THE SEISMIC RESPONSE OF STEEL FRAMES

A thesis
submitted in partial fulfilment
of the requirements for the degree
of
Doctor of Philosophy in Civil Engineering
at the
University of Canterbury
Christchurch
New Zealand

by G. A. MacRae

Supervised by A. J. Carr and W. R. Walpole

October 1989

To my parents

ABSTRACT

The seismic behaviour of moment-resisting and eccentrically-braced steel frames is studied. Inelastic time history analyses are presented to show that simple design techniques may be developed to encourage earthquake resisting structures to behave well, even though their seismic response may be complex.

Complementary to the analytical study, eight steel I-section beam-columns were tested under a regime of cyclic bending. The units exhibited very good hysteretic behaviour prior to their failure by means of fracture or various modes of buckling. The cyclic post-elastic behaviour of beams and beam-columns in steel multistorey frames, and some parameters influencing their deformation capacity are discussed.

ACKNOWLEDGEMENTS

The research described in this thesis was carried out in the Department of Civil Engineering at the University of Canterbury, under the overall guidance of its Head, Professor R. Park. The assistance of the academic staff of this department is gratefully acknowledged.

I am particularly indebted to my supervisors, Dr A. J. Carr and Dr W. R. Walpole for their guidance, constructive criticism and encouragement throughout all stages of this research.

I wish also to acknowledge the encouragement and helpful comments of Mr G. C. Clifton of the New Zealand Heavy Engineering Research Association and of Mr G. W. Butcher, of Morrison, Cooper and Partners who suggested the project. I am also grateful to my friends and fellow students T. Andriono, P. C. Cheung, B. Deam, R. Djaja, L. Dodd, S. Gozali, N. I. Guruparan, M. Mortazavi, Pam H. J., J. Restrepo, N. Smith, M. T. Soesianawati, H. Tanaka, J. A. Tjondro, N. Vitharana, S. Wijanto, F. Yanez and Zhao X. who have not only made the research enjoyable but have contributed many useful comments.

My thanks are extended to the Technical Staff of the Department, especially Messrs G. Hill, R. Allen, B. Hutchison, G. E. Clarke, P. Coursey, H. Crowther, N. Grey, D. MacPherson, P. Murphy, and Ş. Pasa. I also wish to thank Mr. L. H. Gardner for photographic work, Mrs V. J. Grey for assistance with the draughting work and Mr N. Hickey, Mr G. Sim, Mrs W. Hale and Mrs Y. Dench for their interest.

The financial assistance provided by the New Zealand Heavy Engineering Research Association and the University Grants Committee is gratefully acknowledged.

TABLE OF CONTENTS

APPENDICES

NOTATION

a = Distance

A = Area of steel section

A_s = Shear area of steel section

b = Distance

b_1 = Flange outstand

B = Width of section flange or distance

C = Compression force or damping or coefficient for the derivation of V_{base}

C_e = Basic seismic coefficient for the derivation of V_{base} for an elastically responding system

C_μ = Basic seismic coefficient for a load reduction factor of μ.

d = Displacement

d_1, d_2, d_3 = Displacements

d_1 = Length of unsupported web

d' = Displacement

D = Depth of section or Dead load

D' = Distance

D_b = Beam depth

e = Link eccentricity

E = Earthquake inertia load or Modulus of elasticity for steel

$E_{10\%}$ = Modulus of elasticity of steel when the strain = 10%

E_μ = Design level seismic load

$E_{\mu=1}$ = Elastic level earthquake load

E_s = Material strain hardening stiffness

F = Factor of safety or stress

F_r = Residual stress

F_u = Ultimate stress

F_y = Yield stress

F_{yf} = Flange yield strength

F_{ys} = Specified yield strength

F_{yw} = Web yield strength

g = Acceleration due to gravity ≈ 9.81 m/s^2

G_s = Shear modulus

h = Interstorey height

h_b = Depth of reinforced concrete member

H = Height or Lateral load

H_c = Height to centroid of lateral load distribution

H_f = Friction force

H_μ = Lateral load at a particular ductility

I = Second moment of area of a section

I_b = Beam second moment of area

I_c = Column second moment of area

K = 1 + the proportion of shear displacement in the total plastic displacement

K_s = Secant stiffness

l_h = Length

L = Live load or length

L_c = Distance to point of contraflexure

L_{col} = Column clear length

L_p = Plastic hinge length

L_r = Reduced live load

L_s = Service live load or Length

M = Bending moment

M_b = Beam moment

M_c = Column moment

M_{code} = Bending moment derived from code specified lateral seismic loading only (taken at the beam centreline for column members

M_E = Beam fixed end moment

M_i = Initial moments

M_f = Final moments

M_{pb} = Beam plastic moment

M_{pc} = Column plastic moment reduced by axial load

M_p = Plastic moment

$M_{p,col}$ = Plastic unreduced column moment

M_p^o = Overstrength moment = $\phi_o M_{pb}$

$M_{stat,os}$ = Static overstrength column moment

M_u = Factored moment at a section acting with a shear force V_u

M_y = Yield moment

M^*_p = Probable flexural strength

P = Axial load, may be subscripted D for dead load or L_s for reduced live load

P_i = Storey lateral force

P_{eq} = Seismic axial load

P_{oc} = Euler buckling axial load

P_u = Design axial compression force

P_y = Axial load causing yield over the whole section

P_{yc} = Compressive yield stress

R = Risk factor used in the derivation for C_u or strength reduction factor or rotation capacity

R_m = Moment reduction factor

R_v = Axial load reduction factor

S = Plastic modulus of section

S_b = Beam plastic modulus

S_c = Column plastic modulus

t_w = Web thickness

t = Time

T = Flange thickness or Period of vibration

V = Shear force

V_{base} = Design level base shear

V_c = Column shear

V_{code} = Shear force in a member due to code specified lateral seismic loading alone

V_{des} = Design shear

V_E = Beam fixed end shear

V_{link} = Link shear force

V_{max} = Maximum shear

V_{ob} = Maximum earthquake induced shear force at the development of beam flexural overstrengths

V_p = Plastic shear force

V_{pc} = Reduced plastic shear force

$V_{stat,os}$ = Static overstrength column shear

W = Weight

W_i = Storey weight

W_t = Weight

w_v = Dynamic magnification factor for shear

w_m = Dynamic magnification factor for moment

w_f = Dynamic magnification factor for base shear

Z = Elastic modulus of section or Zone factor used in the derivation of C_μ

α = Experimental constant or factor for Rayleigh damping or amplification factor

β = Experimental constant or factor for Rayleigh damping

δ = Displacement

δ_a = Axial displacement

δ_b = Component of plastic displacement from moment alone

δ_p = Plastic displacement

δ_s = Plastic displacement at L_s up specimen height

δ_t = Plastic displacement at point of contraflexure

δ_T = Top displacement

δt = Timestep

δ_o = Interstorey drift

δ_v = Component of plastic displacement from shear alone

δ_y = Yield displacement

δ_μ = Design level interstorey drift or displacement at a particular ductility

$\bar{\delta}$ = Distance

ε = Strain

ε_{av} = Average axial strain

ε_{ax} = Axial strain

ε_f = Flange strain

ε_u = Ultimate strain

ε_y = Yield strain

μ = Displacement ductility factor

μ_{des} = Lateral load reduction factor for frames with periods greater than 0.7 seconds

μ_{max} = Maximum displacement ductility

μ_m = Member displacement ductility

μ_n = Displacement ductility factor incorporating a nominal level of ductility

μ_s = Subassemblage displacement ductility

θ = Rotation or stability coefficient

θ_b = Beam rotation

θ_c = Column rotation

θ_{cr} = Critical rotation

θ_H = Inelastic hinge rotation

θ_p = Plastic hinge rotation

θ_{pc} = Reduced plastic rotation

θ_u = Ultimate rotation

ϕ = Strength reduction factor or curvature

ϕ_{av} = Average curvature

ϕ_y = Yield curvature

ϕ_p = Plastic curvature

ϕ_u = Ultimate curvature

ϕ_o = Material overstrength factor

ϕ_{ob} = Beam overstrength factor

Σ = Symbol denoting summation of a variable

GLOSSARY

CAPACITY DESIGN. In the capacity design of earthquake resistant structures, elements of the primary lateral load resisting system are chosen and suitably detailed for energy dissipation under severe deformations. All other structural elements are then provided with sufficient strength so that the chosen means of energy dissipation may be maintained.

DUCTILITY means the ability to deflect beyond the yield displacement or yield curvature into the plastic range without excessive loss of strength or any critical structural damage.

DUCTILE MOMENT-RESISTING FRAME (DMRF) is a space frame which resists lateral loading primarily by the means of flexure in the beams and columns which are detailed for ductile behaviour.

DUCTILE STRUCTURES resisting seismic loading are required to dissipate energy by ductile flexural, shear, or axial yielding in specified locations in the structure.

ECCENTRICALLY BRACED FRAME (EBF) is that form of braced frame where at least one end of each brace intersects a beam at a point away from a joint.

ELASTICALLY RESPONDING STRUCTURES are not expected to develop significant inelastic deformations while resisting the largest seismic loads specified by the appropriate loadings code.

HYBRID STRUCTURE (or DUAL SYSTEM) consists of at least two forms of structural framing which resist the lateral load.

INTERSTOREY DRIFT is the displacement of one level relative to the level above or below it.

INTERSTOREY DRIFT RATIO is the interstorey drift divided by the storey height.

LIMITED DUCTILITY. Structures of limited ductility are assumed to be required to sustain low levels of inelastic ductility demand and are designed to resist larger seismic loads than fully ductile structures, as specified in the appropriate loadings code. Member strength is determined by either capacity or strength design procedures.

MEMBER DISPLACEMENT DUCTILITY means the ratio of transverse displacement of a member to its plastic displacement.

NEGATIVE (HOGGING) MOMENT causes tension on the top of a member.

OVERSTRENGTH FACTOR takes into account all possible factors that may contribute to strength such as higher than specified strengths of the steel, strain hardening of the steel, the possible variation in section dimensions and the contribution of the floor slab.

P-DELTA EFFECT implies or refers to the increase in overturning moment at any level of the structure caused by the gravity load which is laterally displaced in the deformed structure due to seismic or wind load or other effects.

PLASTIC DISPLACEMENT means the displacement which produces yield point stresses in the extreme fibres, multiplied by the shape factor for the section. It may be reduced by the presence of axial load.

PLASTIC HINGE REGIONS in a member are where significant rotations due to inelastic strains may develop under flexural actions.

POSITIVE MOMENT causes compression on the top of a member.

SECTION CURVATURE DUCTILITY means the ratio of curvature at any cross-section of a member to its plastic curvature.

SECTION CURVATURE DUCTILITY CAPACITY means the ratio of maximum sustainable curvature at any cross-section of a member to its plastic curvature.

SOFT STOREY MECHANISM in the frame occurs when all the columns in a storey yield at both ends at the same time producing a mechanism.

STRENGTH REDUCTION FACTORS are provided to allow for approximations in the calculations and variations in the material strengths, workmanship, and dimensions.

STRENGTH DESIGN is design with factored loads to the strength limit state. This is also known as load and resistance factor design.

WORKING STRESS DESIGN. Member sizes are chosen so that the expected member actions do not cause the allowable working stresses to be exceeded.

YIELD CURVATURE means the curvature which produces yield point stresses in the extreme fibres, multiplied by the shape factor for the section. It may be reduced by the presence of axial load.

DEFINITION OF MEMBER FLEXURAL STRENGTHS

The different levels of member flexural strength used in the following chapters are defined as follows:

1. Ideal Strength (M_p) - theoretical strength calculated using the specified minimum steel strength.

2. Dependable Strength (ϕM_p) is the ideal strength multiplied by strength reduction factors (ϕ) specified by codes to give a statistical lower bound on the member strength.

3. Limited ductility overstrength ($\phi_o' M_p$) is the overstrength factor of steel members expected to be subjected to limited ductility demand.

4. Fully ductile overstrength ($\phi_o'' M_p$) is the overstrength factor of steel members expected to be subjected to full ductility demand.

Inter-Relationship Between Capacities

a) Flexural strengths for beams:

Ideal	: M_p	$= SF_y$	
Dependable	: ϕM_p	$= 1.0\ M_p$	(from reference [2.40])
Overstrength	: $\phi_o' M_p$	$= 1.35 M_p$	(from reference [2.40])
	$\phi_o'' M_p$	$= 1.50 M_p \approx 1.10 \phi_o' M_p$	

b) Flexural strengths for columns:

The moment capacity of columns, M_{pc}, was calculated from the specified minimum value of yield stress, F_y, and was adjusted according to the level of axial load, P.

ABBREVIATIONS

AS - Australian Standard
EBF - Eccentrically braced frame
DMRF - Ductile moment resisting frame
NZS - New Zealand Standard
UBC - Uniform Building Code

Chapter 1

INTRODUCTION

The structural forms of moment-resisting steel frames or eccentrically-braced steel frames are now commonly used in buildings in areas in which there is danger of damage from seismic activity. It is generally regarded as desirable that there should be no loss of life as a result of the collapse of these structural types.

In this report, a study of the response of steel frames to earthquake records which may occur in steel frames is undertaken. The behaviour of these frames is studied particularly from the point of view of determining whether large inelastic deformation demands would occur as a result of an undesirable frame mechanism. An understanding of the behaviour of these structures leads to design guidelines. In particular, a "capacity design" type of approach, in which certain elements in the frame are chosen to yield before others has been presented for the design of moment-resisting and eccentrically-braced steel frames. This means that although the structures may not be strong they will be "tough", so that sudden, brittle or other undesirable failures are discouraged. The results of several computer-based non-linear dynamic analyses modelling the seismic attack on prototype structures are discussed. These were carried out in order to develop and to assess the design procedures.

In view of the large structural displacement ductility demands which may be imposed on a frame during a major seismic event, critical regions of the beams and columns must be able to sustain high local deformations. Thus, complementary to the theoretical study, an experimental investigation of the inelastic cyclic behaviour of some beam-columns was undertaken. Special attention was given to the deformation capacity and to the effect of axial load on the cyclic performance of steel I-shaped beam-columns.

This report is organised into four sections which are presented in the following order.

MOMENT-RESISTING FRAMES

Chapter 2 describes the need for an understanding of moment-resisting steel frames subjected to large ground accelerations. A summary of accepted design philosophies and relevant literature including the existing "capacity design" methods are discussed and the way in which the frames are modelled in the later chapters is described.

Chapter 3 describes some aspects of the dynamic behaviour of moment-resisting steel frames. Problems with the application of the reinforced concrete "capacity design" type of procedure to moment-resisting steel frames are discussed and several methods for designing steel frames are described in the light of the results of dynamic time-history analyses. Finally, a design methodology is presented.

Chapter 4 examines the effect of P-delta forces on the seismic response of steel frames and the previous work undertaken to predict and design for this effect. A design method is then presented.

ECCENTRICALLY BRACED FRAMES

Chapter 5 briefly looks at the problems and the behaviour of K-braced and D-braced steel frames and suggests methods to discourage the formation of soft-storey mechanisms.

COLUMN TESTING

Chapter 6 discusses some aspects of the cyclic behaviour of members. A literature review is given and the need to study the behaviour of steel beam-columns is shown. A discussion of some of the different parameters used for measuring damage is made and relationships between the different parameters are described. Reliable methods for damage measurement are required to relate the design-level earthquake lateral load reduction factor of a frame to the inelastic deformations of the members.

Chapter 7 describes the eight beam-columns tested, test procedure and the performance of each specimen. A general discussion of the behaviour of the test columns follows and the main parameter effecting the cyclic ductility capacity of compact steel beam-columns is identified.

CONCLUSIONS

Finally, Chapter 8 summarizes the work undertaken and restates the main conclusions and recommendations made regarding the design methodologies and the cyclic performance of the column units.

Chapter Two

SEISMIC DESIGN PHILOSOPHY, DESIGN METHODS AND FRAME MODELLING

2.1 INTRODUCTION

This chapter describes the basic aims of building design in order to produce earthquake resistance and shows how these requirements are presently satisfied in New Zealand by means of a "capacity design" philosophy developed for reinforced concrete structures. Some assumptions made in earthquake-resistant design are described and some methods for the design of moment-resisting steel frames are discussed. The modelling assumptions used for the frame members in the following chapters are also described.

2.2 STRUCTURAL DESIGN PHILOSOPHY

An earthquake resistant structure should be designed in such a way [2.1] that it is:

i) stiff, so that there is no non-structural damage in small or moderate earthquakes,

ii) strong, so that in moderate to strong earthquakes the structure will respond elastically and there will be no structural damage, and

iii) ductile, so that the structure may safely sustain the displacements beyond the elastic range that will be imposed upon it in a very strong earthquake.

The overriding concern in seismic design is the prevention of catastrophic failure and hence the loss of life as a possible consequence of a large earthquake that may be expected during the life of the building.

(a) Stiffness, Strength and Ductility

Stiffness is controlled by the appropriate loadings code. The purpose of the interstorey drift limits in the draft New Zealand loadings code [2.2] is to minimize the second order or P-delta effect. These drift limits are zone dependent as a result of some work carried out by Andrews [2.3]. The limits also serve to prevent excessive vibration under service loads and to ensure that no damage will occur in the non-structural or structural frame components during moderate earthquakes.

The minimum strength of a structure is determined from the code load combinations. For combinations including seismic loading, the seismic design level forces are found from the expected elastic response of a structure which is reduced by a load reduction factor. This factor, which may be as large as six, is related to the expected frame displacement ductility.

Ductility is provided by detailing the components which are expected to deform inelastically so that they may sustain the inelastic deformations required of them. In steel structures, brittle components are protected by being provided with sufficient strength so that they do not yield. Compact closely-braced steel members may sustain large inelastic deformations before losing significant load carrying capacity.

2.3 NEW ZEALAND DESIGN APPROACHES

In New Zealand, most detailed design approaches are presently available only for ductile reinforced concrete structures. Commonly accepted design approaches include "capacity design", limited ductility frame design, and elastic design. A design approach for gravity-dominated reinforced concrete and a recent proposed design method for steel framed structures are also available. These are discussed below.

2.3.1 Capacity Design

In "capacity design", a simple deterministic seismic design approach is used in certain types of frame in which the specified lateral loads are used to establish a hierarchy in the development of energy dissipating mechanisms. The members which are selected to deform inelastically are chosen, and each member is given an appropriate strength or resistance to ensure that, when required, only the chosen plastic mechanisms can develop within the structure thus ensuring desirable and predictable inelastic behaviour during an extreme seismic event.

There are three steps in applying the procedure:

1) Selection of desired mechanism. Often a strong column-weak beam design philosophy will be chosen for reinforced concrete framed structures.

2) Detailing ductile components so that they can sustain the deformations required without a large loss of strength.

3) Providing the non-ductile components with sufficient strength to remain essentially elastic throughout the deformations which may occur. In order to provide this strength the forces in these components must be estimated in

some way. The reinforced concrete commentary [2.4] discusses in detail ways of estimating these forces. A detailed description of "capacity design" as applied to reinforced concrete systems has been described by Paulay in references [2.5] and [2.6].

An indiscriminate allocation of strength throughout a structure may decrease the ability of a structure to withstand a particular seismic event rather than increase it depending on which components are strengthened. In "capacity design", an increase in strength of an inelastic element usually requires an increase in strength in other components of a frame so that the same mechanism occurs.

As earthquakes significantly larger than the design level may occur, a "capacity design" approach encouraging a ductile or non-brittle response will give a structure a good chance of survival, however, if the ground excitation is extremely large not even a "capacity designed" structure will necessarily be able to remain standing as the member ductility capacities may be exhausted.

In "capacity design", a desirable mechanism is selected and encouraged while undesirable mechanisms and failure modes are identified and discouraged. This leads to a greater understanding of structural behaviour than from a pure "strength design" method and enables greater control of the structural response. However, "capacity design" methods require more design effort than does a strength design procedure. In the reinforced concrete procedure [2.4] the number of steps in the design procedure is not small.

For some structures "capacity design" methods may result in conservative member sizes if the member sizes are governed by other than seismic loads. This is discussed in more detail in section 3.4.

2.3.2 New Zealand Reinforced Concrete Ductile Moment Resisting Frame Capacity Design Method

In tall reinforced concrete ductile moment-resisting frames, a strong column-weak beam philosophy as shown in Figure 2.1a is generally selected. Beam flexural hinging is the preferred inelastic deformation system. Joint failure, as well as member failure from shear and excessive ductility demand are discouraged. All of these failures may lead to a sudden loss of strength, and to possible collapse.

The New Zealand reinforced concrete code [2.7] seeks to discourage all column hinging except at the bases of those columns at the ground floor. This is because special detailing is required for reinforced concrete columns in order to obtain a significant column ductility capacity. Beam hinging is desired because larger absolute rotations and energy absorption is available than in members in axial compression.

A soft-storey mechanism, such as that shown in Figure 2.1b, has been shown to induce much larger inelastic rotations in the columns than in the beams in the beam sidesway mechanism of Figure 2.1a if the displacements at the top of both frames are the same [2.8]. A soft-storey mechanism is discouraged especially in tall structures because of the increased rotational demand of the soft-storey mechanism, and the smaller rotational capacity of the columns than of the beams. Furthermore, in reinforced concrete structures, if column hinging is able to be avoided altogether, columns may be detailed for much less ductility and the amount of confining steel used may be reduced.

In a tall reinforced concrete frame, the beam sidesway mechanism shown in Figure 2.1a is chosen. The beams are detailed for ductility, and other components are then provided with sufficient strength to ensure that the chosen mechanism occurs. The method by which this is done is briefly explained in the next section.

(a) Details of the Reinforced Concrete DMRF "Capacity Design" Procedure

Seismic-induced lateral loads obtained by elastic static or modal analysis techniques are used simply to ensure that there is a rational distribution of lateral resistance throughout the structure. These loads are reduced by a factor which is related to the expected amount of member ductility. Paulay [2.6] has defined the use of the lateral load distribution as follows:

> "Because of the inevitable gross uncertainties involved in the specifications of building codes for using equivalent lateral static design loads and the uncertainties associated with inelastic dynamic structural response to ground motions, in the context of design for survival, the importance of the accuracy of the of elastic structural analyses is not as important as protection against the undesirable mechanisms."

The beams, which are part of the primary load resisting system and are expected to deform inelastically, are sized according to the actions resulting from the most critical load combination and are detailed appropriately. It is important at this stage to get as close a match as possible between the required member strength and the actual strength of the beams as this will affect the required sizes of the columns and the distribution of ductility throughout the structure. Moment redistribution, as described in section 2.6.4.3, if necessary, may be applied.

The strengths of the columns and beam-column joints, which are not part of the primary seismic induced load resisting system, are based on forces resulting from the strength of the inelastically deforming members. Dynamic and overstrength effects are considered to ensure that the chosen energy dissipating mechanisms may be maintained throughout the deformations that may occur. However, members are not required to be designed for forces larger than the elastic seismic forces. Estimation of member actions is performed as follows.

(i) Column Moments

The New Zealand reinforced concrete code commentary [2.4] states that the column design moment should be:

$$M_{col} = R_m \, (\phi_{ob} W M_{code} - 0.3 h_b V_c) \qquad \text{Equation 2.1}$$

The term for column moment, M_{code}, is calculated from the earthquake load case alone.

The beam overstrength factor, ϕ_{ob}, is the ratio of the sum of the flexural overstrengths developed by the beams, as detailed, to the sum of the flexural strengths required in the given direction by the Code specified earthquake loading alone, both sets of values being taken at the relevant column centreline. This factor needs to be evaluated at each level of each column and effectively distributes the overstrength beam moment to the column in proportion to the column moments from the static earthquake analysis alone. It is calculated as follows:

$$\phi_{ob} = \frac{\phi_o \Sigma M_{pb}}{\Sigma M_{b,code}} \qquad \text{Equation 2.2}$$

In Equation 2.2, $\Sigma M_{b,code}$ is the sum of the beam moments at the joint from the earthquake load case alone, ϕ_o is the material overstrength factor, and ΣM_{pb} is the actual flexural strengths of the beams at the joint.

The dynamic magnification factor, w, is to allow for the actual distribution of moment not being equal to that specified by the static overstrength moments, $\phi_{ob}M_{code}$, alone. Reasons for this may be:

i) that the chosen method of distributing moment by the earthquake moment forces alone, may not be what would occur without dynamic effects, and

ii) that higher mode effects may contribute to the increased moment.

The second term in the brackets is a modification to the column centreline moments in recognition that the maximum column moments occur near the beam face. The value of $0.3h_b$ for the effective rigid end block is used. M_{code} may be determined by either modal analysis or by the Code specified lateral loads.

The moment reduction factor, R_m, is used because in reinforced concrete column design outer columns are usually governed by the forces occurring when the member is in tension. However, because reinforced concrete columns are strong and ductile in tension or with a small compressive axial load, hinging is allowed. Three conditions apply so as to make the amount of hinging acceptable. The first condition is a limit on the axial load ratio which is necessary to ensure that the column yields in bending rather than under tensile axial load, the second is a lower limit on R_m to control the amount of force redistribution so that the ductility demand in that member will not be too large, and the last condition makes sure that the strength lost in the column considered may be redistributed to other columns in the storey so that the storey strength will not be lost. For steel frames, the column loaded in compression is the most critical and a factor such as R_m is not required.

(ii) Column Shear

The reinforced concrete code commentary [2.4] assumes that the maximum expected column shear is given in Equation 2.3, where V_c is the column design shear force, and V_{code} is the column shear force obtained from code specified lateral seismic loading alone.

$$V_c = 1.30\phi_{ov}V_{code} \qquad \text{Equation 2.3}$$

The notation regarding the overstrength factor in the reinforced concrete code commentary [2.4] is ambiguous. It is not spelt out how the factor, ϕ_{ov}, used in Equation 2.3 is calculated. In practice the shear overstrength factor, ϕ_{ov}, is often calculated as the beam overstrength factor, ϕ_{ob}, from the levels above and below the column considered. However, $\phi_{ov}V_{code}$ does not represent the shear on the column resulting from the static overstrength beam moments. It is thought that a more rational formula for the estimation of column shear would be Equation 2.4. In this equation the static overstrength shear is magnified for dynamic effects.

$$V_c = 1.30V_{stat,os} \qquad \text{Equation 2.4}$$

where $V_{stat,os} = (\phi_{ob,top}M_{code,top} + \phi_{ob,bot}M_{code,bot})/L_c$

The factor of 1.30 includes a strength reduction factor (ϕ) of 0.85 and assumes that the column shear force obtained from the code specified lateral seismic loading varies by no more than 20% from the static overstrength shear [2.4].

(iii) Column Axial Loads

Seismic axial loads, P_{eq}, are found from Equation 2.5, where ΣV_{ob} is the sum of the overstrength seismic shear forces from the beams above the level under consideration and R_v is an axial load reduction factor which accounts for the fact that not all of the girders above the level under consideration will necessarily yield at a given instant of time because of higher mode effects. The column design axial load also includes the gravity loading. The value of V_{ob} for a beam is calculated as the the sum of the overstrength moments at each end of the beam divided by the beam clear length.

$$P_{eq} = R_v \Sigma V_{ob} \qquad \text{Equation 2.5}$$

(b) Background to Dynamic Magnification Effects

Values for the factors of shear and moment dynamic magnification, and the axial load reduction factor, were obtained from dynamic analyses of frames. The need for dynamic magnification factors for column moment was shown by Paulay [2.9], however the number of effects determining these factors have made the problem complex. These effects include the number and location of the hinges forming, the natural periods of the structure, and the particular earthquake record which determined how many of the modes were excited.

Because of this complexity, an empirical approach was taken, and analyses were run by Row [2.10], Lindup [2.11], Kelly [2.12] and Jury [2.13], to find reasonable values for the factors to incorporate in a design procedure. These values are given in the reinforced concrete commentary [2.4]. It should be noted that the values used do not represent an upper bound on the member actions from dynamic analyses, because, under very large earthquakes some column yielding is permitted and it has been argued [2.14] that as these high levels of moment often occur for less than 0.05 seconds that there may be insufficient time for very large inelastic demands to occur.

2.3.3 Reinforced Concrete Frames of Limited Ductility

Design provisions for frames of limited ductility are specified in chapter 14 of the present New Zealand reinforced concrete code [2.7] which are only applicable for frames not greater than 4 stories or 18 m in height. Strength design using the load combinations of an appropriate loadings code, rather than "capacity design" is used to size all of the members, but the design level of seismic force used is greater than that required for a fully ductile design. Column detailing requirements are more severe than in the "capacity design" approach to ensure adequate column ductility is available.

The rationale for this kind of approach is that a soft-storey mechanism occurring in a moment-resisting frame is able to be accepted only if the curvature ductility demands are not excessive. In order for the column ductility demand from a soft-storey mechanism to be less than the column ductility capacity a frame must be:

i) Low, so that the displacement at the top of a structure predicted by the equal displacement assumption will be small. The column curvature ductility demand increases with the number of frame stories if a soft-storey mechanism occurs. Park and Paulay [2.8], using a number of assumptions, have shown that if a column sidesway mechanism forms in a reinforced concrete moment-resisting frame with a frame displacement ductility factor, μ, of 4, a 3 storey frame may demand a maximum member curvature ductility, ϕ/ϕ_y, of 34, while a 10 storey frame may demand a maximum member curvature ductility as large as 122. A beam sidesway mechanism may be required to sustain curvature ductilities in the beams of 16.2 and 17.6 respectively for these heights of frames. To find these ductility demands it was assumed that the equal displacement assumption holds so that the displacement at the top of a frame would be the same whether a beam or a column sidesway mechanism occurred.

ii) Designed for a higher level of lateral force than a fully ductile frame. For short frames, the required ductility demand may still be greater than that which may be sustained even with a large amount of detailing. One way of reducing this ductility demand is to increase the seismic design level forces.

iii) Detailed appropriately so the members may sustain the ductility demand imposed on them. The present detailing provisions seem to be inconsistent in the New Zealand reinforced concrete code [2.7]. For example, according to Park and Paulay [2.8], a four storey frame with a soft-storey mechanism and a design displacement ductility, μ, of three will require a curvature ductility, ϕ/ϕ_y, of 31.6 using equations 11.42 and 11.44 in reference [2.8]. This demand is very large and is unlikely to be able to be achieved even by detailing for full ductility (ϕ/ϕ_y=20). To detail the frame for limited ductility (ϕ/ϕ_y=10), as implied by the concrete code [2.7], can be seen to be grossly incautious.

It is suggested that if the method of prediction of member ductility proposed by Park and Paulay [2.8] is used for frames designed to limited ductility forces in which a soft-storey mechanism is likely to form that

i) for one storey frames, column sections detailed for limited ductility deformation capacity should be used, and

ii) for frames of two to three stories, detailing for full ductility should be carried out, and

iii) for frame above three stories in height, no soft-storey mechanism should be permitted to occur.

In actual analyses of frames it should be noted that even if "capacity design" is not specified for reinforced concrete frames, a soft-storey mechanism will not always occur because the strength of the bottom storey is often up to two times the design level strength as the point of contraflexure is often near the top of the bottom storey. The lower stories may be overdesigned because of load cases other than earthquake effecting the member sizes, yielding may occur in more than one level and the assumption that the same displacement will occur at the top of a frame independently of where the hinging occurs may be extremely conservative.

2.3.4 Gravity-Dominated Reinforced Concrete Frames

Some reinforced concrete frames, especially those in regions of low seismic risk with high gravity loads may be gravity-dominated rather than governed by seismic load. Study of the behaviour of these types of frame have been made by Paulay [2.15] and Fenwick and Davidson [2.16].

(a) Paulay's Design Methods for Gravity-dominated Frames

Paulay [2.15] has studied this frame type and has run analyses to investigate the dynamic behaviour of such frames in conjunction with Tompkins [2.14] and Mullaly [2.17]. Further work by Paulay [2.18] has produced two design methods for gravity-dominated reinforced concrete frames. In the first method shown in Figure 2.2a hinging is permitted within the length of the beam by selectively curtailing the reinforcing steel. In the second method shown in Figure 2.2b the outer columns only were kept elastic, but the internal columns were permitted to yield.

(b) Fenwick and Davidson's Analyses of Gravity-dominated Frames

Fenwick and Davidson [2.16] have run a number of analyses of gravity dominated reinforced concrete frames. They showed that as cyclic loading occurs in a subassemblage and yielding occurs in at least one end of the beam, the gravity end moments "shake down" to zero after several cycles of loading. The effect of shakedown was shown from the results of a non-linear analysis. The moments at the end of each beam after the El Centro excitation were much less than those before the analysis.

They showed that yielding will occur in one direction only at each hinge location in gravity-dominated beams where hinging is permitted along the member length and that with each additional cycle of loading the inelastic rotation would accumulate in these regions. It was suggested that the hinge deformation capacity may be exhausted and failure may result if a subassemblage of this type were subjected to the loading regime of the draft New Zealand loadings code. It was found that the beams could be expected to survive 2 to 3 El Centro ground motions before there was any danger of strength degradation in the frames analysed.

A comparison of the dynamic behaviour of earthquake-dominated frames, in which there were no gravity moments, and of gravity-dominated frames, in which hinging could only occur along the beam length, was carried out. These

frames possessed the same stiffness and mass, but different strengths in order to carry the different loads. It was found that the displacements at the roof of the earthquake-dominated frames were generally more than for the gravity-dominated frames. The maximum inelastic beam rotation was larger in the gravity-dominated frames and in most cases equalled the cumulative inelastic rotation showing that there was no load reversal in these hinges. The cumulative inelastic beam rotation was often much larger in the gravity-dominated frames than in the earthquake-dominated frames.

2.3.5 Elastic design

Structures may be designed for the elastic level earthquake forces. "Capacity design" of members is generally not required as the possibility of severe damage is very low even under large earthquakes. Furthermore in "capacity design", members are not generally required to be designed for more than the expected elastic level of response.

2.3.6 Interim Design Procedure for Steel Frames

An interim method has been recommended by Clifton [2.19] to design steel moment-resisting frames in New Zealand until a detailed design philosophy for such frames is available.

In this procedure the overstrength beam moment on one side of the column plus the moment from the earthquake load combination on the other is applied to the column. The axial load on a column is calculated from the summation of the estimated beam shears above the column level under consideration. The beam shears are calculated from the gravity shear plus an estimation of the maximum earthquake shear which assumes that the beam reaches its overstrength moment capacity at one end, and only the moment from the earthquake load combination at the other end.

The method takes some account of the level of gravity loading and encourages beam hinging before column hinging. Although this procedure is less complicated than the reinforced concrete type of procedure, several steps are required in order to obtain the column sizes. The column axial load reduction factor of the reinforced concrete code commentary [2.4] is used but no moment dynamic magnification factor is applied. The required column sizes are dependent upon the level of earthquake force used to obtain the beam design moments.

2.4 OVERSEAS DESIGN APPROACHES

(a) Strength Design

Overseas, and in the past in New Zealand, the strength design method has been used for the design of multistorey steel frames. In this method, the members and connections are both designed for the forces resulting from the expected level of lateral loading on the structure which may be significantly less than the elastic design forces. No consideration is given to the relationship between strengths of members.

Often a mixture of strength and capacity design is used. For example, many codes now require connections in seismic frames to be designed for the full capacity of the member framing into it, yet use the "strength design" method to size members. The strong-column weak-beam design philosophy for moment-resisting steel frames has often been given lip service by engineers but there have been few guidelines to encourage this behaviour.

(b) Bertero and Kamil

Bertero and Kamil (1972) [2.20] carried out research into a non-linear design method for multistorey steel frames. Member forces were obtained by modal analysis techniques, and the most economic frame sizes were found by an iterative optimization procedure based on a series of elastic and inelastic time history analyses.

As part of this procedure the authors chose to minimize the possibility of plastic hinging in the columns by ensuring that the sum of the reduced column moment capacities at any joint, ΣM_{pc}, were greater than a factor of safety, F, multiplied by the sum of the beam strengths framing into the joint, ΣM_{pb}. That is,

$$\Sigma M_{pc} > F \Sigma M_{pb} \qquad \text{Equation 2.6}$$

A value of F of 1.20 was suggested to cover uncertainties in the design of columns as well as the possible non-equal distribution of girder moments between the columns at a joint.

(c) Austin

Austin et al. [2.21] have described a method of optimal frame design. Many time-history analyses were run, design objectives were set, constraints were specified and a linear programming technique was used to find the optimum solution. Although methods such as this may be available for design of frames in the future as computing power becomes more advanced, guidelines will still be required to obtain the initial frame sizes, and interim design methods are still required.

(d) Humar

Humar [2.22] has suggested a method of frame design using modal techniques. In order to protect the columns he has proposed that a lower seismic load reduction factor be applied to the columns than to the beams thereby encouraging beam yielding.

(e) Recommendations for the Uniform Building Code (UBC)

Recent recommendations for the Uniform Building Code [2.23] have used a formula of similar form to that of Bertero and Kamil [2.20] to provide some protection to the columns against a large amount of yielding. The factor of safety, F, was taken as 1.0 and the column plastic flexural strength was conservatively approximated by a straight line between (0, P_y) and (M_p, 0) on the axial-load moment interaction diagram as shown in Figure 2.3. At any moment frame joint, the following relation is to be satisfied if the axial load ratio, P/P_y, is not less than 0.40 for all load combinations.

$$\Sigma S_c (F_{yc} - P/A)/(\Sigma S_b F_{yb}) > 1.0, \quad \text{where } P/P_{yc} \geq 0 \qquad \text{Equation 2.7}$$

This may be rewritten as $\Sigma M_{pc}' > \Sigma M_{pb}$, where $\Sigma M_{pc}' = \Sigma M_{p,col}(1-P/P_y)$.

The limit on the axial load ratio, P/P_y, of 0.4 is possibly based on the recommendations by Popov, Bertero and Chandramoulli [2.24] in which it was found that columns with axial load ratios, P/P_y, greater than 0.50 did not perform well. The lower limit of 0.40 for the axial load ratio, rather than 0.50, may be to allow for the dynamic variation of the distance from the end of the column to the point of contraflexure and the vertical accelerations which may occur during an earthquake.

These recommendations state that columns may be assumed to remain elastic if the sum of the moment-capacities of the columns is greater than

i) 1.25 times the sum of the moment capacity of the beams framing into the joint, or

ii) the gravity forces plus the elastic seismic forces, or

iii) 1.25 times the strength required to cause yielding in the panel zone.

2.5 ESTIMATION OF FORCES AND DISPLACEMENTS IN INELASTIC FRAMES

The forces and displacements in ductile frames are commonly estimated by means of empirical assumptions based on the seismic response of single degree of freedom inelastic oscillators to selected earthquake records. The most common of these are the equal acceleration, equal energy and equal displacement type of approximations which may be used for design. These methods are suitable for design because of the ease with which they may be used with an acceleration response spectrum. For structures with a fundamental period of response greater than about 0.7 seconds, such as those in this report, the equal displacement assumption is generally recognised as being the most suitable method of estimating the maximum structural displacement. This method is discussed in structural dynamics textbooks [2.25]. In this section only the background to and the applicability of the equal displacement assumption is discussed.

An inelastic response involves a lengthening in period of the inelastic structure and increased effective damping from the energy absorbed by the hysteretic behaviour of the members. While estimates of the "effective period" and "effective damping" are able to be used to a limited extent for structures with a single bi-linear degree of freedom such as bridge piers and base isolated structures, a sufficiently accurate method for the routine design of multistorey structures has not yet been developed.

(a) The Equal Displacement Assumption

The equal displacement assumption simply states that the maximum displacement expected in a ductile structure subject to a particular earthquake is approximately equal to the displacement obtained if the structure remained elastic. This effect is shown in Figure 2.4.

(i) Single Degree of Freedom Structures

The equal displacement effect was initially observed on oscillators subjected to the El Centro 1940 N-S ground motion because, for a long time, this was the most severe record in existence. Most of the structures analysed had first mode periods between 0.8 and 2.0 seconds. The El Centro 5% damped spectral displacement spectra is reasonably constant over this range, and hence the displacements for the elastic and inelastic oscillators were similar.

Humar [2.22] has shown that in many cases the elasto-plastic deflection can be very different from the maximum elastic deflection for a particular earthquake record, and that the maximum deflection is sometimes underestimated, especially for short period structures.

Carr and Moss [2.26] have shown that for one storey structures with different hysteresis shapes acted upon by a variety of earthquakes, the equal displacement assumption may be far from accurate, and is sometimes grossly incautious even for periods greater than one second. Even under El Centro type excitation, the maximum displacement may be underestimated by a factor of three.

(ii) Multidegree of Freedom Structures

The equal displacement assumption has traditionally been found to apply approximately to the displacement at the top of a multistorey frame. However, as the interstorey drifts must also be estimated in building design, the equal displacement assumption is often used to determine these drifts [2.2]. An alternative method to find the interstorey drifts is discussed in section 4.4.1.

With all the shortcomings of the equal displacement assumption, it is still regarded as the most suitable method available for the estimation of the maximum displacement of a structure with a first mode response period of greater than approximately 0.7 seconds and the method is still expected to be used for some time into the future.

2.6 METHOD OF FRAME DESIGN

2.6.1 Codes

At the time this work was started, both the steel structures codes and the loadings codes in New Zealand were under review. Frames were designed under the latest codes, where appropriate, in order that the recommendations of this report would be relevant and directly applicable for several years. As the work progressed, revised versions of the drafts became available as well as new draft codes. The codes are referenced where they were used.

In this project frames were designed according to the loads from the draft New Zealand loadings code [2.2]. The newer version draft loadings code [2.27] has some provisions which are significantly different from this. For member design, the relevant code at the time of starting this project was the New Zealand Steel Structures code [2.28], which contained provisions for seismic design, and in its revised version incorporates the Australian Steel Structures code (AS1250) [2.29] for general member and connection design. In this code [2.29], the "capacity design" method was stated as being necessary for tall steel ductile framed structures yet detailed provisions for the capacity design of steel framed structures were not available.

In order to correct some errors in this code [2.29], to provide some further information for the design of the many newer types of structure becoming available, and to give a state-of-the-art review of recent research, the New Zealand study group for the design of steel structures presented some recommendations [2.30]. These recommendations, along with a strength version of AS1250 [2.31], were used for design in this project. One of the faults with the Australian code [2.29] as well as this code [2.31] was that it required all column members in sway frames to be designed as sway members, which, in conjunction with the axial load-moment interaction equation for the strength along the member for columns in sway frames, made it difficult to design inelastic axially loaded members. This requirement was ignored because the appropriate provision of the newer limit state draft Australian Steel Structures code [2.32] shows that a more rational and less conservative approach to column design may be used.

An interim steel structures code [2.33] in an allowable stress format based on some of the recommendations of the New Zealand steel structures study group [2.30] was prepared as a temporary measure until a limit state code to tie in with the new Australian limit state code [2.32] was available. These codes are referenced where they are used.

2.6.2 Loads

Relevant load combinations specified in the draft New Zealand loadings code [2.2] are:

i) $1.20D + 1.60L_r$ Equation 2.8a

ii) $1.20D + 1.20L_s \pm 1.00E_\mu$ Equation 2.8b

and iii) $0.90D \pm 1.00E_\mu$ Equation 2.8c

where D represents dead load,

L_r is the live load which may be reduced if the floor area over which the live load acts is large enough,

L_s is the serviceability live load which is the load which is likely to be on the structure at any time,

and E_μ represents the seismic load which may be reduced from the elastic level load if ductile behaviour is expected.

In the seismic design of steel frames, the second load combination is generally more critical than the third load case, so the latter was ignored. The factor of 1.20 in the second load case, which allows for variation from the specified levels of dead and live load is not required as the actual dead and live loads are known in these analyses and are specified as the input data. For the actual frame design, this factor of 1.20 should be included as the actual masses may be different from those expected. To be consistent when designing with the gravity combination, this too was divided by 1.20. The period of the structure is based on $D+L_s$. For simplicity, the allowable live load reduction factor was ignored and full live load was used.

The load case combinations used for designing frames to be analysed in this report were:

i) $1.00D + 1.33L$ Equation 2.9a

and ii) $1.00D + 1.00L_s \pm 1.00E_\mu$ Equation 2.9b

For office buildings the basic live load (L) = 2.50 kPa, and the service live load (L_s) = 0.80 kPa. It was assumed that the floor slab spanned only one-way onto the beams.

Load combinations involving wind were not considered, neither were serviceability requirements or irregular distributions of gravity load on the different beams. While these effects may in some instances lead to larger member sizes, the same principles of seismic design would apply.

(a) Seismic Load Level

The base shear of the frames was found from the draft New Zealand loadings code [2.2] by means of Equation 2.10.

$$V_{base} = C_\mu * R * Z * W_t \qquad \text{Equation 2.10}$$

where R is the risk factor, which changes according to the importance of the facilities and the possible risk of loss of life which could occur on collapse. For normal office buildings subject to a design level earthquake the value of R is taken as 1.0 which represents an annual probability of exceedence of 1/150 or a return period of 150 years. For R = 2.0, the implied return period is 1000 years as the annual probability of exceedence was 0.001 as shown in Figure 2.6. The design level earthquake is often referred to as that found from R = 1.0 and in this report earthquakes greater than the level implied by R = 2.0 are thought to be unrealistically large,

Z is the zone factor, which is dependent on the probable degree of seismic risk at the site of the structure. The majority of frames were designed for regions of high seismicity such as Wellington, where Z = 0.85. In New Zealand the minimum zone factor used is 0.40 in regions of low seismicity such as Dunedin [2.35]. The zone factor (Z) is shown in Figure 2.7 which is taken from reference [2.36],

W_t is the expected weight of the structure when an earthquake occurs and is found from $1.0D + 1.0L_s$.

The spectrum of the code seismic coefficient, C_μ, is shown for different levels of design ductility and period in Figure 2.5 [2.34]. This coefficient is based on three Japanese earthquake records, namely Hachinohe NS, Tohuku NS, and Sendai Basement, as a similar tectonic environment to that of New Zealand is thought to exist in Japan, and three North American earthquakes, namely El Centro 1940 NS, Parkfield N65E, and Orion Boulevard EW record from the San Fernando earthquake [2.35].

(b) Distribution of Seismic Loads

The loadings code [2.2] equivalent static lateral force distribution for frames with a fundamental period greater than 0.7 seconds consists of a point load at the top of the structure of $0.08V_{base}$ with the rest of the base shear being applied as an inverted triangular distribution as shown in Figure 2.8. Although this code recommends use of the equivalent static lateral load distribution for structures with periods less than one second, a revision of these recommendations has no upper limit on the period [2.27]. This distribution was used for all of the frames designed, because, as stated previously, in the context of "capacity design" the purpose of the seismic induced load distribution is simply to provide a rational distribution of load resistance throughout the height of the structure.

2.6.3 Interstorey Drift

The maximum interstorey drift ratio allowed by the loadings code [2.2] is Z/50, where Z is the zone factor. The actual interstorey drift ratio is calculated as the interstorey drift ratio from the reduced seismic loads multiplied by the elastic load reduction factor, C_e/C_μ.

Buildings in every zone in New Zealand are required to have the same stiffness because the zone factor, Z, is included in the drift ratio limit. This means that steel buildings means should have approximately the same minimum strength. The independence of the drift limit upon the seismic zone is based on work by Andrews [2.3] with the aim of allowing an energy loss due to P-delta of only 10% of the total energy. The limit has also been argued as being necessary to provide sufficient stiffness against serviceability loads such as wind, and vibrations caused by passing heavy vehicles.

2.6.4 Frame Design

Iteration was required in order to obtain suitable member sizes. A computer program was written to calculate the period of a frame by Rayleigh's method [2.2], as well as the base shear and interstorey drifts. The way this program works is shown in Appendix 1. The periods of frames were later verified by modal analysis from the dynamic analysis program [2.37] and were found to be accurate to within 2% of that obtained by Rayleigh's method. A two-dimensional structural analysis program was written which could accept member loads as well as nodal loads and would combine load cases internally. This greatly speeded up the design procedure.

2.6.4.1 Design Tools

The design tools used in this project are those commonly available to engineers in New Zealand. A two dimensional static analysis program incorporating material non-linearity [2.38] was used for the majority of the design, and a modal analysis program [2.39] was occasionally also used to look at the modal effects.

The early part of the computation reported herein was carried out using the University of Canterbury Burroughs B6900. Later the Vax 11/750 of the Department of Civil Engineering and an IBM-like microcomputer were used.

2.6.4.2 General Modelling Assumptions

All analyses were two dimensional and "first order" in the sense that the calculations are based on the initial undeformed structural geometry. Torsion and skew effects on the structures were ignored. Floor slabs were treated as rigid in their own plane, unless otherwise stated, and full foundation fixity for all columns was assumed. Flexural members are usually idealized as line elements and shear deformations were often neglected. Flexibility resulting from connection and the panel zone deformation were assumed to be taken account by neglecting the rigid end blocks. Member centreline dimensions were used.

2.6.4.3 Member Design

An attempt was made to ensure that the frames investigated would have realistic properties and that the number of building variables would be kept to a minimum so that the effects of important parameters could be isolated and studied.

A specified value of steel strength, F_{ys}, of 250 MPa was assumed for all members. The design approach used in this report may be used for members of different strength. The elastic (Young's) modulus, E, was taken as 200 GPa, and the shear modulus was taken as 80 GPa. The shear area was approximated as the depth of the section, D, multiplied by the thickness of the web, t, where shear deformation was included. The flexural strength of the bare steel member, M_p, was calculated as SF_{ys} and the axial strength, P_y, as AF_{ys}.

For some of the frames designed, available steel beam and column sizes were not used as the step between section sizes was large. To choose the most adverse beam and column strengths, intermediate beam and column sizes were required. To obtain intermediate values of plastic moment capacity, moment of inertia and strength, sizes were interpolated between those currently available using a least squares power curve.

For all members a strength reduction factor (ϕ) for material variation of 1.0 was used [2.40]. It was assumed that all sections were compact enough and that braces were spaced closely enough that the member plastic strength could be obtained, as well as the large ductility capacity.

(a) Beam Design

The member forces obtained from the code load combinations in Equation 2.9 were used to determine the minimum size of the beams. For drift governed frames, the beam sizes sometimes were required to be increased above the sizes required for strength. Moment redistribution was performed on the beams if it was required, but because the drift limits often governed the beam sizes it was not necessary in most cases.

Beams were generally assumed to behave compositely over their central region. In accordance with the suggestions by Morrison [2.41], this resulted in an approximate increase in beam stiffness to $1.20I_b$, and an increase in plastic moment capacity to approximately $1.40M_{pb}$ along the member. Careful detailing at the ends of the beams was assumed, as described in section 6.6.1(b), so the plastic moment capacity at these locations was assumed to be equal to that of the member itself. Hinging was assumed to occur only at the beam ends because of the resulting increase in strength along the member from composite action.

(b) Moment Redistribution

In design situations, use may be made of moment redistribution to provide a more uniform and efficient distribution of load resistance in earthquake resistant frames. Inelastic action is permitted in some members under the design lateral seismic load, so that members sizes may be smaller while the design level of lateral load will still be resisted.

Redistribution of moment is not a new concept and occurs in plastically designed frames. When a plastic hinge forms, no more moment may be carried and the load redistributes itself toward the stiffer members.

(i) Aims of moment redistribution

Paulay [2.42] has suggested three aims of moment redistribution for reinforced concrete frames. They are to:

1) Reduce the absolute maximum moment, and compensate for this by increasing the moments in the non-critical moment regions. Thus a better distribution of strength is achieved, particularly along prismatic members.

2) Equalize the moments occurring at a joint in the beams due to the two directions of seismic attack, so that the same size members may be used either side of the joint.

3) To fully utilise the section moment capacity by equalizing the two most critical moment regions in a member so that it will still resist the shear obtained from the elastic moment envelope although the amount of ductility required in each potential hinge location may have changed.

(ii) Reinforced Concrete Redistribution Methods

Limitations on the amount of moment redistribution permitted are required in order to ensure that the ductility demand is not excessive. The New Zealand reinforced concrete code, [2.4] requires that:

i) equilibrium be maintained on every level,

ii) the maximum redistribution is 30% of the maximum moment at a section,

iii) the moment at any section be at least 70% of the unredistributed moment capacity, and

iv) the unredistributed lateral shear force from the storey above that under consideration, plus the shear at that storey be able to be carried to the floor below.

Moment-redistribution may be used in ductile frames under any of the code loading combinations. A technique for carrying out redistribution has been described by Paulay [2.42] for reinforced concrete frames. The same method may also be applied in the design of steel structures.

(iii) Recommendations for the Redistribution Limit

Limits are required on the amount of redistribution allowed to be used in design to ensure that the resulting ductility demand is not too large. However, the codes and recommendations for redistribution in New Zealand are inconsistent. The suggestions of the present steel design code NZS3404:1977

[2.28], the recommendations of Patton [2.40] in the New Zealand steel structures study group [2.30], and the New Zealand reinforced concrete code NZS3101:1982 [2.7], for ductile reinforced concrete structures are shown in Table 2.1.

Table 2.1 Maximum Reduction of Peak Bending Moment

	Dead, Live and Wind Loading Combinations	Load Combinations Including Earthquake	
		Full Ductility	Limited Ductility
NZS3404:1977	35%	15%	15%
Study Group	0%	30%	15%
NZS3101:1982	30%	30%	30%

The study group for the design of steel structures [2.30] has recommended that the amount of redistribution used is to be a function of the type of loading. It is suggested that the amount of redistribution should not be dependent on the magnitude of the loads, but upon the section category of the member. That is, for non-compact category 3 sections, category 2 sections, and very compact category 1 sections, that redistribution limits of 0%, 15% and 30% respectively should apply. The requirements of each section category are described in section 6.4.4.

(iv) Moment Redistribution in Steel Structures

In many steel moment resisting frames, load cases other than seismic may govern the beam sizes and so redistribution may not be necessary. In steel structures, as in reinforced concrete structures, redistribution will result in a more even and economical steel demand at the cost of a small amount of extra ductility demand.

(c) Column Design

One aim of this project was to determine the likely magnitude of the forces required to design columns in earthquake resistant steel frames. A computer program was used for column design which followed the methods in the draft Australian steel code [2.32]. A column effective length factor of unity was used. The column stiffness, I_c, was taken for the bare steel section. The maximum axial load was checked against the limit obtained from the formulae developed by Lay described in the source book to the Australian steel code [2.43] to ensure that there would be available ductility when yielding occurred at the column ends. An estimate of the distance to the column point of contraflexure is required with this formula. Analyses undertaken by

Tompkins [2.14] indicate that the interstorey height may be a reasonable estimate for the maximum likely distance between the position of greatest column moment and the column point of contraflexure at an instant in time. Column sizes, like beam sizes, were in some cases greater than that required from strength considerations alone because of interstorey drift limitations.

2.7 DYNAMIC MODELLING

A general purpose dynamic analysis computer program, RUAUMOKO [2.37], was used for the dynamic modelling. This program was developed by Sharpe [2.44] and has been extended by Carr [2.37]. Analysis results have been compared against those obtained in DRAIN-2D [2.45] by Goodsir [2.46] and it has been used extensively at the University of Canterbury over the past 15 years. As well as performing dynamic inelastic time history analyses, this program also calculates the natural frequencies of vibration, the damping ratio for each mode, and modal participation factors. Mode shapes may also be computed.

The modelling assumptions used in the static analyses were also used in the dynamic analyses. The effects of material variation and overstrength were not included in the analyses as the member strengths were known, but have taken account of in the suggested design procedures.

Other data required for input into the program RUAUMOKO is described below.

2.7.1 Masses and Loads

In the analyses the loads and masses were computed from the load combination of $D+L_s$. Lumped nodal masses were used, primarily for the sake of simplicity, but were justified as the consistent mass matrix bounds the computed frequencies. The nodal translational masses were found from the nodal loads and the uniformly distributed masses were allocated to the nearest node. The rotational mass was calculated from $\Sigma(wl^3)/105$ for all members framing into the joint, where w is the mass per unit length acting on a member, and l is the member length. This term is the diagonal mass coefficient from the consistent mass matrix for a straight beam segment with a uniformly distributed mass [2.47]. Where no uniformly distributed loads were assumed an arbitrary rotational mass was used. At the ends of the beams the fixed-end moments were calculated as $M_E = wl^2/12$, and the fixed-end shear as $V_E = wl/2$. The value of the acceleration of gravity used was $9.81 m/sec^2$.

2.7.2 Stiffness and Strength

The change in slope of the moment-curvature diagram when there was no axial load was assumed to occur at the plastic felxural strength, M_p which was calculated as SF_y, as shown in Figure 2.9, and the maximum axial load P_y was taken as AF_y. Using the plastic moment rather than the yield moment gives a much better approximation to the behaviour of the members. Because of this, the plastic curvature and displacement are used instead of the yield curvature and displacement in the calculations. The Australian steel code [2.29] axial load-moment interaction diagram shown in Figure 2.3 was used as the member yield interaction surface.

The program RUAUMOKO allows the use of many different hysteresis loops. An elastoplastic hysteresis rule was selected for the beams on the grounds of its computational efficiency, a bilinear rule was used for the columns with a small bilinear factor primarily to reduce errors arising from moment overshoot. The elastoplastic rule was thought to be a reasonable representation of the actual behaviour of the steel provided no strain hardening takes place. Stewart [2.48] has shown that the shape of the hysteresis loop does not have a significant effect on the response of a structure.

2.7.3 Damping

Rayleigh damping [2.25], in which the damping matrix [C] is proportional to a combination of the mass [M] and stiffness [K] matrices, based on 5% of critical damping in the first mode and the mode corresponding to the number of stories was generally used. Care was taken to ensure that all modes were sub-critically damped [2.49].

2.7.4 Dynamic Modelling Assumptions

The horizontal deformations of all nodes on the same floor for the moment resisting frames were coupled to reduce the degrees of freedom of the stiffness matrix and the computational solution time for the structure as a whole.

The P-delta effect was generally taken account of by computing the deformed co-ordinates of the structure under gravity load alone. Thereafter, these coordinates were used. In some cases the deformed coordinates were used

throughout the whole analysis, and in other cases the original coordinates were used. Further discussion of modelling for the P-delta effect is given in section 4.5.

Plastic hinges were assumed to be able to occur only at the ends of the members and a plastic hinge length, L_p, equal to the depth of the member, D, was assumed. The assumed length of the hinge affected the curvature ductility recorded as well as the bilinear stiffness of the member [2.44].

2.7.5 Solution Techniques

In the analyses undertaken, the Newmark constant average acceleration method of integration was used with a timestep, δt, of 0.01 seconds. This timestep corresponded to less than one half of the "n"th mode of vibration for an "n" storey frame and has commonly been used in the past.

Whenever the moment was found to exceed the yield moment, corrections for moment overshoot were made in the following timestep and the stiffness matrix was altered. To ensure numerical stability when overshoot occurred, a rotational nodal mass and a bilinear plastic hinge model was used for the post-elastic column stiffness.

2.7.6 Output

The output contains maximum values of member force, deformation, nodal deflection, ductility, and hinge curvature. This information may also be stored on disk at intervals during the analysis. A post processing program DYNAPLOT [2.50], was used in order to obtain interstorey drifts, plots of hysteretic behaviour, and time history graphs of required parameters.

Curvatures, ϕ, and curvature ductilities were computed at every timestep. The curvature ductility, ϕ/ϕ_p, was calculated as the curvature divided by the plastic curvature, ϕ_p rather than the reduced plastic curvature, ϕ_{pc}. The curvature ductility printed is therefore always a lower limit on the actual curvature ductility. The inelastic hinge rotation, θ_H, was calculated manually after the analysis as $\theta_H = (\phi-\phi_p)\ L_p$, where $\phi_p = M_p/EI$. The member displacement ductilities were approximated from Equation 6.7.

While maximum displacements and forces printed were the maximum from every timestep, other parameters, such as the interstorey displacements and values of moment at certain instants in time were calculated from values recorded

every 10 timesteps, or 0.1 seconds, because of data storage constraints. These may give peak values of response slightly less than the actual values.

2.7.7 Limitations of the study

In this study, biaxial effects, out-of plane action, vertical accelerations and column inelastic axial shortening due to flexural yielding were not modelled. The effects of material strain hardening and material variation were also ignored with the hysteresis type used but have been considered in the design procedure.

2.8 EARTHQUAKE RECORDS

The earthquakes used in this report, and the design recommendations made are for frames situated upon normal soils only. Horizontal ground motions of the following earthquake records were chosen for the analyses:

i) Two artificial earthquakes following the draft loadings code design spectrum [2.2] were generated by the program SIMQKE [2.51].

ii) El Centro May 1940 NS. This earthquake was treated as a benchmark or design level earthquake as it has in the past formed the basis of many seismic codes. In areas of low seismic risk, such as Dunedin, the El Centro record is thought to represent the maximum credible level of seismic excitation.

iii) Parkfield No. 2 June 1966 N65°E. This record has large ground accelerations resulting from the direction of wave propagation causing focussing of energy at the recording station.

iv) Pacoima Dam Feb 1971 S16°E is seen as a maximum credible level record and not a design level excitation. A high level of shaking occurs especially for structures with periods of up to 2 seconds. This was part of the San Fernando earthquake recorded at a rock outcrop near the dam.

As each earthquake has different characteristics it will cause different effects on a particular structure of a given period and hysteretic hinge behaviour. Because of this, several earthquake records are required to evaluate the likely overall performance of a structure. The characteristics and principal data of the selected natural ground motions have been discussed in detail by Tompkins [2.14] and Whittaker et al. [2.52].

The natural ground motions were run for a duration of 14 seconds and the artificial records were run for 20 seconds. A scale factor was used on the two artificial records which was equal to the appropriate zone factor, Z

[2.2]. The zone factor generally used was 0.85 for Wellington. The artificial and El Centro records were thought to represent design level excitations.

The two artificial earthquakes were generated to match the spectra of the draft New Zealand Loadings code [2.2] for hard foundations as shown in Figure 2.5. In order to obtain a reasonable match between these spectra, an earthquake record length of 20 seconds was required. The length of high intensity shaking is therefore significantly higher than that of most natural records where the strongest shaking may last for only a few seconds. Whilst the acceleration response spectra shows the maximum response acceleration and displacement it does not show the number of large displacement cycles of the oscillator. Care must be taken with artificially generated records of long duration especially when cumulative ductility effects are considered.

Input parameters for the records are shown in Appendix 2. Artificial earthquake #1 is shown in Figure 2.10 and its acceleration response spectrum is compared with the target code response spectrum [2.2] in Figure 2.11.

2.9 CHAPTER SUMMARY

In this chapter an introduction to the structural design philosophy of earthquake-resistant frames was described. The method of application of this philosophy in New Zealand as it is applied to reinforced concrete frames is known as "capacity design". Other moment-resisting frame design methods used in New Zealand for gravity dominated frames, elastically responding frames, and an interim method for the design of steel frames were discussed. Some overseas methods suggested for the design of frames overseas were also described. Displacements and interstorey drifts of frames of long period to design level excitations are usually estimated by the equal displacement assumption.

The code requirements for frame design and the assumptions made in the modelling of frames in the later chapters was described. Several different earthquake records were used in the dynamic analyses.

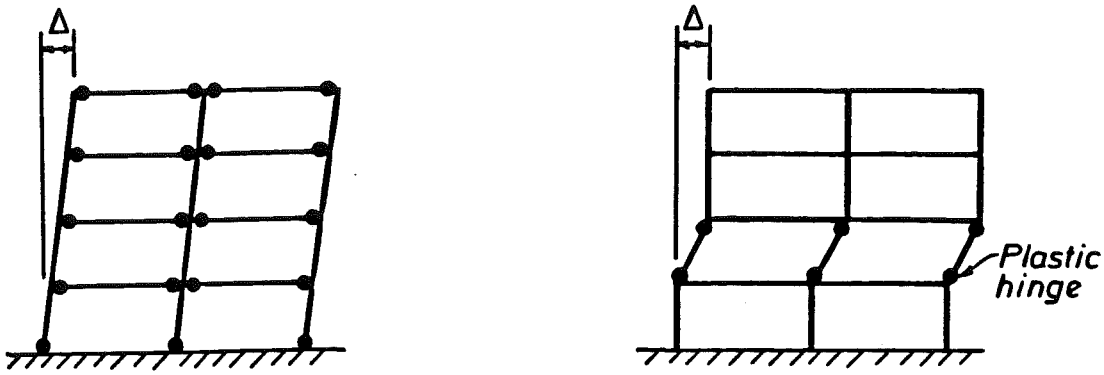

(a)
Strong-column or beam-sidesway mechanism

(b)
Strong-beam or column-sidesway mechanism

Figure 2.1

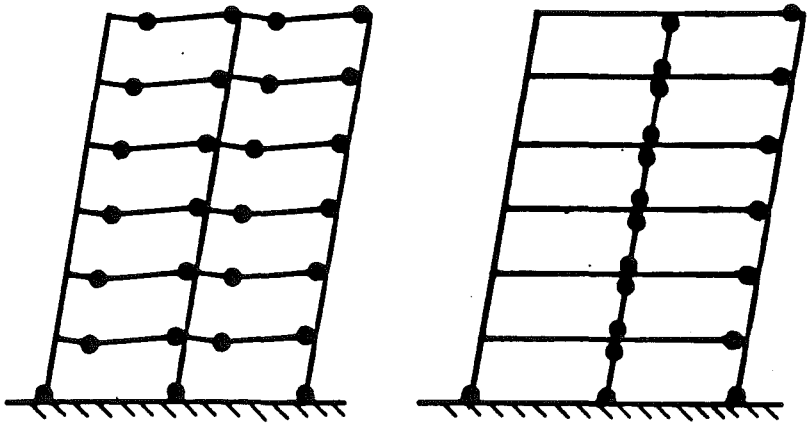

(a) (b)
Hinge patterns in Gravity Dominated Frames
Figure 2.2

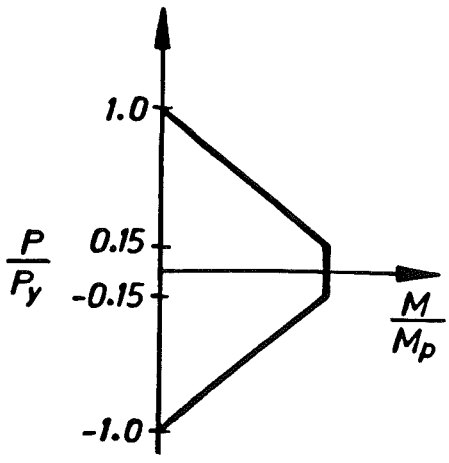

Figure 2.3. Assumed Moment-Axial Load Interaction Diagram for I-Shaped Steel Columns

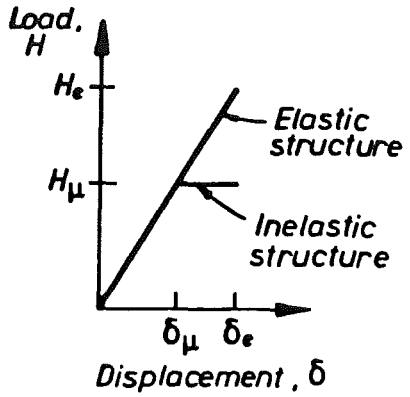

Figure 2.4. Equal Displacement Assumption

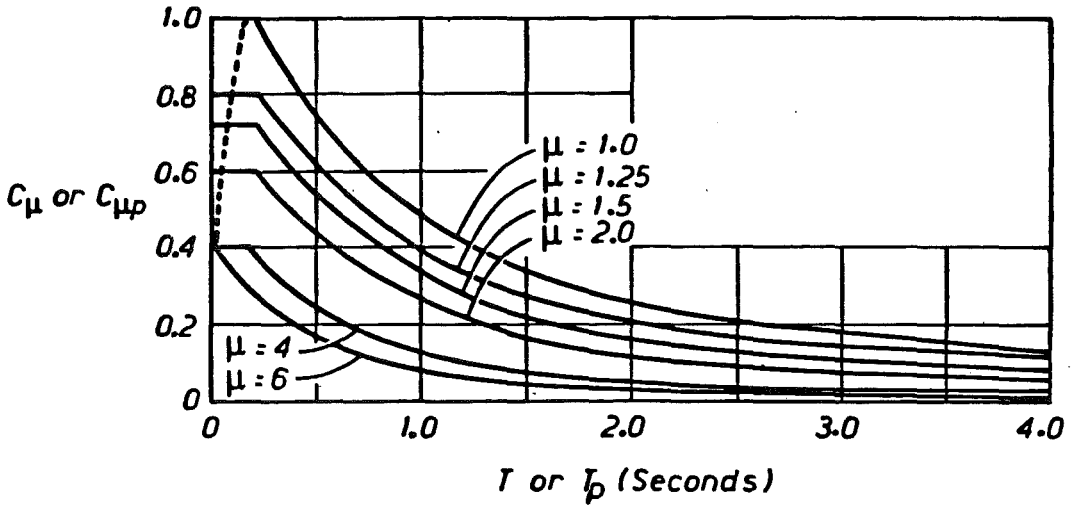

Figure 2.5. Basic Seismic Acceleration Coefficient

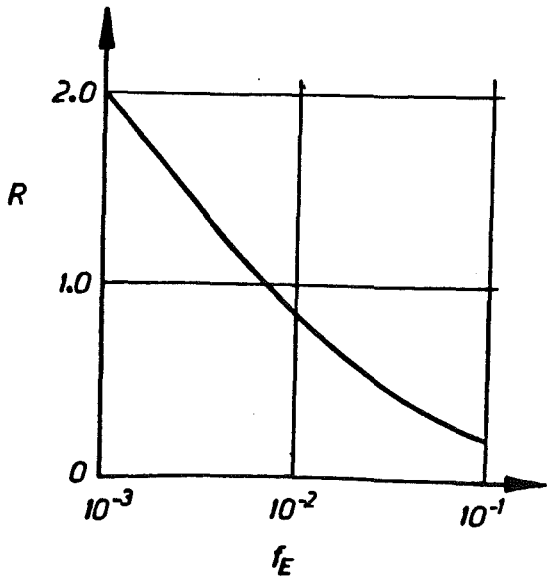

Figure 2.6. Relationship between Risk Factor (R) and Annual Probability of Exceedence (f_E)

ZONE FACTOR FOR MAJOR METROPOLITAN AREAS AND CHATHAM ISLANDS.

		Z
AUCKLAND	: Within boundaries of Auckland Regional Auth.	0.5
HAMILTON	: Within boundaries of Hamilton City Council	0.5
WELLINGTON	: Within boundaries of Wgtn Regional Council	0.85
CHCH	: Within boundaries of ChCh City Council	0.65
DUNEDIN	: Within boundaries of Dunedin City Council	0.4
CHATHAM ISLANDS	:	0.4

Note: Tabulated values take precedence over contours for the areas described.

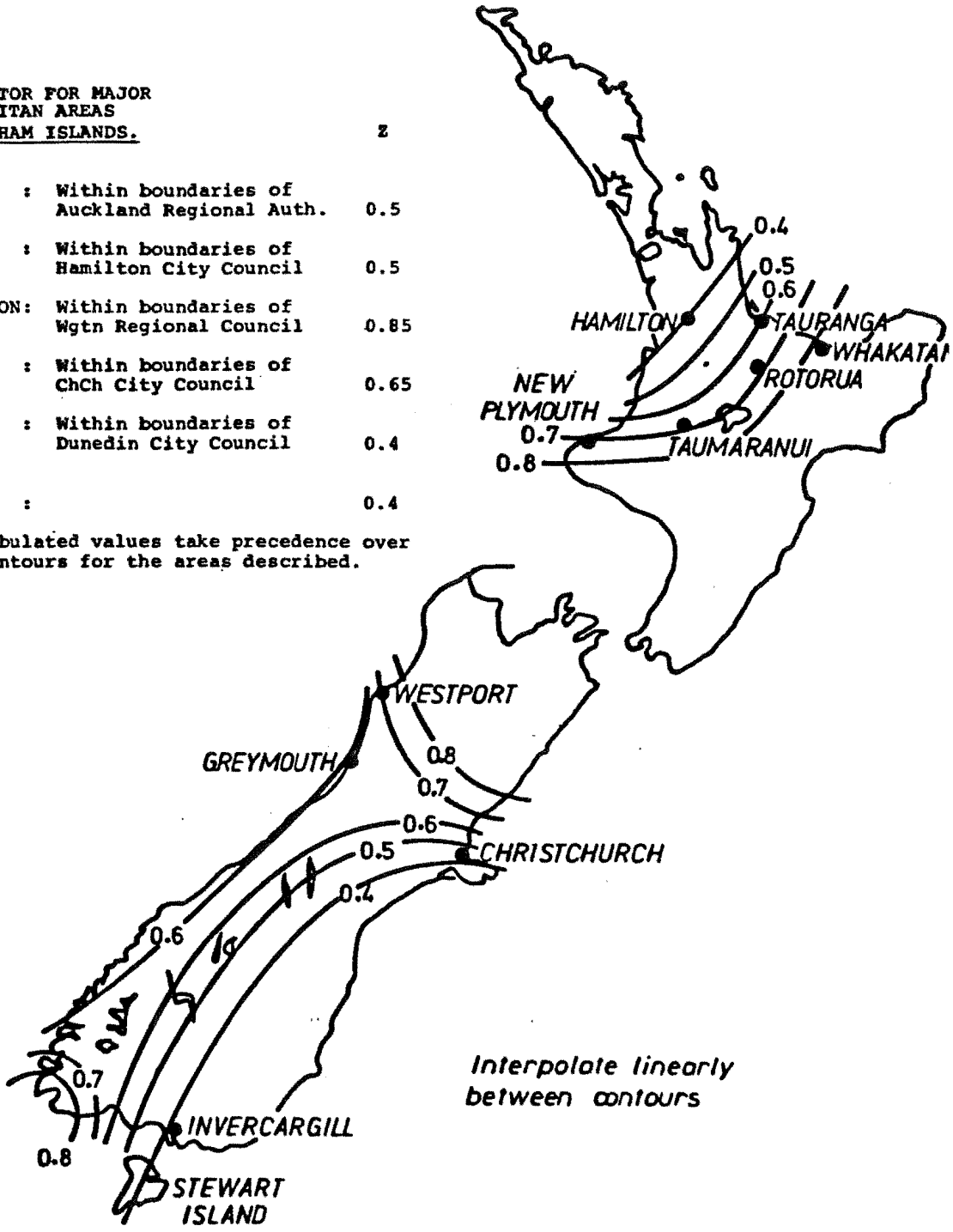

Figure 2.7. Zone Factor (Z)

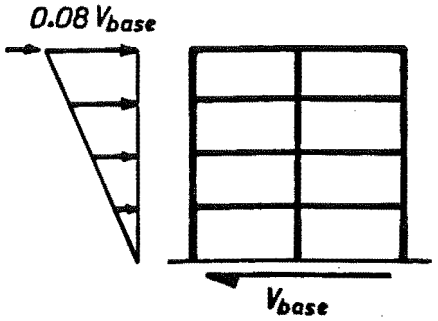

Figure 2.8. Code Static Load Distribution for Long-Period Structures

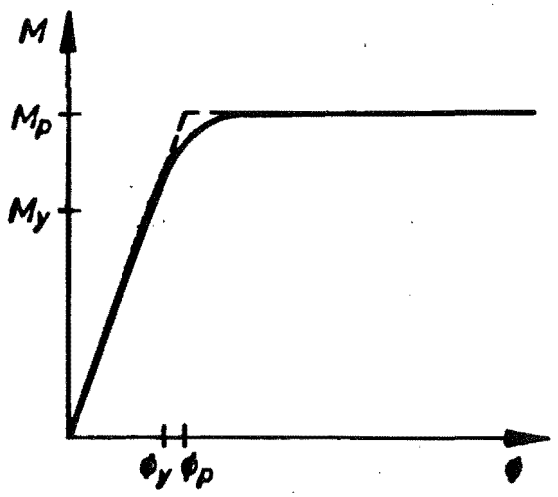

Figure 2.9. Assumed Elasto-plastic Moment-Curvature Relationship of a Steel Member.

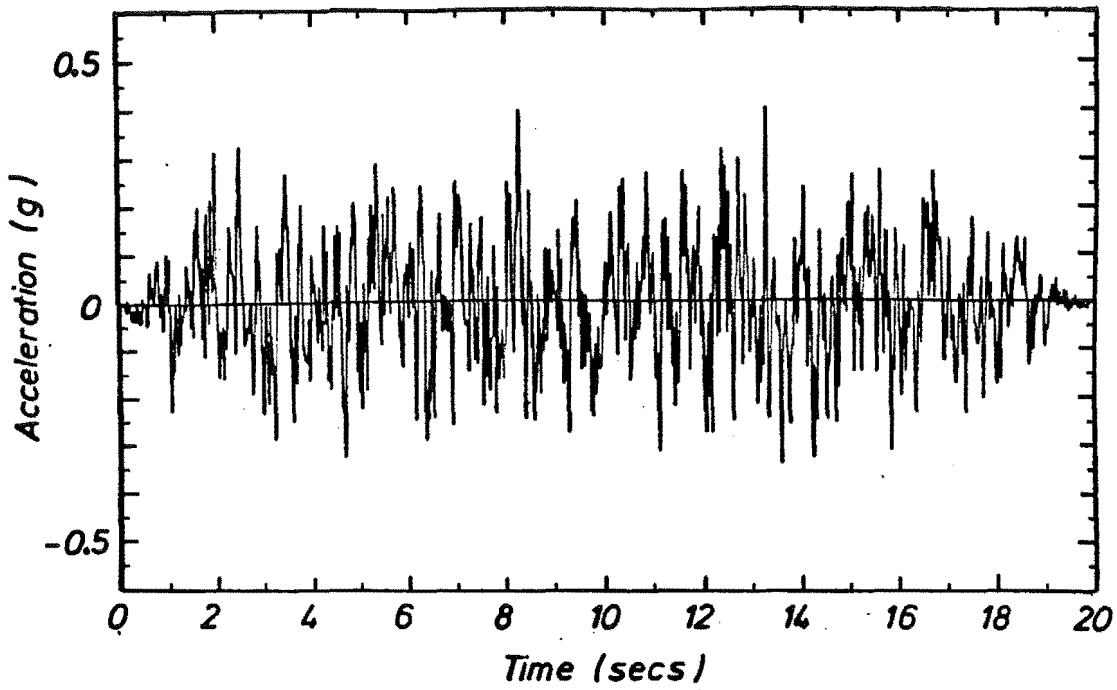

Figure 2.10. Artificial Earthquake #1 -
Ground Acceleration versus Time

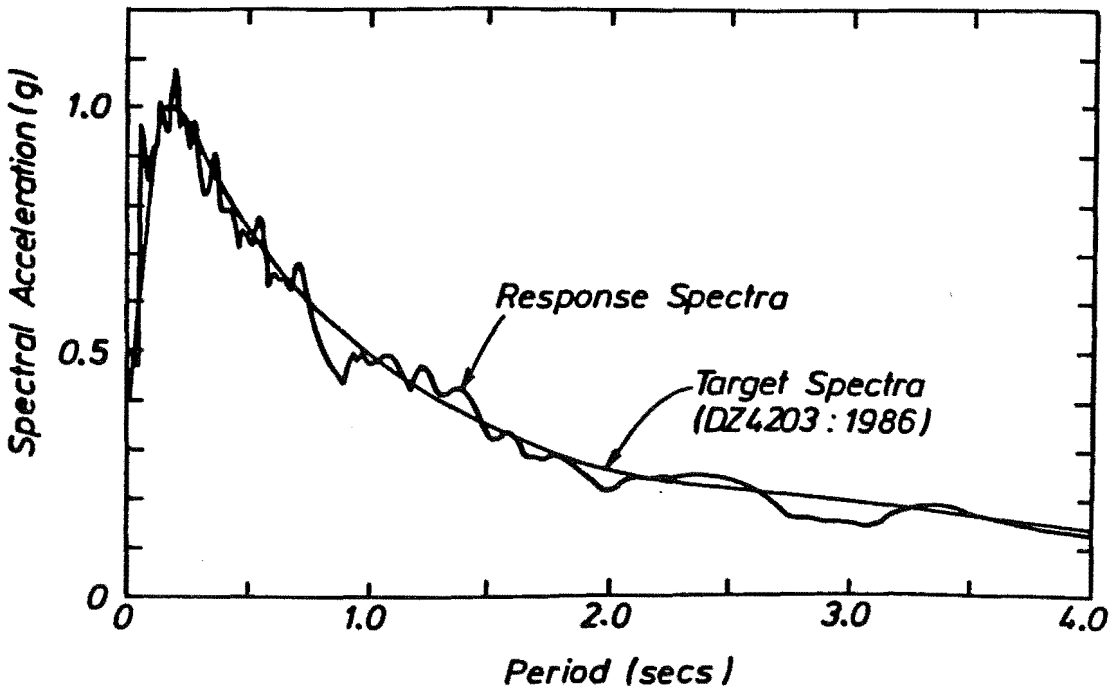

Figure 2.11. Artificial Earthquake #1 -
Comparison of Spectral Acceleration
with Target Spectral Acceleration

2.10 REFERENCES

2.1 Paulay T. 1986. "Structural Walls", Notes for Master of Engineering, Department of Civil Engineering, University of Canterbury.

2.2 SANZ, "General structural design and design loadings for buildings", DZ4203 Draft for comment, New Zealand Standard, 1986.

2.3 Andrews A. L., "Slenderness Effects in Earthquake Resisting Frames", Bull. NZNSEE, Vol. 10, No. 3, Sept 1977, p154-158.

2.4 SANZ, "Commentary: Design of Concrete Structures", NZ3101 Part 2, 1982.

2.5 Paulay T., "Seismic Design in Reinforced Concrete: The State of the Art in New Zealand", Bulletin of the New Zealand National Society for Earthquake Engineering, Vol. 21, No. 3, September 1988, pp208-232.

2.6 Paulay T. "Development in the Design of Ductile Reinforced Concrete Frames", Bulletin of the New Zealand National Society for Earthquake Engineering, Vol. 12, No. 1, pp. 35-48, March 1979.

2.7 SANZ, "Design of Concrete Structures", NZ3101 Part 1, 1982.

2.8 Park R. and Paulay T., "Reinforced Concrete Structures", John Wiley & Sons Inc., 1975.

2.9 Paulay T., "Seismic Design of Ductile Moment-resisting Concrete Frames. Columns - Evaluation of Action", Bulletin of the New Zealand National Society for Earthquake Engineering, Vol. 10, No. 2, Jan. 1977.

2.10 Row D. G., "The Effects of Skew Symmetric Response on Reinforced Concrete Frames", Master of Engineering Report, Department of Civil Engineering, University of Canterbury, 1973.

2.11 Lindup G. P., "Seismic Demands on Columns of Reinforced Concrete Multistorey Frames", Master of Engineering Report, Department of Civil Engineering, University of Canterbury, 1975.

2.12 Kelly T. E., "Some Seismic Design Aspects of Multistorey Concrete Frames", Master of Engineering Report, Department of Civil Engineering, University of Canterbury, 1974.

2.13 Jury R. D., "Seismic Load Demands on Columns of Reinforced Concrete Multistorey Frames", Master of Engineering Report, Department of Civil Engineering, University of Canterbury, 1978.

2.14 Tompkins D. N., "The Seismic Response of Reinforced Concrete Multistorey Frames", Research Report No. 80-5, Department of Civil Engineering, University of Canterbury, 1984.

2.15 Paulay T., "An Application of Capacity Design Philosophy to Gravity Load Dominated Ductile Reinforced Concrete Frames", NZNSEE Vol. 11, No. 1, March 1978, p50-61.

2.16 Fenwick R. C. and Davidson B. J. "Moment-Redistribution in Seismic Resistant Concrete Frames", Pacific Conference on Earthquake Engineering, Wairakei, New Zealand, August 1987, Vol. 1, p95-106.

2.17 Mullaly K. W., "Gravity Dominated Reinforced Concrete Frame Buildings", Master of Engineering Report, Department of Civil Engineering, University of Canterbury, 1986.

2.18 Paulay T., Personal Correspondence, 1987.

2.19 Clifton G. C., "Seismic Design Procedures for Ductile Steel Moment-Resisting and Eccentrically Braced Frames", Pacific Conference on Earthquake Engineering, New Zealand, Vol. 2, pp35-46, 1987.

2.20 Bertero V. V. and Kamil H., "Nonlinear Seismic Design", Can. J. Civ. Eng., Vol. 2, 1975.

2.21 Austin M. A., Pister K. S. and Mahin S. A., "Probabilistic Design of Earthquake-Resistant Structures", *Journal of the Structural Division*, ASCE, Vol. 113, No. 8, August 1987.

2.22 Humar J. L., "Seismic Design of Multstorey Steel-frame Buildings using Dynamic Analysis", Can. J. Civ. Eng., 6, 173-185, 1979.

2.23 -, 1987 Code Change Submittals, UBC, Suggested Revisions to the 1985 Editions of the Uniform Codes. Further Study Items and Submittals for 1987. Building Standards, V. 55, No. 6, Pt 3. Nov-Dec, 1986.

2.24 Popov E. P., Bertero V. V. and Chandramoulli S., "Hysteretic Behaviour of Steel Columns", UCB/EERC 75-11, September 1975.

2.25 Clough R. W. and Penzien J., "Dynamics of Structures", McGraw-Hill, 1982.

2.26 Moss P. J. and Carr A. J. "Seismic Response of Low-Rise Timber Buildings", Pacific Conference on Earthquake Engineering, New Zealand, Vol. 2, pp153-164, 1987.

2.27 SANZ, "General structural design and design loadings for buildings", DZ4203 Draft for comment, New Zealand Standard, 1989.

2.28 SANZ, "Code for Design of Steel Structures (with commentary)", NZS3404, New Zealand Standard, 1977.

2.29 SAA, "SAA Steel Structures Code", Australian Standard AS1250-1981.

2.30 Deliberations of the New Zealand Study Group for the Design of Steel Structures, Bulletin of the New Zealand National Society for Earthquake Engineering, Vol. 18, No. 4, December 1985.

2.31 Walpole W. R. "Draft Strength Method Rules for Structural Steel", Internal Document, Department of Civil Engineering, University of Canterbury, March 1986.

2.32 SAA, "Draft Australian Standard for Comment - Steel Structures", DR 87164, August 1987.

2.33 SANZ, "Code for Design of Steel Structures (with commentary)", NZS3404, New Zealand Standard, 1989.

2.34 Matuscha T., Berryman K. R. et al. "New Zealand Seismic Hazard Analysis", NZNSEE, Vol. 18. No. 4, December 1985, pp313-322.

2.35 Hutchison D. L. et al. "Draft Revision of NZS 4203:1984:Seismic Provisions", NZNSEE, Vol. 19, No. 3, September 1986.

2.36 Park R. et al., "Structures of Limited Ductility", Bulletin of the New Zealand National Society of Earthquake Engineering, Vol. 19, No. 4, December 1986.

2.37 Carr A. J., "RUAUMOKO", Computer Program Library, Department of Civil Engineering, University of Canterbury. May 1986.

2.38 MacRae G. A., "EPF - Two Dimensional Elasto-Plastic Frame Analysis Program". Department of Civil Engineering, University of Canterbury. August 1987.

2.39 Wilson E. L., Hollings J. P., Dovey H. H. and Carr A. J. "ETABS - Three Dimensional Analysis of Building Systems (Extended Version)", Computer Program Library. Department of Civil Engineering, University of Canterbury. August 1981.

2.40 Patton R. N., "Analysis and Design Methods", Section B, Deliberations of the New Zealand Study Group for the Design of Steel Structures, Bulletin of the New Zealand National Society for Earthquake Engineering, Vol. 18, No. 4, December 1985.

2.41 Morrison J., "Design of Continuous Composite Beams for Buildings", Arup Journal, Vol. 9, No. 2, June 1974.

2.42 Paulay T., "Moment Redistribution in Continuous Beams of Earthquake Resistant Multistorey Reinforced Concrete Frames", NZNSEE Vol. 9, No. 4, December 1976, p205-212.

2.43 Lay M. G., "Source Book for the Australian Steel Structures Code AS1250", Australian Institute of Steel Construction, Sydney, 1975.

2.44 Sharpe R. D., "The Seismic Response of Inelastic Structures", Ph.D. Thesis, Department of Civil Engineering, University of Canterbury, 1974.

2.45 Kanaan A. and Powell G. H., "DRAIN-2D, General Purpose Computer Program for Dynamic Response of Plane Structures", Report UCB/EERC 73/6, Earthquake Engineering Research Centre, University of California, Berkeley, 1973.

2.46 Goodsir W. J. et al., "The Design of Coupled Frame-Wall Structures for Seismic Actions", Research Report 85-8, Department of Civil Engineering, University of Canterbury, 1985.

2.47 Archer J. S., "Consistent Mass Matrix for Distributed Mass Systems", *Journal of the Structural Division*, ASCE, Vol. 89, No. ST4, Part 1, August 1963, p161-178.

2.48 Stewart W. G., "The Seismic Design of Plywood Sheathed Shear Walls", Ph.D. Thesis, Department of Civil Engineering, University of Canterbury, 1987.

2.49 Chrisp D. J., "Damping Models for Inelastic Structures", ME Thesis, Department of Civil Engineering, University of Canterbury, 1980.

2.50 Carr A. J., "DYNAPLOT", Computer Program Library. Department of Civil Engineering, University of Canterbury. November 1986.

2.51 MIT and Carr A. J., "SIMQKE : A Program for Artificial Motion Generation", Computer Program Library. Department of Civil Engineering, University of Canterbury. November 1986.

2.52 Whittaker D., Park R. and Carr A. J., "Seismic Performance of Offshore Concrete Gravity Platforms", Research Report 88-1, Department of Civil Engineering, University of Canterbury, January 1988.

Chapter 3

MOMENT-RESISTING STEEL FRAMES

3.1 INTRODUCTION

The benefits of a "capacity design" philosophy for reinforced concrete frames have been expounded in the previous chapter. In this chapter, the aim was to develop a procedure based on the same philosophy for moment-resisting steel frames. It was hoped to produce a design procedure in which undesirable frame mechanisms should be discouraged, as they may lead to excessive ductility demands causing failure and collapse. This procedure was to be simple, rational and not overly conservative.

The behaviour of steel ductile moment-resisting frames (DMRF's) is discussed, the approach and problems encountered in developing design procedures are explained, and finally design recommendations are made. Because most of the frames behaved in a similar manner, only the results of a few frames are described here in order to illustrate the behaviour.

3.2 HISTORICAL BACKGROUND

In the 1950's buildings in New Zealand were designed directly from the forces obtained by the equivalent lateral force method. Reinforced concrete frames tended to be built more frequently than steel frames because, after the Second World War, labour was cheap and the cost of importing steel sections was expensive. Several important steel framed structures were built, such as Aurora house in Wellington, which has a moment resisting steel frame and at the time of completion had more floor area than any other building in New Zealand. The 26 storey Wellington BNZ building was started in 1973 but construction was not completed until 1984, taking over two times the expected construction time, and costing almost three times the originally estimated price because of a long list of problems including contractors' disputes and union labour disputes [3.1]. The possibility of similar union action on further steel buildings, especially where on site welding was required, virtually halted the construction of steel framed office buildings in New Zealand until the mid 1980's.

While steel members were regarded as being naturally ductile this was certainly not the case with reinforced concrete members. The challenge of making these members ductile dominated New Zealand structural research and caused confidence to be gained in reinforced concrete by the building

industry. The accepted method of designing multistorey frames in New Zealand resulting from this research became based on what is known as the "CAPACITY DESIGN" philosophy. This method was developed into design methods by Paulay [3.2], and now a forms a part of the commentary to the New Zealand code for reinforced concrete structures [3.3]. The rational basis of these methods has permeated the thoughts of New Zealand engineers to the extent that non-capacity design methods are treated with suspicion for tall multistorey framed structures.

Unfortunately, a similar method for the design of steel frames was not developed at the same time and the reinforced concrete DMRF design methods were not appropriate for steel DMRF's. However, the New Zealand steel code [3.4] stated that "All structures except small buildings of limited ductility ... shall be designed taking into account capacity design ..". The definition of capacity design was that given in the reinforced concrete code [3.3], which is repeated in the glossary of this report. "Capacity design" was therefore required, yet no suitable static based method for steel structures had been written or developed. If designers had ignored the "capacity design" requirements and designed their buildings by "strength design" as was done overseas, they would have found that the code provisions for inelastic column design were very confusing. The only way of being reasonably sure that no hinging would not occur was to use the reinforced concrete "capacity design" methods which were excessively conservative, or to run dynamic inelastic time-history analyses for every building designed. To analyse frames dynamically was expensive and there was no guarantee that the earthquake records used were appropriate. This proved to be another major disincentive for the design of steel-framed buildings. The design profession in New Zealand therefore tended to use reinforced concrete frames instead of steel frames for office buildings.

In engineering education, the lack of a "capacity design" procedure for steel frames meant that the academics instructing in steel design could suggest either an overseas approach, for which there was no guarantee against undesirable frame behaviour, or to suggest the use of the reinforced concrete procedure.

The New Zealand Heavy Engineering Research Association (HERA), was established in 1978 with its prime objectives being to promote, supervise and conduct research and scientific work in connection with heavy engineering. Since its establishment, HERA has promoted the use of steel as a structural material in New Zealand. With the advent of shop welding and site bolting fabrication techniques, steel construction has moved forward,

particularly in Auckland where the seismic design forces are lower and economical section sizes may be obtained from the elastic design level earthquake. Other buildings were constructed which used a steel frame with pinned-type connections at the expected points of contraflexure in the beam from gravity loading alone. This frame was designed to carry gravity load only, while reinforced concrete shear walls were to resist the lateral load.

Overseas, codes generally used the lateral force or modal analysis methods for determination of the elastic level member forces. These forces were reduced to allow for ductility. The first attempt of codification of a "capacity design" method for steel frames found by the author was in late 1986 [3.5]. This method was only for columns in which the axial load ratio, P/P_y, was greater than 0.40. Realistic methods of determining the expected column axial loads were also made.

The shortage of information about steel framed structures in New Zealand was widely appreciated, and a study group was set up by the New Zealand Earthquake Engineering society in 1984 to collect the latest and most relevant material for steel members subjected to an earthquake-induced loading. This was so that recommendations for design could be made and the information could be used as a resource for future steel codes. It also was used to correct some of the interaction formulae in the New Zealand Steel Structures Code [3.4]. The deliberations of this group were published in December 1985 [3.6].

At the beginning of 1986, this project was started with one of its objectives being to study the behaviour of moment-resisting frames from the point of view of ensuring that only "desirable" types of mechanism occurred, and that ductility demand would not be too high. It was hoped that a "capacity design" type of method would be proposed for steel ductile moment-resisting frames (DMRF's) similar to that applied to reinforced concrete DMRF's which would reflect the differences between steel and reinforced concrete frames but provide a similar degree of protection.

Design philosophies used for frames developed in New Zealand have tended to be reasonably rational [3.7] reflecting the degree of uncertainty estimating the seismic induced forces, the physical frame parameters (such as the frame strength, loading and stiffness), and the current understanding of the seismic response of frames. This has resulted in design methods which are conservative, but in which desirable seismic response is almost certain, even during large earthquakes. However, as understanding of structural seismic response increases, conservatism in design procedures is able to be

reduced. It is anticipated that the design methods developed in this report may still be slightly conservative and that further refinement may be desirable.

3.3 MECHANISMS IN STEEL STRUCTURES

Many energy dissipating mechanisms are possible in steel ductile moment-resisting frames. In this report it is assumed that connections are provided with enough strength so that they do not yield and that the majority of the energy dissipated is not in the panel zones. Only mechanisms involving beam and column hinging are considered to occur.

The most desirable mechanism in a steel moment-resisting frame, is the beam-sidesway mechanism shown in Figure 2.1a which is predominantly a first mode response with hinging occurring in the beams and in the columns at the base of the frame. It is desirable because many hinges will form in the beams thereby absorbing a large amount of energy. The member ductility demands found from analyses of frames behaving in this manner are generally smaller than from other mechanisms.

The soft-storey (or column-sidesway) mechanism shown in Figure 2.1b is of concern in steel frames as it is in reinforced concrete frames because excessive ductility demand may occur with only a small amount of energy dissipation possibly leading to a catastrophic collapse and loss of life. This kind of mechanism is to be discouraged. One other type of possible mechanism is the partial sidesway mechanism, which is a combination of both beam and column sidesway, and is shown in Figure 3.1. Martinez-Romero [3.8], in a report about the behaviour of buildings in the 1985 Mexico City earthquake, found that 40% of the collapses involved an intermediate storey failure, 38% involved an upper storey failure, and 8% involved a weak first storey. Although many of these failures may be attributed to poor detailing, fabrication and quality control, the fact that so many occurred show that it is prudent to consider the possibility of a storey mechanism in structural design.

3.4 TRIAL DESIGN METHOD #1 : Reinforced Concrete Capacity Design Procedure

The reinforced concrete capacity design procedure was applied to steel frames designed to the loads described in section 2.6. Excessively conservative column sizes resulted because of the difference between the behaviour of reinforced concrete and steel moment-resisting frames.

Differences in the behaviour of steel and reinforced concrete members may cause limit states other than earthquake to govern the member sizes in steel frames.

3.4.1 Member Differences

The differences between reinforced concrete members and steel members are:

1) the ratio of the strength to stiffness of steel members is very high compared to other commonly used structural materials. For example, the strength to stiffness ratio of a steel beam is typically 3 to 4 times that of a reinforced concrete T-beam of the same depth. This means that longer spans may be used,

2) the moment capacity of a bare steel section is usually uniform along the member length and cannot be varied easily to match the required strength so the overstrength beam moment applied to a column using the reinforced concrete capacity design procedure is fixed. However, the reinforced concrete code [3.4] allows the positive beam flexural strength to be as small as one half of the negative beam flexural strength by curtailing the reinforcing steel in the beams away from the joint,

3) the high gravity moments acting on bare steel beams having a large span may cause hinging away from the member ends as shown in Figure 2.2a. This may be avoided in reinforced concrete frames by selective curtailing of the reinforcing steel. Composite design may be used to a limited extent in a similar way for steel beams,

4) for compact steel sections large curvature ductility capacities are generally available without special detailing. As steel columns are generally able to sustain some inelastic rotation, it is unnecessary to eliminate all plastic hinging in the columns. Reinforced concrete columns may require special detailing to obtain reasonable ductilities, and

5) some ductility is available in both column shear and panel zone deformation in steel members. The panel zones may be designed to dissipate reasonably large amounts of energy. This is not done in reinforced concrete joints.

3.4.2 Limit State Sizing Differences

Because of the material differences between steel and reinforced concrete members, it was found that if the reinforced concrete "capacity design" philosophy was applied to steel frames, the required column sizes are very large. While many reinforced concrete moment-resisting frames are earthquake dominated, (that is, the gravity moments may be redistributed out and earthquake moments alone govern the size of the beams), member sizes in steel frames may be controlled by a combination of other limit states such as those described below.

3.4.2.1 Gravity Dominated Frames

The ratio of beam gravity moments to seismic-induced moments is often considerably greater in a steel frame than in a reinforced concrete frame because the relatively long spans, and the small stiffness-to-strength ratio of steel beams when compared to reinforced concrete beams. This causes steel frames to be much more flexible than reinforced concrete frames having a longer period of vibration and lower seismic forces if the acceleration response spectra follows the shape of most hard-ground design spectra. Gravity moments are often large enough that the seismic moments alone do not govern the beam size even when redistribution is used.

The effect of the large gravity loading may be seen in the first-half cycle of loading in the gravity dominated subassemblage shown in Figure 3.2. As the level of seismic-induced loading increases, yielding will first occur in the beam at the end with negative seismic moment. At the "positive seismic moment" end, the gravity moment, which is negative, will act in opposition to the seismic moment. The effect of seismic moment is initially to reduce the total moment at that end. If the seismic moment is large enough, yielding in the "positive" direction may then occur at, or near the "positive seismic moment" end of the beam. Depending on the magnitude of the seismic load, the formation of a hinge at the "positive seismic moment" end of the beam may be suppressed. Curvature ductility demand will be greatest at the "negative seismic moment" end of the beam.

3.4.2.2 Drift Governed Frames

The result of the high stiffness-to-strength ratio of the members is that the strength requirements of a ductile steel frame are often satisfied if the stiffness of the frame is within the limits of the draft loadings code

[3.9]. This causes frames to be stronger than required by the code and ductility demands to be lower.

3.4.2.3 Displacement Controlled

When the frame is connected to a stiffer structure which takes the majority of the seismic loading, the displacements of the moment resisting frame are controlled by the stiffer structure.

3.4.2.4 Other Limit States

Member sizes may also be controlled by other limit states such as wind or serviceability considerations in order to keep service vibrations to a minimum.

3.4.3 Inapplicability of Reinforced Concrete Procedure to Steel Frames

In the reinforced concrete "capacity design" method, the column is designed for moments resulting from the sum of the magnified beam overstrength moments at a joint in order to reduce the possibility of column hinging. This method is inappropriate for steel frames for the following reasons,

i) The beam size is generally larger than what would be required if the frame were earthquake-dominated, resulting in large column sizes,

ii) Because many frames are gravity-dominated, the beam framing in on one side of the column which is subject to positive seismic moment may not come close to yielding, therefore, the application of the beam overstrength moments from both sides of the column will be overly cautious, also resulting in large column sizes, and

iii) As columns possess some ductility and there is no reason why all hinging should be totally discouraged during an extreme earthquake.

For these reasons given above column strengths may therefore be significantly smaller than those obtained with the reinforced concrete "capacity design" philosophy without any decrease in the seismic performance.

The reinforced concrete "capacity design" type of formulation, or even an adaption of it is inappropriate, because limit states other than earthquake may govern the sizes of members and the member behaviour is such that

limited column hinging will not present any problems. The rigid application of the "capacity design" procedure results in excessively conservative column sizes.

Because of these differences it was necessary to develop for steel moment-resisting frames a new methodology to remove the excessive conservatisms which occur when the reinforced concrete "capacity design" procedure is applied to these structures, and yet retain the same margin of safety afforded by reinforced concrete frames if subjected to the same level of seismic excitation.

3.5 TRIAL DESIGN METHOD #2 : Stiffening of Capacity Designed Frames

Before being fully aware of the aforementioned differences in the behaviour of reinforced concrete and steel frames, a method of capacity design was attempted. The frame was to be designed initially by the reinforced concrete "capacity design" procedure with the drift limits ignored. The frames were then to be stiffened with a beam-to-column stiffening ratio which would allow, but not encourage column hinging.

The method proved to be totally unsatisfactory as the preliminary sizes required for strength were small due to the low seismic forces resulting from the long first mode period of the structure. At this stage in the process, a designer would have no feel of what the final member sizes should be. When the frame was stiffened up the seismic forces became higher so another check was therefore required to check that the implicit design level ductility was not too high. The applicability of the reinforced concrete capacity design procedure for steel framed structures was still uncertain. For these reasons this method was not used.

3.6 BEHAVIOUR OF A STEEL FRAME

3.6.1 Frame Type and Period

In order to understand the behaviour of steel moment-resisting frames, the six storey three bay frame, hereafter referred to as Frame #1, shown in Figure 3.3.1 was analysed. This frame was designed to the loadings code [3.9] drift limits and the columns were made stronger than the beams. Limited ductility design was used with an elastic load reduction factor of 3. The same column size was used throughout each level. The loads and input data for RUAUMOKO [3.10] for all frames in this report are given in Appendix 3. The first mode response period was calculated by Rayleighs method [3.9]

as 1.62 seconds. This was confirmed by modal analysis in RUAUMOKO in which the period was also computed as 1.62 seconds, however, as the stiffness of the columns of the frame was altered to allow for gravity loading, the first mode response period calculated by RUAUMOKO increased to 1.66 seconds. The frame was analysed both with and without slaving of the horizontal degrees of freedom of the nodes on each level, and the period and response were found in each case to be almost identical.

3.6.2 Hinge formation

It may be seen from the pattern of hinge formation during the El Centro excitation shown in Figure 3.3.2 that beam hinges tended to form in groups which moved up and down the structure. This was thought to have been caused by the higher mode effects. Hinging occurred only at one end of the beam at a time because of the effect of gravity loads.

During more severe excitation, caused by the Pacoima Dam and Parkfield records, more hinges tended to form. At one stage, shown in Figure 3.3.3, almost a complete beam-sidesway mechanism had formed during the Pacoima ground motion with both ends of the beams yielding. Limited column hinging at the base of the structure and also above the base occurred at different intervals during the analysis.

At 8.10 seconds through the artificial earthquake #1 excitation, EQ/ART1, a beam hinged at one end while the other beams on the same level hinged at the other ends of their bays as is seen in Figure 3.3.3. In this case the negative gravity moment and the positive gravity moment at one end of the beam sum to a greater absolute magnitude than the negative gravity moment and negative gravity moment at the other end of the beam. This is caused by a "shakedown" of the gravity moments at the ends of the beams which is discussed in section 3.11.

3.6.3 Ductility Demand

The beam and column curvature ductility demands under the various earthquakes are shown in Figure 3.3.4 at the different levels. It may be seen that beam ductility demand is spread over the height of the structure. The maximum ductility demands for the different ground motions are given in Table 3.1.

The displacement ductility, $\mu \approx (\phi/\phi_p + 1)/2$, according to Equation 6.8. The maximum beam displacement ductility demand, δ/δ_p, from Table 3.1 will

therefore be approximately 3 during a design level earthquake, and around 8 for the Pacoima and Parkfield records. Very little column yielding occurred during the design level earthquakes and a maximum column displacement ductility, δ/δ_p of about 3 to 4 may be demanded during the Parkfield excitation because yielding occurred only at the ground floor level and the ratio of L_c/L_p would be greater than that assumed in Equation 6.8. The hysteresis of the column hinging during the Parkfield excitation is shown in Figure 3.3.5. It may be seen that very little load reversal occurred. The curvature ductility obtained from this graph represents the true curvature ductility, ϕ/ϕ_{pc}, which is greater that the curvature ductility in which axial load is ignored, ϕ/ϕ_p, obtained from the output of RUAUMOKO [3.10]. Galambos and Lay [3.11] have shown that beams satisfying the New Zealand limited ductility section slenderness requirements should be able to sustain strains of at least 3.5% under monotonic loading before local buckling occurs and that the strength degrades slowly after the occurrence of local buckling. It is therefore thought by the present writer that members detailed to sustain limited ductility demand with the present New Zealand detailing requirements would all be able to sustain the curvature ductility of 14 which is equivalent to a plastic rotation, θ_R, of 3.1% and that collapse would not necessarily occur even under the Pacoima excitation.

Table 3.1 Maximum Curvature Ductilities

Earthquake Record	Beam Curvature Ductility (ϕ_{max}/ϕ_p)	Column Curvature Ductility (ϕ_{max}/ϕ_p)
Eq/Art1	5.2	1.6
Eq/Art2	6.5	1.1
El Centro	5.6	-
Parkfield	12.3	7.9
Pacoima	14.1	5.0

The ends of each beam tended to yield mainly in either positive or negative flexure rather than equally in each direction during the El Centro excitation. as shown in the pattern of hinge formation in Figure 3.3.2. A moment-curvature hysteresis diagram for end-one of beam member 28, the left-hand-side of the second floor beam on the left-hand bay, is shown in Figure 3.3.6 during the El Centro excitation. It deformed inelastically only in negative flexure and each time it yielded, the negative curvature ductility accumulated. In the time-history of the moment shown in Figure 3.3.7 the reason for this yielding occurring may be observed. Before the shaking started there was an initial moment on the beam caused by gravity load. This encouraged yielding to occur first when the gravity moment and the seismic

moment were of the same sign. It may also be seen in this figure that the peak moment may last for a very short time, sometimes less than 0.10 seconds.

3.6.4 Fundamental Response

The displacement of the top of the structure varying with time is shown in Figure 3.3.8 for several different earthquakes. It may be seen that the top of the structure moves with a response period approximately equal to the natural period of 1.66 seconds even though the structure has become inelastic. Higher modes cause this response to vary slightly.

3.6.5 Comparison between the different types of P-delta Analysis

To gauge the effect of the way in which the P-delta effect should be considered in the frame, analyses were carried out in which

i) the P-delta effect was totally ignored,

ii) the column geometric stiffnesses were recalculated and updated at each timestep throughout the analysis, and

iii) the deformed frame co-ordinates were calculated after the static analysis and the column geometric stiffnesses were updated for the axial forces due to gravity loading only.

Further discussion of these analysis types is given in Chapter 4.

The difference between the maximum displacements for the frame subjected to the El Centro record analysed with different types of P-delta analysis is shown in Figure 3.3.9. It was observed that these maximum displacements occurred at approximately the same time in all of the analyses, and it may be seen from the diagrams that the maximum values are very similar. It was decided to analyse most other frames by updating the co-ordinates and column geometric stiffnesses at the beginning of the analysis only.

3.6.6 Interstorey Drift Envelopes

Interstorey drift envelopes for the different earthquake records and the expected design level interstorey drift calculated by the equal displacement assumption are shown in Figure 3.3.10. In this figure it may be seen that the design level drift is a conservative estimate of the drifts obtained from design level earthquakes but is exceeded by Parkfield and Pacoima excitations.

3.6.7 Structure Deflected Shape

The deflected shape envelope and the deflected shape of the structure at different time intervals for the different excitations is shown in Figure 3.3.11. The shape predicted in the design stage making use of the equal displacement assumption is also shown in this figure. The deformed shape of a structure at an instant during an earthquake may be similar to the envelope of the deflected shapes. Only Parkfield and Pacoima earthquakes exceed the predicted design level displacement.

3.6.8 Magnification of Column Actions

The magnification of the column moments and shears above the values found from the static overstrength distribution are shown in Figure 3.3.12 and Figure 3.3.13 respectively. These have been calculated only for the exterior columns as the static overstrength beam moments are not always reached simultaneously at both sides of the interior columns during the design level earthquake. Enhancement of moment on an interior column may be caused by the beams resisting higher forces than the design level or because of higher mode effects.

The column bending moment magnification factor, w_b, was calculated as

$$w_b = \frac{M_{c,max}}{M_{stat,os}} \qquad \text{Equation 3.1a}$$

where $M_{c,max}$ is the maximum column moment found from dynamic analysis either above or below the joint, whichever is being considered, and $M_{stat,os}$ is the static overstrength moment. The static overstrength moment is given in the reinforced concrete code as

$$M_{stat,os} = \phi_{ob}\, M_{c,code} \qquad \text{Equation 3.1b}$$

where $M_{c,code}$ is the maximum column moment from above or below the joint, which is found from the static earthquake loading alone.

$$\phi_{ob} = \frac{\phi_o\, \Sigma M_{pb}}{\Sigma M_{b,code}} \qquad \text{Equation 3.1c}$$

M_{pb} is the ideal strength of the actual beam used. At any joint the column moments from the earthquake load case should equal those in the beams, so $\Sigma M_{c,code} = \Sigma M_{b,code}$, so

$$M_{stat,os} = \phi_o\, \Sigma M_{pb}\, \frac{M_{c,code}}{\Sigma M_{c,code}} \qquad \text{Equation 3.2}$$

In Equation 3.2 the static overstrength moment may be envisaged easily as the overstrength beam moment, $\phi_o M_{pb}$, distributed above and below the joint in proportion to the moments found from the static earthquake loading alone.

For an exterior column, $\Sigma M_{pb} = M_{pb}$ and $M_{b,code} = \Sigma M_{b,code}$. The strengths of the members analysed were known so the material overstrength factor, ϕ_o, was taken as 1.0 giving Equation 3.3.

$$M_{stat,os} = M_{pb} \frac{M_{c,code}}{\Sigma M_{c,code}} \qquad \text{Equation 3.3}$$

The maximum beam moments are compared with the column static overstrength moments and those from the earthquakes in Table 3.2. The dynamic magnification factors in this table are calculated as the maximum moment at a joint divided by the maximum joint overstrength moment as this is what is considered in design. Lines were drawn between the peak moments in Figure 3.3.12 to show which earthquake caused the response but the slope of these lines do not give the column shear as the peak moments at the ends of the columns may have occurred at different times.

The column shear magnification factor was calculated as

$$w_v = \frac{V_{c,max}}{V_{stat,os}} \qquad \text{Equation 3.4a}$$

where $$V_{stat,os} = (M_{stat,os,t} + M_{stat,os,b})/L_c \qquad \text{Equation 3.4b}$$

and the subscripts $,b$ and $,t$ relate to the moments on the column at the joints at the bottom and top of the column in respectively and L_c is the clear length of that column. The overstrength column shear and the shears obtained from the analyses, with the shear dynamic magnification factors are shown in Table 3.3.

It may be seen that the maximum values of dynamic magnification of moment are greater toward the base of the frame. The shear dynamic magnification factor seems to be approximately constant over the height of the frame but is less than the maximum values of moment magnification obtained. These results agree with those obtained by Jury [3.12] and those presented in the reinforced concrete code commentary [3.3] in which the moment dynamic magnification factor may be as large as 1.90, but the shear dynamic magnification factor was assumed to be not greater than 1.20. The dynamic magnification factor for shear was generally around 1.20, however, analyses of other frames have shown that shear magnification factors of up to 1.40 are not uncommon.

Table 3.2
Frame #1. Exterior Column Moment Dynamic Magnification Factors

P-delta flag = 2 (No P-delta considered after analysis started)

Level	O/Strength Moment	EQ/ART1		El Centro		Parkfield		Pacoima	
		Moment	Mom Mag	Moment	Mom Mag	Moment	Mom Mag	Moment	Mom Mag
6	262	212	.81	207	.79	237	.90	258	.98
	42	155		164		179		238	
5	220	192	.87	211	.96	254	1.15	296	1.35
	86	178		179		248		248	
4	176	205	1.16	170	1.02	248	1.41	318	1.81
	128	203		240		274		271	
3	170	235	1.38	224	1.41	287	1.69	317	1.86
	141	200		226		300		351	
2	157	244	1.55	260	1.66	371	2.36	355	2.26
	206	250		223		393		501	
1	92	177	1.21	159	1.08	227	1.91	304	2.43
	-	561		438		579		577	

Table 3.3
Frame #1. Exterior Column Shear Dynamic Magnification Factors

P-delta flag = 2 (No P-delta considered after analysis started)

Level	O/Strength Shear	EQ/ART1		El Centro		Parkfield		Pacoima	
		Shear	Sh Mag	Shear	Sh Mag	Shear	Sh Mag	Shear	Sh Mag
5-6	87	104	1.20	106	1.22	112	1.29	132	1.52
4-5	87	95	1.09	103	1.18	118	1.36	141	1.62
3-4	87	106	1.22	103	1.18	118	1.36	140	1.61
2-3	89	106	1.19	97	1.09	127	1.43	149	1.67
1-2	104	129	1.24	121	1.16	135	1.30	148	1.42
-		200		163		230		237	

Distributions of column bending moments are shown at different intervals during the Parkfield and Pacoima excitations in Figure 3.3.14. It may be seen that these distributions differ from the static distribution and in some cases cause high shears or high moments. At some instances of time there is no point of contraflexure in the column. Tompkins [3.13] has suggested that when design is being carried out for the maximum moment at one end of a column, the most critical moment at the other end of the column should be taken as zero. The column is therefore considered to be bending in single curvature. This recommendation seems reasonable for the analyses undertaken. The moments at each end of the column must be known in order to find the most critical end-moment ratio, β, for the purposes of buckling and for ensuring that column ductility capacity will be available at the ends of the member.

3.6.9 Base Shear and Centre of Force Distribution

The maximum base shear which occurred during the different earthquake records is shown in Table 3.4. The design level base shear which was calculated using a force reduction factor, μ, of 3 was 358 kN.

Table 3.4
Maximum Frame Base Shear

Earthquake Record	Base Shear (kN)
Eq/Art1	793
Eq/Art2	678
El Centro	667
Parkfield	888
Pacoima	886

The maximum base shear for the frame assuming a triangular load distribution may be found from Figure 3.3.15. It may be seen that if a beam-sidesway mechanism occurs, the base shear $V_b = \Sigma F_i$. Moment equilibrium at the base of the structure must be satisfied, so

$$\Sigma F_i h_i = P\ 3L + 4M_{pc} \qquad \text{Equation 3.5}$$

If the code lateral force distribution is used, the centre of the lateral force distribution will act at 0.744H for a six storey frame, therefore the base shear, V_b is given as:

$$V_b = \Sigma F_i = (P\ 3L + 4M_{pc})/(0.744H) \qquad \text{Equation 3.6}$$

where

$$P = \Sigma V_b = 2\ \Sigma M_p/L = 2/7\ (298*3 + 262*3) = 480\ kN$$

The average column axial load ratio was 0.228 at the base of the structure causing an average column plastic moment reduced by axial load, M_{pc}, of 524 kNm there. The value of base shear may therefore be calculated as:

$$V_b = (P\ 3L + 4M_{pc})/(0.744H) = (480*3*7 + 4*524)/(0.744*21) = 779\ kN$$

This is equivalent to designing for a frame force reduction factor, μ, of 1.38. Because the base shear forces obtained by the Pacoima and Parkfield excitations are greater than 779 kN without a full mechanism being formed, it indicates that the centre of the load distribution must have been lower than that assumed in the code lateral load distribution.

3.6.10 Axial Load Effects

3.6.10.1 Maximum Column Axial Load

In the interior columns at the base of the building the axial load varied from 1242kN to 1306kN during the El Centro excitation while the gravity load was 1270kN. This variation in the axial load of this internal column was small because the seismic shears either side of the joint almost cancelled each other out as may be seen in Figure 3.2b.

In the exterior columns, the seismic-induced axial load may form a high percentage of the total axial load. A comparison of the axial loads in the outer columns during different earthquakes is given in Table 3.5 and Figure 3.3.16. In this table, the "Gravity" row was calculated as the sum of the fixed end gravity shears plus the sum of the nodal loads above the level considered, and the "Maximum Possible" row was calculated from the "Gravity" shear plus the sum of the shears caused by earthquake if the beams above the level considered yielded at both ends. The axial load in the "D + L_s + $E_{(\mu=1)}$", "D + L_s + $E_{(\mu=3)}$" and "D + L_s + $E_{(\mu=6)}$" rows were taken directly from the static analysis output. The axial load obtained from an incremental

elasto-plastic analysis program is also given in Table 3.5. The formation of the hinges and the top displacement plotted against base shear during the elasto-plastic analysis are shown in Figure 3.3.17.

Table 3.5
Exterior Column Axial Load Levels (kN)

Level	1	2	3	4	5	6
Gravity	732	610	488	366	244	122
$D+L_s+E_{(\mu=1)}$	1409	1147	867	599	364	161
$D+L_s+E_{(\mu=3)}$	951	784	610	440	281	132
$D+L_s+E_{(\mu=6)}$	837	693	546	400	260	125
Max. Poss.	1212	1007	784	591	395	197
Incr. E. P.	1147	962	764	562	368	176
EQ/ART1	1132	926	722	518	325	156
El Centro	1048	886	714	530	345	163
Parkfield	1151	950	764	562	362	166
Pacoima	1183	976	766	591	386	181

The maximum axial loads were greater than the design level, "$D + L_s + E_{(\mu=3)}$", but were less than the maximum possible axial load. The frame could just as easily have been designed for fully ductile response in which case the design level loading would have been "$D + L_s + E_{(\mu=6)}$". In this case it may be seen that the axial loads observed are significantly greater than the design level. This effect has been observed previously by Goel [3.14] who, in a limited study, has shown that maximum axial loads may be 3½ times that given by the static design loads. The ratio of the maximum observed axial load to the "Maximum Possible" axial load decreased near the top of the structure because elastic "$D + L_s + E_{(\mu=1)}$" axial forces were less than the "Maximum Possible" forces in the upper stories. The axial forces from an elasto-plastic incremental analysis approximate the design level axial forces well.

(a) Reason for the High Level of Seismic Axial Load

The reason that the axial load increases in the outer columns of steel DMRFs is that a full plastic mechanism may not occur in these frames. This allows forces higher than the design level to act upon the structure. This will result in higher member moments which may cause flexural yielding, which is generally acceptable, but it will also cause higher axial loads. The effects of the increase in axial load include:

i) reduction in column rotation capacity. This effect will usually be negligible as long as local buckling is prevented, as steel is a naturally ductile material,

ii) a decrease in column moment capacity and rotational stiffness,
iii) greater problems with buckling, and
iv) more column shortening.

Reinforced concrete moment-resisting frames generally form a full plastic mechanism and the base shear which may enter into the structure is limited. In this case the column axial loads may be easily be obtained from the overstrength beam shears.

(b) Overseas Design Approaches

Possible revisions to the Uniform Building Code suggested in Building Standards [3.5] use a factor of $3R_w/8$ by which to multiply the seismic axial loads from the factored down static analysis. This value is described by Krawinkler [3.15,3.16] as "an elastic estimate of the maximum force demand". and is also used to compute the expected displacements.

(c) Design for Axial load

The results above have shown that the actual axial loads observed may be significantly greater than that estimated from the design level load cases for earthquake plus gravity loading. This has been particularly pronounced in the outer columns where axial load due to earthquake is larger than in the inner columns. Columns should be designed for axial loads greater than those found from design level load cases with reduced seismic loading in order to represent the actual axial loads to which they may be subject.

It is suggested by the present writer that the columns be designed for the lesser of:
i) the sum of the overstrength seismic shears of the beams framing into the column above the level under consideration plus the gravity load, or
ii) a combination of gravity loading and a high level of lateral seismic loading. This level of load must lie somewhere between the fully elastic (μ=1) and the design level of axial load. For ductile frames, an nominally elastic estimate of the actual force demand will generally be cautious. The nominal value may be used because in a ductile frame, as hinging occurs throughout the structure, the base shear and member forces will be reduced. The nominally elastic force reduction factor, μ_n, suggested by the new draft loadings code is 1.25.

3.6.10.2 Axial Load Reduction In Capacity Designed Frames

For the following reasons it is recommended that no axial load reduction factor, R_v, such as that described in section 2.3.2a(iii) be used in a design procedure for steel DMRFs.

1) The column design axial load may be more dependent upon the level of earthquake load rather than the overstrength beam shears because the beams may not yield at both ends simultaneously in a design level earthquake. In this case the axial load to be reduced is often determined as a function of the earthquake rather than of the structure so there is no natural upper limit for column axial load. To determine a sensible axial load reduction factor may therefore be very difficult.

2) The axial load reduction factor, as it is used for reinforced concrete frames, is effectively a correction on the dynamic magnification factor (which is a correction to the static loading distribution) and is close to unity. While it makes a difference to the seismic axial forces it makes very little difference to the total column axial forces.

3) The effects of vertical accelerations may cause additional axial load which is not taken account of in most design procedures.

4) If plastic hinging occurs in any column, this will be associated with axial shortening of that column and redistribution of axial load to the other columns. These other columns may be required to carry larger axial loads than their design level.

3.6.11 Shakedown of Beam Gravity Moments

The shakedown of the beam gravity moments is shown for beam member 28, the second floor beam on the left hand bay of the frame, in Figure 3.3.18. The average moment at each end of the beam is plotted against time during several different earthquake excitations in this figure. The initial average moment is from gravity loading alone. It may be seen that the average end moment becomes smaller as cyclic yielding occurs in the member. The reasons for this phenomena have been described by Fenwick and Davidson [3.17] and is illustrated below.

A gravity dominated subassemblage with a composite beam allowing hinging at the ends only, and with initial end moments equal to M_1, such as that shown in Figure 3.3.19a, is considered. The first plastic hinge will to occur when the gravity and the seismic load cause the plastic moment capacity of the beam to be reached during the initial cycle of loading as shown in Figure 3.3.19b. The moment at the right-hand side of the beam will remain constant at the beam plastic moment capacity and inelastic rotation will occur as the

displacement of the subassemblage increases, but the moment at the other end of the beam will become more positive until the required maximum displacement is reached. This is shown in Figure 3.3.19c. The moments at each end of the beam must be the same when the lateral load is removed because the beam is not required to carry any seismic shear. The moments at each end of the beam, M_2, will be less than the initial end moments, M_1, upon elastic unloading as shown in Figure 3.3.19d because redistribution of moment has taken place. This is known as the "shakedown" of gravity moments. After this removal of lateral load, the displacement of the subassemblage has not yet returned to the initial position. As further yielding of the subassemblage occurs, or if hinging occurs at both ends of the beam simultaneously, the bending moment diagram considering gravity load only may drop to the level shown in Figure 3.3.19e where the end moments are zero.

The total moment from the beams applied to the internal second storey column during the various earthquake records is shown in Figure 3.3.20. The moment applied to the internal column in order to obtain the maximum column displacement may be similar to that shown in Figure 3.2c before the "shakedown" of gravity moment occurs. Larger beam shears may occur in the subassemblage after the shakedown has started because higher forces are required to produce yielding. For example, after sufficient "shakedown" of gravity moments has occurred, the beam may behave elastically. Larger beam shears than those expected during the first cycle may also occur when the excitation is greater than the design level. The sum of the beam moments on the internal second-storey column from an elasto-plastic analysis where the top of the frame is deformed to the elastic design level displacement was equal to $2M_{pb}$, or 596kN, as the beams either side of the column had yielded.

Some effects of this redistribution have been described by Fenwick and Davidson [3.17]. During design-level earthquakes, the ductility demands at the end of the member will decrease during the subsequent cycles. The beam ductility demand in the later cycles is likely to be reduced because a larger level of lateral load than that assumed in design is required to produce beam yielding. If the beams are not strong enough over their length, the redistributed gravity load may cause yielding near the middle of the member. In a multibay frame, the total moment from the beams to which the columns (and panel zone) may be subjected during a design level earthquake may change from M_1, as shown in Figure 3.3.21 during the initial cycle of loading, to M_f, during the later cycles, where M_f is larger than M_1.

It may be seen in Figure 3.3.18 that the average gravity moment decreases abruptly during the Parkfield and Pacoima records as these excitations cause hinging to occur at both ends of the member simultaneously. The times at which the average moment decreases most corresponds to large change in the displacement at the top of the frame as shown in Figure 3.3.8. The average gravity moments occurring during the artificial earthquakes and the El Centro excitations drop away less rapidly than they do during the Parkfield and Pacoima excitations as yielding occurs these beams. In Figure 3.3.8 it may be seen that large displacements occur at the top of the structure while shakedown is taking place during all of these earthquakes and also after shakedown has occurred. The duration of the earthquakes is therefore long enough to cause significant beam forces on the column after shakedown has occurred.

Yielding was expected to occur in beam member 28, the second floor beam on the left hand bay of the frame when the design level earthquake lateral load reduction factor, μ, equals 3.0. The elastic member moment divided by the plastic flexural strength was 2.20. A more rapid decrease in the magnitude of the average end moment would be expected in members of frames which were designed for a higher level of ductility.

Shakedown of the gravity moments may cause different levels of force to act on the structure during the later cycles of loading than during the initial cycle. These forces should be considered during design.

3.7 TRIAL DESIGN METHOD #3 : GRAVITY DOMINATED FRAME PROCEDURE

Two methods suggested by Paulay [3.18] for the design of gravity-dominated reinforced concrete moment-resisting frames have been described in section 2.3.4. It was decided to try to use these methods to see if they were suitable for design of steel framed structures.

The first method, which uses the hinge pattern shown in Figure 2.2a is specific to reinforced concrete frames where the position of the desired beam hinge may be controlled by the positioning of the reinforcing steel. For standard bare steel beams, this method is not suitable, and even with composite beams only a limited control of the hinge location is possible.

The second method, shown in Figure 2.2b, in which the exterior columns are strong and interior columns are permitted to yield is more suitable. It was this method which was selected and adapted for trial in the procedure described below.

3.7.1 Modifications to Paulay's Method

It was found that the method of Paulay could be described generally as an "strong" column method where the "strong" column may be either internal or external.

In order for a soft-storey mechanism to be prevented in a particular storey, only one end of this "strong" column is required not to hinge at the top and the bottom at the same time during an earthquake. To discourage formation of hinges at the top and bottom of a storey in a column at the same time, the maximum moment gradient, which is the column shear, must be prevented from becoming large enough to cause column hinging at both ends simultaneously. It may be seen in Figure 3.4 that while a large peak value of moment may cause hinging at one end of a column, a high moment gradient will cause both ends to yield. Therefore, if in at least one column in every storey Equation 3.7 is satisfied, then no soft storey mechanism will occur.

$$V_{max} < (M_{pc,top} + M_{pc,bot})/L_{col} \qquad \text{Equation 3.7}$$

where V_{max} is the maximum column shear force imposed during an earthquake, and

M_{pc} is the moment capacity of the column allowing for axial load, and

L_{col} is the column clear length.

The dynamic magnification factors required for steel frames which are based on the variation of column shear should be less than those for reinforced concrete which are based on the variation of column moment. This is because the column shear dynamic magnification factor, w_v, was found to be less than the moment magnification factor, w_b, in the lower stories.

The "strong" columns may be discouraged from hinging at both ends simultaneously by modifying the capacity design procedure which is used for reinforced concrete. That is, the overstrength flexural capacity of the beam may be applied to the column and distributed above and below the joint in proportion to the moments produced by the earthquake load case alone to obtain the static overstrength moments. These static overstrength moments are then multiplied by the shear dynamic magnification factor, w_v, which allows for higher mode effects, to obtain the column design moments.

The "weak" columns in the frames designed were reduced to the smallest realistic size that would sustain the loads from the code specified load

combinations to obtain the maximum member ductilities. The "strong" columns were required to be very large in order to control the drift. It is desirable to decrease the ratio of the actual strengths of the inelastically responding members to those required by the code toward the top of the building to encourage uniform ductility demand over the height of the structure.

3.7.2 Benefits of using "Strong" Outer Columns

One frame was designed using a "strong" internal column and "weak" external columns, however, there were several benefits in using a "strong" outer column rather than an "strong" internal column. These are:

1) There is only one beam framing into an exterior beam-column joint so that the sum of the beam overstrength moments at the joint will be one half of that for an interior column,

2) If an inner column is chosen to be "strong" and gravity moment is large so that yielding of the beam occurs on one side of the column only, then designing by this method may cause the interior column size to be larger than is necessary,

3) If the exterior columns are chosen to be "strong", the same sized column, or one near it is often able to be used across the frame,

4) Non-structural damage on the exterior of the frame may be less possibly decreasing the likelihood of frame cladding and glazing becoming detached during an earthquake.

3.7.3 Dynamic Magnification Factors

From the analyses run, a value of between 1.20 and 1.40 for the shear dynamic magnification factor, w_v, was found to be appropriate for all the frames subjected to design level earthquakes. This value appeared to be dependent on the height of the frame rather than the number of bays in the frame. Taller frames with longer fundamental periods seemed to have larger dynamic magnification factors as a result of the higher modes being excited more. A factor of 1.20 for shear magnification has been recommended in the commentary to the reinforced concrete code [3.3].

3.7.4 Prevention of Partial Sway Mechanism

The partial storey sway mechanism was described in section 3.3. This mechanism is more desirable than the so-called soft-storey mechanism but is less desirable than a full beam-sidesway mechanism. In the design

methodology described no attempt has been made to inhibit this mechanism. However, if columns are designed according to the method already outlined, then some protection is already provided. For example, if the partial sway mechanism occurs over two stories, and the column shear dynamic magnification factor, w_v = 1.20 say, then in this mechanism, the central beam must yield, giving an average moment above and below the joint on the exterior column of $M_{pb}/2$, which in the middle stories of a frame will be approximately equal to $\phi_{ob}M_{code}$. At the column ends away from the yielding beam, the moments must reach $1.20\phi_{ob}M_{code}$ as shown in Figure 3.5. The average shear on the columns to cause this type of mechanism is $1.10\phi_{ob}V_{code}$ if ϕ_{ob} is approximately constant in each storey as $V_{code} = (M_{code,t} + M_{code,b})/L$. This has a lower factor of safety than the design value of $1.20\phi_{ob}V_{code}$ for one column. However the number of hinges formed has increased so member forces will be less. If the partial sway mechanism extends over n stories then the required value of $1.10\phi_{ob}V_{code}$ will still be required in the upper most and lowest columns in the sway part of the frame, but many more hinges will be required to form. The partial sway mechanism is most likely to form over two stories.

3.7.5 Frame Behaviour

A six storey two bay frame with elastic outer columns was designed to allow the internal column to yield. The sizes of the frame, referred to as Frame #2, are given in Appendix 3. The outer columns were designed to be stronger than the required for strength in order to satisfy the drift requirements [3.9].

Consideration of the P-delta effect in the dynamic analyses increased the total frame displacement in some instances as is shown in Figure 3.6.1.

It may be seen that the maximum shears given in Table 3.6 for the frame with and without P-delta effects included were of approximately the same magnitude. The maximum shear magnification was less than 1.20 during the design level earthquakes but was greater in some instances during the Pacoima and Parkfield excitations.

The maximum axial load which occurred in the external columns is shown in Figure 3.6.2. In this frame the elastic level of earthquake load is less than that obtained from the maximum possible axial load calculated from the overstrength beam shears and gravity loading. It was found that the axial load during an earthquake may be 4.5 times the seismic design level (μ=6)

Dynamic Magnification Factors for Frame #2. This is a six storey two bay frame with strong outer columns.

Six Storey Heavy Frame - P-delta flag = 2 (No P-delta considered after analysis started)

Level	Overstrength Forces		EQ/ART1		EQ/ART2		El Centro		Parkfield		Pacoima	
	Moment	Shear	Shear	Sh Mag	Shear	Sh Mag	Shear	Sh Mag	Shear	Sh Mag	Shear	Sh Mag
Top	645	232	221	.95	230	.99	248	1.07	223	.96	236	1.02
6B	166											
5T	479	209	201	.96	225	1.08	209	1.00	253	1.21	237	1.14
5B	251											
4T	393	202	211	1.04	223	1.10	193	.96	226	1.12	250	1.24
4B	314											
3T	387	211	216	1.03	207	.98	193	.92	239	1.14	316	1.50
3B	350											
2T	352	245	243	.99	281	1.15	247	1.01	322	1.31	275	1.12
2B	506											
1T	196		275		288		280		369		352	
Ground	387											

Six Storey Heavy Frame - P-delta flag = 1 (P-delta analysis at every time-step)

Level	Overstrength Forces		EQ/ART1		EQ/ART2		El Centro		Parkfield		Pacoima	
	Moment	Shear	Shear	Sh Mag	Shear	Sh Mag	Shear	Sh Mag	Shear	Sh Mag	Shear	Sh Mag
Top	645	232	208	.90	230	.99	255	1.10	223	.96	239	1.03
6B	166											
5T	479	209	195	.93	206	.99	210	1.01	262	1.26	226	1.08
5B	251											
4T	393	202	209	1.03	226	1.12	184	.91	214	1.06	262	1.30
4B	314											
3T	387	211	216	1.03	209	.99	209	.99	238	1.13	314	1.49
3B	350											
2T	352	245	242	.99	264	1.08	239	.97	334	1.36	304	1.24
2B	506											
1T	196		284		277		257		388		376	
Ground												

Table 3.6
Frame #2. Exterior Column Shear Dynamic Magnification Factors

axial load causing an increase in the total column axial load of 40% for design level earthquakes. The axial loads in the columns in the upper stories often exceeded the axial load from the elastic (μ=1) earthquake load combination. This is because the static elastic load distribution underestimates the likely maximum shear force in the upper stories.

Table 3.7
Maximum Hinge Rotations and Ductility Demands

Earthquake	Maximum Inelastic Hinge Rotation (radians)	Maximum Ductility Demand (ϕ/ϕ_p)
EQ/ART1	0.0072	2.83
EQ/ART2	0.0060	2.59
El Centro	0.0050	2.14
Parkfield	0.0218	7.11
Pacoima	0.0256	8.28

The maximum column plastic rotations, θ_R, and curvature ductility demands (ϕ/ϕ_p) are given in Table 3.7. This frame was designed for a displacement ductility of three. The ductility demands from the computer output shown in the table are lower than the actual ductility demands (ϕ/ϕ_{pc}) which account for the actual levels of axial load. The maximum interior column axial load ratio, P/P_y, was 0.32 resulting in actual curvature ductility demands (ϕ/ϕ_{pc}) being up to 1.25 times greater than those recorded (ϕ/ϕ_p). Considering that the displacement ductility demand is approximately one half of the curvature ductility demand as shown in section 6.7.3(b), the ductilities demanded are small. Even under the Parkfield and Pacoima excitations the inelastic rotation and ductility demands could be met.

3.7.6 Problems with this Procedure

In all of the frames analysed the dynamic behaviour is good. However, there are some problems with the implementation of this procedure in irregular structures, and the factor of safety associated with providing "strong" columns is not uniform for multibay frames. For these reasons, which are expounded below, it is recommended that the "strong" column method should not be used to guarantee satisfactory behaviour of multistorey steel ductile moment-resisting frames.

(a) Minimum Column Stiffness

The first of these problems is that there is no minimum stiffness required of the elastic outer columns. Their design is based completely on strength. It is therefore conceptually possible that an elastic outer column may be

very small if it is made from high strength steel and the beams are connected to the outer column shear connectors. Therefore if a storey is displaced laterally and all of the columns yield except the "strong" column, this column may provide very little resistance against further deformation. With large deformations, P-delta effects may become large on this column.

(b) Storey Behaviour

To critically appraise this procedure it is necessary to understand the behaviour of a frame rather than just the possible magnification of moments near the joints. Each floor with mass is excited relative to the floors above and beneath it. If only the columns yield, the stiffness of each storey may be represented by the elasto-plastic load-displacement curve shown in Curve "A" of Figure 3.7. If the columns behave in a bilinear manner the load-displacement curve may be more like Curve "B".

For a frame which is designed by the "strong" outer column concept with all of the columns behaving elasto-plastically, the hysteretic behaviour will be like Curve "B" because the internal columns may yield, whereas the outer columns will remain elastic causing an overall positive storey stiffness. A soft-storey mechanism with bilinear hysteretic behaviour may therefore behave in a similar way to a system with stiff beams and elastic outer columns.

If the frame designed by the "strong" outer column concept is now considered to be many bays wide, the bilinear stiffness of the storey will be a much lower proportion of the initial elastic stiffness, and in the extreme case, the bilinear stiffness of the storey with an infinite number of bays will tend to zero. It may be seen that the level of safety associated with this method is not uniform and decreases as the number of bays increases.

It is suggested that the reason that multibay frames behaved well is that the seismic behaviour of all regular steel multistorey ductile moment-resisting frames is good. It is unknown how much protection against large ductility demands caused by soft-storey mechanisms is given by the elastic outer columns.

It should be noted that in the designs carried out for structures designed by the "strong" outer column concept, large columns were required to enable them to fulfill the drift requirements and for frames of many bays the elastic outer columns had to be very stiff. This would have provided the

storey with a large amount of bilinear stiffness. The forces on this outer column seldom seemed to be of the same magnitude found in frames when all columns were elastic.

P-delta forces are also present in real frames possibly causing a negative post-elastic stiffness as shown in Curve "C" of Figure 3.7. It is thought that the absolute value of the post-elastic stiffness is not as important as the relative stiffnesses of the adjacent stories. Further research is required to study this behaviour.

(c) Irregular Frames

Difficulties in finding a rational position for a strong column may exist in irregular frames such as the frame with no moment connection to an outer column and the frame with a setback shown in Figure 3.8. Irregular frames tend to be commonly designed in practice.

(d) Column Yielding

The "strong" column method, as described by Paulay [3.18], allows plastic hinges to form in the internal columns. It is shown in chapter 6 that there are potential problems with allowing large amounts of flexural yielding to occur in the columns, and column yielding is shown to be not as desirable as beam yielding. Column hinging is therefore best discouraged in steel framed structures from being the primary-energy dissipating mechanism.

3.8 Tolerance of Steel Frames

In order to protect frames against the possibility of soft-storey behaviour it desirable to see under what conditions a soft-storey mechanism occurs and then to design against it. Many regular steel frames of different sizes were analysed but a soft storey mechanism was not observed to develop in any of these frames. Tjondro [3.19] also analysed several frames which had been designed for drift in which all of the columns in any storey were the same size and very little column hinging was observed.

The lack of undesirable behaviour is fortunate for steel frames showing that they are tolerant, however it was difficult to form a design strategy based on eliminating the possibility of such a mechanism. The purpose of a "capacity design" procedure protects against undesirable behaviour. If no undesirable behaviour occurs then a pure strength design procedure will be satisfactory.

The tolerance of steel frames was shown in that the structural damage which was reported from the 1985 Mexico City earthquake [3.8] occurred in frames with poor detailing. No reports were given of structures in which an undesirable frame mechanism occurred in which the member ductility demands to be high.

While the steel frames analysed in this study may be tolerant against forming a mechanism, large plastic rotations may be demanded from the members. Only regular frames with a constant interstorey height have been studied here. For frames of different configurations a soft-storey mechanism may possibly occur.

(a) Testing of Tolerance of Steel Frames Buildings

The tolerance of steel frames was shown by:

1) no mechanism forming in frames subjected to two times the design level earthquake. The expected return period of an earthquake of that magnitude is 1000 years. It was not considered necessary to analyse structures for earthquakes to greater than this level of excitation. The frames were analysed for the full P-delta effects. In Frame #1 and Frame #3, described in section 4.6, the required curvature ductilities were 8.9 and 12.9 respectively during EQ/ART1 multiplied by 2.

2) no mechanism forming in frames when all elements except the columns at the bottom storey or first storey level were forced to remain elastic.

(b) Reasons for Tolerance of Steel Moment-Resisting Frames

There are several possible reasons for the tolerant behaviour of steel frames. These are:

1) Members in steel moment-resisting frames often have a small second moment of area and may span over a large distance while the members are strong. This causes the frames to be strong and flexible, attracting only low levels of seismic force and demanding low levels of ductility. The floor dead load per unit area of a steel structure is often small compared to that of an equivalent reinforced concrete structure. The draft New Zealand loadings code [3.9] is conservative in its estimation of forces for long period structures. For most natural earthquakes the longer period response drops away rapidly. Therefore, while design is carried out according to the loadings code, actual earthquake accelerograms may be unable to excite much inelastic response. The level of lateral load required to produce a full frame mechanism may be similar to that of the elastic design level

earthquake. This was found to be the case for buildings with internal frames, and external frames in which closely spaced columns were used to resist the full earthquake inertial load of a storey and internal frames were considered to carry gravity loads only.

2) The gravity moments form a large proportion of the maximum column moment because of the flexibility of the frames. This may result in yielding at one end of the beams only during design level excitation. Therefore the outer column on the tension side of the frame may be unlikely to yield as the moments from the beam framing into it may be very small (before a large amount of "shakedown" of member moments occurs) thereby discouraging the possibility of a soft-storey mechanism in frames with a small number of bays.

3) The beams and columns may be stiff in the bottom stories of tall steel frames, however, the period of their first mode response will generally be very long. For example, one 18 storey frame analysed had a first mode response period of 4.15 seconds. Because of this, limit states other than earthquake may govern the member sizes. In tall frames the column sizes near the base of the frame are required to be large to carry the axial load from the upper stories. If there is a reasonable limit on the column axial load ratios to control frame buckling under the gravity load combination alone, sufficient column strength may be available to discourage large column ductility demands under the earthquake load cases.

In order to understand the inelastic seismic behaviour of these frames in greater detail, more reliable methods for the prediction of the inelastic seismic response of structures than those presently available must be developed.

3.9 SUMMARY OF THE BEHAVIOUR OF FRAMES

In the analyses of the frames undertaken the hinges tended to move up and down the frame in bands. A full frame mechanism was seldom observed, especially in the larger frames, however high member rotations were observed during severe excitations. It was quite common for hinging to occur at one end of a beam only at any instant in time.

The member displacement ductility demands which were estimated from the curvature ductility demands were approximately the same as the elastic force reduction factor, μ, under the design level earthquakes. This was because even though the displacements were slightly less under the design

level earthquakes than those predicted by the equal displacement assumption, the member ductilities were more than the subassemblage ductilities as described in section 6.7.3(d). Initially the plastic hinges tended to yield predominantly in one direction because of the initial gravity loading on the structure. The magnitude of the average moment at the ends of the beam decreased with the amount of hinging which occurred in the beam. Therefore both the magnitude of the ground acceleration and the length of earthquake affected the maximum inelastic deformations. For the earthquakes of large magnitude, inelastic hinge rotations of over 5% were sometimes demanded for frames designed with a load reduction factor of three.

It is thought that the maximum allowable load reduction factor of six [3.9] is too large for frames as it can result in member displacement ductilities much larger than six, perhaps up to ten under design level loading. As the strength to stiffness ratio, M_P/EI (which is the plastic curvature, ϕ_P), of steel frames is high, large displacement ductilities will result in large inelastic hinge deformations. However, large inelastic rotations are not generally likely in steel frames as limit states other than earthquake often govern the member sizes. Members in frames are therefore likely to be subjected to displacement ductilities significantly less than the maximum allowable load reduction factors imply so these large allowable load reduction factors do not present a problem.

The fundamental displacement response as seen from the displacement of the top stories was predominantly that of the first mode.

In frames in which no soft-storey mechanism occurred, the interstorey drift envelopes were shown to be conservatively predicted by the code simplified frame design method which was used for design level earthquakes. Lateral forces calculated by modal analysis techniques are smaller than those obtained from the simplified frame design method. It is expected that displacements obtained from modal analysis rather than from the code equivalent static lateral force distribution would more accurately predict the frame response to the design level earthquakes.

The deflected shapes of the structures at certain instances of time were often found to be close to that of the displacement envelope. The displacement envelope from design level earthquakes was found to be less than that predicted by the equal displacement assumption.

Forces higher than those implied by the lateral load reduction factor, μ, may enter the structure because a full frame mechanism seldom occurred. This causes base shears and column axial loads higher than those calculated from the design level forces. Realistic values for the higher axial loads during design level earthquakes may be approximated and used for column design.

In the lower stories of a frame, the storey shear is underestimated by the code lateral load distribution because the centre of applied load moves down the frame. This causes larger base shears than the code loading distribution implies. The actual storey shears are also underestimated in the upper stories where the so-called whiplash effect occurs.

3.10 BEHAVIOUR OF COLUMNS AND PANEL ZONES

In order to provide a satisfactory design philosophy for steel framed structures, the inelastic behaviour of frame components which may possibly yield must be understood. It is well accepted that the inelastic behaviour of well detailed beams is good. The behaviour and recommended use of columns and panel zones in frames is discussed below.

(a) Panel Zone Behaviour

Testing of panel zones [3.20] has shown that some inelastic panel zone behaviour may be tolerated in steel structures. Reasonably accurate predictions of panel zone strength may now be made including the effect of the strength of the column flanges and the level of column axial load [3.21]. Dependable shear rotations of over 0.06 radians may be obtained from well detailed panel zones [3.15]. Panel zone deformation is shown in Figure 3.9.

Krawinkler [3.16] has analysed two frames with different panel zone strengths and found that the lateral displacements were not increased if the frames had weak panel zones. He also states that if all of the energy dissipation occurs in the joints throughout a frame that the panel zones may have to undergo large distortions which may lead to problems outside the joint at the corners where beam flanges are usually welded to the column flanges. Fracture of these welds caused by high curvatures at the joint corners has been observed in past experiments. It was shown that the lateral load resistance of frames may be considerably reduced by weak

joints. For these reasons it was recommended that sharing of inelastic deformations between the joints and beams be carried out in a well balanced manner.

(b) Column behaviour

Column hinging is best discouraged in frames for the reasons that will be given in section 6.6.2. If hinging is permitted, and a column sustains four cycles of loading with an inelastic rotation of 0.02 radians, the amount of axial shortening of each hinge will be approximately 16mm according to Equation 7.15b if A_s/A is assumed to be 0.20, L_p = 300mm, and P/P_y = 0.40. This may be a very severe case, but even if there was 3mm of shortening in the hinges at the top and bottom of every storey, this would result in a 48mm difference in floor level at the ninth storey. This may result in major structural effects and the non-structural components contributing to the response. It is suggested that a large amount of column hinging be discouraged. This will also discourage the possibility of a soft-storey mechanism.

3.11 TRIAL DESIGN METHOD #4 : ELASTO-PLASTIC DESIGN PROCEDURE

3.11.1 Design Philosophy in the Elasto-Plastic Design Method

The design philosophy for this method is as follows :

> Only beam hinging, and possibly column hinging at the ground floor level should occur during the deformations to which the frame is expected to be subjected during the design level earthquake on the first cycle of loading. Panel zone and column hinging, preferably in that sequence, may occur during earthquakes of greater magnitude than this and when higher mode effects become significant. Connections are expected to remain elastic and no member yielding in shear is expected.

3.11.2 Discussion of Elasto-Plastic Design Method

This philosophy will discourage column hinging and the possibility of soft-storey behaviour during the first cycle, or first few cycles of loading in both regular and irregular frames. A certain amount of column or panel zone yielding may occur during large earthquakes because of higher mode effects or during earthquakes of average to long duration. Columns should therefore be designed to limited ductility requirements. The concept of protection

against seismic attack is that of dissipating most of the energy in the beams and sharing the inelastic demand from higher mode effects and large earthquakes between other ductile components of a frame.

A typical joint moment pattern from an elasto-plastic analysis may be similar to that shown in Figure 3.10a. If the sum of the beam moments at the joint are greater than the design level, as shown in Figure 3.10b, this will cause either panel zone or column yielding depending upon the relative strength of these elements. However, if higher mode effects occur, such as is shown in Figure 3.10c, the net joint moment will not increase, so panel zone yielding will not occur, but column yielding may occur instead.

3.11.3 Application of Elasto-Plastic Design Method

In this method, an static elasto-plastic frame analysis modelling the overstrength beam strengths is used to follow a gravity loaded frame through to the expected elastic displacements ($\mu = 1$) calculated by means of the equal displacement assumption. Columns are designed so that they will not yield in flexure under the forces obtained from this type of analysis.

The panel zone is designed for the member forces from the elasto-plastic analysis program and the column shear strength should be strong enough to resist 1.20 times the shear from the analysis.

The frame may be deformed to the expected displacements with an elasto-plastic analysis program by applying lateral loads to struts at each level as shown in Figure 3.11a. The forces applied to struts at each level, P_i, may be calculated from Equation 3.8 where the expected displacements, δ_i, are calculated as $C_e/C_\mu . \delta_{\mu i}$ and ΣP_i is much greater than the frame base shear, V_{base}. This method of design is not straight-forward to apply.

$$P_i = \frac{A_i E_i}{L} \delta_i \qquad \text{Equation 3.8}$$

The member forces may be approximated more simply than by the method described above by using the incremental elasto-plastic analysis program to displace the structure until deformations are greater than or equal to those predicted by the equal displacement assumption are obtained or until a full frame mechanism forms. In regular frames, when the top of the frame reaches the required elastic top storey displacement, the displacements of the rest of the structure are also generally of a slightly greater magnitude than that required.

If the elasto-plastic design method is used, it is suggested that the lateral forces be applied using the code lateral load distribution. The possible hinge formation pattern resulting from such an analysis on a steel frame is shown in Figure 3.11b. Computer programs to perform this kind of analysis are freely available [3.22]. The elasto-plastic design method has some similarities with the method proposed by Clifton [3.23] which was mentioned in section 2.3.6.

3.11.4 Examples of Elasto-Plastic Design Method on Frames Analysed

The elasto-plastic analysis computer program was used on two of the frames analysed in this report to illustrate the application of this method. The code static force distribution was incremented while the gravity loads remained constant. For Frame #1, described in section 3.6, the order of the formation of hinges and the base shear force-top displacement curve is shown in Figure 3.3.17, the exterior column axial loads are compared with the design level and earthquake axial loads in Figure 3.3.16 and the design level displacements and interstorey drifts are compared with those from the elasto-plastic analysis in Figures 3.3.10 and 3.3.11.

The order of the formation of hinges and the base shear force-top displacement curve are shown in Figure 3.12 for Frame #3, which is described in section 4.6 of the next chapter. The design level displacements and interstorey drifts are compared with the design method in Figures 4.5 and 4.6.

(a) Results from Elasto-Plastic Analysis

The base shear was 665 kN at the expected displacement when the incremental elasto-plastic method is applied to Frame #1, and the maximum base shear was 779 kN when the last hinge formed in the full beam-sidesway mechanism. This is the same as that calculated in section 3.6.9.

The base shear of 665 kN was exceeded in all of the earthquakes as shown in Table 3.4, even though, in earthquakes such as El Centro and EQ/ART1 the displacements observed were significantly smaller than those used in the incremental elasto-plastic method. Considerably greater base shears were observed during Pacoima and Parkfield excitations. The magnification of the shears at the base of the columns effecting the foundation design are referred to as w_f. A value of w_f of 1.20 would be required to estimate the maximum base shear which occurred during EQ/ART1.

At the top of the structure the maximum storey shear was 365kN during the El Centro record while the predicted storey shear by the incremental elasto-plastic design method was 229 kN.

Storey shears within the structure, at the top and at the base, were greater than that predicted by the elasto-plastic design method. This is because the code force distribution which was used in the design method was not the most critical.

It is seen that the loading distribution used does not give the maximum storey shear at either the top or at the bottom of the frame. Robinson [3.24] has recommended that several different loading patterns be used to find the maximum higher mode forces. A single point load could be used on the structure to obtain the maximum shears in the upper stories, but the long lever arm from the top of the structure to the frame base would result in the base shear being small. A distribution with a low centre of force, such as a rectangular or inverted triangular distribution would produce a high base shear but very small top-storey shears at the required displacements.

Frame #1 was pushed to the desired top displacement from the equal displacement assumption of 0.292m with a point load at the top, a rectangular distribution and the code load distribution. The base shears when the frame top displacement reached the expected level under these lateral load patterns were 483kN, 670kN and 884kN respectively. The base shears when a full frame mechanism formed were 580kN, 779kN and 994kN respectively. The exterior compression column axial load is shown in Figure 3.13 for the frame. The point load at the top produces the highest level of axial load, while the rectangular distribution causes the greatest base shear. If the maximum storey shears throughout the frame are required to be designed for, two or more static load distributions should be used.

According to the stated design methodology, the higher modal contributions are to be ignored. Higher storey shears occur than those anticipated may result in limited column hinging. This is not generally a problem. The foundations are, however, required to be designed for the larger shear force, and this larger force must get to the foundations through the columns at the base of the structure.

3.11.5 Problems with the Elasto-Plastic Design Method

The major problems with this method are that the column forces are based on the monotonic frame deformation and the effects of "shakedown" are not included. It was shown in section 3.6.11 that to ignore the "shakedown" may cause underestimation of the actual beam moments applied to the columns. The columns may possibly become the primary energy dissipating elements and the beams may dissipate no energy in the later cycles. This is not desirable.

The problems with this method lead on to the proposed design procedure for steel ductile moment-resisting framed structures.

3.12 DESIGN PROCEDURE #5 - RECOMMENDED DESIGN METHOD

3.12.1 Basis for Design Procedure

The behaviour of steel frames discussed below forms the background to the proposed design recommendations.

i) Traditional reinforced concrete "capacity" design methods are not suitable for steel frame design as they require excessively large column sizes,

ii) The design method in which at least one of the columns is kept elastic, does not provide a uniform level of protection against soft-storey mechanisms, and for frames with a large number of bays there is no real benefit from this type of system,

iii) The elasto-plastic method of design does not consider the likely column forces on the later cycles of loading,

iv) Steel frames are very tolerant and the possibility of a soft-storey mechanism is very low so protection against this type of mechanism is not a primary consideration, and

v) Although columns and panel zones both possess ductility, there may be problems if too much ductility is demanded of either of these elements. These elements should therefore not be the primary methods by which energy should be dissipated. The phenomena of shakedown of beam gravity moments may mean that the moments applied from the beams to the columns may be greater than what is expected on the first cycle of loading.

Many design procedures could be based on these points. The procedure described was selected because it was thought to be reasonable and simple to apply.

3.12.2 Proposed Design Philosophy

The proposed design philosophy is given below:

> Only beam hinging, and possibly column hinging at the ground floor level should occur during the first mode response of a frame. Column hinging may occur when higher mode effects become significant. Connections are expected to remain elastic and no member yielding in shear is expected.

3.12.3 Application of Proposed Design Method

The first step of the design is to select member sizes. These will often be governed by drift limitations. Beams should be designed to resist the reduced code level design forces. Beams are also expected to be designed as closely as possible to the same level of ductility so that yielding will not just occur in one storey but will be spread throughout the height of the structure. The beam shear strength should be sufficient to resist the maximum expected shear. This may be the "nominally elastic" level of shear or may result from simultaneous gravity loading and yielding at the both ends of the beam. The composite beams should be designed to carry the moments expected along the midspan of the member when the "shakedown of gravity moments" has fully occurred unless hinging along the beam length is desired.

In this method, the sum of the overstrength beam moments at a joint are applied to the column and distributed above and below the joint in proportion to the column moments above and below the joint found previously under the earthquake load case alone to obtain the column design moment. The moments from the earthquake load case alone may be found by simple methods such as the Muto analysis, or by a more exact elastic analysis.

The column should be designed to limited ductility requirements and designed to carry the design moment and axial load. No member in a frame is required to be designed for forces greater than those given by load combinations using the nominal ($\mu = 1.25$) level of earthquake load. Lateral buckling of the columns should be considered in design and the column slenderness should be checked, with a ratio of end moments, β, equal to zero, to ensure that there is sufficient ductility capacity at the ends of the member. This is to allow for the variation of the column moment from the static overstrength distribution as described in section 3.6.8.

Enhancement of end moments in the plane of bending should not be considered during first mode response as these moments are limited by the plastic strength of the beams.

It is proposed that the dependable column shear strength should be greater than the lesser of 1.20 times the expected column shear, or the shear if hinging occurs at both ends of the column or the "nominally elastic" column shear. The value of 1.20 is from the shear dynamic magnification, w_v, and is used by the reinforced concrete code commentary [3.3]. Mortazavi [3.25] has shown that during the yielding of unstiffened webs in columns that the hysteresis loops may have a negative slope as the web buckles are straightened out changing to a positive slope as the buckles reform in the other direction. In these tests the columns yielded earlier in shear than in flexure as their shear strength was less than their bending strength. The strength of these units degraded more rapidly than would be expected in a compact column yielding in flexure.

Panel zones should be designed for the forces expected to occur in conjunction with the overstrength beam moments, or from the nominally elastic design forces.

Connections should be designed for the overstrength member inputs or for at least the elastic (μ = 1.0) level earthquake.

(a) Discussion of Design Procedure

The design philosophy described encourages weak-beam strong-column behaviour. Rather than allow only beam hinging during a very large earthquake and when higher mode effects become significant, a sharing of inelasticity throughout the ductile components of a frame is permitted.

Panel zones and columns are both discouraged from dissipating large amounts of energy for the reasons described in section 3.10. However, there is no reason why they cannot be the primary energy dissipating elements if the amount of inelasticity expected in these elements is very low. This case is covered to some extent by the nominally elastic design factor (μ=1.25) for all steel frames [3.26]. Inelasticity may occur in these elements if they are designed for the nominally elastic level forces and earthquakes greater than that implied by this level of loading occur. Columns may also be permitted to dissipate all of the energy in low rise steel frames if these

are designed for high forces implying low levels of ductility. Further recommendations are required for the maximum levels of ductility to which panel zones in frames may be subject.

The procedure presented is based on the analyses of frames where hinging may only occur at the ends of the member. The procedure will still be valid, but may be slightly conservative for frames in which hinging may occur along the beam length. This is because after shakedown of gravity moments, the moments at the end of the beams may be greater than zero as shown by Fenwick and Davidson [3.17]. It is suggested that the procedure described be applied to beams in which gravity forces are permitted to cause hinging along the member, and that the beams be detailed for ductility along their length.

3.12.4 Simplification of this Design Procedure

This method may be simplified to estimate the design column moment in a similar way to that of Kamil and Bertero [3.27] described in section 2.4 where the factor, F, defined in that section, is chosen as $1.0\phi_o$. Kamil and Bertero's method does not allow for the possible uneven distribution of column bending moments above and below the joints and may allow slightly more column yielding in the columns near the top and near the base of the frame than the method described above.

3.12.5 Comparison between the Design Proposal and the Elasto-Plastic Method

This method is more conservative than the elasto-plastic design method. However, similar results will be obtained using the two methods if

1) the effects of earthquake loading are much more significant in determining the beam sizes than the gravity forces. In this case hinging would be expected to occur at both ends of the beams, or there would be an elastic response, or if

2) the member forces as a result of earthquake are very small compared to the gravity forces. The columns may then be designed elastically.

"Shakedown" of gravity moments occurs when gravity and earthquake loading are both significant. Frames of this type are generally expected to sustain only limited levels of ductility demand in a design level earthquake.

The consequence of "shakedown" is that is that after the first few cycles of displacement, beam yielding may no longer be the main means of energy dissipation within the frame, and energy and inelastic deformation may take

place in the internal columns instead of in the beams at these joints. There did not seem to be a problem in the frames described in this report with excessive column yielding. This is because the columns were generally strong enough to resist yielding of the beams at either side of the joint as shown in Figure 3.3.3. As the effects of shakedown in beams may be significant, this conservative treatment of shakedown is felt to be appropriate for design.

3.12.6 Design of Ground Floor Columns

Design of the column at the ground level of a frame must be different from the design further up the column because there may be no beams at the base of this column, and if there are, these foundation beams are often designed to remain elastic.

It is recommended that the size of a column should not increase up the height of a structure. The size of the column at the base of the frame may therefore often be determined by the required column size above that level. It is recommended that the columns be designed for the load combinations with no greater than a limited ductility (μ=3) level of elastic seismic force reduction.

Storey shears greater than the design level were found to occur in the frames analysed. This caused an increase in column shear as a result of the centroid of the lateral earthquake inertia force distribution being lower than that assumed by the code lateral load distribution as described in section 3.11.4(a). This will not usually cause hinging at both ends of the bottom storey columns because, under the design level loading, the moment demand at the top of the ground floor column is approximately zero but the flexural strength is high. An increase in shear can usually be carried without a soft-storey mechanism forming. No problems occurred in any of the frames analysed in this study.

Foundation design is outside the scope of this report, but a dynamic magnification factor for the foundation shear, w_f, is required as the presently used design forces are incautious if the foundation is to be designed to remain elastic.

3.12.7 Summary of Design Procedure

The simplified version of the design method is recommended. This will allow slightly more column hinging than if the design method described above is used but beam hinging will be the primary energy dissipating mechanism.

The columns should be designed for the moments found from Equation 3.9 where N_b and N_c are the number of beams and the number of columns in the plane of loading framing in to the joint considered. At the ground floor level the column should be designed for limited ductility forces. The column axial load may be found from the sum of the overstrength shears from all of the beams above the level under consideration plus the gravity loads, or from the load combination including the nominally elastic earthquake forces. The column shear strength should be greater than 1.20 $(M_{c,top} + M_{c,bot})/L_c$, $2\phi_o M_{pc}/L_c$ or the forces from the nominally elastic earthquake load case.

$$M_c \geq \frac{N_b}{N_c} \phi_o M_{pb} \qquad \text{Equation 3.9}$$

Panel zones should be designed for the forces expected to occur in conjunction with the overstrength beam moments, or from the nominally elastic design forces.

Connections should be designed to the overstrength or elastic (μ=1.0) member forces.

3.12.8 Factors of Safety against Collapse

The method presented may be conservative in some instances such as when the frame is not earthquake dominated and strength governs the column sizes or when the duration of the strong-motion is not long. It considers that large frame displacements may occur after the "shakedown" of the beam gravity moments.

Some other possible factors of safety in frames designed according to the method described above which may assist a structure to sustain an earthquake of greater magnitude than the design level are:

1) the possible participation of non-structural components moving through the large displacements,

2) the column on the tension side of the frame may remain elastic because of large gravity moments on the beams as shown in Figure 3.2 reducing the moment input to the columns,

3) the ratio of the column-to-beam yield strength possibly being greater than that implied by the overstrength factors,

4) strain hardening in the columns will increase their strength,

5) the dynamic response of a storey may be such that even if a soft-storey mechanism does occur it will not lead to collapse. The magnitude and alternating direction of the seismic excitation may limit the ductility demand in the members.

In the analyses carried out in this project no frame mechanism occurred during even the Pacoima or Parkfield excitations. For the above reasons it is hoped that collapse will not occur in any steel DMRF even during a maximum credible seismic event.

3.13 CONCLUSIONS

In this chapter some reasons for the low number of steel buildings designed in New Zealand are described and the need for a design philosophy for such frames is stated.

The behaviour of steel moment-resisting frames has been shown to be different from reinforced concrete frames because of the difference between steel and reinforced concrete members. Steel members have a very large strength-to-stiffness ratio and the strength along the steel members cannot be altered with ease. Steel members also possess a large ductility capacity without specific detailing. This causes limit states other than earthquake forces, such as gravity loading and interstorey drift limitations to often govern the member sizes.

The reinforced concrete design methodology was applied to steel moment-resisting frames and was found to cause excessively large column sizes because these frames were not earthquake dominated. A second method for the design of frames was attempted in which the reinforced concrete design methodology was used and the frame was subsequently stiffened up to satisfy the drift limits. This method was found to be inappropriate in its goals and in its implementation. A third method of design, in which at least one "strong" column was used to prevent a soft-storey mechanism was also studied. This method was easy to apply to regular frames, but not to irregular frames. The degree of protection against a soft-storey mechanism was believed to decrease as the number of bays in the frame increased. A method of frame design using the elasto-plastic design method was

described, however, this method was based on the first cycle of frame loading and did not consider the effects of reverse loading and "shakedown" of gravity moments.)

The results of regular frames analysed by inelastic dynamic time history analyses were shown. From these analyses it was found that axial loads greater than the design level axial loads occurred in the columns, no soft-storey mechanism occurred in the frames which were analysed, large variations of column moment may occur during the analyses, shakedown of beam gravity moments may occur with progressive cycles of beam yielding and dynamic shear magnification was observed in the columns.

Based on these results it was recommended that:

i) columns be designed for a realistic level of axial load. A value of seismic lateral load corresponding to the nominally elastic seismic force, $\mu = 1.25$, or the overstrength beam forces should be used to calculate the column axial loads,

ii) column shear strength should be at least 1.20 times the expected shear force at the expected design displacement,

iii) the ratio of the column end moments, β, be taken as zero in the design of columns for maximum axial load, and

iii) no specific protection need be provided against soft-storey mechanisms in regular steel frames as they do not seem to occur.)

The dynamic behaviour of inelastic frames is complex, yet by making some simplifications and assumptions, reasonable design methods may be found. A design philosophy was suggested. It was recommended that the beams and the columns at the base of the frame yield during the first mode response of a frame. It was recommended that a large amount of energy should not be dissipated in panel zones and column yielding.)

The simple design method was described which is different from that specified for reinforced concrete frames because of the different behaviour of the two types of frame. "Capacity design" principles are used, and beam hinging is encouraged to occur first thereby discouraging undesirable mechanisms from occurring. No dynamic magnification or axial load reduction factors are used. For larger excitations, the design methods allow for a sharing of inelastic demand with other ductile frame components, such as the columns and panel zone, so that the total beam inelastic demands do not become too large. This approach is different from the reinforced concrete

"capacity design" approach in which a desirable mechanism is chosen and the members detailed to behave inelastically are expected to sustain all of the inelastic demand.

Further work is required to study the seismic response of irregular frames. When more realistic modelling of the response of a frame is carried out than that used in this report, incorporating inelastic axial deformation of column members and inelastic panel zone deformation, it may be found that relaxation of the design recommendations made may be acceptable, particularly in regard to the amount of panel zone deformation permitted.

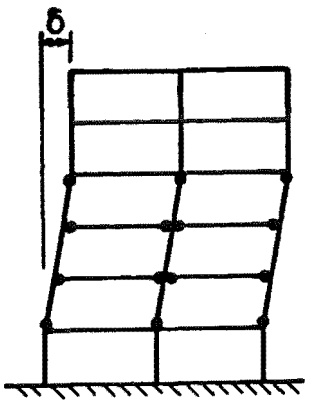

Figure 3.1. Partial Sidesway Mechanism

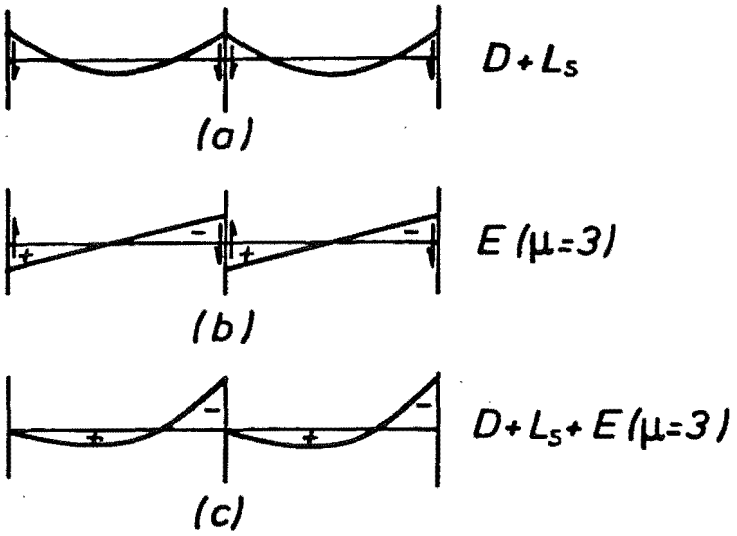

Figure 3.2. Gravity and Earthquake Moments
on First Cycle of Frame Displacement

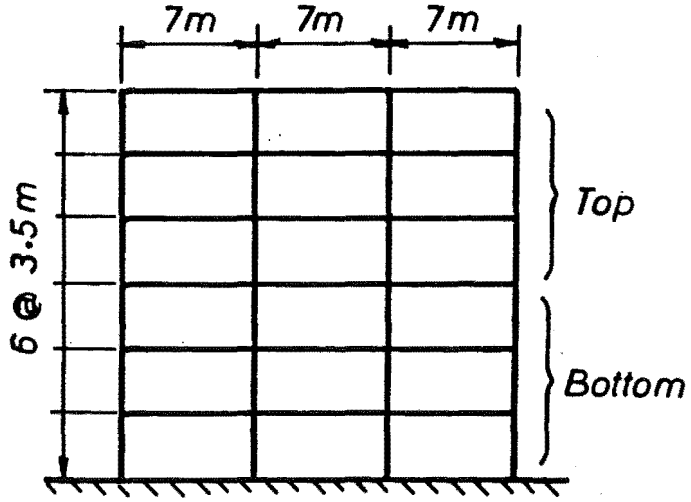

	Top	Bottom
Beams	410UB60	410 UB 54
Columns	310 UC118	310 UC 137

Figure 3.3.1. Frame #1 Dimensions and Member Sizes

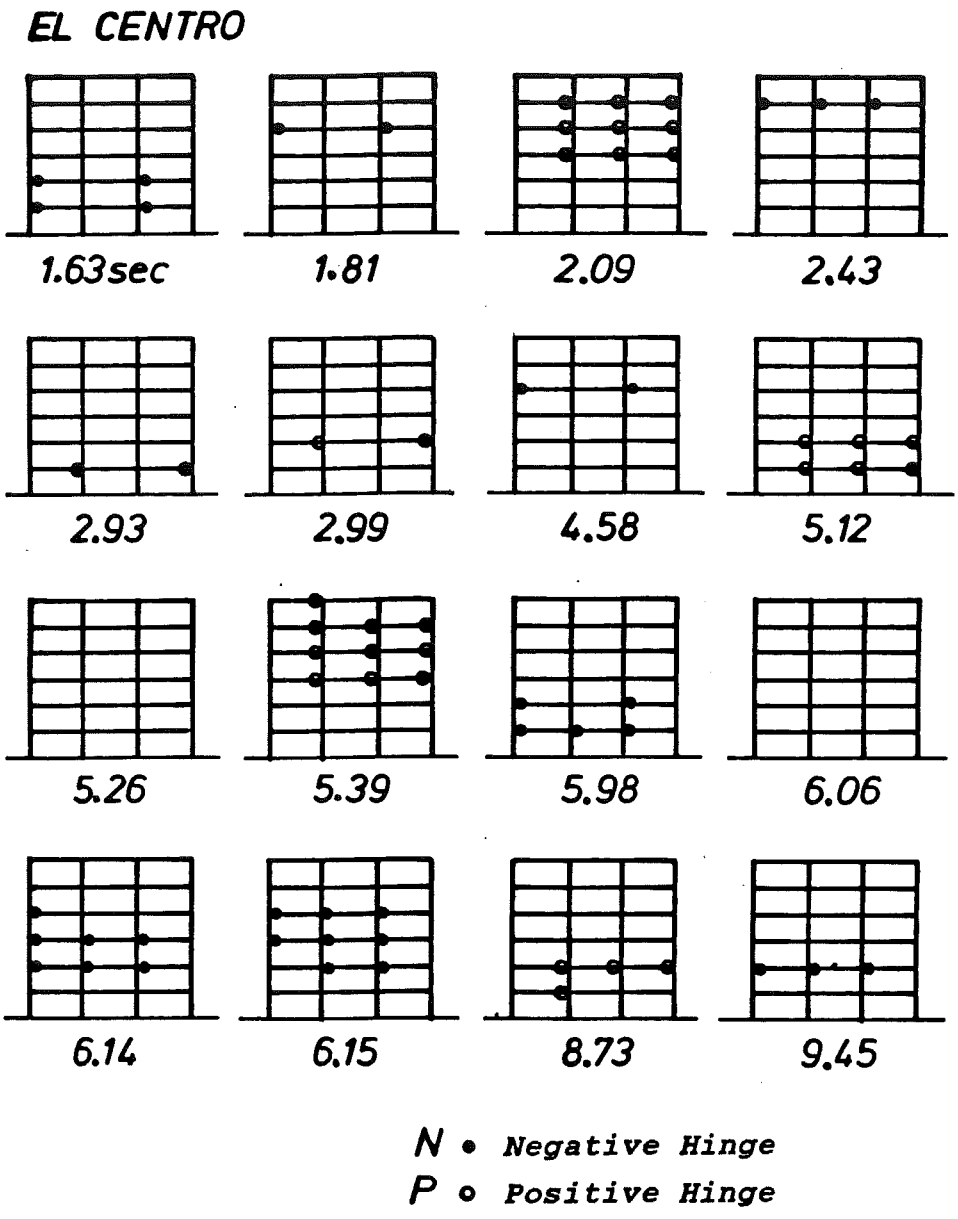

Figure 3.3.2. Hinge Formation in Frame #1
during the El Centro Earthquake

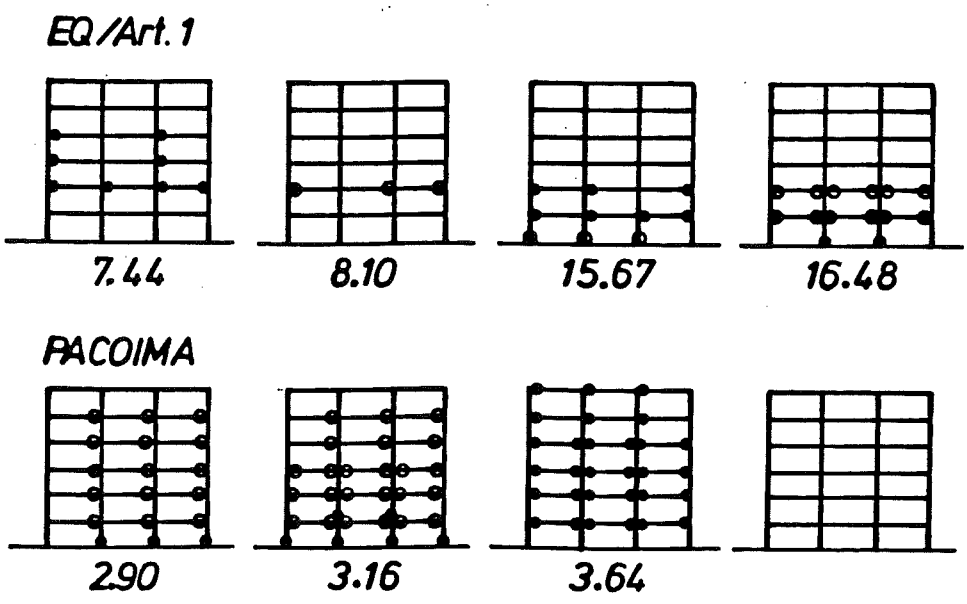

Figure 3.3.3. Hinge Formation in Frame #1
during EQ/ART1 and Pacoima Excitations

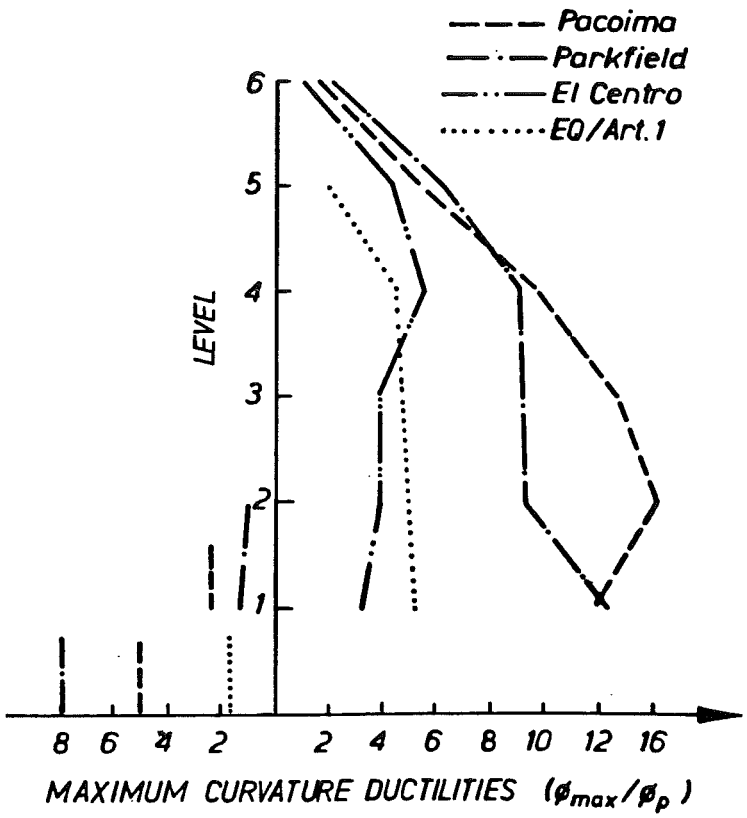

Figure 3.3.4. Frame #1 Maximum Member Curvature Ductilities

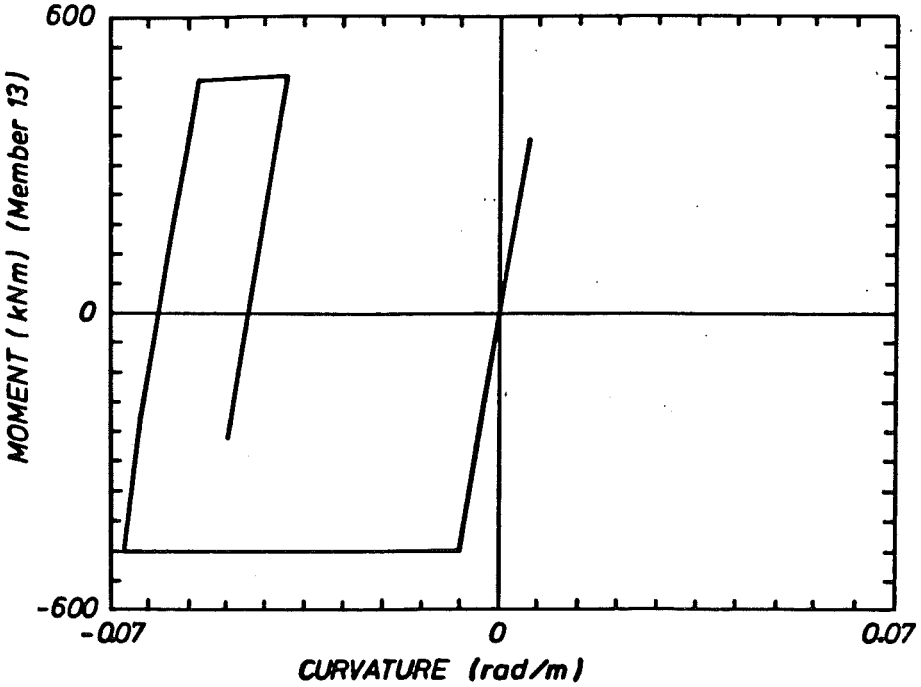

Figure 3.3.5. Moment-Curvature Relationship
at the Base of the External Column
during the Parkfield Excitation

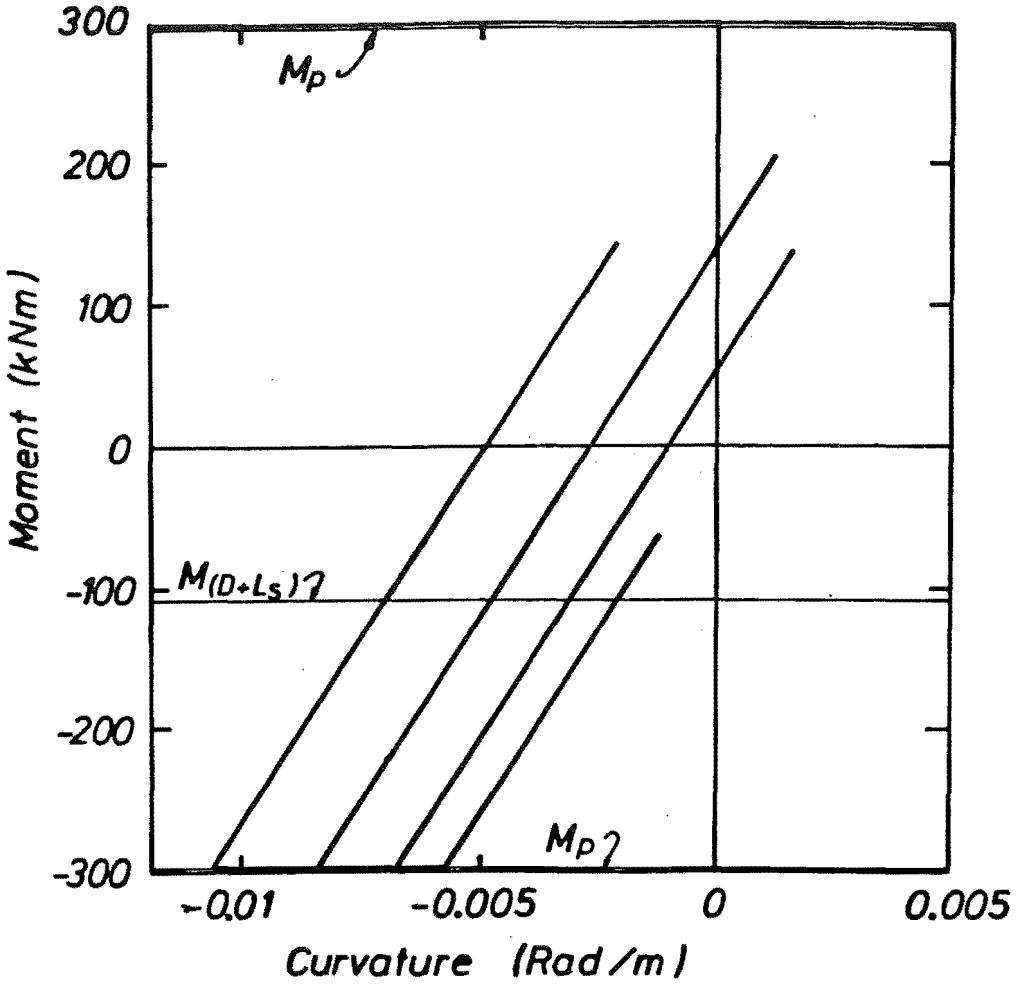

Figure 3.3.6. Moment-Curvature Relationship in the Second Storey Beam beside the External Column during the El Centro Excitation

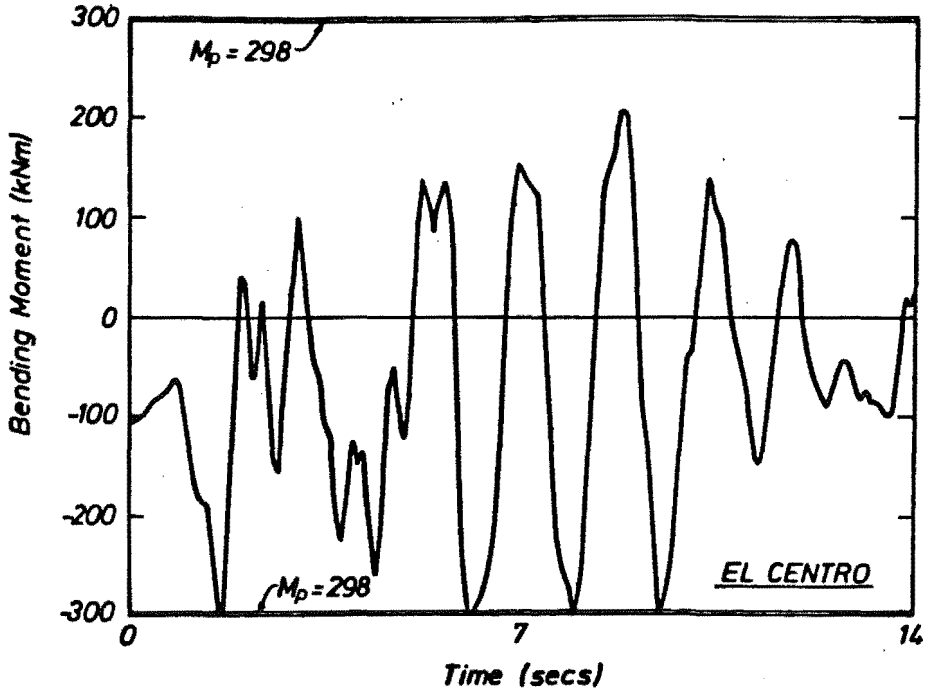

Figure 3.3.7. Bending Moment in the Second Storey Beam beside the External Column during the El Centro Excitation

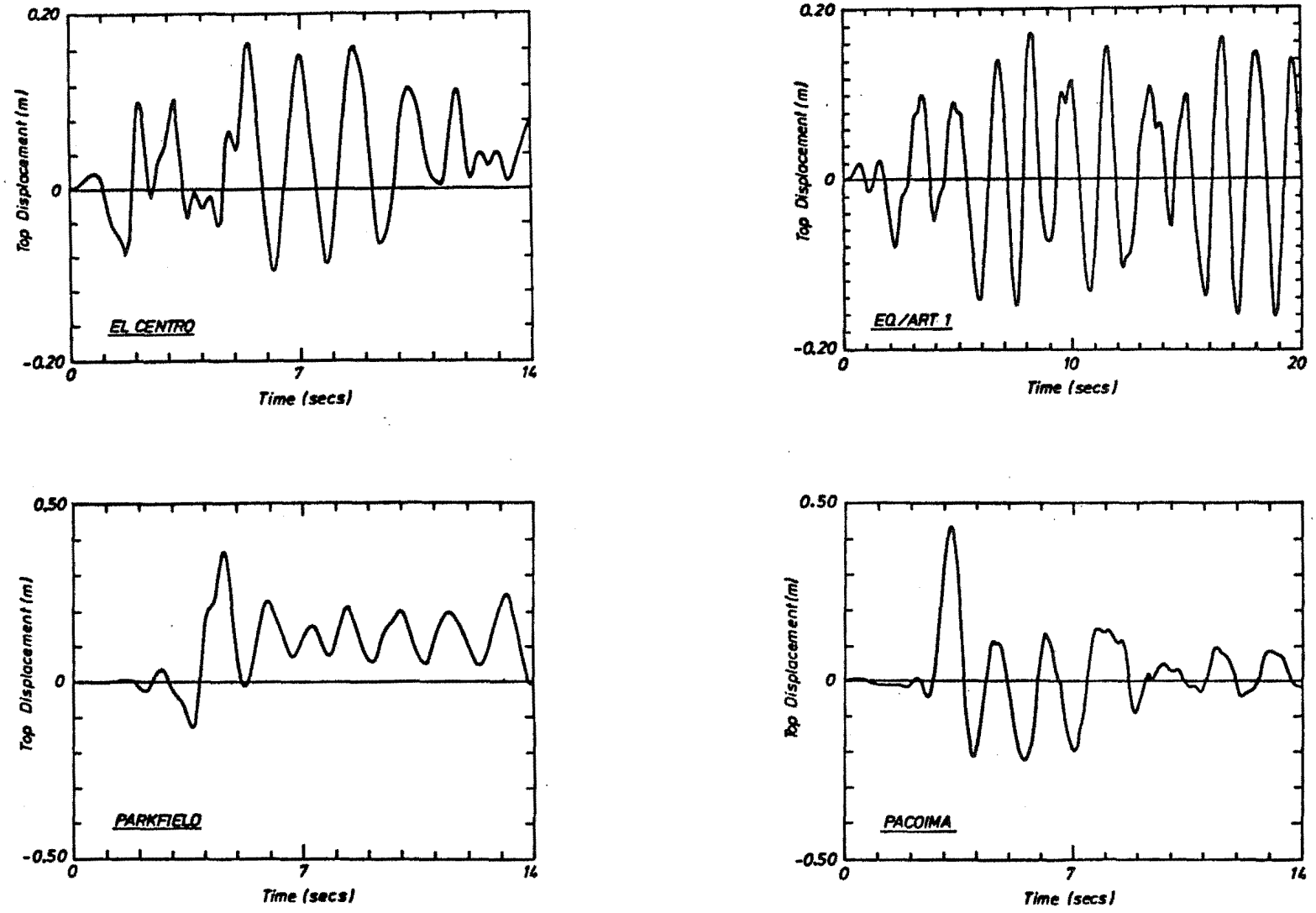

Figure 3.3.8. Displacement at the top of Frame #1 during various earthquake records

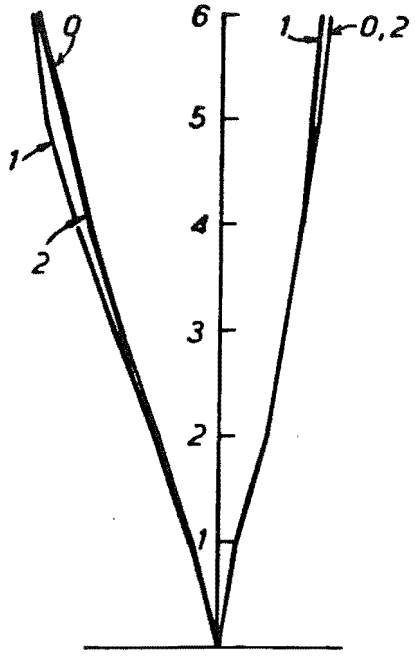

Figure 3.3.9. Effect of the P-delta Flag on the Displacement Envelopes of Frame #1 during the El Centro Excitation

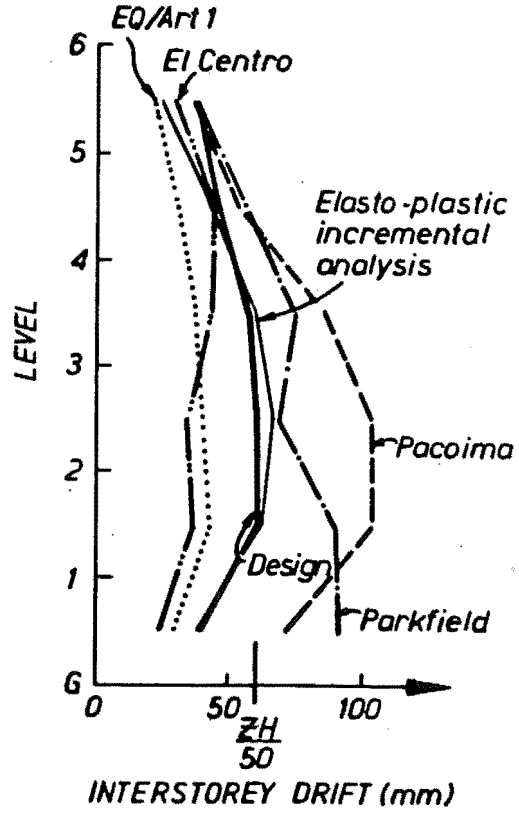

Figure 3.3.10. Interstorey Drift Envelopes during Different Earthquake Records

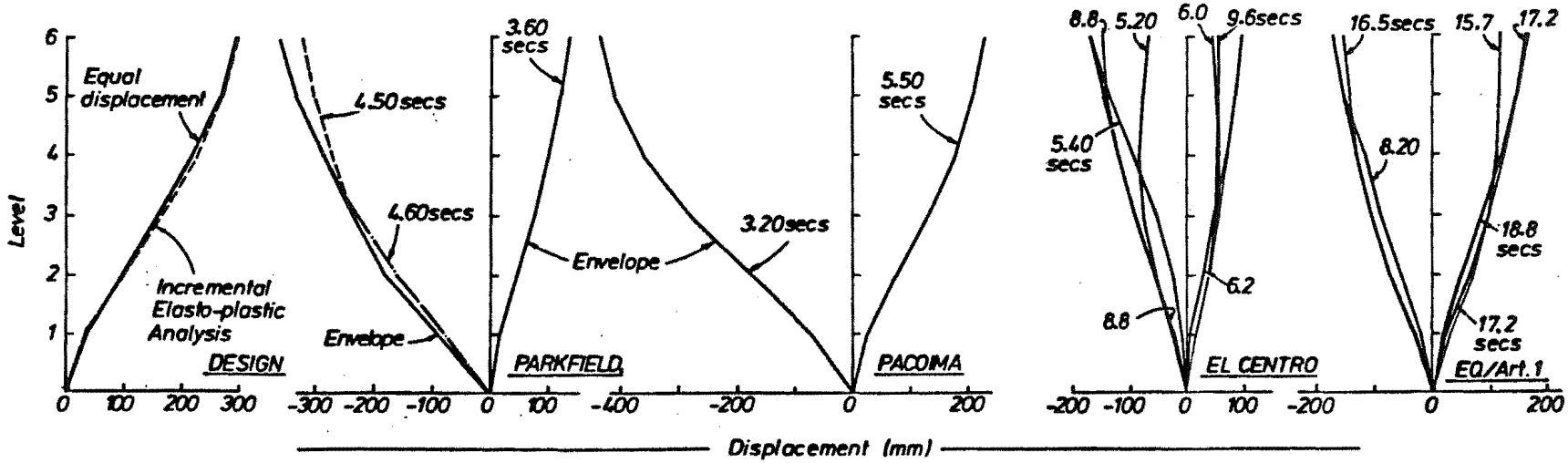

Figure 3.3.11. Displacement Envelopes
and Deflected Shapes at Specified Intervals
of Time of Frame #1

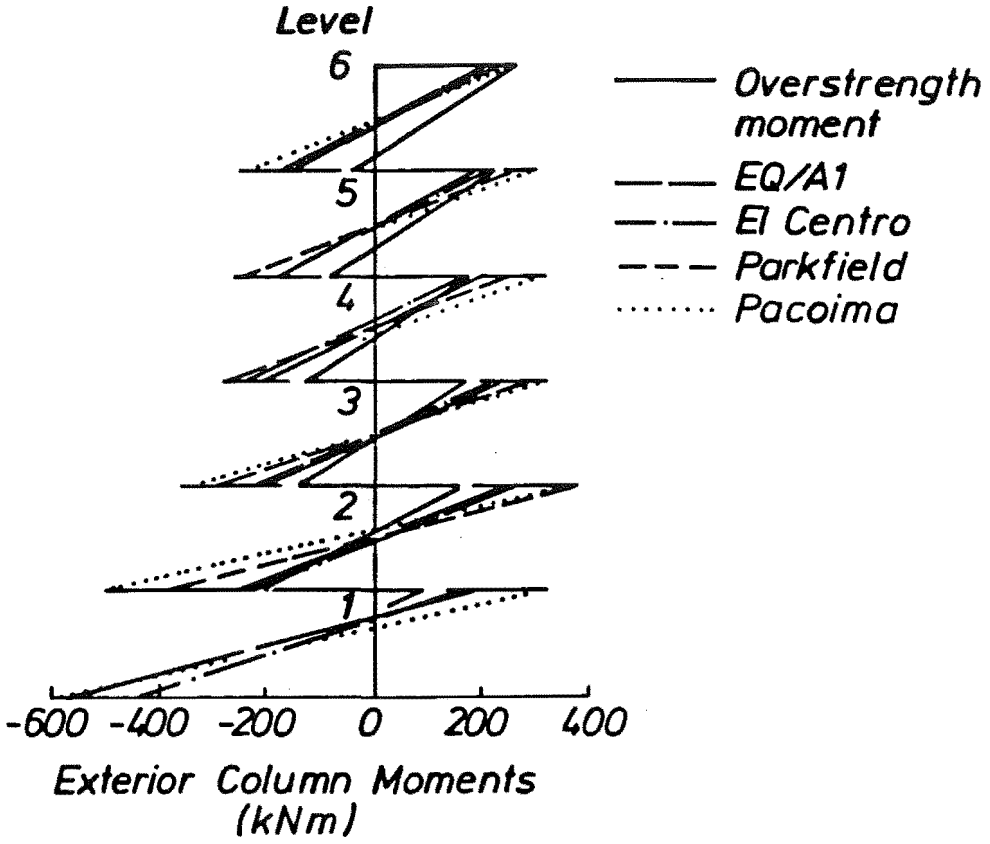

Figure 3.3.12. Frame #1 Exterior Column Moments (kNm)

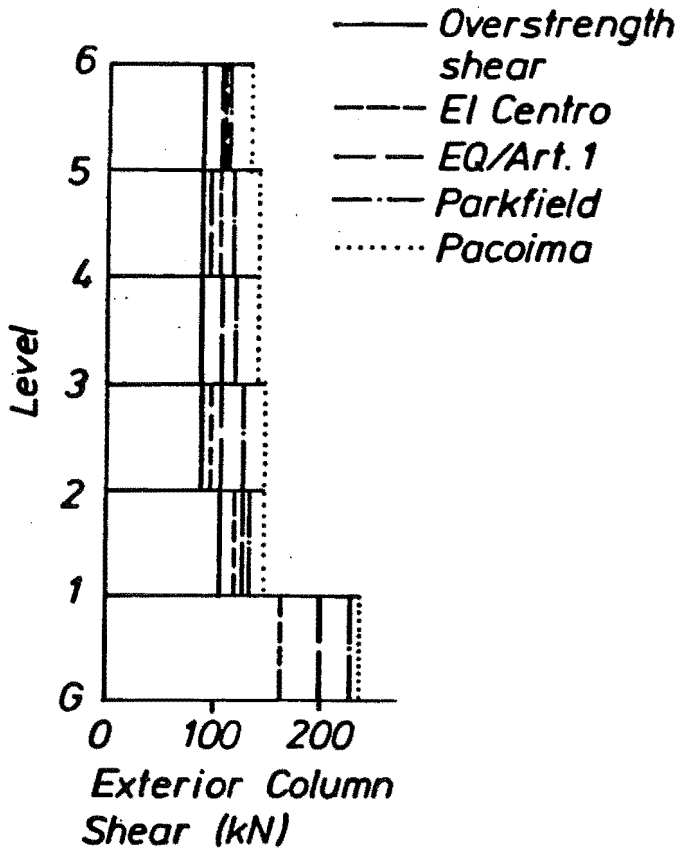

Figure 3.3.13. Frame #1 Exterior Column Shears (kN)

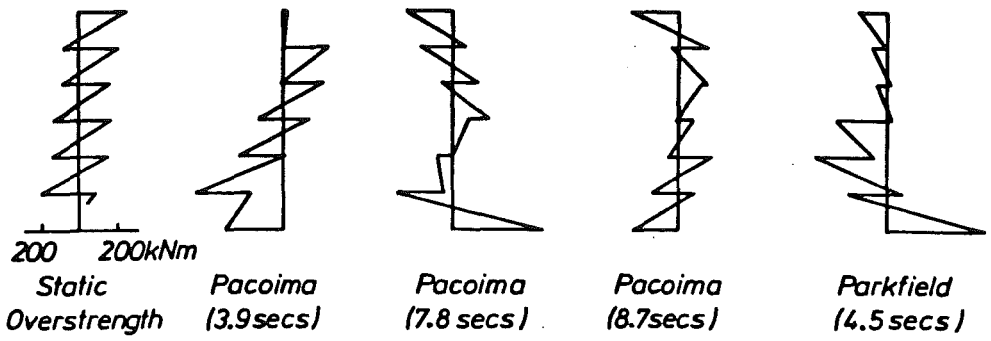

Figure 3.3.14. Frame #1 Exterior Column Moments at Specified Times

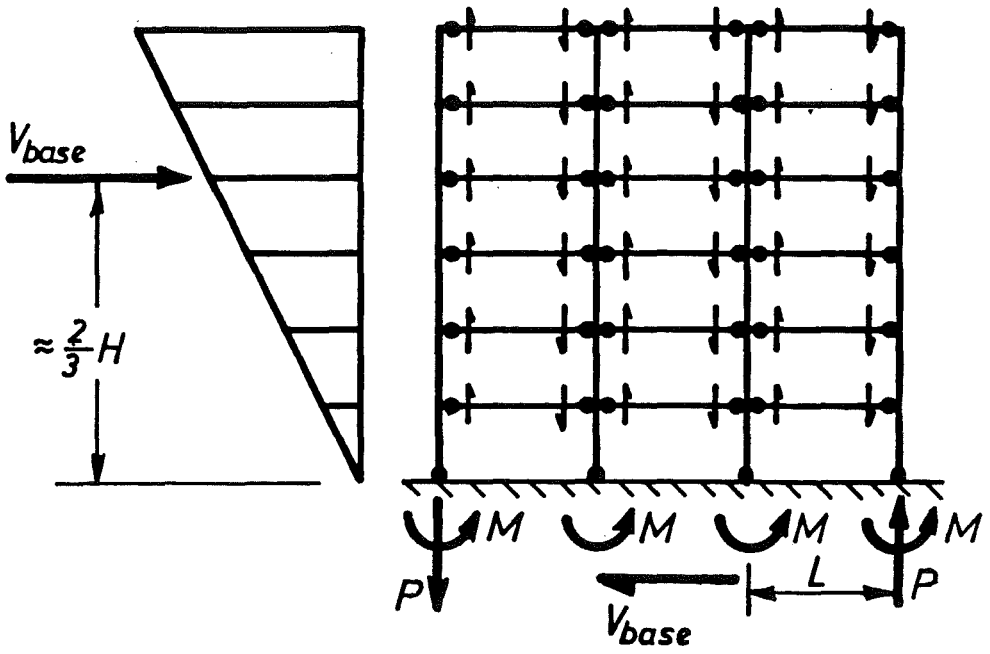

Figure 3.3.15. Forces for the Calculation of the Maximum Likely Base Shear

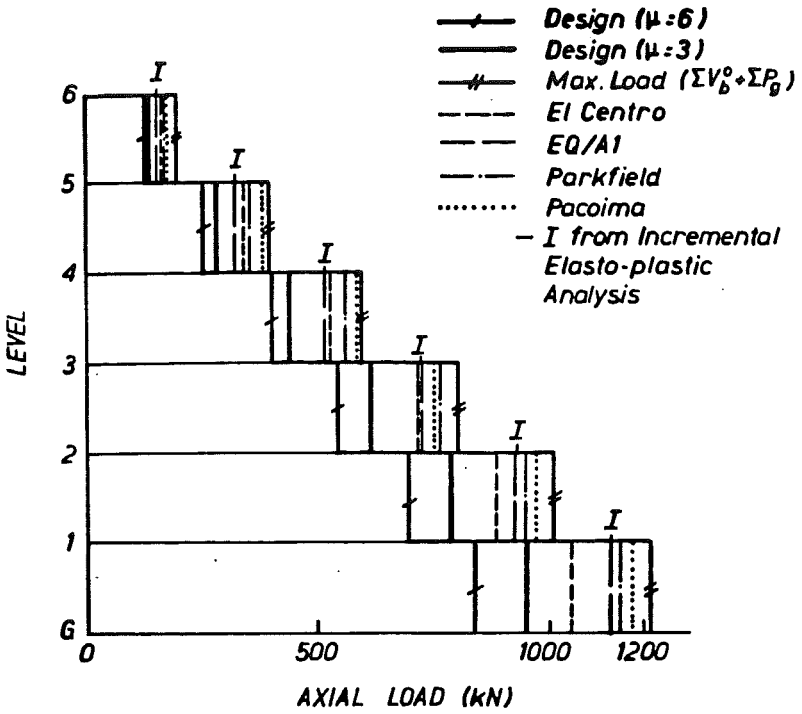

Figure 3.3.16. Frame #1 Exterior Column Axial Load

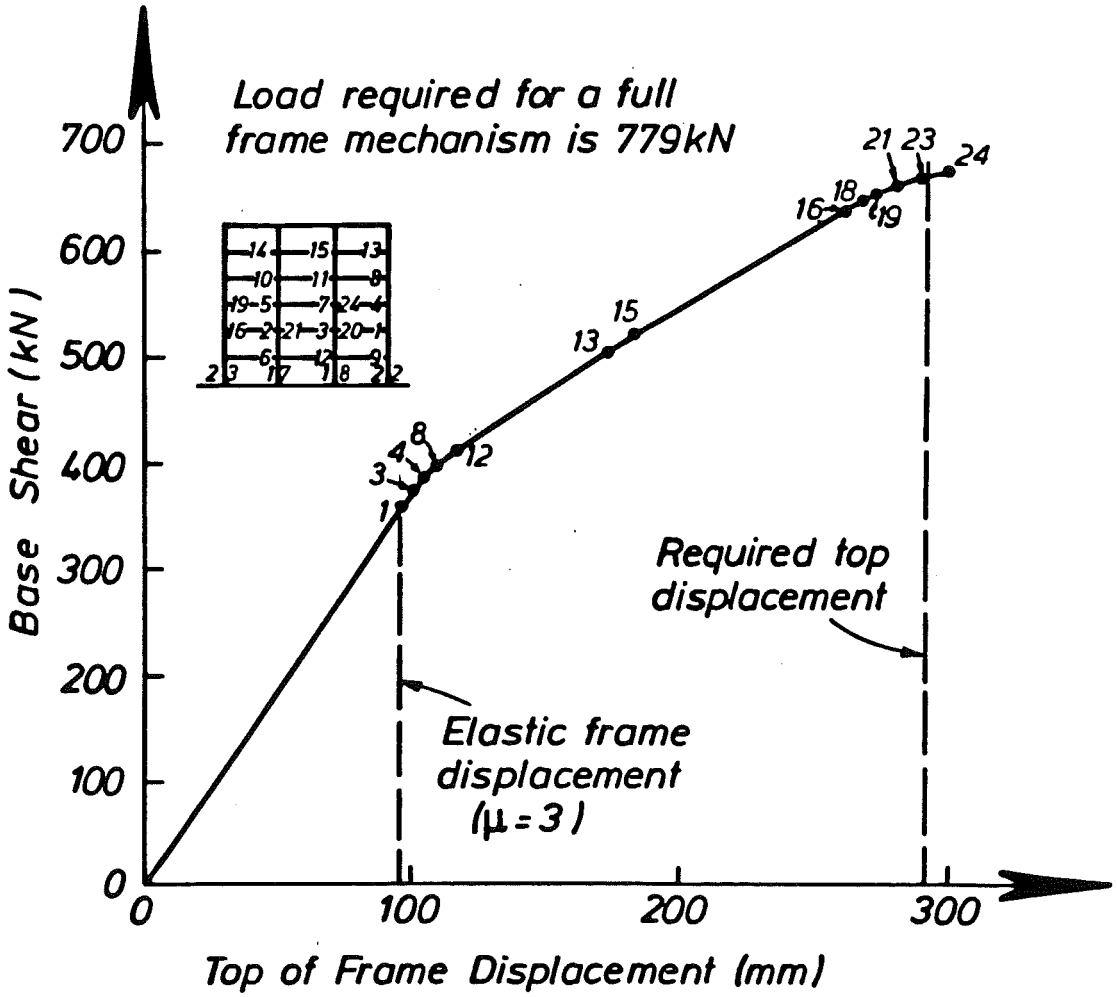

Figure 3.3.17. Frame #1 Top of Frame Displacement versus Base Shear and Order of Hinge formation during Elasto-plastic Analysis

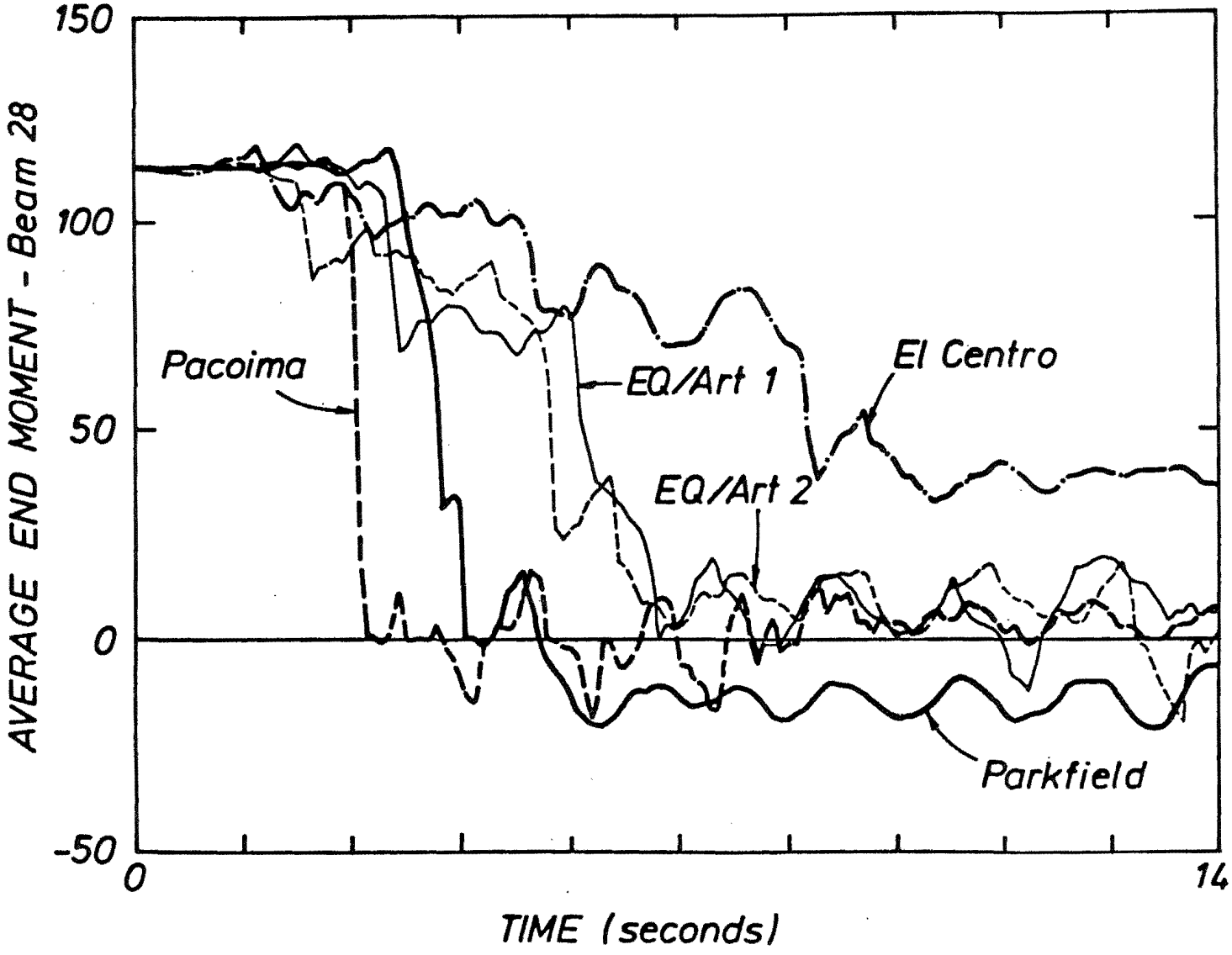

Figure 3.3.18. Average End Moment in the Exterior Second Storey Beam in Frame #1

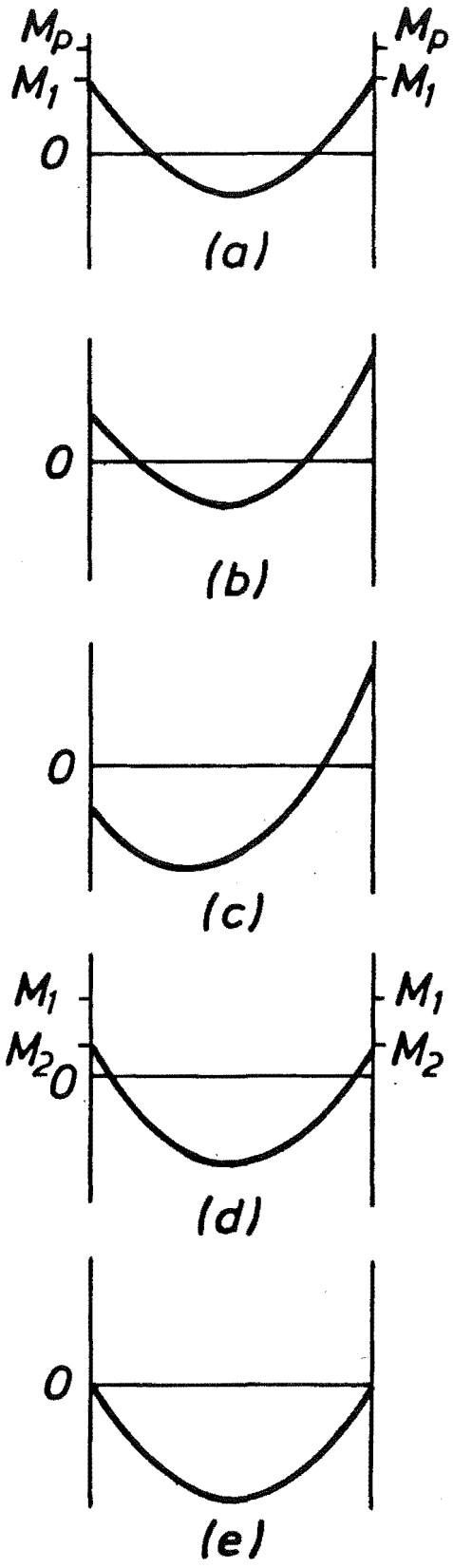

Figure 3.3.19. Shakedown of Beam Gravity Moments

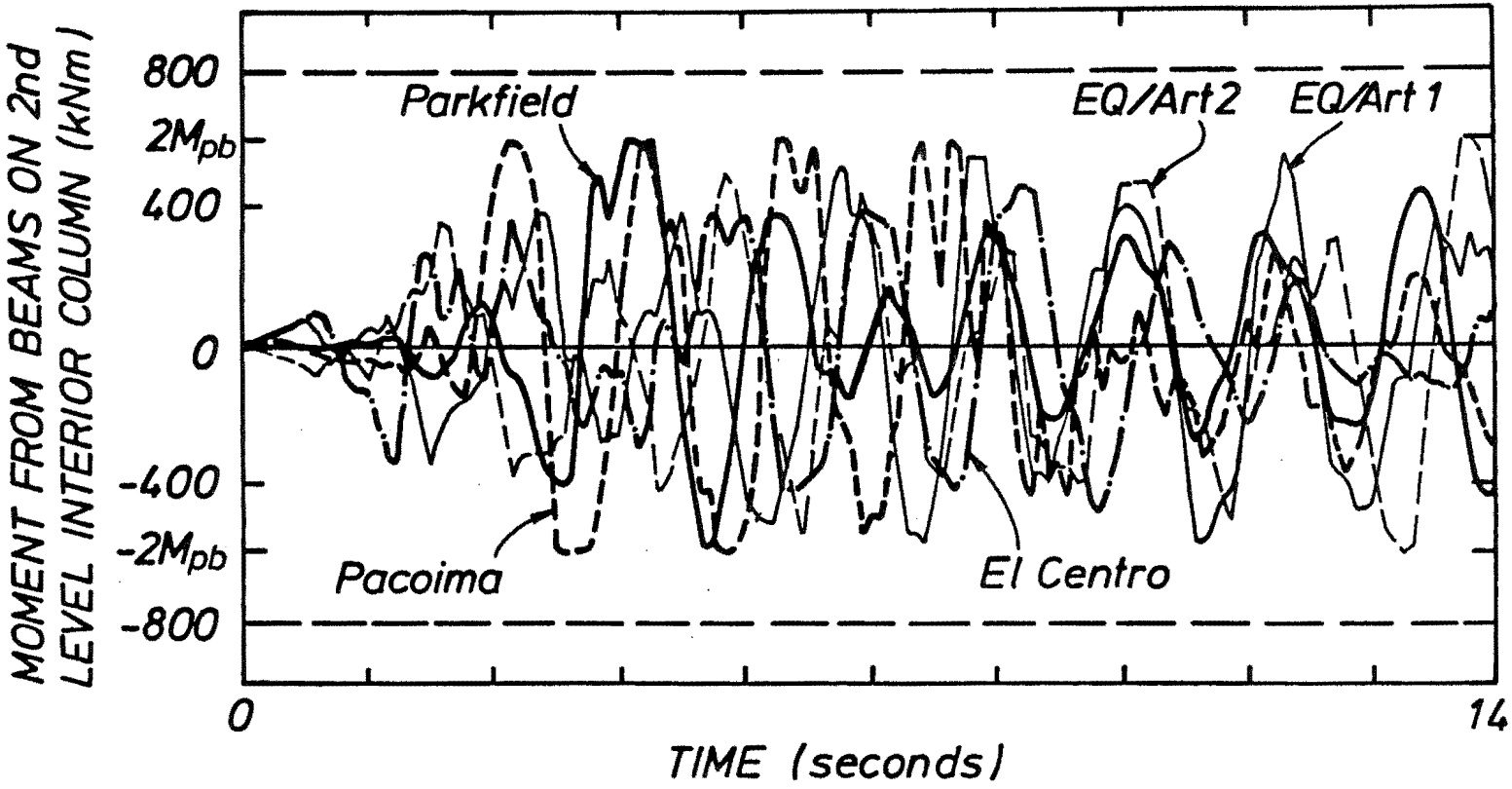

Figure 3.3.20. Moment from Beams on the Internal Column at the Second Storey of Frame #1 during Various Excitations

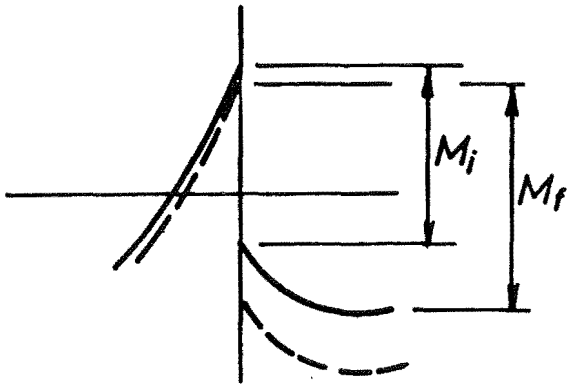

Figure 3.3.21. Possible Beam Moments applied to an Internal Column

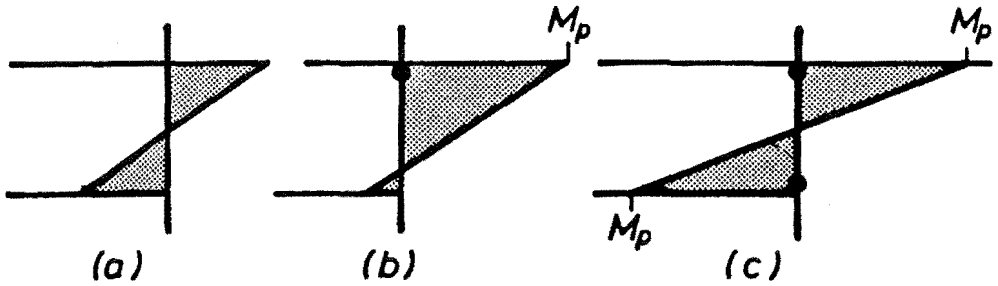

Figure 3.4. Hinging of a Column

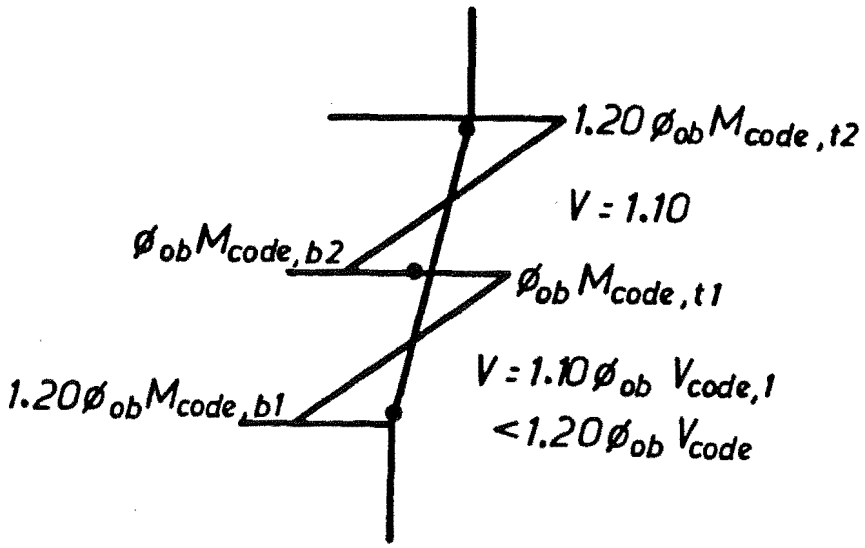

Figure 3.5. Protection Against Formation of a Partial Sidesway Mechanism

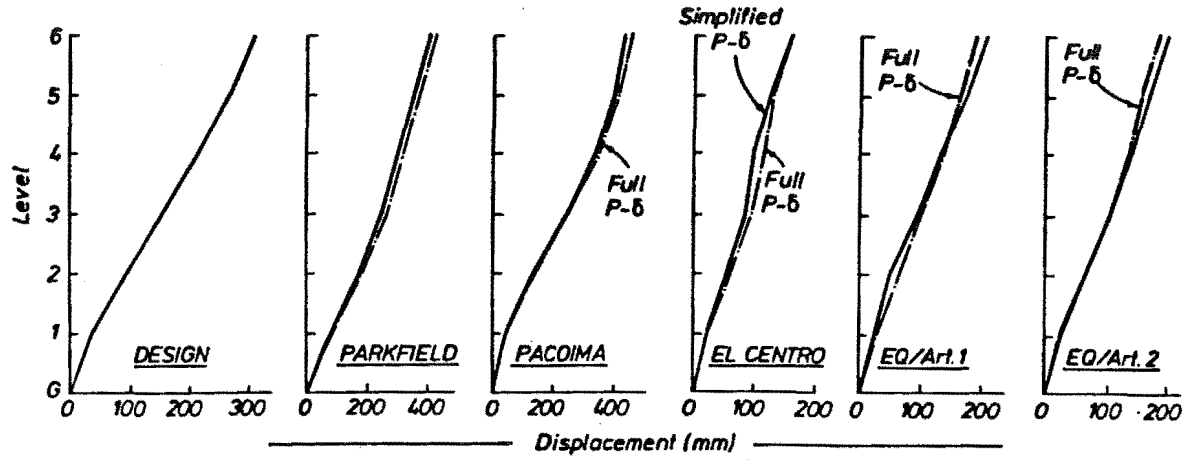

Figure 3.6.1. Frame #2 Displacement Envelopes

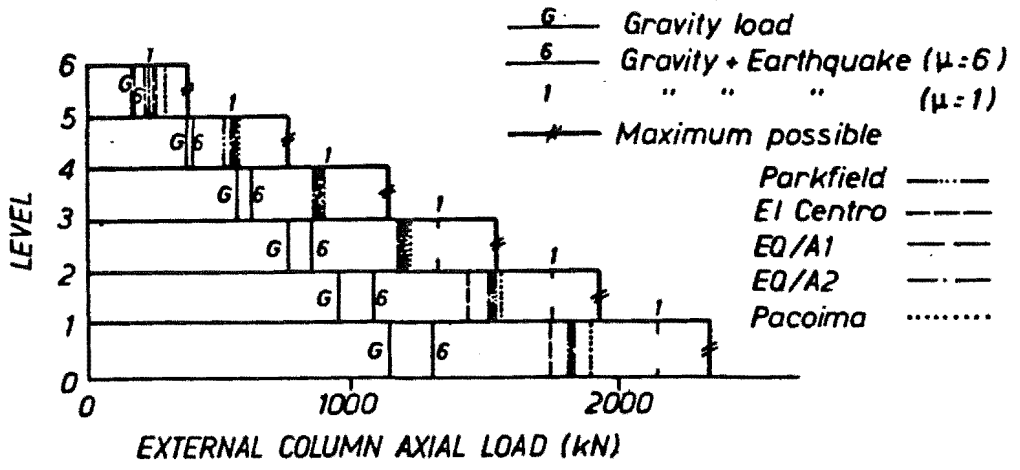

Figure 3.6.2. Frame #2 External Column Gravity Load

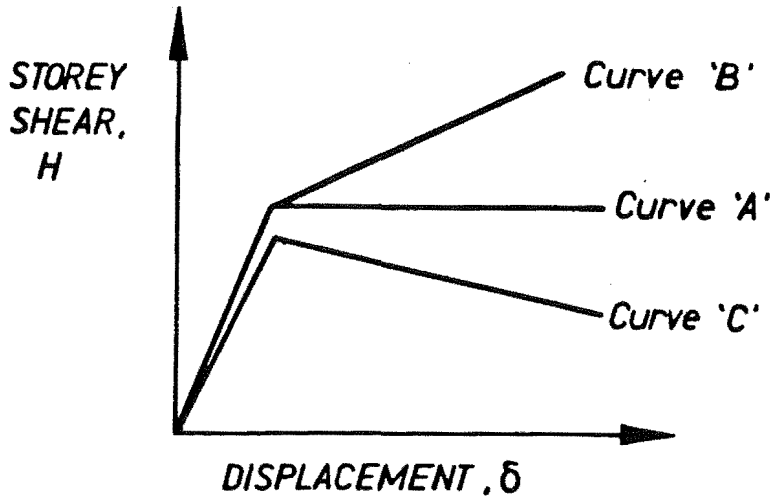

Figure 3.7. Storey Stiffness

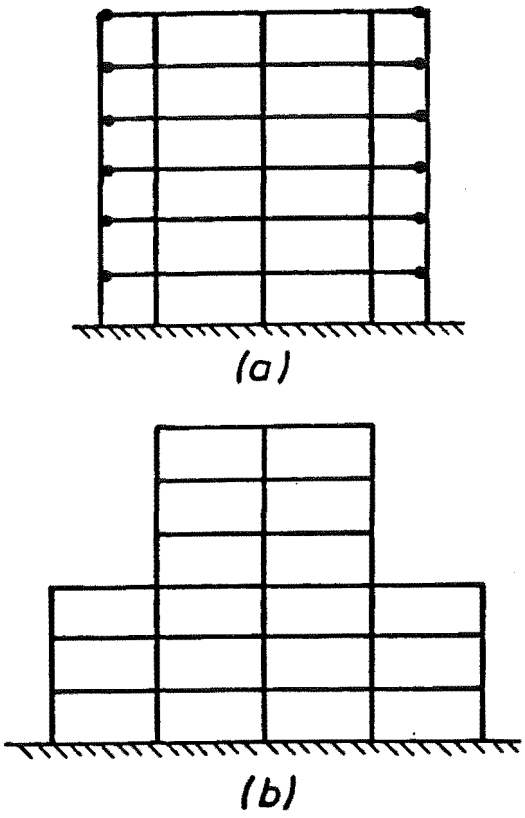

Figure 3.8. Irregular Frames

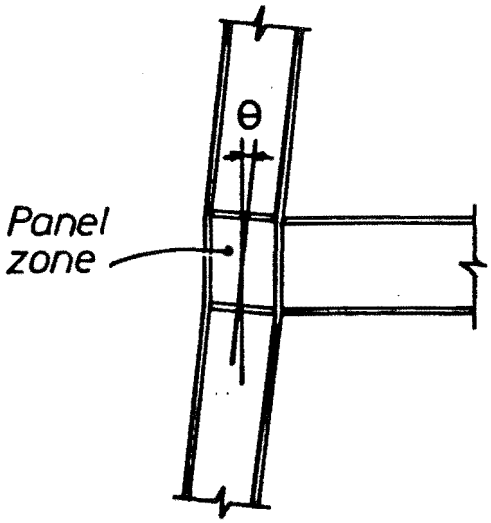

Figure 3.9. Panel Zone Deformation

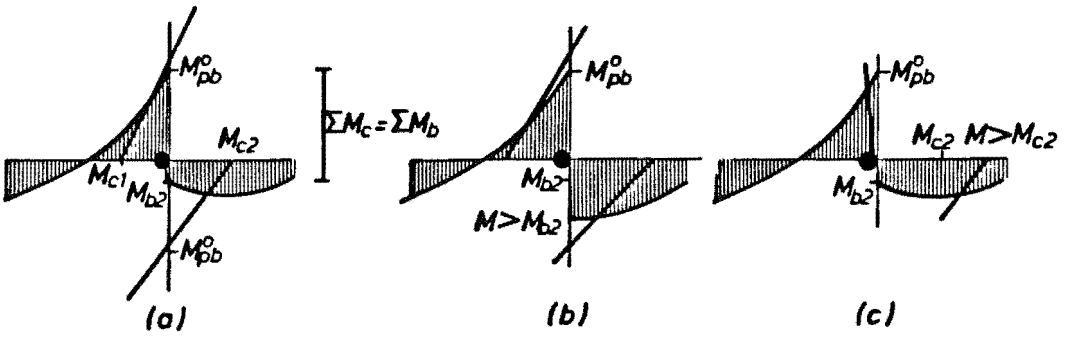

Figure 3.10. Column Design Moments

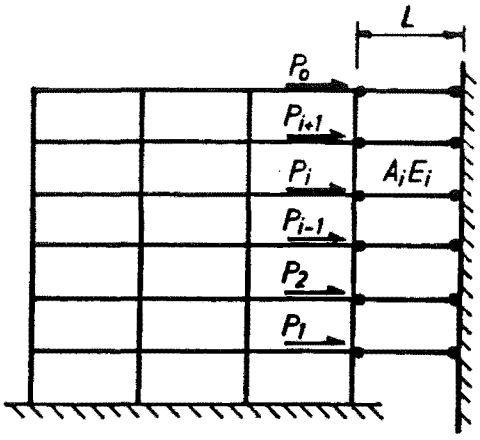

(a)

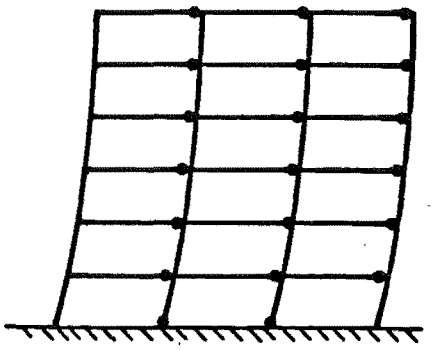

(b)

Figure 3.11. Deforming frame to Desired Displacements

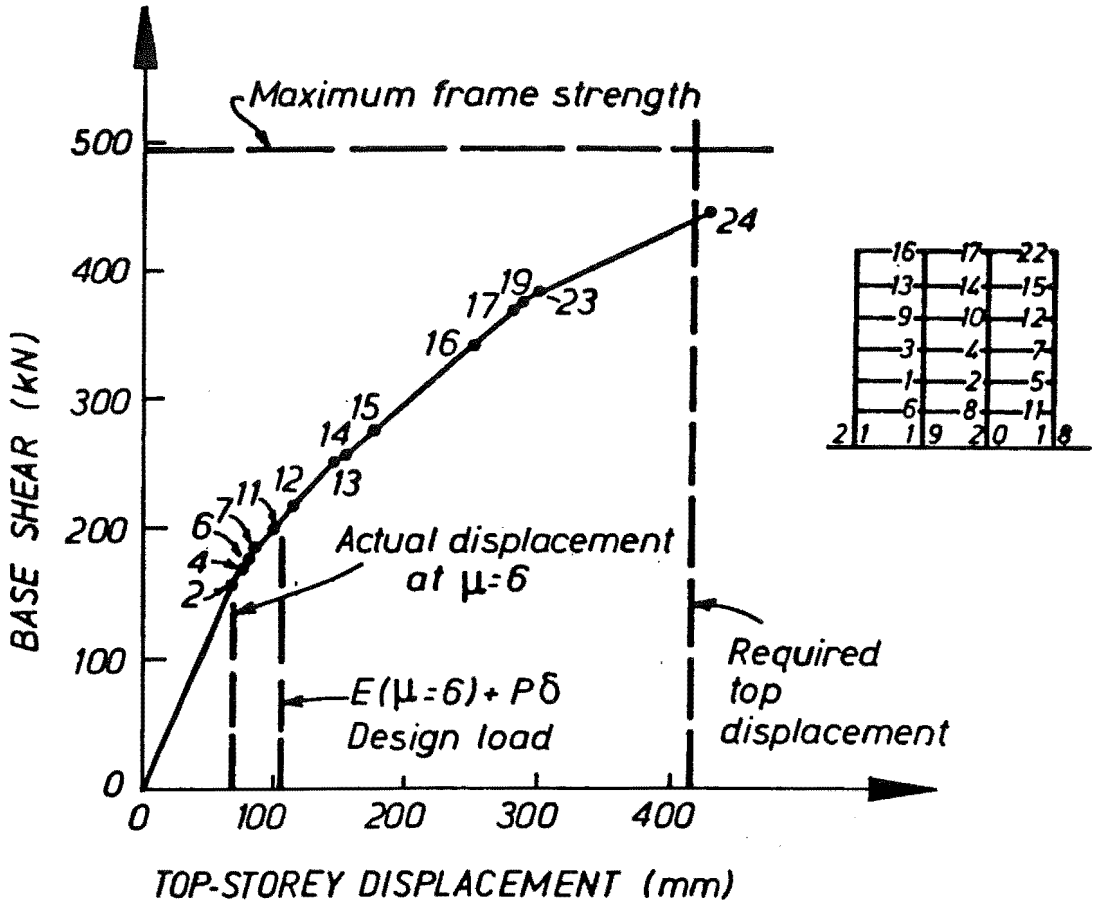

Figure 3.12. Frame #3 Top of Frame Displacement versus Base Shear and Order of Hinge formation during Elasto-plastic Analysis

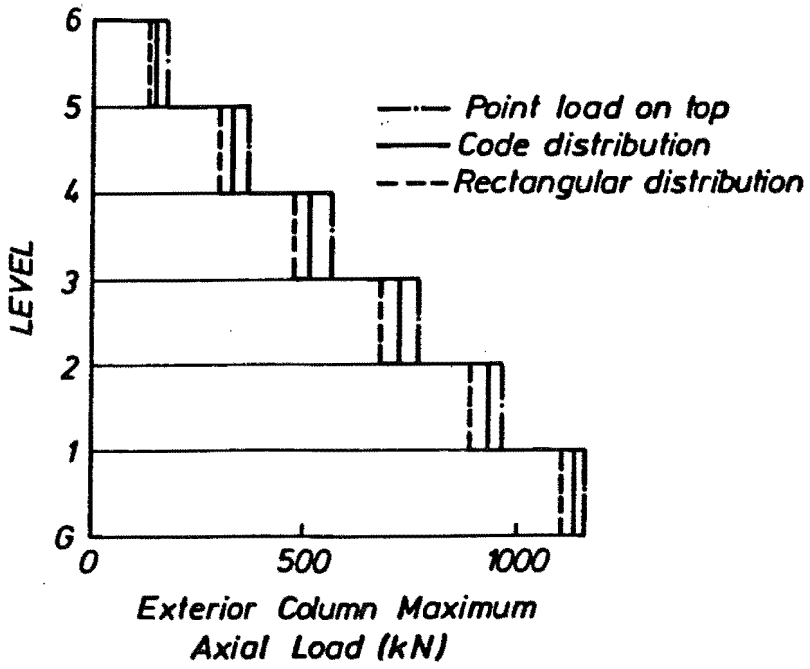

Figure 3.13. Frame #1 Exterior Column Axial Load during Elasto-plastic Analysis with Different Load Distributions

3.14 REFERENCES

3.1 Abernethy P., "Steel Frames back in High-Rise Favour", National Business Review, p15, November 5, 1987.

3.2 Paulay T., "Seismic Design of Ductile Moment-resisting Concrete Frames. Columns - Evaluation of Action", Bulletin of the New Zealand National Society for Earthquake Engineering, Vol. 10, No. 2, Jan. 1977.

3.3 SANZ, "Commentary: Design of Concrete Structures", NZ3101 Part 2, 1982.

3.4 SANZ, "Code for Design of Steel Structures (with commentary)", NZS3404, New Zealand Standard, 1977.

3.5 -, 1987 Code Change Submittals, UBC, Suggested Revisions to the 1985 Editions of the Uniform Codes. Further Study Items and Submittals for 1987. Building Standards, V. 55, No. 6, Pt 3. Nov-Dec, 1986.

3.6 Deliberations of the New Zealand Study Group for the Design of Steel Structures, Bulletin of the New Zealand National Society for Earthquake Engineering, Vol. 18, No. 4, December 1985.

3.7 Paulay T., "Seismic Design in Reinforced Concrete: The State of the Art in New Zealand", Bulletin of the New Zealand National Society for Earthquake Engineering, Vol. 21, No. 3, September 1988, pp208-232.

3.8 Martinez-Romero E., "The Behaviour of Steel Buildings after the Earthquakes of September 1985", Bulletin of the New Zealand National Society for Earthquake Engineering, Vol. 20, No. 1, March 1987.

3.9 SANZ, "General structural design and design loadings for buildings", DZ4203 Draft for comment, New Zealand Standard, 1986.

3.10 Carr A. J., "RUAUMOKO", Computer Program Library, Department of Civil Engineering, University of Canterbury. May 1986.

3.11 Galambos T. V. and Lay M. G., "Studies on the Ductility of Steel Structures", *Journal of the Structural Division*, ASCE, Vol 91, ST4 (1965).

3.12 Jury R. D., "Seismic Load Demands on Columns of Reinforced Concrete Multistorey Frames", Master of Engineering Report, Department of Civil Engineering, University of Canterbury, 1978.

3.13 Tompkins D. N., "The Seismic Response of Reinforced Concrete Multistorey Frames", Research Report No. 80-5, Department of Civil Engineering, University of Canterbury, 1984.

3.14 Goel S.C., "P-delta and Axial Column Deformation in Aseismic frames", J. Struct", *Journal of the Structural Division*, ASCE, Vol. 95, No. ST8, August 1969.

3.15 Krawinkler H., "Seismic Code Developments for Steel Structures", Pacific Structural Steel Conference, Vol. 3, p361-372. Auckland, 1986.

3.16 Krawinkler H., "Tentative Lateral Force Requirements Background to Selected Steel Provisions", 54th Convention of the Structural Engineers Association of California, San Diego, 1985.

3.17 Fenwick R. C. and Davidson B. J. "Moment-Redistribution in Seismic Resistant Concrete Frames", Pacific Conference on Earthquake Engineering, Wairakei, New Zealand, August 1987, Vol. 1, p95-106.

3.18 Paulay T., Personal Correspondence, 1987.

3.19 Tjondro J. A., "Analytical Investigation of P-delta Effects in Medium Height Steel Moment-Resisting Frames", Master of Engineering Report, Department of Civil Engineering, University of Canterbury, 1988.

3.20 Krawinkler H., Popov E. P. and Bertero V. V., "Inelastic Behaviour of Steel Beam-to-Column Subassemblages", UCB/EERC 71-7, Oct 1971.

3.21 SANZ, "Code for Design of Steel Structures (with commentary)", NZS3404, New Zealand Standard, 1989.

3.22 MacRae G. A., "EPF - Two Dimensional Elasto-Plastic Frame Analysis Program". Department of Civil Engineering, University of Canterbury. August 1987.

3.23 Clifton G. C., "Seismic Design Procedures for Ductile Steel Moment-Resisting and Eccentrically Braced Frames", Pacific Conference on Earthquake Engineering, New Zealand, Vol. 2, pp35-46, 1987.

3.24 Robinson L. M., "Towards a General Capacity Design Procedure for Buildings", IPENZ Conference, Dunedin, pp95-106.

3.25 Mortazavi M. R., "The Influence of Section Slenderness on the Inelastic Rotation Capacity of I-shaped Steel Columns", ME Thesis, Department of Civil Engineering, University of Canterbury, February 1989.

3.26 SANZ, "General structural design and design loadings for buildings", DZ4203 Draft for comment, New Zealand Standard, 1989.

3.27 Bertero V. V. and Kamil H., "Nonlinear Seismic Design", Can. J. Civ. Eng., Vol. 2, 1975.

Chapter 4

Second Order Effects

4.1 INTRODUCTION

Traditionally, linear elastic analyses have been used in the design and analysis of multistorey steel frames. These analytical techniques usually ignore the influence of geometric effects on the response of a structure. In more recent times there has been increased interest in these second order effects and in particular that due to the combination of gravity loads and large displacements, commonly known as the P-delta effect, and its consequences on the response of members in a frame.

The study of the P-delta effect has usually been carried out on elastic structures subjected to static loading conditions. More recently, inelastic effects have been studied. Very little research has been carried out into the P-delta effects of frames responding inelastically to earthquakes. The design approach in New Zealand has been to minimise the possible influence of P-delta effects by tightly controlling the frame design lateral displacements. These deflection limits often determine the sizes of members in steel structures. If this design approach could be modified to account for actual P-delta forces acting on the frames, less strict limits on displacement may be permitted and a saving of material may result.

The seismic response of frames incorporating the P-delta effect is complex as the gravity forces alter the period of the frame and thus the amount of excitation to which the frame may be subjected. For elasto-plastically responding structures the axial forces may cause a negative post-elastic lateral stiffness. Krawinkler [4.1] has stated that "The P-delta effect may cause negative structural stiffness and consequently the drifting of the seismic response and the amplification of lateral deflection to the point of dynamic instability." This is contrary to the assumptions of the equal displacement concept in which the displacement which occurs is assumed to be independent of the post-elastic stiffness of the deforming elements. It is also contrary to the results obtained by Stewart [4.2] for frames with different positive values of post-elastic stiffness which show that there is no correlation between the displacement measured and the post-elastic stiffness used. However, for negative values of post-elastic stiffness, a positive correlation has been found by Bernal [4.3] between the amount of negative post-elastic stiffness and the increase in response.

4.2 LITERATURE SUMMARY

Previous analyses and recommended design methods for the P-delta effect in frames responding inelastically to earthquake ground motions are described below.

Goel [4.4] found that while the response of elastic frames was influenced by as much as 10%, the P-delta effect on the inelastically responding frames was insignificant, the change being of the order of 1%. The periods of the frames analysed were 1.25 and 1.36 seconds and interstorey displacements were low.

Andrews [4.5] has obtained drift limits for frames using static methods to keep the energy lost by the P-delta effect to less than 10% of the total hysteretic energy. If the displacement ductility is 4, limiting the energy loss to 10% is similar to limiting the loss of strength at first yield to 5% of the yield strength as suggested by the steel structures code [4.6] . The drift limits derived are zone dependent. That is, in regions of low seismicity the drift limits are more severe than in regions of high seismicity. Recommendations in the draft loadings code [4.7] cause the minimum stiffness of buildings in every seismic zone to be the same. These drift limits often govern the sizes of members in steel frames in regions of high seismicity, and will almost always govern member sizes of frames in regions of low seismicity.

Paulay [4.8] has suggested that the P-delta effect may be ignored in reinforced concrete frames when the stability index $W\delta_o/(Vh)$ is less than 0.15. The ratio V/W is the ratio of the base shear to the weight of the structure and δ_o/h is the interstorey drift index. It was also suggested that a suitable method for compensating for the effect of P-delta secondary moments is to increase the strength of the structure without altering the member sizes.

Paulay's stability index is shown as a function of period and ductility in Table 4.1. The interstorey drift ratio of 0.017 (Z/50 with Z = 0.85 [4.7]) was assumed and the value of V/W of $C_\mu RZ$ was used, where Z was taken as 0.85 and R was taken as 1.0. In Table 4.1, Paulay's stability index increases with period and displacement ductility. Therefore, the P-delta effects would be expected to be less significant in elastically-responding frames with shorter natural periods than in inelastically-responding frames or in frames with long natural periods. If a lower zone factor is used, this will

decrease the base shear ratio, V/W, and P-delta effects would also be expected to increase. The dependence of the zone factor upon the magnitude of the P-delta forces has already been shown by by Andrews [4.5].

Montgomery [4.9] suggested that P-delta effects need only to be considered when the ratio of the maximum storey drift to the yield storey drift is greater than 2, or when the ratio of the base shear to the weight of the structure, V/W, is less than 0.10. These recommendations are very similar to those of Paulay [4.8]. If the interstorey drift index is assumed to be 0.017, an equivalent stability index in the form that Paulay uses is $W\delta_o/(Vh)$ is less than 0.17 for P-delta to be insignificant. A stability factor approach was also shown to be a reasonable means of representing the P-delta effect for structures which respond in an elastic, or nearly elastic manner.

Table 4.1
Paulay's Stability Coefficient for different Periods and Ductilities

Period (secs)	0.5	1.0	1.5	2.0	2.5	3.0	3.5	4.0
$W\delta_o/Vh$ μ=1	.027	.040	.058	.080	.095	.105	.121	.143
$W\delta_o/Vh$ μ=6	.122	.240	.353	.480	.558	.632	.727	.827

Bernal [4.3], based on the work of Jennings and Husid [4.10], Takizawa and Jennings [4.11], and his own previous work [4.12] has shown that the change in response resulting from dynamic P-delta effects is usually negligible in structures which respond elastically, but may become the dominant factor in the behaviour of structures in which significant yielding occurs.

Bernal examined P-delta effects from the perspective of inelastic spectral ordinates which were found by the difference between the results of analyses of single degree of freedom oscillators subjected to specified earthquake records with and without the P-delta effect. Amplification factors were obtained statistically reflecting the P-delta effect for the particular ductility and the stability index selected. Dynamic analyses indicated that there was no significant correlation between the displacement amplification and the natural period. The amplification, α, is a function of the stability coefficient, θ, and the design displacement ductility, μ. The stability coefficient, θ, is equal to $\delta_o/(hC_e)$, where C_e is the elastic base shear coefficient. The amplification factor was found from Equation 4.1 which is based on a regression analysis.

$$\alpha = \frac{1 + \beta\theta}{1 - \theta} \qquad \text{Equation 4.1}$$

The maximum suggested value of interstorey drift assuming an amplification of 10% is $\delta_o/h = 0.1C_e/(\beta + 1.1)$, where $\beta = 1.87(\mu-1)$. This approximately corresponds to a maximum value of Paulay's stability index, $W\delta_o/(Vh)$, of 0.06 for P-delta effects to be able to be ignored. This value is much more conservative than that calculated by Paulay.

Tjondro [4.13] found that P-delta effects altered the response after the interstorey drift ratio was larger than 0.02. An approximately linear relationship between the interstorey drift and the beam inelastic rotation demand for the frames analysed was established. From these results it seems that the maximum design level drift should not be too large or beam inelastic rotation capacities may be exceeded.

Galambos [4.14] described a method in which a column with a negative stiffness slaved to the horizontal displacements of a frame can model the P-delta effect on that frame.

The New Zealand steel code [4.6] states that if P-delta moments "at a level exceed 5% of the plastic moment capacity of the beams framing into the column at that level, then the strength of the frame shall be increased to carry the P-delta moments". The P-delta forces must be calculated in order to verify that the P-delta moments are not more than 5% of the total moments so that P-delta effects may be ignored.

The AISC-LRFD code [4.15] suggests that the inelastic column moments may be magnified by $1/(1 - \Sigma P_u(\delta_o/\Sigma HL)$ to allow for the second order effect.

The emphasis is on the column strength in both of the code methods [4.6,4.15]. An additional effect which is not taken into account is that the ductility demands of the inelastic members must increase to sustain the increased displacements expected as a result of the P-delta effect.

4.3 METHODS OF DESIGN FOR THE P-DELTA EFFECT

In the literature summary most of the papers dealing with P-delta discussed interstorey drift limits under which the P-delta effect would be negligible. Only two of the papers discussed the influence of P-delta on the behaviour of a frame beyond these limits. Those were the papers of Bernal [4.3], in which the displacements were amplified, and that of Paulay [4.8] in which it

was suggested that the frame be strengthened to allow for P-delta effects. Bernal [4.16] has incorporated his method for the estimation of P-delta effects, based on the results of 4 earthquake records, into a design procedure.

Paulay's method states that the strength of the structure may be enhanced to cope with the P-delta effect and as shown in Figure 4.1. It is this method which is suggested because of its conceptual simplicity and ease of implementation, however further verification of its validity is required. In Figure 4.1 the lateral force at the maximum displacement is the same both when there is no P-delta effect, and when the P-delta effect is included in design. At this point the secant stiffness, K_s, is the same in both cases. The secant stiffness has been shown to be very important in the estimation of the seismic response by both Turkington [4.17] and Andriono [4.18].

A method used by Galambos [4.14] with the negative stiffness of the columns enhanced to represent the actual displacements could well be used with Paulay's method, but the modelling required is slightly more complex than the modelling method described below.

4.4 PROPOSED DESIGN METHOD

There are two effects which should be considered in the design for the P-delta effect. They are:

1) the softening of the structure due to gravity loads in the columns, and
2) the overturning forces caused by the structure being laterally displaced.

The draft Australian steel structures code [4.19] indicates that the softening of the structure may be ignored if the sum of the column axial loads to the Euler axial load, $\Sigma(P/P_{oc}) \leq 0.20$ in each storey. If $\Sigma(P/P_{oc}) > 0.20$, the structure should have its stiffness and coordinates updated to account for the effect of gravity loading. The overturning forces were considered only in this project because the softening will increase the period thereby decreasing the lateral inertia forces on structures on stiff soil sites during an earthquake. However, these inertia forces will cause a larger displacement in the structure than if the structure were not as soft. The effect of the softening was ignored as these two effects were assumed to compensate for each other.

It was assumed that the effect of P-delta forces may be taken into account by means of an extra set of lateral forces to the frame. The effect of these increased lateral forces is to reduce the elastic force reduction factor, μ, for which the structure is designed. The static lateral forces, P_i, shown in Figure 4.2, are required to produce the same storey shears, moments, and interstorey drifts that are caused by the storey weights, W_i, acting through the displacements expected in the frame. The P-delta moments and shears from the actual storey masses being displaced laterally are compared with the moments and shears from an equivalent lateral P-delta force distribution below. These sets of storey shears and moments were calculated from the forces on the frame shown in Figure 4.2. The modelled P-delta forces must produce shears and moments equal to those obtained from the actual P-delta forces if they are to accurately model the actual P-delta effect.

	Actual P-delta Forces	Modelled P-delta Forces
Moments:	$M_1 = W_1 \delta_1$	$M_1 = P_1 h_1$
	$M_2 = W_1 (\delta_1+\delta_2) + W_2 \delta_2$	$M_2 = P_1 (h_1+h_2) + P_2 h_2$
	$M_n = \sum_{j=1}^{n} (W_j \sum_{i=1}^{j} \delta_i)$	$M_n = \sum_{j=1}^{n} (P_j \sum_{i=1}^{j} h_i)$
Shears:	$V_1 = W_1 \delta_1 / h_1$	$V_1 = P_1$
	$V_n = \delta_n / h_n \ \Sigma W_i$	$V_n = \Sigma P_i$

The interstorey height, h_i, above the level under consideration must be considered to be a constant value, h, to obtain further simplification. If the interstorey height, h, is not constant, the smallest value of interstorey height above the level considered will conservatively estimate the actual P-delta forces.

Moments:	$M_n = \sum_{j=1}^{n} (W_j \sum_{i=1}^{j} \delta_i)$	$M_n = \sum_{j=1}^{n} P_j jh$
Shears:	$V_n = \delta_n / h \ \Sigma W_i$	$V_n = \Sigma P_i$

A further simplification is required in order for the moments and shears from the lateral loads to be the same as those from the actual vertical loads. The value of interstorey drift, δ_i, above the level under consideration must be chosen to be a constant value, δ. In most frames the interstorey drift, δ, varies with height, however, a value which is the maximum for all stories above the level under consideration will

conservatively estimate the actual P-delta forces. This leads to the following relationship between the lateral loads at each level, P_i, and the storey masses, W_i.

$$P_i = W_i \delta/h \qquad \text{Equation 4.2}$$

Equation 4.2 may be used to conservatively approximate the P-delta forces at any level. However, it is cumbersome to estimate the P-delta forces at each level separately in turn. To avoid this, a further very useful approximation may be made. The P-delta forces may be conservatively modelled using Equation 4.2 by a single lateral load distribution if the largest interstorey drift, δ, expected in the frame, rather than the largest interstorey drift expected above the level under consideration, is used.

It is proposed that the P-delta forces should be taken into account by the application of a single lateral load distribution. The largest value of interstorey drift, δ, expected in the frame should be used in the calculation of the lateral loads in each level, P_i, found from Equation 4.2.

(a) Obtaining Interstorey Drifts

In the analyses of frames in this report the equal displacement assumption usually conservatively predicts the actual displacements and interstorey drifts in multistorey steel frames during design level earthquakes as long as a soft-storey mechanism does not occur. A similar finding was made by Tjondro [4.13], although it appears that multistorey reinforced concrete frames may behave somewhat differently [4.8].

It is therefore recommended that the interstorey drifts from the earthquake forces for steel framed structures be obtained from the equal displacement assumption. However, the application of the P-delta static load distribution to the frame causes the interstorey displacements to increase above that expected by the equal displacement assumption. Higher P-delta static loads are therefore required to model this increase in displacement. The maximum expected interstorey drift may be estimated in order to avoid iteration. The P-delta forces may then be found from Equation 4.2 using this estimated drift. The total frame displacements are found by the equal displacement assumption as C_e/C_μ multiplied by the design level frame displacements plus the displacements obtained from the P-delta lateral forces. The drifts obtained from these displacements should then be checked to ensure that they are less than the estimated level of drift.

Paulay [4.8] has indicated that while the expected deformed shape of the reinforced concrete structures may be similar to that shown in curve "a" of Figure 4.3, which is found from the equal displacement assumption. The shape of the actual displacement and interstorey drift envelopes of an inelastically responding reinforced concrete frame may be similar to curve "b". The interstorey drifts shown in curve "b" are larger in the lower floors than those predicted by the equal displacement assumption. Paulay has suggested that curve "c" may be used to estimate the actual interstorey displacements in the lower stories rather than the equal displacement assumption. This shape does not seem to be as noticeable in moment-resisting steel frames as it is in reinforced concrete frames possibly because there is much less hinging of the columns at the base of steel frames during design level earthquakes.

Building Standards suggested revisions for the Uniform Building Code [4.20] allow interstorey drift ratios of up to 3% if the P-delta effect is considered in design. It is felt by the author that interstorey drift ratios greater than this level should not be used so that the inelastic rotation capacity of the members is not exhausted and non-structural damage is not too severe.

(b) Summary of Design Procedure

An extra set of lateral forces is applied to a frame in the design stage to consider the P-delta effects. These forces may be obtained from Equation 4.2, where the interstorey drift may be obtained by means of the equal displacement assumption.

4.5 MODELLING

The dynamic inelastic time-history frame analysis program, RUAUMOKO [4.21], which is used in this project has three analysis options for the consideration of P-delta effects. They are:

i) No P-delta effects are taken into account and the initial structural configuration is used throughout the analysis. (P-delta flag = 0).

ii) The geometry and stiffness of the frame are updated before the time-history analysis is started to allow for the axial forces in the columns due to static loads. The structure is less stiff than if the undeformed structure is used thereby resulting in a longer initial period. Moss and Carr [4.22] have recommended that this method be used for all frames as very little extra computational work is required. However, it does not take account of the overturning effects on the structure. (P-delta flag = 2).

iii) The deformed frame coordinates and column geometric stiffnesses are recalculated and updated at every timestep throughout the analyses. This is the full P-delta effect which includes the calculation of the overturning forces. (P-delta flag = 1).

4.6 APPLICATION OF THE P-DELTA DESIGN METHOD

In order to illustrate how the P-delta method was applied, Frame #1 was redesigned. The beams were designed to carry the moments from the dead load case alone and, based on the beam strengths, column sizes were selected. The sizes for this frame, referred to as Frame #3, are given in Appendix 3.

The period of the structure was calculated to be 2.09 seconds, and the base shear was calculated as 138 kN which was based on a lateral load reduction factor, μ, of 6. The interstorey drift which resulted from the code lateral load distribution was 2.33%. The static load distribution is shown in Figure 4.4a. It was thought that the total interstorey drift, δ/h, may reach 3% once P-delta forces were included. The magnitude of P-delta forces shown in Figure 4.4b were calculated by Equation 4.2 as 666kN * 0.03 = 20 kN at each level. The maximum interstorey drift including the P-delta forces increased to 2.59%. The sizes chosen for the structure could carry the total lateral loads from Figure 4.4 with some redistribution, so no revision of the magnitude of the P-delta forces was made.

(a) Frame Performance

The displacements and interstorey drifts of the frame with and without the inclusion of the P-delta effect from design level loading, as well as those obtained and from 5 ground excitations are shown in Figures 4.5 and 4.6. Frame displacements may either increase or decrease when the P-delta effect is included because the period of the frame increases, and the frame response to a particular earthquake record is altered. It is difficult to make generalisations based on a small number of analyses, but in the analyses carried out in this project, the frame response increased when the P-delta effects were included more often than they decreased. This is in agreement with research by Bernal [4.3] who has undertaken many analyses of single degree of freedom systems.

The response of the frame to the design level earthquakes was less than that predicted by the equal displacement assumption and the deformation envelopes were not of the shape observed by Paulay [4.8] for reinforced concrete frames. The displacements during the El Centro excitation were thought to be

low because the spectral acceleration of the El Centro record is lower than the design level spectral acceleration at the frame fundamental period of 2.09 seconds.

The increase in frame displacements from the P-delta forces in the static design load case looks to be an acceptable, perhaps slightly conservative, estimate of the likely increase in deformation due to P-delta effects in an earthquake.

The response of the top of the frame during artificial earthquake #2 with and without the P-delta effect is shown in Figure 4.7. It may be seen that the peak displacements are sometimes larger with P-delta effects and sometimes they are not. It may also be seen that the response period of the structure with P-delta is longer than when it is not included as the peak responses move out of phase near the end of the earthquake.

Beam hinging occurred throughout the frame even though the beams were made the same size over the frame height. The maximum beam curvature ductilities when the P-delta effect was not included were 8.55, 7.45, 8.04, 12.4 and 17.0 during the EQ/ART1, EQ/ART2, El Centro, Parkfield, and Pacoima excitations. The maximum beam curvature ductilities when the P-delta effect was included were 7.73, 8.37, 7.38, 11.8 and 20.3 during EQ/ART1, EQ/ART2, El Centro, Parkfield and Pacoima excitations. The increase or decrease in maximum displacement was generally associated with an increase or decrease in maximum beam curvature ductility resulting from the P-delta effects. There was no column hinging during most of the design level level records.

The Parkfield and Pacoima excitations both caused displacements larger than those associated with the design level earthquake. A maximum column curvature ductility (ϕ/ϕ_p) of 10 was demanded during the Pacoima excitation at the base of one of the internal columns and the maximum beam curvature ductility of 20.3 corresponded to an inelastic hinge rotation, θ_H, of 0.0545 radians. It is thought unlikely that this rotation could be sustained without a large amount of buckling and loss of strength. However, these excitations are much greater than the design level excitations under which the frames behaved well.

P-delta forces can often be carried without any increase in member size as steel moment-resisting frames are generally much stronger than they are required to be to resist seismic lateral load. Steel eccentrically and concentrically braced frames are often stiff so that the displacements are

small and the P-delta forces are small. It is therefore thought that P-delta effects will not be very significant in the design of most steel-framed structures.

4.7 SUMMARY

There are very few methods for the estimation and design of P-delta effects in inelastically responding moment-resisting frames. This is because the response of these frames is complex and is very dependent upon the earthquake record used for analysis. In some cases the effect of P-delta forces is to increase the displacements and in other cases the displacements are decreased. However, design for P-delta effects should be carried out as the risk of collapse from overturning, amplification of forces or inelastic deformations must be considered.

In this chapter, a simple rational method has been suggested to design, to some extent, against possible undesirable behaviour as a result of P-delta effects. In this method, the actual displacements through which the gravity loads are expected to move are considered in the calculation of the P-delta forces. The frame is made stronger than what is required to resist the lateral earthquake loads alone. All approximations may be clearly seen and very few assumptions are required apart from those used by Paulay [4.8].

In the design method, the P-delta forces are approximated by a static lateral load distribution. The magnitude of the static lateral loads at each level is found from Equation 4.2. The equal displacement assumption may be used to find the interstorey drifts, from the seismic load, to be used in this equation.

It is recommended that this method should be used for all frames in which the displacements are sufficiently large that the P-delta effects are unable to be ignored. Serviceability criteria, which may often be critical, should be designed for separately.

4.7.1 Further Research

There is very little justification presently available for the method used by Paulay [4.8] of increasing the strength of the structure to allow for P-delta effects. The method for P-delta design in this chapter is based upon this method. Although this method seemed to be appropriate for the framed structures studied, further verification of this treatment is required for single degree of freedom oscillators and for multi-storey frames.

Further research is required to estimate when P-delta forces are likely to become larger than the seismic restoring forces, thereby causing dynamic instability and overturning of the inelastically responding structures. It is thought that if the overturning limit state is understood, even though it is hoped that overturning is avoided in real structures, further understanding of the amplification of displacements and likely increase in curvature ductility may be obtained.

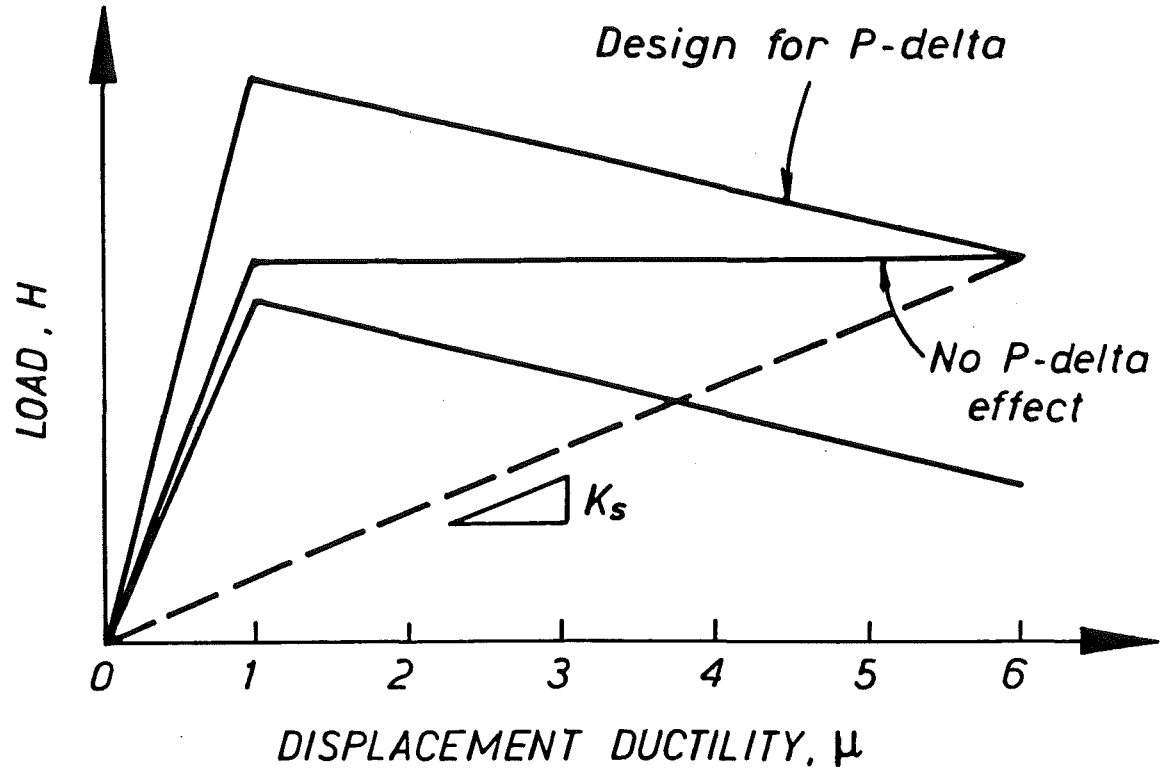

Figure 4.1. Increase of Strength to Design For P-Delta

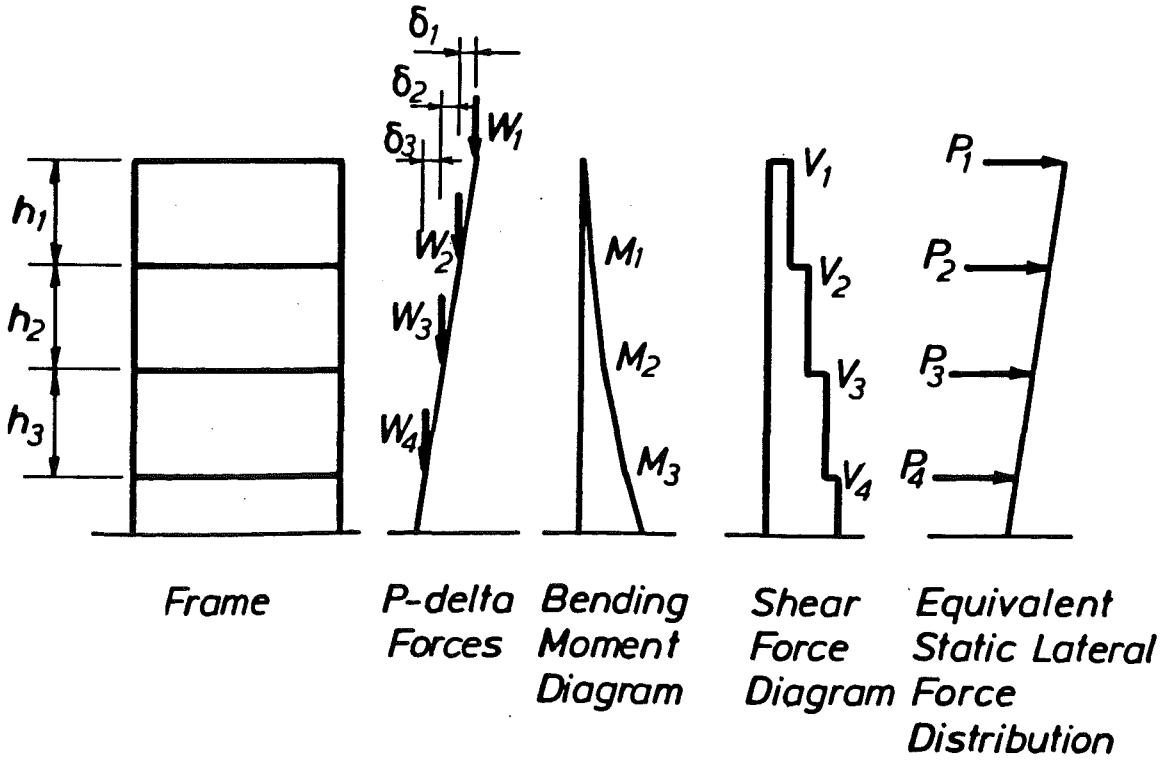

Figure 4.2. Equivalent Lateral P-delta Forces

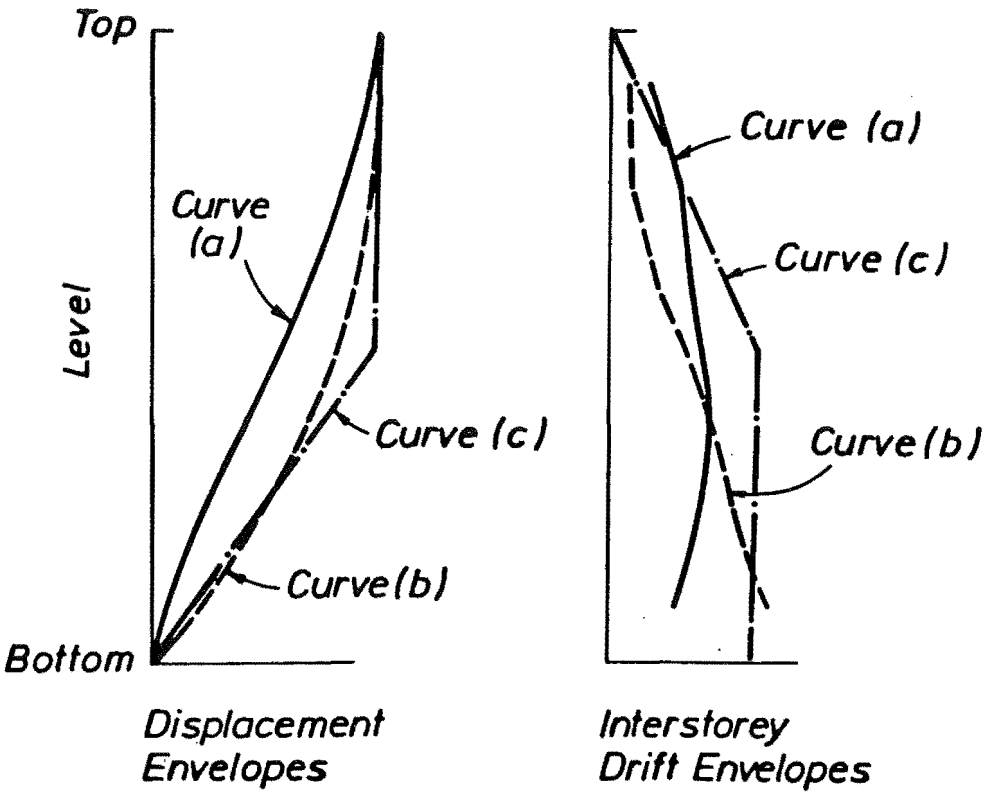

Figure 4.3. Displacement and Interstorey Drift Envelopes

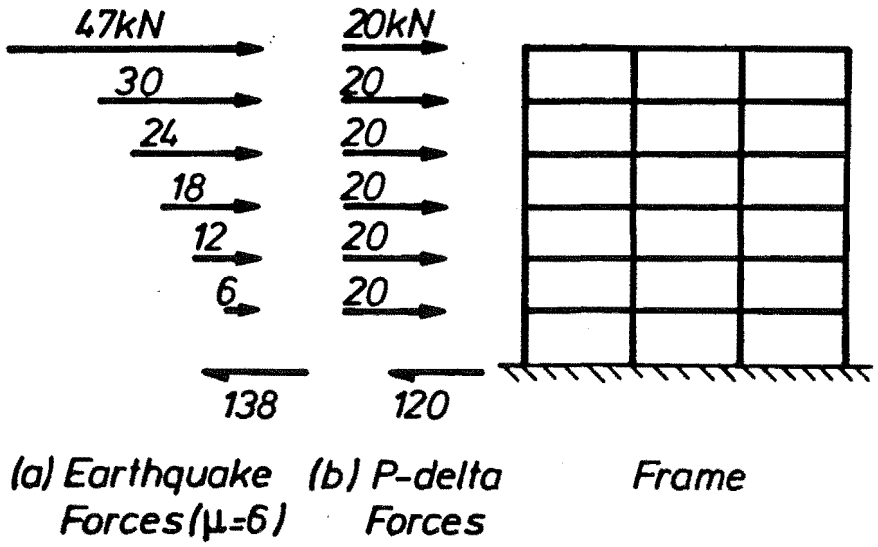

Figure 4.4. Application of P-delta Design Method to Frame #3

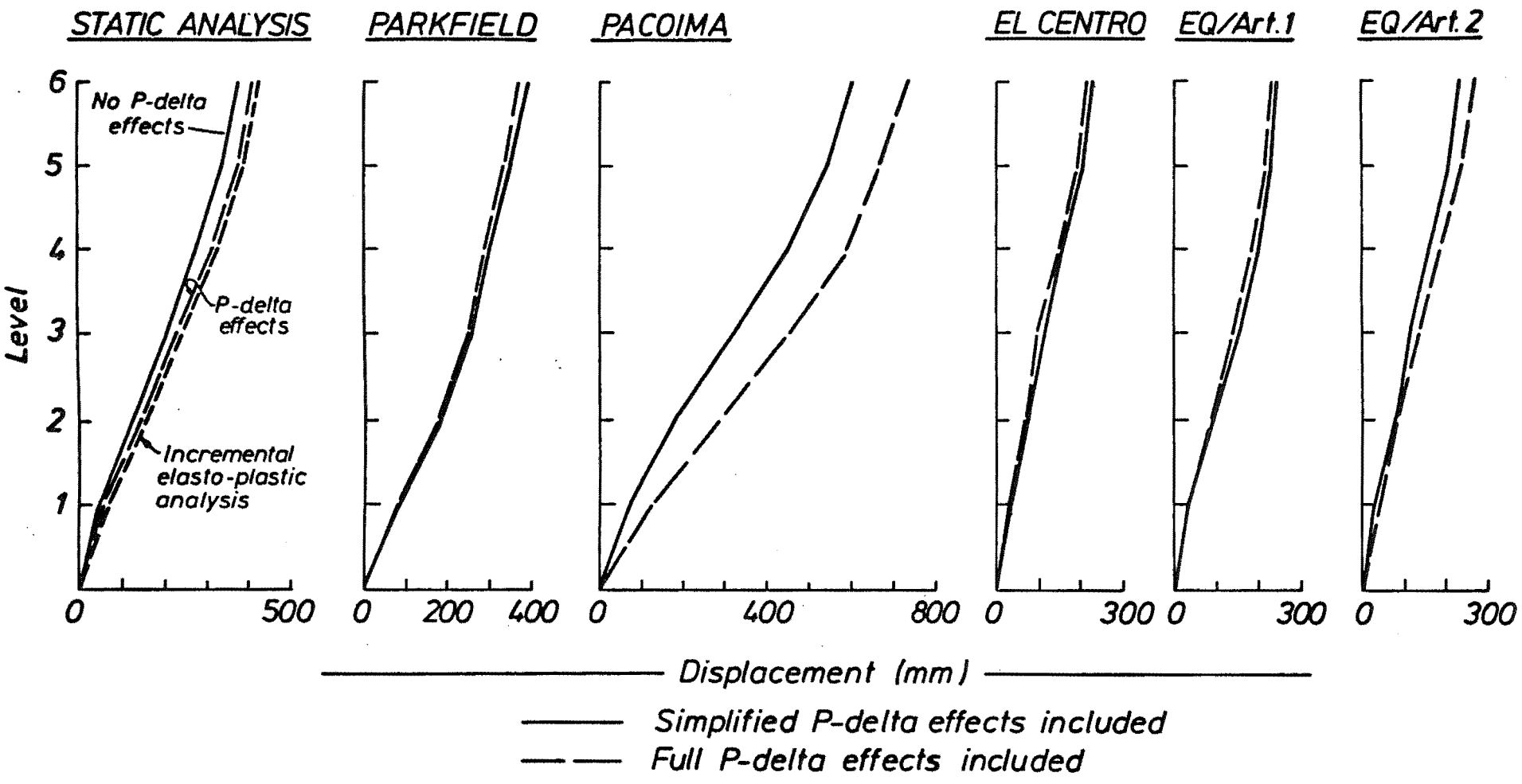

Figure 4.5. Frame #3 Displacement Envelopes

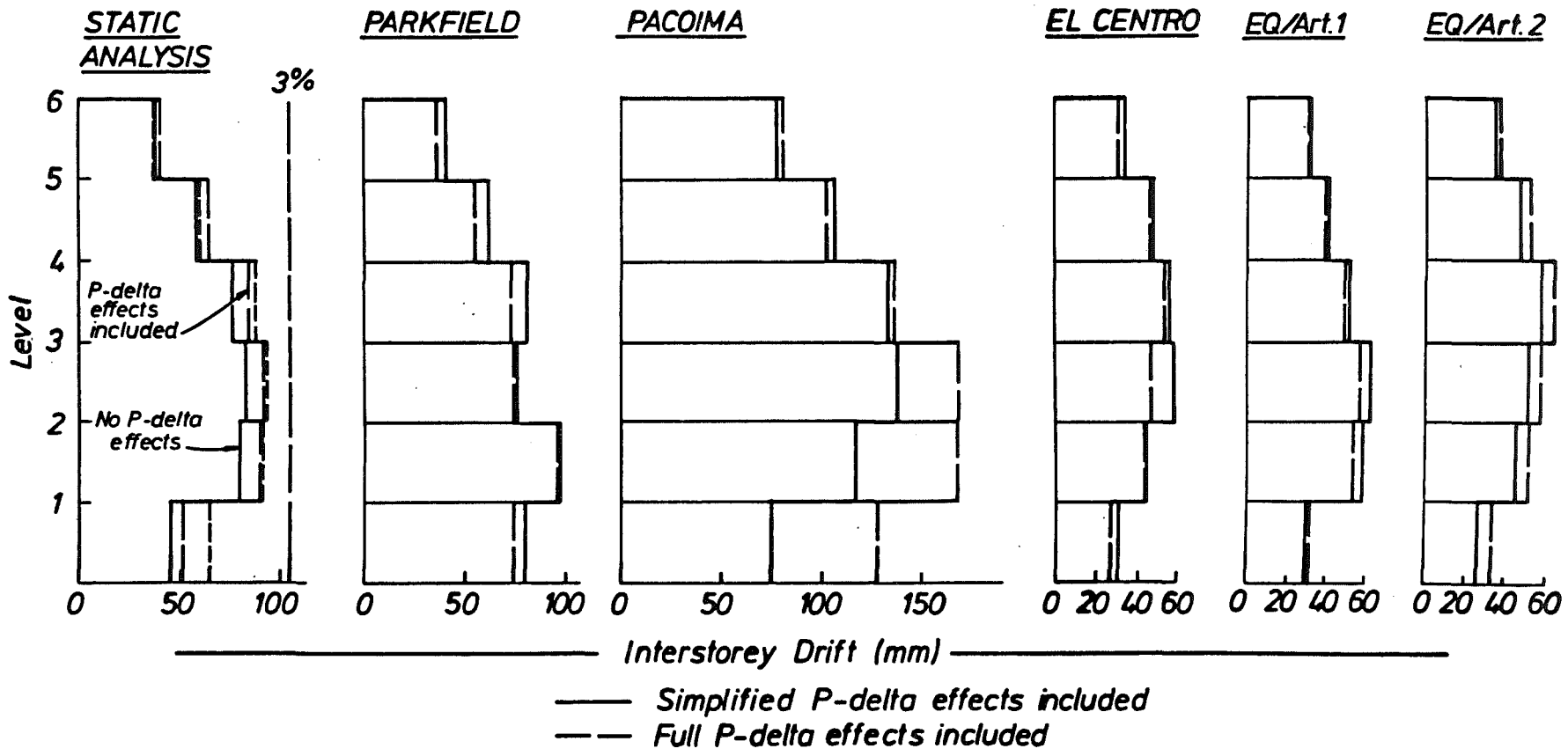

Figure 4.6. Frame #3 Interstorey Drift Envelopes

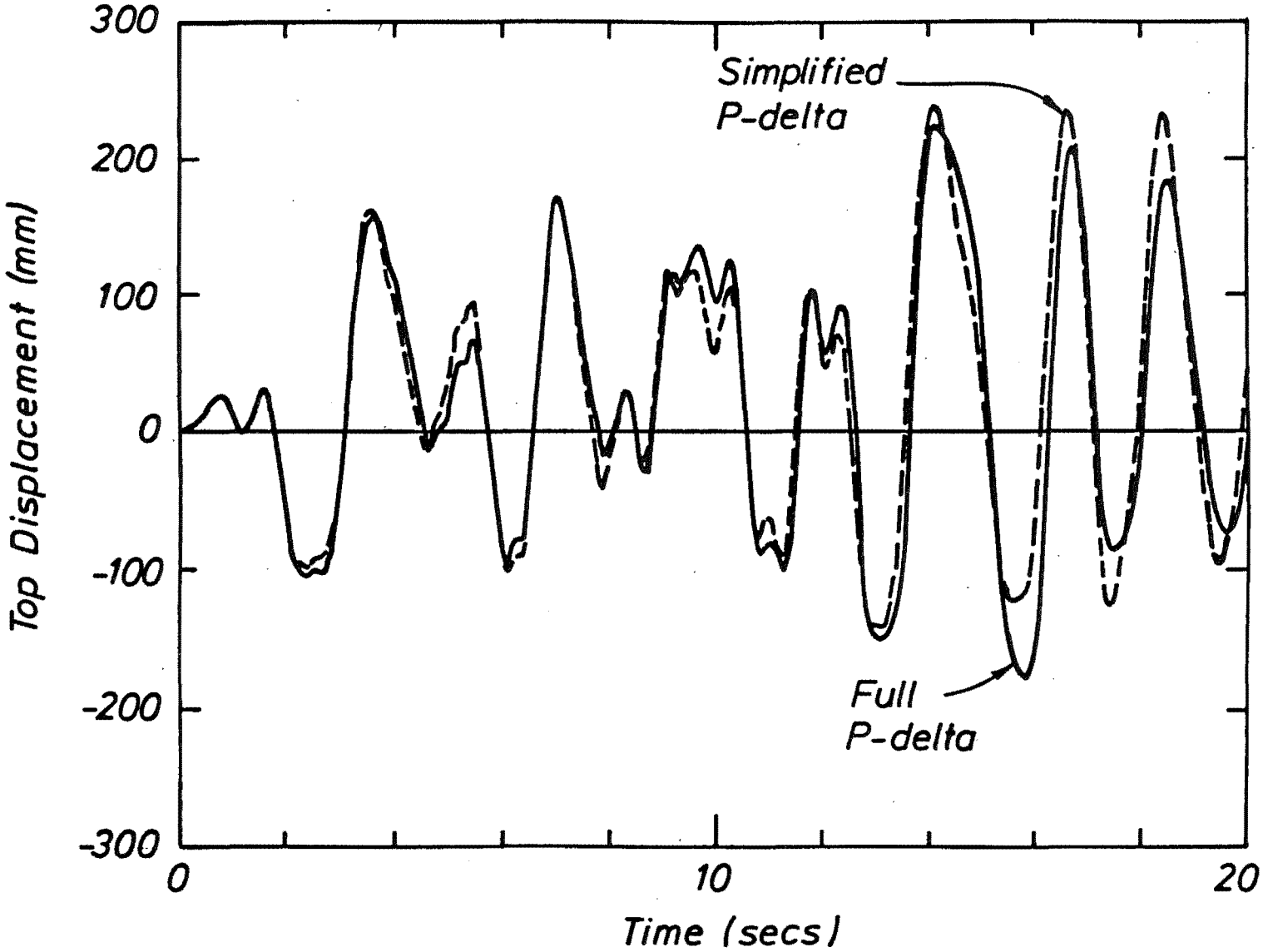

Figure 4.7. Comparison of Displacement at the Top of Frame #3 with and without P-delta Effects Included

4.8 REFERENCES

4.1 Krawinkler H., "Seismic Code Developments for Steel Structures", Pacific Structural Steel Conference, Vol. 3, p361-372. Auckland, 1986.

4.2 Stewart W. G., "The Seismic Design of Plywood Sheathed Shear Walls", Ph.D. Thesis, Department of Civil Engineering, University of Canterbury, 1987.

4.3 Bernal D. "Amplification Factors for Inelastic Dynamic P-delta Effects in Earthquake Analysis", Earthquake Engineering and Structural Dynamics, Vol. 15, 635-651, 1987.

4.4 Goel S.C., "P-delta and Axial Column Deformation in Aseismic frames", J. Struct", *Journal of the Structural Division*, ASCE, Vol. 95, No. ST8, August 1969.

4.5 Andrews A. L., "Slenderness Effects in Earthquake Resisting Frames", Bull. NZNSEE, Vol. 10, No. 3, Sept 1977, p154-158.

4.6 SANZ, "Code for Design of Steel Structures (with commentary)", NZS3404, New Zealand Standard, 1977.

4.7 SANZ, "General structural design and design loadings for buildings", DZ4203 Draft for comment, New Zealand Standard, 1986.

4.8 Paulay T., "A Consideration of P-delta Effects in Ductile Reinforced Concrete Frames", Bulletin of the New Zealand National Society for Earthquake Engineering, Vol. 111, No. 3, September 1978.

4.9 Montgomery C. J. "Influence of P-delta on Seismic Design", Can. J. Civ. Eng. 8, 31-43, 1981.

4.10 Jennings P. C. and Husid R., "Collapse of Yielding Structures Under Earthquakes", *Journal of the Engineering Mechanics Division*, ASCE, Vol. 94, 1045-1065, 1968.

4.11 Tazikawa H. and Jennings P. C., "Collapse of a Model for Ductile Reinforced Concrete Frames under extreme Earthquake Motions", Earthquake Engineering and Structural Dynamics, 8, 117-144, 1980.

4.12 Bernal D., "P-δ Effects in Nonlinear Seismic Response", Direccion General de Reglamentos y Sistemas, Serie de Publicaciones Technicas PT-1, SEOPC, 1-31, 1985 (in Spanish).

4.13 Tjondro J. A., "Analytical Investigation of P-delta Effects in Medium Height Steel Moment-Resisting Frames", Master of Engineering Report, Department of Civil Engineering, University of Canterbury, 1988.

4.14 Galambos T. V. "Guide to Stability Design Criteria for Metal Structures", 4th ed., edited by T. V. Galambos, Wiley, 1988.

4.15 AISC, "Load and Resistance Factor Design Specification for structural steel buildings", American Institute of Steel Construction Inc., 1986.

4.16 Bernal D., "P-delta effects in the Inelastic Response of Multistorey Buildings", Proc. Pacific Conference on Earthquake Engineering, New Zealand, Volume 2, pp221-230, August 1987.

4.17 Turkington D. H. et al. "Seismic Design of Bridges on Lead-Rubber Bearings", Research Report 87/2, Department of Civil Engineering, University of Canterbury, 1987.

4.18 Andriono T. "Seismic Resistant Design of Base-Isolated Multistorey Structures", Ph.D. thesis, Department of Civil Engineering, University of Canterbury, in preparation.

4.19 SAA, "Draft Australian Standard for Comment - Steel Structures", DR 87164, August 1987.

4.20 -, 1987 Code Change Submittals, UBC, Suggested Revisions to the 1985 Editions of the Uniform Codes. Further Study Items and Submittals for 1987. Building Standards, V. 55, No. 6, Pt 3. Nov-Dec, 1986.

4.21 Carr A. J., "RUAUMOKO", Computer Program Library, Department of Civil Engineering, University of Canterbury. May 1986.

4.22 Moss P. J. and Carr A. J., "The Effects of Large Displacements on the Earthquake Response of Tall Frame Structures", NZNSEE, Vol. 13, No. 4, Dec 1980.

Chapter 5

ECCENTRICALLY-BRACED FRAMES

5.1 INTRODUCTION

Eccentrically-braced frames (EBFs) are a relatively new form of construction having been used in buildings since only 1977. Development of design provisions has been carried out predominantly at the University of California, Berkeley, under the guidance of Professor E. P. Popov where a large amount of testing of the inelastic components and subassemblages has been carried out.

The two desirable attributes of properly detailed EBFs are that they are ductile, having fat hysteresis loops like moment-resisting frames, and that they are stiff, like concentrically-braced frames.

Several forms of eccentrically-braced frame may be used. V-braced or inverted V-braced frames (VBF), and D-braced frames (DBF) are shown in Figure 5.1. In both of these frames the braces frame into the beam at a distance "e" from the other joints. This length of beam, known as the "active link", is where most of the deformation is expected to occur.

5.2 AIM OF THIS STUDY

This study was carried out in order to satisfy the requirement of New Zealand engineers that the dynamic behaviour of EBFs was desirable, and particularly to show that there is only a small possibility that a "soft-storey" mechanism, such as that shown in Figure 5.2a, may form.

According to design procedures for VBFs suggested by Popov, Kasai and Engelhardt [5.1], the columns are generally not required to resist flexure as the braces and columns resist load predominantly by strut and tie (truss) behaviour. While it is desirable that the magnitude of the column moments is small, methods to predict the magnitude of these moments are currently not available. Because of this it is uncertain as to whether or not the chosen mechanism of energy dissipation, with only the links yielding, may be maintained.

The use of ties between stories, as shown in Figure 5.2b, has been tentatively suggested by New Zealand designers as a means of avoiding a soft-storey mechanism.

It was desired to see if the moments on the column could be predicted approximately by any existing methods for DBFs.

5.3 LITERATURE SUMMARY

The literature available on the behaviour of EBFs is reasonably extensive, and is well covered by Engelhardt and Popov [5.2]. In this summary, some aspects of interest are mentioned, particularly in relation to the maximum deformation capacity of shear links and the way members are sized for the different forces.

Malley and Popov [5.3] tested several links and found that:

i) properly designed and detailed links can dissipate large amounts of energy regardless of the loading history. Monotonic shear link rotations of up to 0.20 radians may occur without significant loss in strength, and

ii) link rotations may be calculated approximately and slightly conservatively assuming the behaviour of the frame was perfectly-plastic. The angle of plastic link rotation, $\tau = \theta L/e$, for VBFs and DBFs where these symbols are shown in Figure 5.3.

Kasai and Popov [5.4] found on testing some well detailed specimens that

i) maximum link rotations of 0.14 to 0.16 radians were achieved under cyclic loading,

ii) no interaction of shear strength, V_p, and flexural strength, M_p, need be considered even in the presence of axial force. The shear and flexural strengths may be calculated from Equations 5.1 and 5.2 respectively,

$$(P/P_y)^2 + (V/V_p)^2 = 1 \qquad \text{Equation 5.1}$$

$$P/P_y + M/(1.18M_p) = 1,\ M \leq M_p \qquad \text{Equation 5.2}$$

iii) with large axial force, flange buckling may become a potential cause of premature failure,

iv) the limitations of shear link length of $1.6M_p/V_p$ seem to be reasonable for avoiding failure mechanisms due to excessive bending, and for assuring most of the inelastic deformation is due to shear,

v) web buckling cannot be predicted on the basis of cumulative energy, but a relation between the critical link rotation and the web stiffener spacing exists regardless of the amount of energy dissipation, cumulative shear ductility or the number of cycles of loading unless they are excessively large.

Kasai and Popov [5.5] have also found that the maximum inelastic shear deformation is more important in the determination of the link deformation than the amount of energy absorbed. They suggested that link web buckling is the most appropriate limit state to consider for link ultimate design because buckling is the direct cause of deterioration of the link hysteretic behaviour as post-buckling behaviour and failure are difficult to predict.

It has been suggested in Building Standards [5.6] that the maximum link rotations should be a function of the amount of shear or flexural yielding expected as shown in Figure 5.4. These rotations are less that the achievable rotation angles for a well detailed link because of uncertainties in the behaviour of frames. Maximum link rotations of up to 0.10 radians were demanded in some frames that were designed to these rotation limits when they were analysed by Ricles and Popov [5.7] under various earthquakes. This is about the dependable limit of link rotation in real frames.

Ricles and Popov [5.7] in their analytical studies suggested that the dynamic magnification factors used for reinforced concrete moment-resisting frames in New Zealand [5.8] may be used to model the maximum column moments in DBFs. It was also advised that to stop the majority of the inelastic deformation occurring in only a few links, the V_p/V_{code} ratio should be as close as possible to the same value, but a smaller V_p/V_{code} ratio for the upper links relative to the lower links is more advantageous than vice-versa.

Popov [5.9] has recommended that for links carrying axial load greater than $0.15P_y$, the moment and axial load should be transmitted by the flanges only.

Very recent studies carried out by Engelhardt and Popov [5.2] on the behaviour of long links in EBFs have shown that the beam next to the link must be protected by capacity design type formulations against excessive yielding, and that long links framing into a column should not be used. Revised maximum allowable design rotation limits for links are given in Figure 5.4. These are more liberal than those suggested in Building Standards [5.6].

5.4 V-BRACED FRAMES

5.4.1 Difficulties in V-braced Frame Design

During design of the V-braced frames the following difficulties were encountered.

The link rotational limitations were found to govern the structural configuration and the size of the frames. Because of these limitations it was found to be difficult to design a frame with normal interstorey heights which had V-bracing over the full height. Possible means of decreasing the link rotations are to:

1) increase the length of the link beam, or
2) increase the stiffness of the structure, or
3) change the structural configuration.

An increase in the length of the link beams causes less rotation capacity to be available, and an increase in the stiffness of the frame caused it to respond more highly as it had a shorter period. Problems were experienced in stiffening the structure significantly because EBFs resist forces by truss behaviour, so that the stiffness of all members was related to their cross-sectional areas or to the shear area of the link. Therefore, to increase the frame stiffness by a factor of two would result in a doubling of the areas of the members and of the amount of steel used. For moment-resisting frames a much smaller increase in section size may cause a large increase the member second moment of area and stiffness.

For these reasons, the third option of changing the structural configuration is generally the most practical. To use a D-braced frame, rather than a V-braced frame allows approximately twice the interstorey displacement for the same plastic hinge deformation. D-bracing is thought to be generally suitable at the base of most frames in regions of high seismicity. Here the required drifts are generally greatest. V-bracing may be suitable near the top of the frames where the forces and required drifts are lower.

5.4.2 Frame Design

The ten storey V-braced EBF, referred to as Frame #4, shown in Figures 5.5 and 5.6 was designed for an average gravity dead and reduced live load per square metre of 5 kPa. Only the V-braced part of the frame shown in Figure 5.7a was modelled. The level of seismic load reduction, μ, does not relate directly to an expected link ductility for EBFs but it represents the minimum level of resistance which a frame may possess. The link ductility is a function of the structural configuration as well as the seismic load reduction factor. The period of the frame was 2.05 seconds.

Only the links and the members at the base of the frame were expected to yield and it was hoped that the braces, beams and columns would remain

elastic. To decrease the ratio of V_p/V_{code} towards the top of the frame was not easy as the size of link required there was very small. This did not seem to cause any problems with the behaviour of the frames.

The frame was reanalysed with the beams, braces, and the column at one end all pinned, as shown in Figure 5.7b, in order to study the response as the method of load resistance was predominantly by truss action. The fundamental period was 2.10 seconds. This pinned frame is of particular interest because when the link at any level yields, the frame at that level becomes a soft-storey. In fact, there are many soft-story mechanisms on top of each other when extensive link yielding occurs. It is well known that a soft-storey mechanism may demand very large inelastic deformations in the level in which it occurs. However, the mechanism of resisting load is predominantly by the truss mechanism is the same in the frames in both Figure 5.7a and 5.7b, so it may be expected that both of these frames should behave in a similar way. The dynamic behaviour of the pinned frame will be shown in section 5.4.7.

The design interstorey drift was 45.7mm which corresponds to a link rotation, τ, of 0.104 radians. This is greater than the maximum value of 0.08 radians suggested by Engelhardt and Popov. However this frame may be representative of frames designed before any limitations for rotation were published. A lower hinge rotation would have been obtained if a modal approach had been used to obtain the static lateral load distribution. Even though the link rotation limits are not met, the behaviour of this frame is useful in describing the behaviour of eccentrically-braced frames.

The ratio of the maximum column axial load, found by summing up the gravity loads and the overstrength link shears, to the section yield axial load, P_y, was 0.63 at the base of the frame. Further up the frame the axial load ratio was considerably less than this. The input data for the dynamic analyses is given in Appendix 3.

(a) Attempted Frame Design Using Ties

Several frames were designed using ties to inhibit the mechanism shown in Figure 5.2b. In order to do this the ties had to be designed to resist the forces from all of the links either above or below the level considered. In the middle stories of a frame the required tie sizes were found to be excessively large. Analyses of the frames with ties, with and without the modelling of tie slackness, did show some reduction in the column moments. However, as many well designed EBF's have been analysed and observed to behave well there is no reason why ties should be required in frames.

5.4.3 Column Moments in V-braced Frames

The pattern of column moments required in order to obtain a soft-storey mechanism under a particular direction of loading is shown in Figure 5.8. It was found that the moment pattern did not depend upon whether the hinges formed in the column of the storey considered, the column next to the storey considered, the beam or the brace.

The gravity moments at the member ends, (without showing the variation of moment along the member,) and the seismic moments, μ=6, are shown in Figures 5.9a and 5.9b respectively. In the elastic analysis, the seismic moment pattern for the columns was the same as that shown in Figure 5.9b over the full height of the frame. It may be seen that these moments from the elastic loading occur in the opposite direction to the moments required to form a soft-storey mechanism. If the seismic moments act in opposition to those required to form a soft-storey mechanism also during inelastic analyses, then a soft-storey mechanism will not form.

The moment pattern shown in Figure 5.10 at level 3 of the frame was found by pushing the frame with the code load distribution until a full frame mechanism occurred and all of the links yielded. This was carried out by means of an incremental elasto-plastic static analysis program. It may be seen that the moment distribution on the columns at level 3 is the same as that required to cause a soft-storey mechanism and different from that obtained from the elastic analysis. A soft-storey mechanism may be able occur in frames in which inelastic link action occurs.

The maximum column bending moments from the elastic analyses, above the ground floor level, were 38kNm and 151kNm for load reduction factors, μ, of six and one respectively. The maximum column moment above the base, found from the elasto-plastic analysis, was 440kNm which was approximately the same as the column reduced moment capacity. The column axial load at this moment was $0.55P_y$. It may be seen in Figure 5.11 that the flexural strength of the 310 UC 240 section used is similar about the weak and strong axes for high levels of axial load. Weak axis column bending may be preferable as the member is less stiff and will therefore require less force for the same rotation, however, because it is less stiff, second order effects along the member will be greater increasing the member moments.

If the beam and brace next to the column are pinned it is expected that smaller column moments will initially occur.

5.4.4 Frame Base Shear

The base shear when Frame #4 forms a full mechanism under the code lateral force distribution was calculated as:

$$V_b = (L\Sigma V^o_{p,i} + \Sigma M_{pb})/H_c$$
$$= (8 * (6*178/0.5+4*142/0.5) + 1721*2 + 220*2)/(.7240*35)$$
$$= 1186 \text{ kN}$$

The amount of load reduction was not as large as the maximum permissible value, μ, of 6 because of the limitations on plastic hinge rotation. The degree of base shear reduction from the elastic base shear, 4020 kN, was 3.4.

5.4.5 Modelling the Frames

To design and dynamically model the frames, several assumptions were made relating to the shear link, the horizontal slaving of nodes and the damping forces in the dynamic modelling are discussed below.

(a) Modelling the Shear link

In order to investigate the mechanisms previously mentioned and to evaluate the approximate column ductilities, a crude shear link model was thought to provide sufficient accuracy.

The length of the links, e, was chosen to be close to that recommended by Kasai and Popov [5.4] for predominantly shear yielding. This length, or eccentricity, e, is $1.60M_p/V_p$, which for all of the beams used was approximately equal to 1 metre. Realistic shear and flexural stiffnesses were used to model the elastic deformations.

The computer models used do not model inelastic shear deformation of members so, as the links are required to deform inelastically in shear, a fictitious flexural strength was used to give the required link shear strength. The link was assumed to deform elasto-plastically with a flexural strength, M_{pl}, equal to $eV_p/2$. Using the eccentricity, e, of $1.60M_p/V_p$ means that the link flexural strength, M_{pl}, is also equal to $0.80M_p$. The link strength would be the same as if the link had deformed inelastically in shear when flexural hinges occurred at both ends of the link, however there may be a difference in the moments at the ends of the link. This difference was ignored.

(b) Nodal Coupling

The period was calculated by Rayleighs method as 2.05 seconds, while the period calculated by modal analysis was 1.92 seconds. The shorter period in the modal analysis was because of the nodes at each level were slaved horizontally to reduce the number of degrees of freedom in the solution procedure. When these restraints were removed, the period calculated by the modal analysis was also 2.05 seconds. When the columns were rotated so that they bent about their weak axis, the period was increased only slightly to 2.07 seconds showing that the column resisted axial load rather than flexure. The frame described here was modelled with the nodes uncoupled, (assuming that no composite action occurred,) and with the columns bending about their strong axis.

(c) Damping

Large damping forces were observed to occur in the dynamic time-history response of the frames. The joint damping forces tended to become large when the links became inelastic. In one case the damping force in one direction of loading was 22% of the magnitude of the component of the maximum member force at that joint in the direction considered. The large damping forces caused base shears which were considerably greater than the maximum possible shear, assuming a mechanism, from static considerations. All frequencies were subcritically damped and there was no possibility of instability resulting from moment overshoot.

Many different types of modelling were attempted to see if these damping forces could be reduced. Masses for every degree of freedom were placed on the nodes and the full P-delta analysis was attempted. The damping forces however remained very high when Rayleigh damping was used. The reason for this is thought to be because the contributions of the higher modes may be very high when the structure becomes inelastic. The timestep of the step-by-step integration was shortened but this also showed no significant effect on the damping forces.

The use of the tangent stiffness damping model caused some decrease in the damping forces. In this model, the maximum damping forces are based upon the initial elastic frame stiffness so that as inelasticity occurs, the damping forces decrease until there are no damping forces when the structure forms a full elasto-plastic mechanism. As the high damping forces were observed only when large amounts of inelasticity occurred with the Rayleigh damping model, the damping forces would be expected to be decreased when the tangent

stiffness damping model is used. Although this decrease in damping forces was observed with the tangent stiffness damping model, it is thought that this model does not realistically model damping forces because the amount of damping in a frame should not be dependent upon the tangent stiffness.

Constant modal damping, with 5% of critical damping in every mode, was used to reduce the damping forces to what was felt to be a reasonable level. Further study is required to investigate when the damping forces are likely to become very large.

5.4.6 Dynamic Response

The response of the frame to the the El Centro, Parkfield, Pacoima, and the EQ/ART1 and EQ/ART2 records are described below.

All of the links except the one at the top became plastic at some stage during every earthquake record. All of the links yielded at the same time during the Pacoima excitation and up to 8 hinges yielded simultaneously during the design level earthquakes. In a DMRF, perhaps only 4 stories would be expected to yield at the same time during a design level earthquake.

The deflected shapes shown in Figure 5.12 from the dynamic analyses are a different shape than that obtained from the loadings code [5.10], which is based on the equal displacement assumption, and the interstorey drifts were much larger near the base of the frame than near the top. The two line approximation suggested by Paulay [5.11], and described in section 4.4(a) would be appropriate to predict the shape of the displacement envelope of this frame. However, even though the shape was different from that obtained from the loadings code the magnitude of these displacements in the design level earthquakes was predicted reasonably accurately by the equal displacement methods of the loadings code.

The interstorey drifts are shown in Figure 5.13. The design level displacements from the loadings code [5.10], which are based on the equal displacement assumption, overestimate the response of all of the design level earthquakes near the top of the structure, and predict the response well in the bottom stories, although slightly non-conservatively. An incremental static elasto-plastic analysis overestimates the interstorey drifts from the design level earthquakes near the base of the frame by a factor of over two and underestimates them near the top. If an incremental elasto-plastic analysis is used to design a frame, the interstorey displacement and link rotation demand will therefore be overestimated near

the base of the frame. This may cause the design to be excessively conservative as link rotation capacity generally governs the member sizes in these frames.

The base shears during the design level earthquakes shown in Table 5.1 were of approximately the same magnitude as the 1186kN calculated in section 5.4.4. During the Pacoima and Parkfield records the maximum base shear was significantly larger than this level because the centre of the lateral inertia loading was lower down the structure than that implied by the code lateral load distribution.

Table 5.1

Maximum Inelastic Hinge Rotation and Base Shear		
Earthquake Record	Inelastic Hinge Rotation (radians)	Base Shear (kN)
Eq/Art1	0.080	1157
Eq/Art2	0.091	1260
El Centro	0.069	1185
Parkfield	0.197	1473
Pacoima	0.279	1561

The inelastic link rotations demanded during the design level earthquakes, as shown in Table 5.1, were less than the expected total rotations, calculated from the expected interstorey drifts of 0.104 radians. It is thought to be unlikely that the large inelastic link rotations demanded during the Pacoima and Parkfield records could be sustained. The component of the total rotation which is elastic is usually very small in shear links, often less than 3% of the total allowable rotation, and a direct comparison between inelastic rotation and total rotation is therefore reasonable.

Inelastic rotations were observed in the beams next to the active link during the Pacoima and Parkfield excitations. These rotations were very small with the largest inelastic rotation being 0.003 radians. The flexural strength of the beam next to the link, ignoring the effect of axial load, was 1.25 times the maximum link end moment, M_{p1}, because $M_{p1} = 0.80M_p$ as described in section 5.4.5a. However, the maximum beam axial load from the incremental elasto-plastic analysis was $0.31P_y$ thereby reducing the beam moment capacity to $0.81M_p$. The reduced flexural strength of the beam next to the link was $0.81*1.25M_{p1}$, or 1.02 times the link strength. Yielding may occur in the beam beside the link depending on the direction and magnitude of the moments in the brace, the beam axial load level, and the damping forces. The strength of the beams may need to be increased to reduce the possibility of excessive beam yielding especially in frames where the links

are yielding in flexure. Engelhardt and Popov [5.2] have suggested that some limited beam yielding during maximum credible level earthquakes may be beneficial and reduce the link ductility demand slightly.

Some column hinging at the base of the frame was observed during the Parkfield and Pacoima excitations. The maximum column inelastic rotation demand was 0.023 radians during the Pacoima excitation. There was only one major inelastic cycle to this displacement. The maximum axial load in this column was $0.63P_y$ as described in section 5.4.2. A column tested and described in chapter 7 with an axial load ratio of 0.60 sustained many displacement cycles and obtained an inelastic rotation of 0.025 radians before it was considered to have failed. It is therefore thought that the inelastic rotation demand of 0.023 radians should be able to be sustained.

The maximum column moments were 314kNm, 400kNm, 300kNm, 593kNm and 691kNm which occurred during earthquakes EQ/ART1, EQ/ART2, El Centro, Parkfield and Pacoima respectively. These are much larger than those expected if the structure behaved elastically. However the moments from the design level earthquakes are less than that the maximum column moment from an incremental elasto-plastic analysis of 440kNm.

The maximum column moments occurring over the height of the structure during the design level earthquakes are compared with those found from the load combination, $D + L_s + E_{(\mu=1)}$, and with those from an incremental analysis in Figure 5.14. It may be seen that the load combination, $D + L_s + E_{(\mu=1)}$, underestimated all of these earthquake moments over most of the height of the structure. The moments from the load combination, $D + L_s + E_{(\mu=6)}$, would underestimate these moments much more. The magnitude of the actual column moments cannot be estimated from an elastic analysis. It may be seen that the magnitude of the moments from the static elasto-plastic analysis was similar to the magnitude of the moments obtained from the earthquake records. In this analysis, the displacement at the top of the structure was approximately the same as that estimated by the loadings code [5.10]. However, at some locations such as the third storey, the moments from the static elasto-plastic analysis underestimate the observed moments by a factor of three. The static elasto-plastic method provides a conservative estimate of the maximum likely column moment in some, but not at all levels. A further problem in using the static elasto-plastic method is that the predicted hinge rotations and interstorey drifts are much greater than those observed during actual earthquake records near the base of the frame as shown in Figure 5.13.

The response with and without modelling the P-delta effect was very similar. This was also observed by Ricles and Popov [5.7].

5.4.7 Dynamic Analyses of Pinned Frames

Many analyses of frames with rigid connections have been carried out and good behaviour has been observed. However as the frames resist load predominantly by truss action, and no minimum column flexural stiffness or strength is required in design, the behaviour of a frame with no column flexural strength as shown in Figure 5.7b, is of interest. It was desired to find out the answers to the following questions:- "If no minimum column strength is provided, allowing soft-storey behaviour, will the levels of inelastic deformation demand be excessive?", and "If the inelastic deformation demand is excessive, what level of column stiffness and strength is required to make a soft-storey mechanism unlikely?"

To answer the first of these questions some analyses were carried out on Frame #4, where pinned type connections were included in the structure at the positions shown in Figure 5.7b. It was recognised that this frame is not at all representative of the type of frame expected in a real building because as soon as link yielding occurs, a soft-storey mechanism forms.

The displacements and interstorey drifts of the pinned frame to the Pacoima and EQ/ART2 records are shown in Figures 5.15 and 5.16. It may be seen that the deformations at the bottom storey were much larger than the design level deformations and were unacceptably large. The incremental elasto-plastic design method was unable to be applied to this frame because as soon as a link yielded, an infinite displacement would be obtained.

The maximum possible base shear from static considerations is found when the bottom link yielded. It may be seen in Figure 5.17 that this shear was equal to $V_{link}B/h$, which in this case was equal to 813kN. The base shear corresponding to a displacement ductility, μ, of 6 was 662kN. The base shears recorded during the Parkfield and EQ/ART2 excitations, in which constant modal damping was used, were 849kN and 872kN respectively. The fact that the base shears from these analyses are different than the maximum possible base shear during static loading, even though the mechanism shown in Figure 5.17 occurred, is a result of the damping forces. Rayleigh damping, with 5% of critical damping specified in modes 1 and 10 was used as well as the constant modal damping model. The base shear obtained during

EQ/ART2 when the Rayleigh damping model was used was 1099kN. This was considered to be unacceptably large and unrealistic being 35% greater than the maximum static base shear.

The maximum inelastic link rotations demands were 0.196, 0.398, 0.833, 0.164 and 0.401 radians during the El Centro, Parkfield, Pacoima, EQ/ART1 and EQ/ART2 records respectively. These inelastic deformation demands are excessively large if a soft-storey mechanism forms.

5.4.8 Column Design

An estimate of the required column stiffness and strength must be made to limit the possibility of a soft-storey mechanism.

Columns are not designed for any moment in the hand methods for the design of V-braced frames and in the computer methods, a reasonable prediction of the likely column moment demand is difficult to obtain. For these reasons it may be difficult to prevent all column yielding.

If column yielding is allowed to occur, precautions must be made so that the column ductility demand will not be excessive. Popov, Bertero and Chandramoulli [5.12] have found that the ductility capacity of columns in both weak and strong-axis bending is not good for axial load ratios exceeding 0.50. In the design of real frames this ratio may need to be reduced to 0.40 to allow for axial load variation as a result of vertical seismic accelerations.

If the column axial load ratio is limited to provide the column with ductility capacity this will have the added benefit of providing the column with a certain minimum flexural strength. The frame analysed with a maximum column axial load ratio of 0.63 at the base of the frame sustained some minor yielding at the base but not over the height of the structure. If the axial load ratio of all columns is limited then undesirable behaviour may be unlikely to occur. Further work is required to study the behaviour of more of these frames to observe if this is likely to be the case.

While this method of design made by limiting the column axial load ratios in frames may be satisfactory for frames such as that shown in Figure 5.5, where the beams next to the EBF bay are pinned, in many cases these beams will have a rigid connection to the columns. Further investigation is required to see how large these moments are, and to see how much they influence the ductility demand in the columns of the VBFs.

(a) Proposed Design Procedure for Columns of V-braced Frames

It is proposed that the maximum axial load ratio which is likely to occur during a earthquake should be limited to 0.40 in order to discourage column yielding and provide ductility capacity in the columns if yielding does occur.

5.4.9 Summary of the Behaviour of VBFs

In this brief and limited study, some possible problems relating to a soft-storey behaviour of V-braced frames have been discussed. The column moments from the beams during the elastic loading have been seen to discourage a soft-storey mechanism, the change in sign of column moments resulting from inelastic link action was observed, and the difficulty in prediction of the actual column moments with both a static elastic modal analysis and with a static elasto-plastic incremental analysis have been discussed. If no strength and stiffness is provided at the column ends, a soft-storey mechanism was shown to produce unacceptably large deformations.

As analyses for V-braced frames are often carried out by hand and no design column moment is used it is suggested that the maximum axial load ratio in the columns in both strong and weak axis bending be limited to 0.40 in order to provide strength and deformation capacity until further study of the possibility of the soft-storey mechanism is carried out.

5.5 D-BRACED FRAMES

D-braced frames (DBFs) are good structural systems for resisting earthquakes when the expected frame displacements are larger than V-braced frames may resist. The major problem with DBFs is the estimation of the moment on the column beside the link. Ricles and Popov [5.7] have suggested that a method similar to the New Zealand reinforced concrete capacity design procedure [5.8] which empirically estimate the column moments from a yielded beam in a moment-resisting frame may be used to determine the column forces.

In this section, a frame was designed and analysed and the column moments were compared with the column design moments suggested in the New Zealand reinforced concrete capacity design procedure [5.8]. There are two ways in which the columns next to the link may be designed depending upon their ductility capacities. Higher dynamic magnification factors should be used for columns in which no or very minor levels of ductility demand can be sustained than for columns in which limited ductility capacity is available.

In this brief study of the behaviour of D-braced frames no column yielding is desired during a design level earthquake. The columns may therefore be detailed for a nominally elastic level of ductility demand. Section slenderness properties for members expected to sustain nominally elastic levels of ductility given in the new New Zealand steel structures code [5.13]. It is suggested that the dynamic magnification factor in bending, w_b, from the New Zealand reinforced concrete code [5.8] should be used to obtain the design forces for these columns. Further study will be required to find the level of column ductility expected during design level excitations if lower values of dynamic magnification factor are used.

5.5.1 Frame Design

The 5 storey frame shown in Figure 5.18 was analysed. The input parameters for the dynamic analysis are given in Appendix 3. Loading from two directions was considered in the design because the frame was not symmetric. The period of the structure was 1.23 seconds.

5.5.2 DBF Frame Behaviour

This frame was subjected to the same earthquake records as was the V-braced frame and sustained hinging in all links only during the Pacoima earthquake. All links, except the link at the top yielded during the other records. Hinging occurred in the columns and brace at the base of the structure during the Pacoima and Parkfield excitations, and a few hinges occurred in the columns further up the structure during the Parkfield excitation.

Table 5.2

Maximum Inelastic Hinge Rotation and Base Shear		
Earthquake Record	Inelastic Hinge Rotation (radians)	Base Shear (kN)
Eq/Art1	0.0396	364
Eq/Art2	0.0193	355
El Centro	0.0196	337
Parkfield	0.126	493
Pacoima	0.155	515

The maximum base shear occurring during each record is given in Table 5.2. The maximum base shear expected is 426kN if a full static mechanism forms and the code specified lateral loading distribution is used. During the design level earthquakes a full mechanism did not occur and the base shears

observed were less than this level. The fact that a base shear larger than 426kN occurred during some excitations is because the centre of applied load was lower than the code load distribution implied.

The maximum axial loads at the base of the column into which the links framed were 1157kN, 1237kN, 1265kN, 1309kN and 1290kN which occurred during earthquakes EQ/ART1, EQ/ART2, El Centro, Parkfield and Pacoima respectively. The maximum possible axial load from static considerations was 1419 kN and was not reached as all of the links did not yield at the same time. The axial load expected if the structure remained elastic is 3778 kN implying a lateral load reduction factor, μ, of 2.66.

The maximum inelastic hinge rotations are also given in Table 5.2. The rotation demands were small during the design level earthquakes and could easily have been sustained by well detailed real links. However the rotations occurring during the Parkfield and Pacoima ground excitations were much larger.

The displacement envelopes are given in Figure 5.19 where it may be seen that the shape of the envelope for all earthquakes is different than the displacement envelope from the loadings code [5.10]. The loadings code conservatively predicts the interstorey displacements during the design level earthquakes as shown in Figure 5.20.

The moments on the columns next to the links are shown in Table 5.3. The maximum column moment at a beam-column joint has been divided by the maximum static overstrength moment at that joint in order to obtain the dynamic magnification factor, w_b. It may be seen that the dynamic magnification factor suggested in the reinforced concrete code, w_b, is generally a conservative estimate of the moments which occurred during the design level earthquakes, but may be non-conservative for larger earthquakes. The degree of variation of these column moments even during the design level earthquakes shows that any recommended factors to allow for dynamic magnification will be extremely approximate as a close estimate to the actual moments expected cannot be obtained.

The dynamic magnification factor was greater than unity at the top storey during the Pacoima excitation because of the damping forces in the constant modal damping model.

Table 5.3
D-Braced Frame Moment Dynamic Magnification Factors

Dynamic Magnification Factors for 5 storey DBF.													
Level	Overstrength Moment (kNm)	RC code Moment Magnif.	Simple Method Moment Magnif.	EQ/ART1		EQ/ART2		El Centro		Parkfield		Pacoima	
				Moment (kNm)	Moment Magnif.	Moment (kNm)	Moment Magnif.	Moment (kNm)	Moment Magnif.	Moment (kNm)	Moment Magnif.	Moment (kNm)	Moment Magnif.
Top	112.5	1.00	1.00	73	.65	65	.58	78	.69	82	.73	121	1.08
5B	50.9			61		56		61		63		99	
4T	61.6	1.30	1.58	63	1.02	63	1.02	72	1.17	76	1.23	82	1.61
4B	51.4			63		60		78		107		125	
3T	61.1	1.58	1.58	69	1.13	66	1.08	73	1.28	112	1.83	163	2.67
3B	54.3			88		73		72		110		158	
2T	58.1	1.58	1.58	91	1.57	74	1.27	74	1.27	135	2.32	185	3.18
2B	64.3			92		86		81		143		151	
1T	48.2	1.39	1.58	80	1.43	75	1.34	79	1.26	133	2.22	179	2.78
Ground	34.7	1.00	1.00	106		105		71		220		220	

5.5.3 Summary of Behaviour

The dynamic magnification factors from the reinforced concrete code [5.8] seem to be able to be approximate the dynamic magnification factors obtained from the computer analyses. The loadings code method [5.10], which is based on the equal displacement assumption, conservatively predicts the interstorey displacements of the frame during design level excitations.

5.5.4 Simplified "Capacity Design" Method

Although the reinforced concrete capacity design procedure seems to predict the moments reasonably well in these frames and provides some insight into the structural behaviour, it is thought that the procedure is unnecessarily complex for routine design.

The aim of "capacity design" in reinforced concrete moment-resisting frames is to protect the structure against undesirable mechanisms, because the exact magnitude and response periods of an expected earthquake are unknown. However, to provide the degree of protection required, some estimate of the maximum forces has to be obtained. In the reinforced concrete capacity design procedure, these are represented by the dynamic magnification factors, w_b, and axial load reduction factors, R_v. These factors were obtained from the analysis of regular frames under design level earthquakes. The reinforced concrete "capacity design" procedure as it presently stands, is still earthquake dependent, even though "capacity design" was primarily put in place as a result of the difficulty of knowing the expected seismic forces. The number of steps in the application of the reinforced concrete design method [5.8] to steel frames is thought to be more than can be justified from the variation of the response to design level earthquakes.

It is felt that for frames with large dynamic magnification factors where the columns are designed according Equation 5.3 that a simpler, and only slightly less accurate estimate of the required ideal column moment capacity may be found using a formula of the form given in Equation 5.4. The variables in both equations are described in detail in section 2.3.2.

$$M_c \geq \phi_{ob}\, w_b\, M_{code} \qquad \text{Equation 5.3}$$

$$M_c \geq w_b' \frac{N_b}{N_c} \phi_o\, M_{pb} \qquad \text{Equation 5.4}$$

where N_b is the number of beams, and N_c is the number of columns at the joint. A formula of the form of Equation 5.4 is easy to use as $\phi_o M_{pb}$ is easy to obtain, and w_b' is a dynamic magnification factor which is constant

over the height of the structure. At the beam-column joint just above ground level, the static overstrength moment, $\phi_{ob}M_{code}$, at the bottom of the second storey is large because the point of contraflexure is near the top of the ground floor column storey. However the dynamic magnification factor, w_b, from the reinforced concrete method is low. This high value of static overstrength moment and the low dynamic magnification factor, w_b, is also observable in the upper stories. In the middle stories, where the points of contraflexure of the columns are near the middle of each storey, the static overstrength moment is low and the value of w_b is high. Instead of having these two factors which will multiply together to be a reasonably constant number over the height of most columns in frames it is suggested that a constant dynamic magnification factor, w_b, known as w_b', be used in the design of steel D-braced frames, except at the top storey and at the base, even though slightly less accuracy may be obtained. A value of w_b' of 1.0 at the top of the frame and at the base of the ground floor column is reasonable as hinging should not be detrimental in these positions. A suitable way of finding the value of w_b' over the rest of the frame may be to take it as the value of w_b recommended by the reinforced concrete code [5.8] over the middle stories of the structure. If Equation 5.4 is applied to the frame analysed above, where w_b' is 1.58, the expected column moment will be 1.58 * 1/2 * 112.5kNm = 88kNm. The dynamic magnification factors from the simplified design method are shown in Table 5.3. If this value is used for the design column moment over the height of the structure, it may be seen that it would be a reasonable approximation to the observed column moments.

If the point of contraflexure is at 0.8 of the height of the column at the base of the frame, and a factor of 1.30, as suggested by the reinforced concrete code commentary is used on the beam strength, and in the middle stories of a column where the point of contraflexure is at one half of the column height, and the dynamic magnification of 1.80 is used, the required column moment would be 15% more at the bottom of the frame than in the middle stories. It may be seen from the analyses that the variation of column moment is so large that an accuracy of 15% is well within the limits of accuracy available from the analyses.

The axial load reduction factors, R_v, used in the reinforced concrete code cause only a small decrease in the column design axial load. Hinging may occur over most of the height of an EBF at the same time if link sizes are chosen to decrease with the height of the structure. It is recommended that

the axial load reduction factor, R_v, used in the capacity design of steel frames should not be used. Further reasons were given in the discussion of the behaviour of moment-resisting frames in section 3.6.10.2.

The simplified method of "capacity design" is similar to that recommended by Kamil and Bertero [5.14] which is described in section 2.4(b).

5.5.5 Suggested Design Procedure for Columns of DBFs

An interim design procedure is suggested for the columns in steel DBFs. In this design procedure, yielding is discouraged from occurring in the columns of the frame during design level earthquakes. The columns therefore are required to be detailed to the nominally elastic section requirements which are described in the new New Zealand steel structures code [5.13].

In this design procedure, which is based on the suggestion of Ricles and Popov [5.7], column design moments over the height of the structure may be obtained from Equation 5.4, where the dynamic magnification factor, w_b', is the maximum value of dynamic magnification over the height of the column assessed as in the reinforced concrete code, or all of the column design moments may be obtained using methods used in the reinforced concrete code. The column design axial load should be obtained from the sum of the overstrength beam shears and no axial load reduction factor should be applied.

These tentative design suggestions are limited to DBFs which do not have beams framing in on the other side of the column. Further study is required for hybrid structures. DBFs with columns able to sustain limited ductility demand should be able to be designed for lower dynamic magnification forces than those used in this design procedure. Further investigation of the behaviour of DBFs is required.

5.6 CHAPTER SUMMARY

In V-braced frames with fixed-end beams, the direction of the static elastic design column moments act in a different direction to that required to form a soft-storey mechanism, however, pseudo-static elasto-plastic analyses have shown that the column moments may be in the direction required to form a soft-storey mechanism when the links yield. The magnitude of the column moments occurring in an earthquake may be much greater than the elastic design level moments.

The problems associated in estimating column design moments to provide a degree of safety against the soft-storey mechanism were discussed and interim recommendations to limit the amount of column yielding by limiting the design axial load were made until further research on this type of structure has been carried out.

It was found that the moments in the columns next to the links in D-braced frames occurring during design level earthquakes could be reasonably accurately predicted by the dynamic magnification factors, w_b, used in the New Zealand reinforced concrete code commentary [5.8]. It was recommended that reinforced concrete design procedure, or a simplified method of this procedure, be applied to obtain the design moments of columns in DBFs. It was also recommended that no axial load reduction factor be used.

The design methods proposed by the draft New Zealand loadings code, in which the equal displacement assumption is used, appears to be reasonable for the estimation of displacements and interstorey drifts. It was found that the behaviour of well designed VBFs and DBFs was good under the design level earthquakes.

(a) Further Research

Research is required on "appropriate" damping models in order to obtain realistic levels of damping forces.

The recommendations made for VBFs and DBFs in this report are from only preliminary analyses and further study is required to determine whether the recommendations made are suitable for frames of other heights and types. Further research into the likelihood of a soft-storey mechanism in V-braced frames should be carried out and the column ductility demand in DBFs for which low values of dynamic magnification are used should be investigated. As eccentrically-braced frames generally act in conjunction with frames carrying gravity load, studies are required to advise on design methods for these hybrid structures.

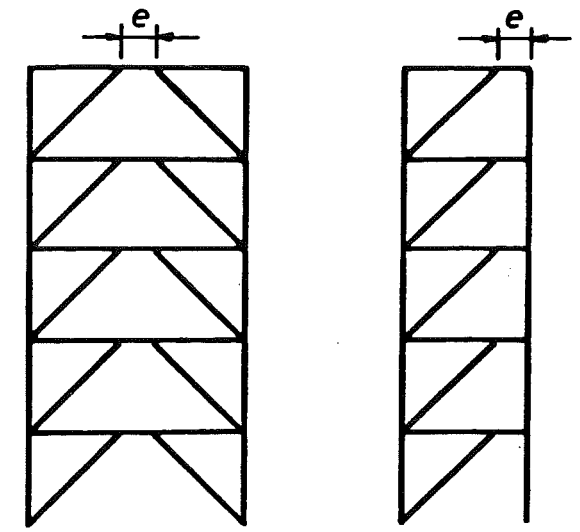

(a) Inverted V-braced Frame (b) D-braced Frame

Figure 5.1. Common Forms of Eccentrically Braced Frame (EBF)

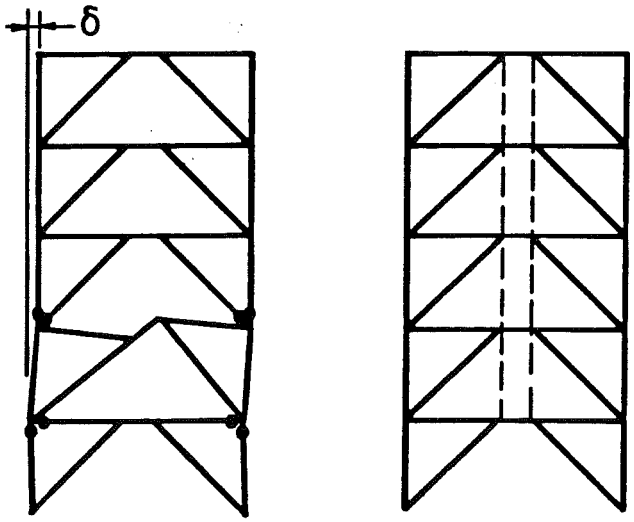

(a) Soft-Storey (b) Frame with Ties

Figure 5.2. EBF Forming a Soft-Storey Mechanism and EBF with ties

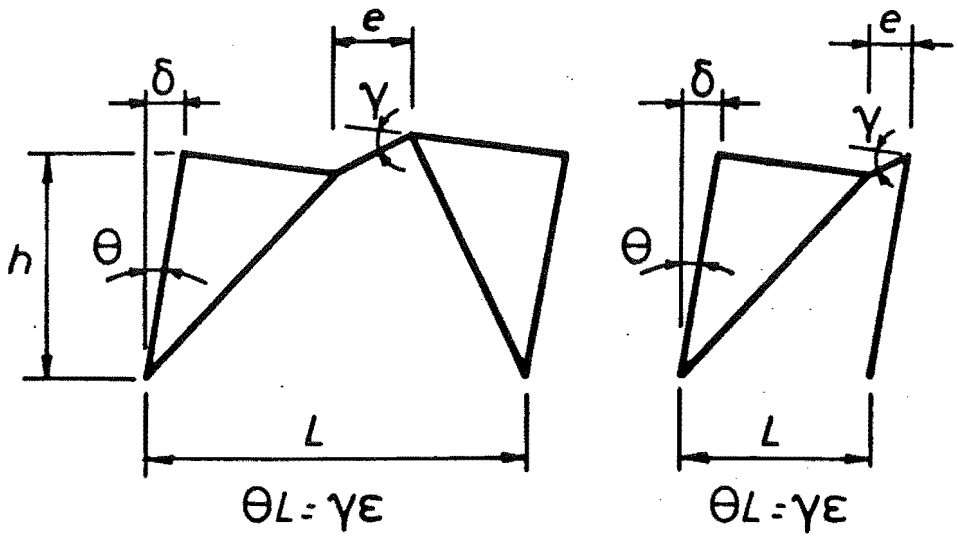

Figure 5.3. Idealised Link Rotations

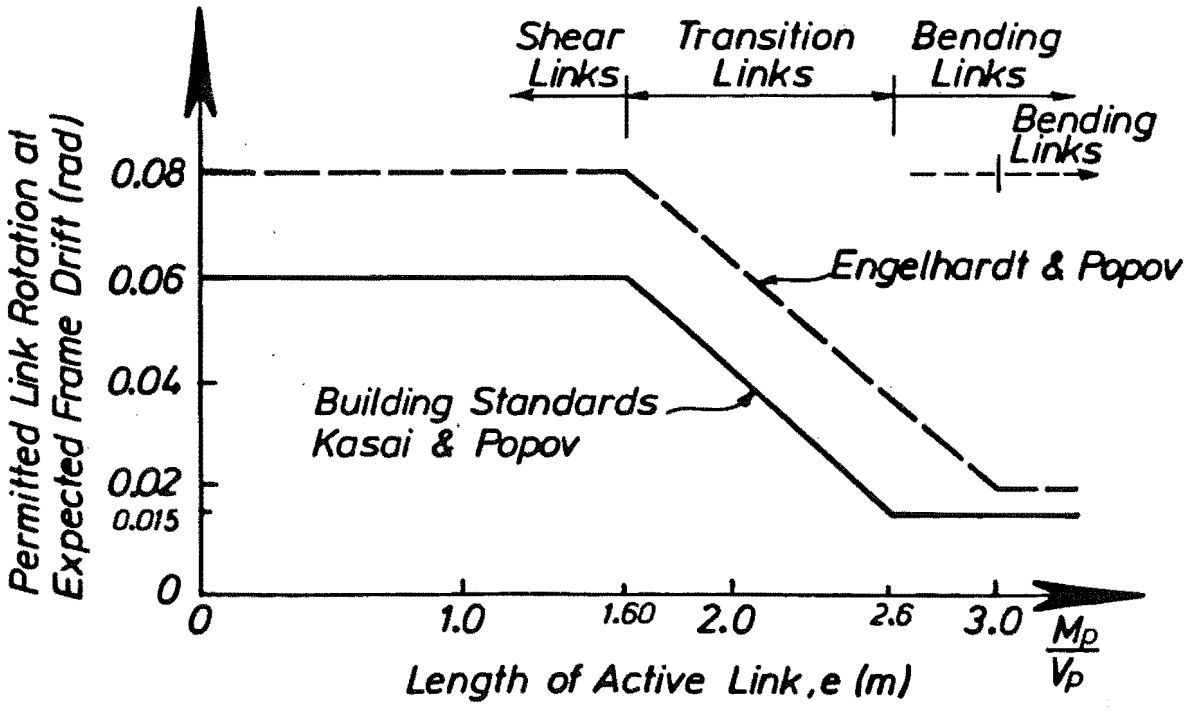

Figure 5.4. Maximum Allowable Link Rotations

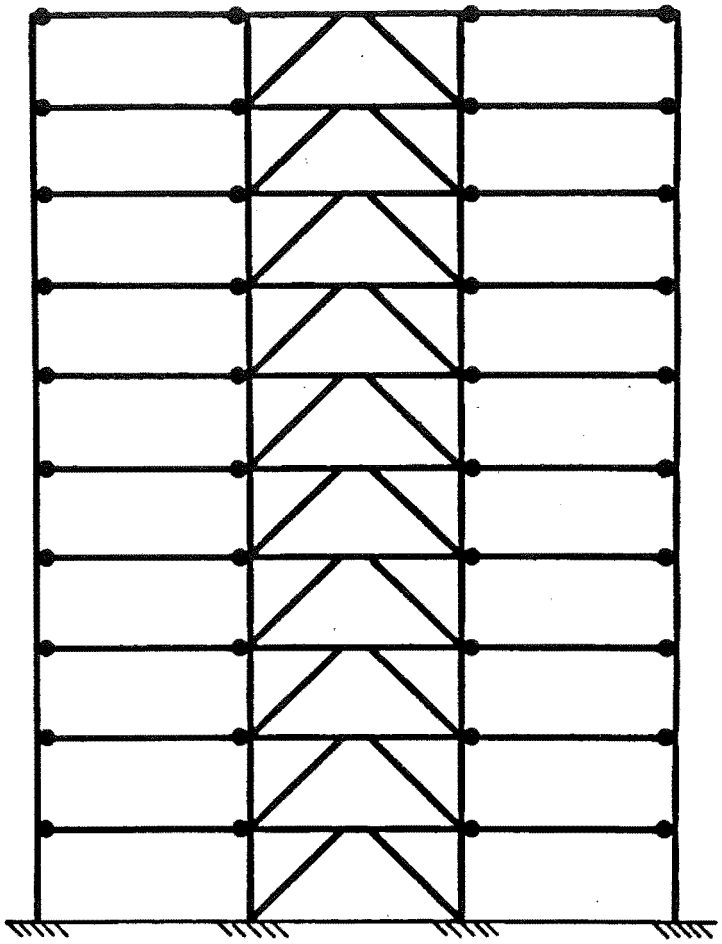

Figure 5.5. Elevation of V-Braced Frame (VBF) Analysed

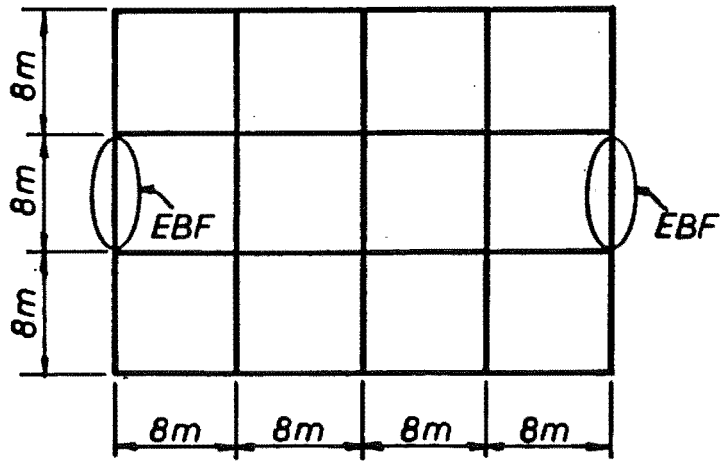

Figure 5.6. Plan of VBF Analysed

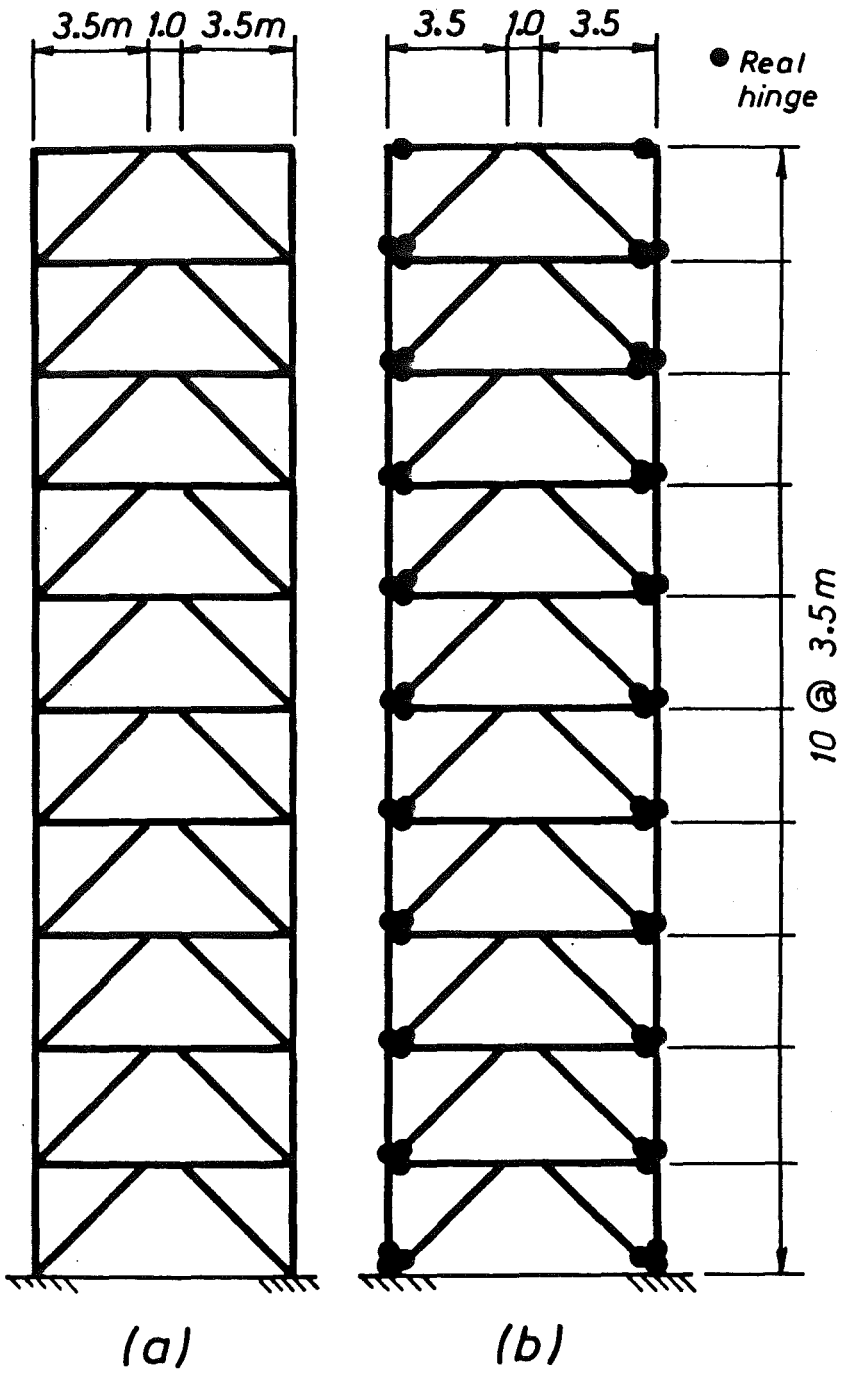

Figure 5.7. Dimensions of VBFs Analysed

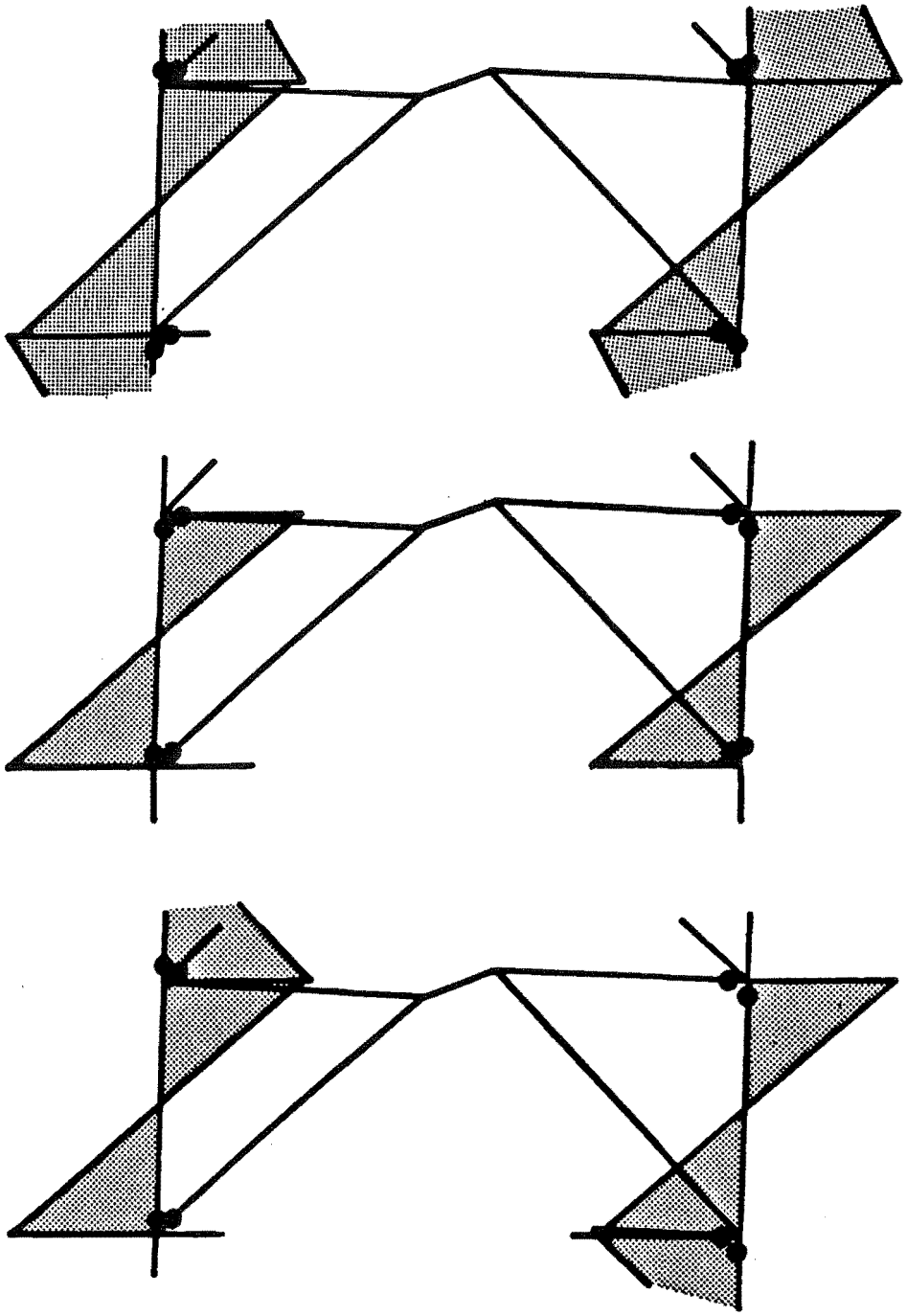

Figure 5.8. Moments in Columns During Soft-Storey Mechanism

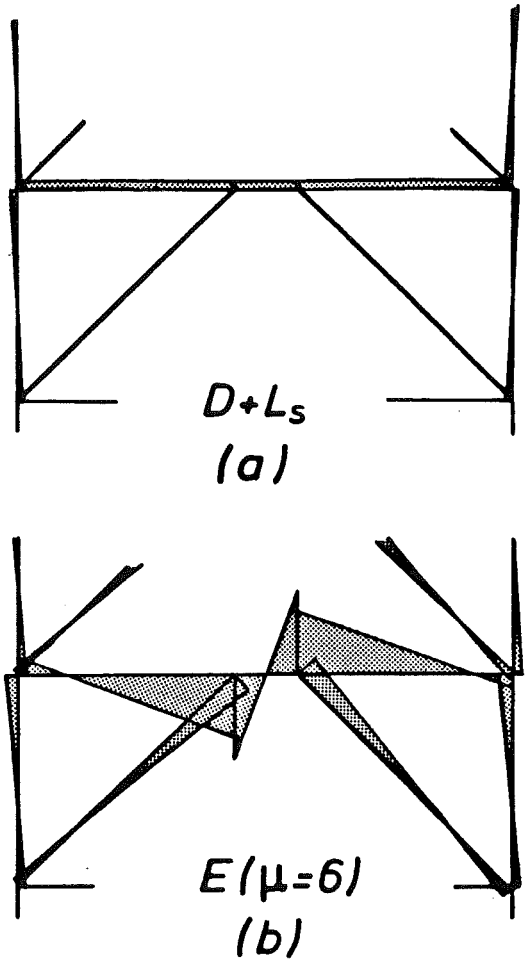

Figure 5.9. Design Level Elastic Subassemblage Moments

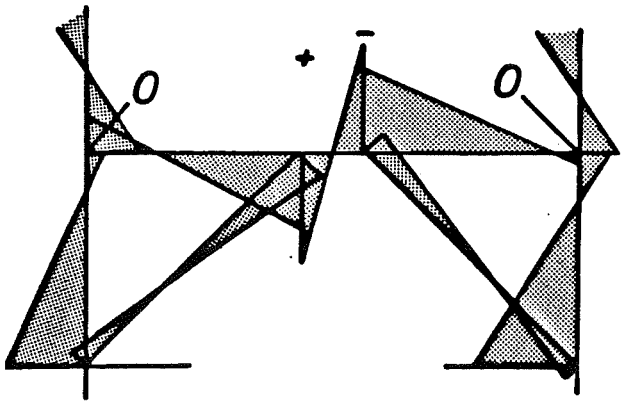

Figure 5.10. Bending Moments at the Third Level During a Static Elasto-Plastic Analysis

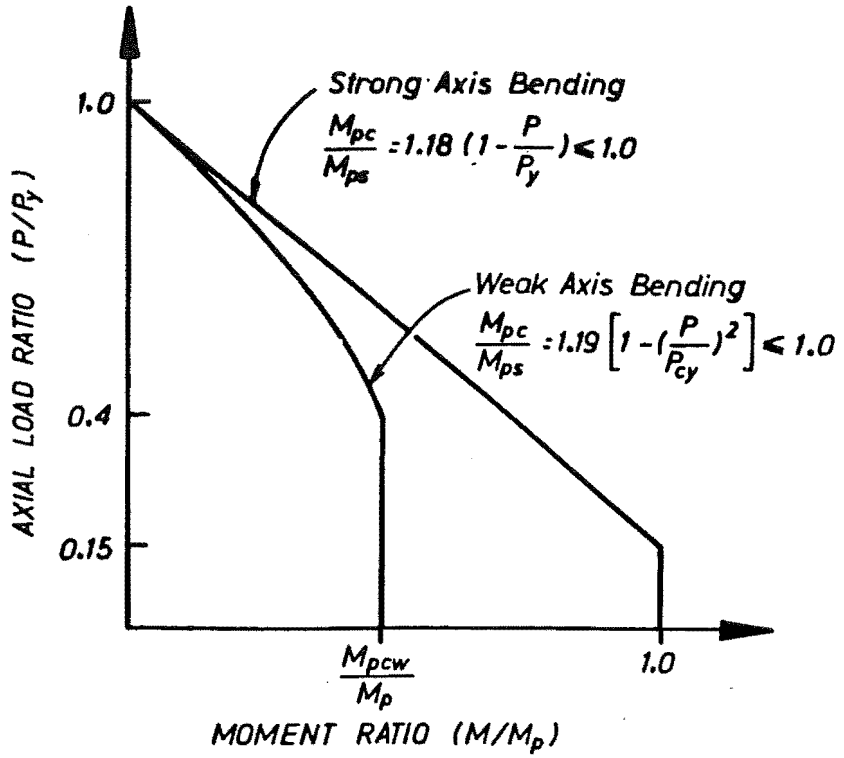

Figure 5.11. Moment-Axial Load Interaction Diagram For 310 UC 240

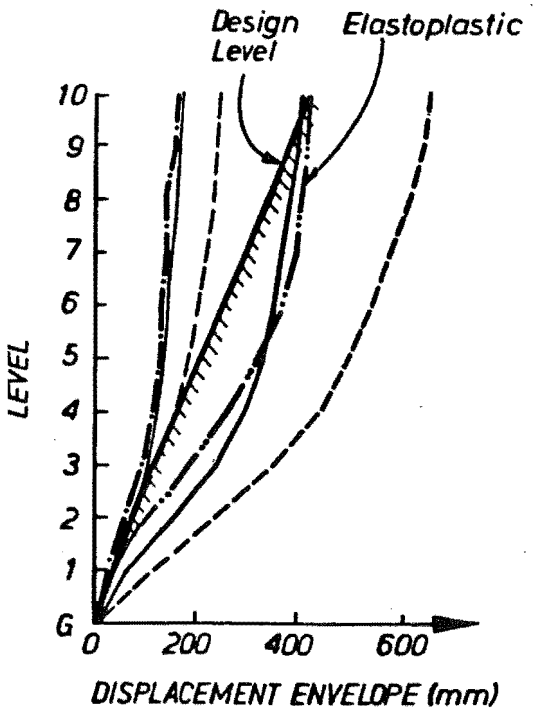

Figure 5.12. Displacement Envelopes of VBF

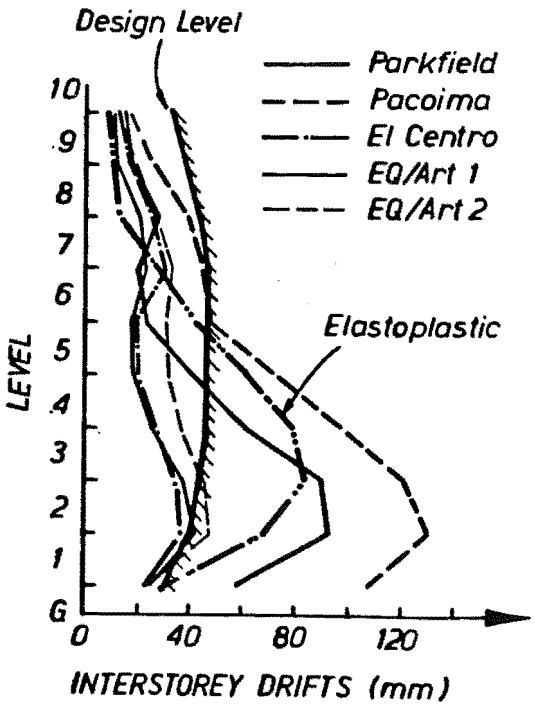

Figure 5.13. Interstorey Drift Envelopes of VBF

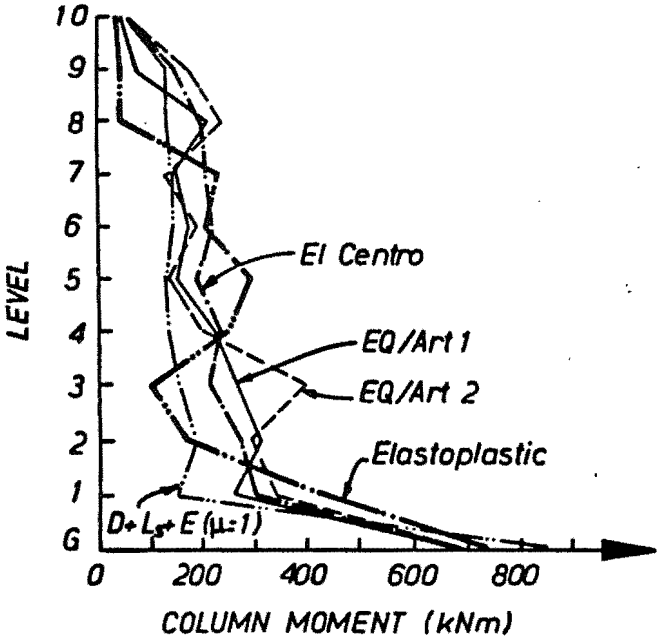

Figure 5.14. Maximum Column Moments in Ordinary VBF

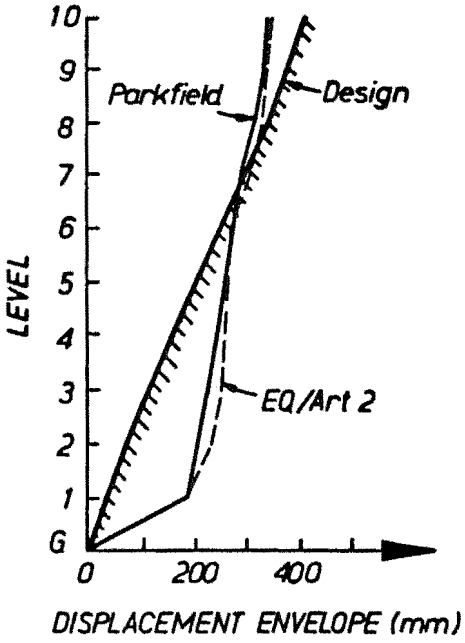

Figure 5.15. Displacement Envelopes of Pinned VBF

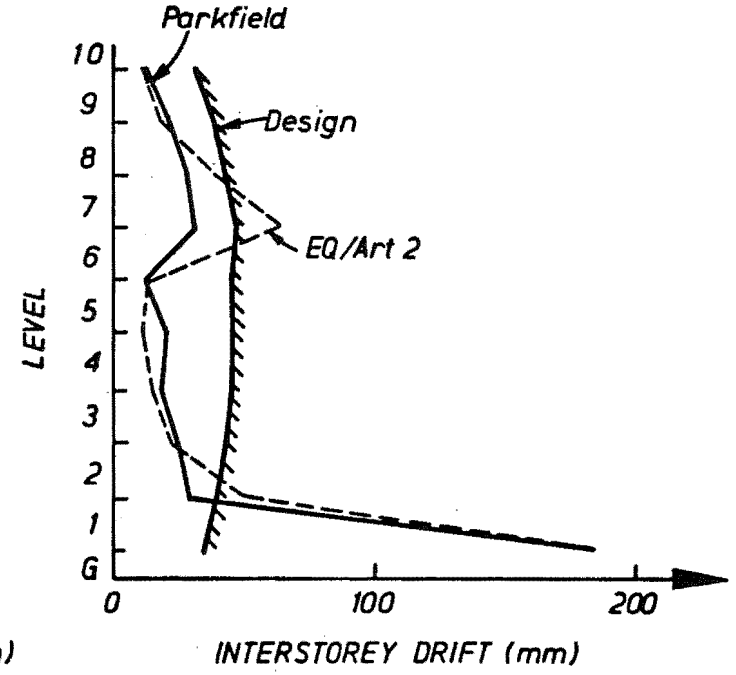

Figure 5.16. Interstorey Drift Envelopes of Pinned VBF

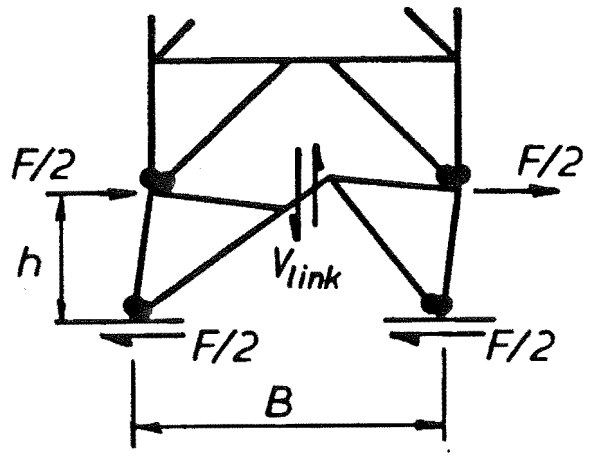

Figure 5.17. Mechanism to Obtain Base Shear

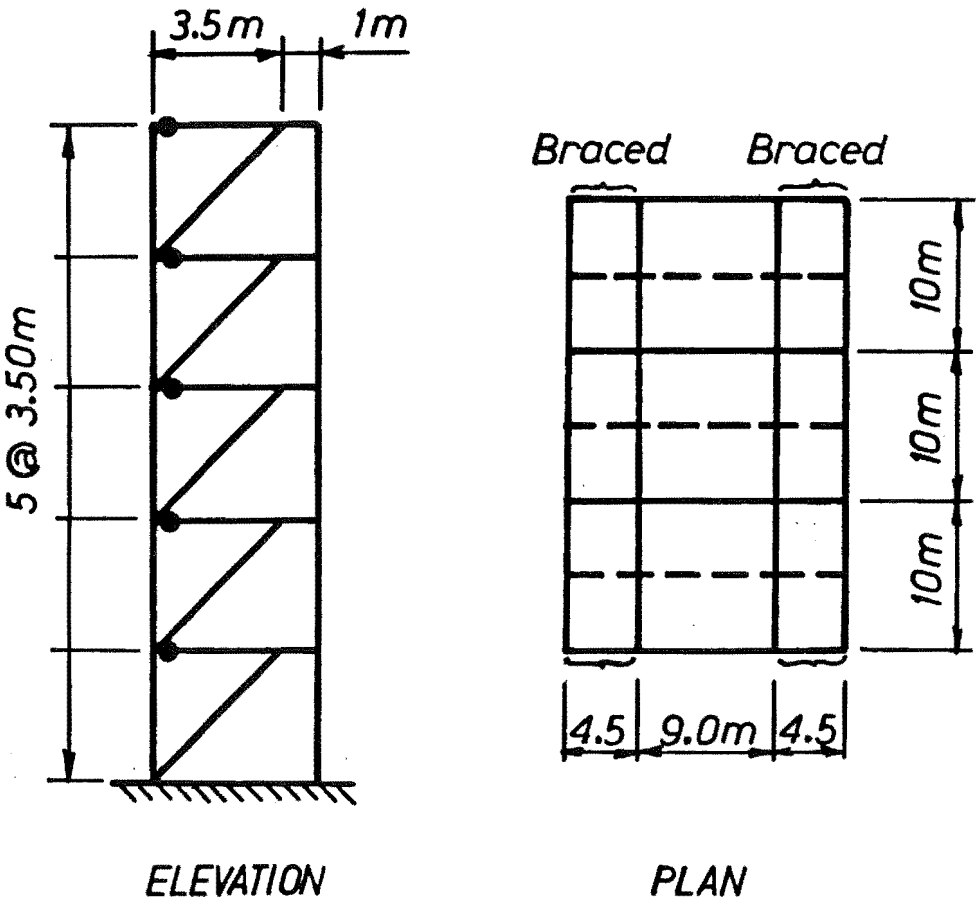

Figure 5.18. Dimensions of D-Braced Frame (DBF)

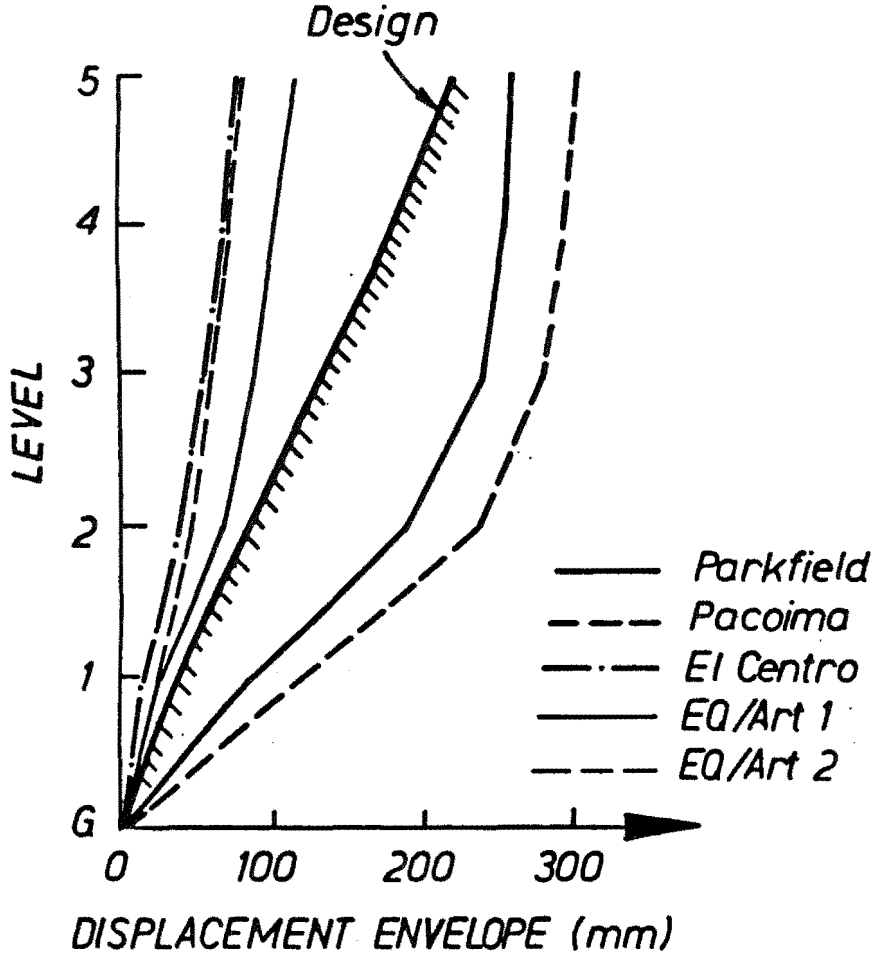

Figure 5.19. DBF Displacement Envelopes

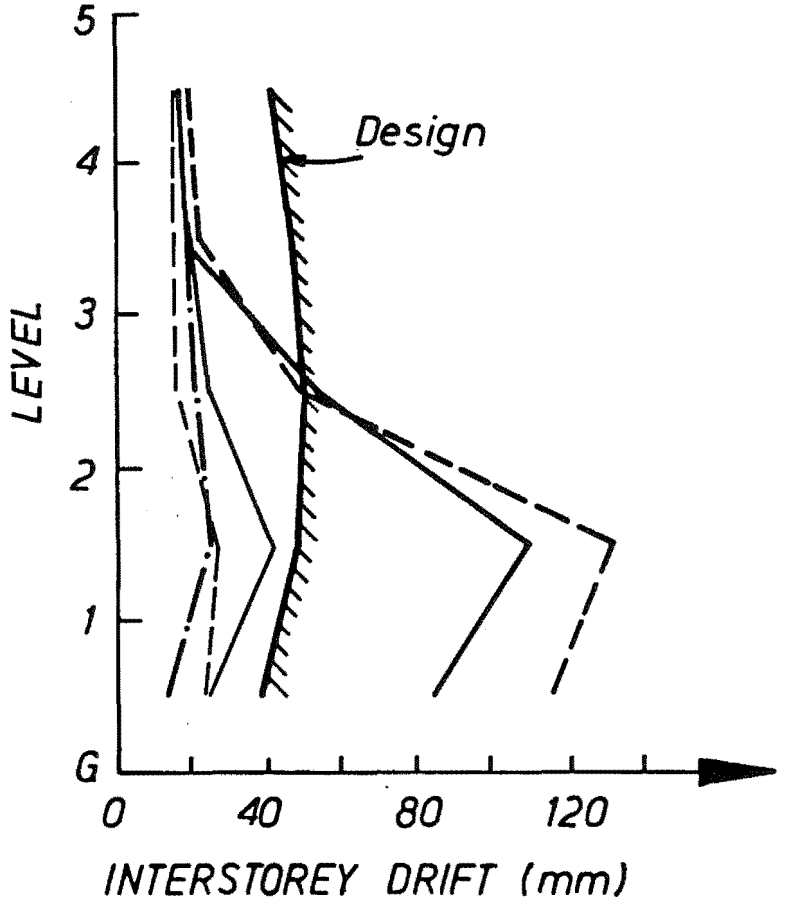

Figure 5.20. DBF Interstorey Drift Envelopes

5.7 REFERENCES

5.1 Popov E. P., Kasai K., and Engelhardt M. D., "Advances in Design of Eccentrically Braced Frames", Pacific Structural Steel Conference, Auckland, 1986, Vol. 1, p85-95.

5.2 Engelhardt M. D. and Popov E. P., "Behaviour of Long Links in Eccentrically Braced frames", Report No. UCB/EERC - 89/01. Earthquake Engineering Research Centre, University of California, Berkeley, 1989.

5.3 Malley J. O. and Popov E. P., "Shear links in Eccentrically Braced Frames", *Journal of the Structural Division*, ASCE, Vol. 110, No. 9, September 1989.

5.4 Kasai K. and Popov E. P., "General Behaviour of WF Steel Shear Link Beams", *Journal of the Structural Division*, ASCE, Vol. 112, No. 2, February 1986.

5.5 Kasai K. and Popov E. P., "Cyclic Web Buckling Control for Shear Link Beams", *Journal of the Structural Division*, ASCE, Vol. 112, No. 3, March 1986.

5.6 -, 1987 Code Change Submittals, UBC, Suggested Revisions to the 1985 Editions of the Uniform Codes. Further Study Items and Submittals for 1987. Building Standards, V. 55, No. 6, Pt 3. Nov-Dec, 1986.

5.7 Ricles J. M. and Popov E. P., "Dynamic Analysis of Seismically Resistant Eccentrically Braced Frames", Report No. UCB/EERC-87/07, June 1987.

5.8 SANZ, "Commentary: Design of Concrete Structures", NZ3101 Part 2, 1982.

5.9 Popov E. P., Correspondence on the updated draft comments to the AISC Specifications Task Committee on Seismic Design, 28 August, 1987.

5.10 Paulay T., "A Consideration of P-delta Effects in Ductile Reinforced Concrete Frames", Bulletin of the New Zealand National Society for Earthquake Engineering, Vol. 111, No. 3, September 1978.

5.11 SANZ, "General structural design and design loadings for buildings", DZ4203, Draft for comment, New Zealand Standard, 1986.

5.12 Popov E. P., Bertero V. V. and Chandramoulli S., "Hysteretic Behaviour of Steel Columns", UCB/EERC 75-11, September 1975.

5.13 SANZ, "General structural design and design loadings for buildings", DZ4203, Draft for comment, New Zealand Standard, 1989.

5.14 Bertero V. V. and Kamil H., "Nonlinear Seismic Design", Can. J. Civ. Eng., Vol. 2, 1975.

Chapter 6

BEHAVIOUR OF STEEL MEMBERS

6.1 SYNOPSIS

In this chapter some parameters affecting the behaviour of steel I-shape members subject to cyclic loading are described. The present New Zealand section limitations for members to provide adequate ductility capacity are discussed as is the cyclic behaviour of the steel material, steel sections, and steel members. A background to the cyclic testing of steel-beam columns, and previous work undertaken to find the achievable ductility of such members is given. Relationships between different forms of damage measurement such as ductility and rotation are also described.

6.2 INTRODUCTION

In the analyses of frames which have been carried out in the previous chapters, results from experimental tests relating to the initial stiffness, strength and post-elastic behaviour of members have been used in frame modelling. The inelastic member demands obtained from computer analyses were then compared with the experimental deformation capacities.

Test results of the inelastic cyclic behaviour of beams are readily available but relatively little has been written on the ductility capacity of cyclically loaded steel beam-columns. This may be because only a limited amount of column hinging is expected at the base of most frames in an earthquake. It was therefore decided to test some beam-columns with section properties similar to those used in steel ductile moment-resisting frames. This testing is described in the following chapter but the background to the testing describing some aspects of the behaviour of steel beam-columns is discussed in this chapter as well as the behaviour of the steel material, the behaviour of the members and the behaviour of these members in frames.

Some comments are made regarding the methods of testing, the methods by which damage is measured and the relationship between these methods because of the importance of the relationships between the analytical and experimental work.

6.3 MATERIAL CHARACTERISTICS

In order to understand the cyclic behaviour of members it is necessary to firstly understand the behaviour of the material. This has been described in detail by many authors such as Lay [6.1] for monotonic loading conditions. The monotonic stress strain curves are shown in Figure 6.1. In this figure the true stress-strain curve is based on the force acting on the actual cross-sectional area of the specimen, which changes during testing, whereas the compression and tensile test curves are based on the cross-sectional area before the testing started. During the tensile tests the area decreases because of Poisson's ratio effects and necking resulting in a true stress larger than that implied from the tensile test curve. During compression, the area over which the force acts increases, thereby decreasing the true stress. The average strain hardening stiffness of steel in compression was 38% greater than the average strain hardening stiffness in tension in tests carried out by Mander [6.2].

Methods for predicting the cyclic behaviour of steel have been described by Kato [6.3], Mander et al. [6.2], Peterson and Popov [6.4] and Beamish [6.5] and methods for determining the low-cycle fatigue fracture limits of test samples, such as Miners rule, the Manson-Coffin hypothesis, and the dissipated energy hypothesis have been discussed by Popov [6.6]. A further method has been described by Kikukawa and Jono [6.7].

6.3.1 Stress-Strain Behaviour

In this section, the steel yield stress, the length of flange yield plateau and strain hardening are discussed.

(a) Yield Strength

The yield strength of steel is usually the basis for selecting the maximum force for which a steel element should be designed. In capacity design, the probable strength variation between the beams and the columns is incorporated into the beam overstrength factor to limit the possibility of column yielding. A factor of 1.35 to allow for the variation of yield strength between sections has been suggested by Patton [6.8].

(b) Yield Plateau

Patton [6.8] has recommended that, for sections of full and limited ductility, the minimum length of the yield plateau should be at least $10\varepsilon_y$,

and $3\varepsilon_y$ respectively. However, the section slenderness limitations suggested by Walpole and Butcher [6.9] for limited ductility are based on monotonic tests in which the minimum length of the yield plateau was $10\varepsilon_y$.

Sections subjected to limited ductility demand with a yield plateau length of $3\varepsilon_y$ may attain approximately the same strength as a fully ductile member with a yield plateau length of $10\varepsilon_y$ because strain hardening will occur at a smaller displacement in the limited ductility section. It is therefore suggested that if the minimum length of yield plateau is $10\varepsilon_y$ for both limited and fully ductile sections, the recommended overstrength values of 1.35 and 1.50 should be used for the respective ductility demands. However, if steels with a minimum yield plateau length of less than $10\varepsilon_y$ are to be used in members of limited ductility a larger overstrength factor than 1.35 may be required.

Lay [6.1] has described the monotonic post-elastic behaviour of steel in the yield plateau region. The cyclic behaviour of steel from Petersen and Popov [6.4] is shown in Figure 6.2. Lay [6.1] assumes that the full length of yield plateau is available in compression after yielding has occurred in tension. However, other authors such as Mander et al. [6.2], Petersen and Popov [6.4], and Kato [6.3] have shown that if strain hardening occurs in one direction of loading that there will be no yield plateau in the other direction. Tests by Mander et al. [6.2] indicate that the length of the yield plateau in compression may be less than in tension.

The use of yield strength as a parameter in members responding inelastically to cyclic loading is not as important as it is in elastic design. After the yield plateau has been exhausted during cyclic loading there is no abrupt change in the material behaviour at the yield strength, but there is a gradual change in stiffness as deformation occurs in the strain hardening range. The maximum strength is related to the ultimate test specimen strength rather than to the yield strength.

Kato and Akiyama [6.10] and Kato, Akiyama and Yamanouchi [6.11] have developed a method which seems to predict the cyclic hysteresis curve for steel from the monotonic curve and vice-versa if there is no buckling.

(c) Strain Hardening

The effect of strain hardening of steel has been studied by many researchers amongst whom are Kato and Akiyama [6.10]. It occurs when the material strain is greater than the strain-hardening strain, ε_s, or when the yield plateau

has been expended as a result of cyclic loading allowing the strength to become greater than the yield strength. The principal effect of strain hardening is to increase the strength of steel and reduce the material stiffness. It may be seen from Figure 6.1 that steel can carry greater load in compression than in tension before buckling. This results in a compressive overstrength factor greater than that obtained from the commonly used tensile test. If the material post-elastic stiffness is high, this will cause large member overstrength forces which are not desirable, whereas, if it is low there will be low overstrength forces. However, a low stiffness will increase the likelihood of buckling.

A relative strain hardening factor of 1.10 has been recommended by Patton [6.8] to allow for the overstrength of steel beams and is based on work by Erasmus [6.12]. Member overstrength factors of 1.50 (≈1.35*1.10) and 1.35 have been recommended for full and limited ductility design respectively as no strain hardening is assumed to occur in limited ductility members. Further analytical modelling is required in order to determine the overstrength values of typical steel sections subjected to cyclic loading with different values of post-elastic stiffness and different lengths of yield plateau.

The minimum strength of steel is specified in New Zealand, but there are no specifications for the maximum level. It is suggested by the present writer that an upper limit on the ultimate strength of steel sections expected to deform inelastically in a seismic event be specified so that the maximum beam strength may be realistically approximated.

6.3.2 Effect of the Cyclic Loading on Steel

Cyclic testing has indicated that the strength of the specimens increases with each cycle when the strain hardening range is reached and then, at some point, fracture occurs. The two mechanism by which strength increase and fracture occur are described below.

1) Strength increase. As energy is absorbed during load cycles, crystals are stretched and compressed causing crystaline defects to be removed and bonding to become stronger. This results in an increase in strength and decreases the material post-elastic stiffness. In this process, often referred to as work hardening, the molecules do not return to the initial configuration. After a few cycles of loading, the material strain is usually in the strain-hardening region and the yield plateau has been expended.

2) Fracture. Strain is not spread uniformly throughout the material but is concentrated in certain locations. This phenomena is shown by the necking of steel in the tensile yield test. If many inelastic load cycles are applied, a low-cycle fatigue fracture may occur resulting from a cumulative localised strain which exceeds the material ultimate strain. A small initial fracture may rapidly propagate throughout other parts of the material causing a sudden decrease in strength.

Excessive buckling and discontinuities in the member or in the material may increase the possibility of strain concentration at a location, possibly leading to fracture.

6.4 MEMBER BEHAVIOUR

6.4.1 Residual Stresses

Residual stresses result from non-uniform cooling of a section or plate which has been rolled or welded. These stresses are in equilibrium over a member cross-section. The residual stress profiles on actual steel sections have been obtained by Tall [6.13] and Popov et al. [6.14]. Approximations to these residual stress profiles, such as that shown for an I-shaped member in Figure 6.3, are commonly assumed in computer analyses. The value of the maximum residual stress, F_r, is often taken as 0.30 F_y [6.15]. The uneven distribution of residual stresses means that some of the fibres in the section will yield before others leading to a decrease in stiffness and a possible decrease in strength.

A comparison between the load displacement relation of a compact section in flexure with and without residual stresses is shown in Figure 6.4 [6.1]. Analytical studies by Kulak and Dawe [6.15] have shown that residual stresses have more effect on the behaviour of a non-compact member than on a compact member. According to the column design curves for the draft Australian steel code [6.16], Tall [6.13] and Mitani, Makino, and Matsui [6.17] residual stresses in built-up welded sections are more critical than in rolled sections.

It is well known that any weld may cause yielding of the material next to the weld. If a weld is defective, and is cut out, and the material rewelded several times strain may accumulate in the material beside the weld as shown in the stress-strain diagram in Figure 6.5. This does not present any major

problems with the high quality of steel generally presently available in New Zealand, however potential problems are best avoided by obtaining a good weld the first time.

6.4.2 Effect of Shear Interaction

In plastic design, shear and flexural yielding may interact to reduce the strength of a section. Members in moment-resisting frames are generally designed to deform inelastically in bending, and a capacity design type of approach may be used to design against a large amount of shear yielding. The relative shear and flexural strengths in the presence of axial load may be calculated in the manner described in section 7.3. If shear yielding is to be an energy dissipating mechanism, the web should be detailed as a shear link with web stiffeners to avoid rapid degradation of strength.

6.4.3 Parameters Affecting the Member Failure

Galambos and Lay [6.18] have listed the factors which affect the deformation capacity of as-rolled structural steel wide-flange beams. They are, moment gradient, spacing of lateral bracing, the end restraint provided by spans adjacent to the inelastic span, properties of the lateral bracing, local buckling, material and cross-sectional properties of the beam, and lateral and torsional buckling. The loading regime and axial load ratio will also affect the behaviour of columns tested under repeated loading.

Failure of members may result from high-cycle fatigue fracture, buckling or low-cycle fatigue fracture. Only the last two mechanisms of buckling and low cycle fatigue fracture are expected during an earthquake.

6.4.4 Buckling

The two main forms of buckling are section local buckling, in which the section shape changes as a result of web or flange buckling, and member lateral, or lateral-torsional buckling in which the member as a whole distorts. As strength loss may result from buckling the parameters affecting buckling should be controlled. The different forms of buckling interact, but for simplicity in design they are generally considered independently.

(a) Local Buckling

Several parameters affect the likelihood of buckling of steel members. These include the length of member yield and the section slenderness ratios. The flange tips of I-shaped members may deform in the different modes shown in Figure 6.6.

Lay [6.19] has stated that for local buckling to occur it is necessary for a longitudinal length greater than or equal to one half of a buckle wavelength to be fully yielded, and if the ends of the buckling region are well restrained, it will be necessary for a full wavelength to have yielded. The wavelength of a buckle is a function of the material post-elastic stiffness.

If the length of flange which has yielded is not long enough to permit buckling, further cycles of loading may decrease the material tangential stiffness to the stage when a smaller buckle wavelength is required for buckling.

The length of flange which has yielded is a function of the distance to the point of contraflexure, the overstrength moment, M_p^o, and the yield moment, M_y, as shown in Figure 6.7. If the minimum length of yielded flange required for buckling to take place is equal to the breadth of a section, B, then flange buckling is not expected to take place while Equation 6.1 is satisfied.

$$(M_p^o/M_y - 1) \leq B/L \qquad \text{Equation 6.1}$$

Local buckling is generally controlled by limitations on the section slenderness ratios, B/T and D/t. The following flange and web slenderness ratios for I-sections reproduced in Table 6.1 have been suggested by Walpole and Butcher [6.9]. Some of the assumptions about the behaviour of specimens which have been made in order to obtain these values are described below. The length of flange outstand, b_1, is $(B-t_w)/2$, and the unsupported length of web, d_1, is (D-2T) is shown in Figure 6.8. The flange and web slenderness limits are considered independently although flange and web buckling are generally both required to occur before there is any strength loss.

In the New Zealand loadings code [6.20], category one (full ductility) and two (limited ductility) members are expected to be able to withstand four cycles of loading to displacement ductilities of 6 and 3 respectively before losing 30% of their ideal strength. Category three members are expected to be able to attain the yield strength of the section.

Table 6.1
Suggested Section Slenderness Ratios

Category		1	2	3
Flanges or plates in compression with one unstiffened edge.	$\frac{b_1\sqrt{F_y}}{T}$	120	136	256
Webs under flexural compression	$\frac{d_1\sqrt{F_y}}{T}$	1000	1120	1340
Webs under uniform axial compression	$\frac{d_1\sqrt{F_y}}{t_w}$	500	512	560

Limiting ratios of section slenderness are generally made to discourage local buckling. These limitations are generally proportional to the inverse of the square root of the yield stress, $1/\sqrt{F_y}$, and are also dependent on the square root of the tangent stiffness of steel, $\sqrt{E_T}$. When steel is loaded in the strain-hardening range, the force carried by strain-hardening steel increases, the tangent stiffness decreases causing the likelihood of buckling to increase.

The values for category 3 members were obtained from the provisions of the Australian steel code [6.16]. The background literature for category 1 and 2 members is described by Walpole and Butcher [6.9]. Slenderness ratio limits of category 2 members are to allow a specimen to attain the plastic moment with some redistribution under monotonic loading before buckling and the section slenderness values for category 1 members were obtained by "engineering judgement" based on a literature study of previous cyclic testing and were made slightly more restrictive than those of category 2 members. These restrictions allow for the possibly increased stress and the lower tangent stiffness in members which are expected to be subjected to higher levels of ductility demand.

The present rules for the flange and web slenderness ratio limitations of beams are governed by a philosophy of discouraging buckling during monotonic loading before strain hardening occurs. This simple approach is felt to be overly severe as the literature has shown that significant local buckling may occur before member strength is lost even during cyclic loading. While rational models have led to slenderness ratios for buckling both in the elastic and strain-hardening range under monotonic loading, this has not yet been done for cyclic loading.

Beamish [6.21] has developed a finite element program to predict the inelastic response of I-section beam-columns under cyclic loading. If the

future results of the analyses compare well with experimental data, the program may be used to obtain flange and member slenderness ratios for cyclic loading so that recommendations may be made for limiting the values of section slenderness for full and limited ductility response.

(b) Lateral Buckling

Walpole and Butcher [6.9] and Butterworth and Spring [6.22] have suggested minimum spacings of lateral restraints in order to control lateral and lateral-torsional buckling in members expected to be subjected to limited and full ductility demands.

(c) Strength Loss from Buckling

Popov and Pinkney [6.23] have shown that strength degradation occurs slowly with local buckling in 8WF20 sections. These sections were very compact with a flange slenderness ratio, B/2T, of 6.60, and a web slenderness ratio, D/t, of 33.1. A slow, rather than a sudden or brittle loss of strength may reduce the possibility of catastrophic failure.

A member flange or web may have to resist bending forces in addition to direct axial forces caused by the eccentricity in the flange or web being away from the line of action of applied force when local buckling has started as shown in Figure 6.9. The maximum axial load which may be carried is reduced by the interaction with the bending stresses which occur at the same time.

Local buckling of beam flanges leads to buckling or twisting of the web and the movement of the centre of the flange away from the line of applied force as shown in Figure 6.10. A moment is introduced which will accentuate the local buckling of the whole section and cause strength degradation as the flange has to resist axial load and bending. It is quite commonly found in testing [6.24] that these buckles do not straighten out during reverse loading, but cause a shortening of the beam. If the lateral slenderness of the beam is high, the effect of local buckling will be more pronounced causing a greater rate of strength degradation.

If the same type of local buckling deformation occurs at both the top and bottom of a column it may cause eccentricities which affect the lateral buckling of the column as a whole. For example, if the flange tips move at both ends of a column in the way shown in Figure 6.6d, then eccentricities may be caused near the middle of the column as shown in Figure 6.11. This

will cause P-delta effects and will possibly lead to yielding of the centre of the column by bending in the weak axis. Similar behaviour may result if the flanges at both ends of the column move in the way shown in Figure 6.6c except a lateral-torsional buckling mode in the column may result. Because severe buckling of these types may affect the behaviour of the rest of a frame, it is desirable large amounts of buckling should not occur.

6.4.5 Previous Work on the Monotonic Deformation Capacity of Beams

Some previous studies of the deformation capacity of monotonically loaded beams are described below.

(a) Galambos and Lay

Galambos and Lay [6.18] developed an equation to estimate the inelastic deformation capacity of beams in which it is implied that the moment capacity would drop below the plastic flexural strength, M_p, at the onset of local buckling [6.25]. Local buckling was only considered to occur when the yielded length of flange is greater than an optimum length, which is approximately equal to the breadth of the flange, B, for the compact sections used. They found that inelastic rotations of over 0.035 radians may be obtained for these sections with closely spaced flange braces, and that as member lateral slenderness ratios seldom exceed 50 and axial loads seldom exceed $0.30P_y$, the beam-columns will behave primarily as beams and deliver end rotations approximately one half that of beams before local buckling occurs.

(b) Lukey and Adams

Lukey and Adams [6.25] found that the length of buckle was dependent on the member shear and varied from the full yielded length to approximately one half of the yielded length for the specimens tested. The rotation capacity suggested by Galambos and Lay [6.18] was modified to include the effects of the member shear.

The relationship between rotation capacity and the flange slenderness ratio, B/T, was found to be gradual and did not show any abrupt improvement when the flange slenderness attained the compact value. The load-carrying capacity of compact sections tended to decrease more gradually than it did with non-compact sections.

(c) Kemp

Kemp [6.26,6.27] suggested a theoretical model for the local buckling of beams using techniques developed by Galambos and Lay [6.18]. The model predicted the maximum moment and the plastic rotation capacity of steel members and was consistent with experimental results. Kemp observed that enhanced levels of ductility may be achieved by ensuring that limiting conditions for both lateral and local buckling do not occur simultaneously and that tighter limits for the flange slenderness ratio are required for columns than for beams.

6.4.6 Cyclically-Loaded Beams

(a) Buckling

Popov and Pinkney [6.23] have carried out cyclic cantilever bending tests on very compact steel beams and concluded that the load-deflection hysteresis loops keep remarkably stable shapes and that the onset of flange buckling does not imply an immediate loss of strength when closely braced compact members are used.

(b) Low-Cycle Fatigue Fracture

Although the form of the equations for low-cycle fatigue fracture have been used with some success to estimate the damage and ductility capacity of steel members by Yamada [6.28,6.29], low-cycle fatigue fracture would not usually be expected to occur in well detailed members during an earthquake for the following reasons:

i) The magnitude and number of cycles of loading occurring in an earthquake are generally smaller than that which would cause low-cycle fatigue fracture in New Zealand steel sections. Tests by Popov and Pinkney [6.23], and Johnstone and Walpole [6.30] have shown for beams that many cycles of loading may be required before a large amount of strength is lost.

ii) Members tend to lose strength by means of buckling rather than by fracture. Testing carried out in this report, as well as further testing carried out at the University of Canterbury [6.24,6.31] have shown that after many cycles of loading to high displacement ductilities, large amounts of buckling occurred prior to any fracturing.

Popov [6.6], in a summary paper of experiments of steel members and their connections stated that for steel beams, low-cycle fatigue is not a serious problem.

6.4.7 Member Behaviour Under Monotonic and Cyclic Loading

Popov [6.6] suggested that as requirements for repeated loading are more severe than for monotonic loading, it is prudent to be more conservative in assigning section slenderness ratios for cyclically loaded members rather than for those which are monotonically loaded.

Members which are able to satisfy a certain monotonic ductility rating may not be able to perform to that same cyclic ductility for the following reasons:

i) the range of displacement covered during cyclic loading from $+\delta$ to $-\delta$ is twice the range of deformation for monotonic loading from 0.0 to $+\delta$ for the same displacement ductility,

ii) after the first inelastic cycle the length of the yield plateau will be reduced considerably or may have disappeared completely, and

iii) the ductility capacity of a member decreases as increasing numbers of cycles are applied.

6.5 BEAM-COLUMNS

The deformation capacity of beam-columns is affected by the level of applied axial load in addition to the parameters which affect the behaviour of beams. In this section New Zealand design recommendations for steel beam-columns are described and a literature summary are given. Axial deformation, the shape of the hysteresis loops, and the ultimate column strength is discussed below.

6.5.1 Design of Beam-Columns

Butterworth and Spring, as part of the New Zealand study group for the design of steel structures [6.22] have recommended that maximum axial load ratios (P/P_y) for sections which are to perform to full ductility and limited ductility levels of seismic loading should be 0.5 and 0.7 respectively. Possible reasons for these limits for fully ductile members are described in section 5.4.8. The axial load limits for limited ductility members is possibly based on test results and engineering judgement. Requirements to provide sufficient rotation capacity for hinging at the column ends are also incorporated in the recommended axial load ratio limits [6.22] shown in Figure 6.12.

Butterworth and Spring [6.22] have also recommended that the flange slenderness requirements of columns should be the same as that given in

Table 6.1 for beams and the web slenderness should be based on uniform axial compression acting over the whole web independently of the actual column axial load level. Column webs will normally be subjected to both flexural and axial compression so these recommendations of Butterworth and Spring [6.22] are somewhat conservative. Experimental tests and calculations [6.32] have shown the required web slenderness ratio to be a function of the axial load ratio and approximate relationships for web slenderness ratio as a function of the axial load ratio for design have been suggested by Lay [6.33] and recently by the new New Zealand steel structures code [6.34].

6.5.2 Literature on the Cyclic Testing of Beam-Columns

Mitani, Makino and Matsui [6.17] studied the influence of local buckling on the cyclic behaviour of steel beam-columns. For tests of specimens with B/2T=8 to ductilities from 10 to 15, the strength was maintained until web buckling occurred. Three types of behaviour were observed for specimens tested at low ductility levels from 2 to 5. In the first the strength decreased gradually for members with B/2T=8, P/P_y=0 independently of the D/t ratio and for B/2T=8, D/t<40 for P/P_y= 0.30 and 0.60. In the second type there was a large decrease in strength with each cycle of loading which was observed when B/2T=8 and D/t>40 and P/P_y=0.30, and B/2T=11 and 16, P/P_y=0.60 regardless of the value of D/t. In the last type, a gradual decrease in strength occurred after a large decrease in the first few cycles when B/2T=11 and 16 and P/P_y = 0.0 and 0.3 regardless of the D/t ratio.

Mitani, Makino and Matsui [6.35] have performed many tests and developed an empirical formula for the estimation of rotation capacity of steel beam-column members. Although cyclic testing seems to have been carried out, the rotation capacity (R) was defined on the virgin or monotonic loading curve. The equation takes into account both the member and section slenderness ratios. Results indicate that most of the steel sections commonly available in New Zealand have monotonic rotational capacities ($R = \theta_{cr}/\theta_{pc} - 1$) greater than ten. The flange slenderness ratios (B/2T) varied from between 8 and 16 and the web slenderness ratios varied from between 17 and 70. The ductility capacity of each column type with axial load ratios between 0.3 and 0.6 was found to be approximately constant and approximately 30% of the rotation capacity if no axial load were applied.

Testing has been carried out by Yamada [6.28,6.29], and formulae for low-cycle fatigue fracture were applied to a steel section subjected to different levels of axial load. A straight line on a log-log graph as shown in Figure 6.13 was found to approximate the number of loading cycles an

axially loaded member could sustain to a given displacement. The number of cycles of loading was found to be an important factor in determining the rotation capacity of members. The reasons for the relationship were stated as not being known at the time the papers were published. The effects of strain-hardening were described, as were the shape of the hysteresis loops. The section had flange (b_1/T) and web (d_1/t) slenderness ratios of 9.9 and 17.4 respectively. Yamada defined failure as when fracture occurred, rather than on the basis of strength loss.

Popov, Bertero and Chandramoulli [6.36] tested four beam-columns in bending about their strong axis as part of a subassemblage with axial load ratios, P/P_y, of 0.8, 0.6, 0.5, and 0.3. They found that the specimens with axial load ratios of up to 0.50 behaved very well. Yielding was observed to occur below the joint in one direction of loading and above the joint in the other direction producing cumulative column curvatures and deforming the column into a "C" shape. A large amount of axial shortening was also observed to occur but no reasons were given for this. All of the sections were compact having a flange slenderness ratio (b_1/T) of either 5.92 or 7.00.

Cyclic testing of steel columns has also been carried out by other authors such as Yokoo, Nakamura and Komiyama [6.37], Kato and Akiyama [6.10], and Igarashi, Matsui and Yoshimura [6.38] who were studying the shape of the hysteresis loop.

It may be seen from this literature survey that very little inelastic cyclic testing of columns has been carried out to date. Popov [6.6], in a summary paper of experiments of steel members and their connections stated that the commonly accepted approach of designing moment-resisting frames tries to avoid significant inelastic action in the columns. A concentration of work in beam testing, rather than column testing has resulted from the acceptance of this strong-column weak-beam philosophy in the design of frames causing the likely beam ductility demand to be greater than that in the columns. In a review of the behaviour of steel members in earthquake resistant frames, De Buen [6.39] has observed that information on the cyclic behaviour of steel beam-columns is scanty.

It is necessary to understand the inelastic cyclic behaviour of columns because, in a beam-sidesway mechanism, the columns at the base of the structure are expected to yield, and although most codes recommend strong-column weak-beam design, provisions which do exist are insufficient to guarantee that column hinging will be totally inhibited throughout a structure. The limited amount of experimental data available [6.29,6.36]

indicates that large ductilities may be obtained from some columns subjected to inelastic load reversals. A limited amount of hinging may be permitted in some columns in moment-resisting frames without a large loss in member strength. It is also necessary to verify whether the axial load limitations recommended by Butterworth and Spring [6.22] are reasonable for steel members.

It is desirable that further testing testing be carried out in order to gain more information about the deformation capacity of steel members, the amount of axial shortening which is likely to occur, and the mechanisms by which failure occurs.

6.5.3 Column Axial Deformation

It has been observed previously only by Popov at al. [6.36] that considerable axial shortening may occur in a column with a compressive axial load before its lateral load carrying capacity is lost, but no reasons were given.

The behaviour of a rectangular cross-section is shown in Figure 6.14a and an elasto-plastic stress-strain rule was assumed for simplicity. The section was initially subjected to an axial load ratio, P/P_y, of 0.50 to obtain the section stresses and strains of Figure 6.14b. A moment was then applied, which in this case corresponded to the yield moment of the section with no axial load, resulting in the stress and strain distribution of Figure 6.14c. When this moment was removed it may be seen from Figure 6.14d that there was a residual average axial strain equal to the yield strain, ε_y. If a moment slightly greater than the yield moment is applied in the other direction, yielding will predominantly occur at the top of the specimen and further axial strain will result. As cyclic loading is carried out, more and more axial shortening will occur. Drawing these stress and strain diagrams for further cycles becomes complex so a computer model would best be used. The hysteretic behaviour of point "P" at the bottom of the cross-section is shown in Figure 6.14e. The dotted line indicates the stress and strain behaviour which would take place in later cycles. The hysteresis loop for point "P" is expected to be symmetric and centred about the origin for sections with no axial load if the top of the specimen is subjected to equal displacements in each direction because the neutral axis will be in the centre of the section so the extreme fibres will deform equally in tension and compression. For members with a high level of axial loading, yielding of these fibres in one direction is possible resulting in a monotonic type of stress-strain curve.

The amount of axial shortening depends on the magnitude of the axial load, the length of the member which has yielded, the stress-strain characteristics of the material, the number of cycles of load applied and the displacement magnitude of those cycles, but it is not affected by buckling until the later cycles. If stress-strain rules of steel were identical in tension and in compression then any compressive axial load with inelastic cyclic column bending would result in axial shortening.

As flange strains build up in the columns subjected to cyclic load, the tangent stiffness of the flange stress-strain diagram is expected to decrease leading to a greater likelihood of local buckling. It is also expected that the buckles, once formed, will not straighten during load reversal. Present requirements of section slenderness for columns do not include this cumulative effect.

In real columns major axial deformation comes from two sources,

1) that occurring in columns before the occurrence of buckling in which the position of the neutral axis moves within the section. It is expected that axial deformation of this sort will accumulate in proportion to the amount of inelastic action occurring in a column, and

2) that occurring as a result of member buckling in which the neutral axis moves within the section because the compressive stiffness is less than the tensile stiffness. This occurs in beams [6.24] as well as in columns.

6.5.4 Member Hysteresis

(a) Shape of Loops

Hysteresis loops for beams have been shown by writers such as Popov [6.6] to be very rounded, whereas the shape of the hysteresis loops for columns have been shown by Yamada [6.28,6.29] to be almost parallelograms. For most steel beams and columns "fat" load-displacement hysteresis loops occur for members deforming in flexure implying good energy dissipation.

It is thought that the smooth rounded hysteresis shape of the beams is a result of the progressive yielding of the web. For the column section shown in Figure 6.15 it may be seen that the neutral axis of the section is in one of the flanges. On the first cycle of loading it may be expected that point "B" will yield before point "A". This will give a rounded stress-strain curve. However, when the lateral load is removed, the hysteretic diagrams shown in Figure 6.15 will result. For loading in the other direction, the neutral axis will move into the other flange and no yielding will occur at

"A" or "B". When loading is again carried out in the initial direction, the points "A" and "B" will yield at approximately the same time. In columns in which a large amount of axial shortening has taken place, the material will be well into the strain hardening range and the post-elastic stiffness will be very low. This will mean that there will be a relatively abrupt change in slope from the elastic stiffness to the post-elastic stiffness, and the parallelogram shaped loops observed by Yamada will result.

Hysteresis loops have generally been considered good if they absorb a large amount of energy. This has been thought to mean that collapse will be slow and safe and has also been thought to reduce the expected displacements of frames during earthquakes. However, recently the importance of the shape of the hysteresis loops has been questioned. Stewart [6.40] has shown that by running many analyses of single degree of freedom systems with different ground motion records that there were no trends in behaviour from the different hysteresis loops used.

It is thought that the amount of ductility and the effective change in period of the structure is of more importance than the energy absorbed by the loop. The fatness of the loop is therefore not regarded as being very important. However, very pinched loops may sometimes cause impact forces and loops with a negative post-elastic slope may increase the likelihood of overturning of a structure. More research is required to study both of these effects. Hysteretic loops often do not show the effects of reversibility or accumulation of damage such as may occur in the columns. It is thought that the reversibility of deformation is a more important factor than the actual shape of the loops themselves.

(b) Ultimate Strength of Sections

The ultimate flexural strength of beams is not generally as high as $F_{max}/F_y.M_p$, where F_{max} and F_y are the maximum stress and the yield stress found the test results of the tensile test pieces. Possible reasons for this are that buckling rather than tensile yield will often govern the maximum stress and every fibre within the section will not reach its ultimate stress at the same time. The stresses on an elasto-plastic section which is at its plastic flexural strength assumes an infinite curvature at the neutral axis of the section. Lay [6.19], based on test results, has suggested that the maximum flexural strength of beams may be estimated as $(F_{max}/F_y + 1)/2.M_p$.

The ratio of the maximum strength to the plastic strength of columns is expected to be different than that of beams. Reasons for this are described below and are illustrated on a rectangular section in Figure 6.16.

If the maximum stress of a steel fibre in tension or compression is assumed to be $\phi_o F_y$ and if every fibre on the section reaches its maximum stress at the same time, then the maximum beam strength, M_{max}, will be equal to $\phi_o M_p$.

Ideal stresses in a column when the section is plastic are shown in Figure 6.16a. The plastic moment capacity, M_{pc}, may be calculated from these stresses. The stress distribution shown in Figure 6.16b will result if the axial load on the section remains constant, overstrength stresses are considered and every fibre on the section reaches the maximum stress at the same time. This allows the neutral axis to move toward the section centroid so that more of the section will be available to resist flexure than is the case in Figure 6.16a. A larger moment than $\phi_o M_{pc}$ may be carried in the column section and the flexural overstrength ratio, M_{max}/M_{pc}, will increase as the level of applied axial load increases.

In any "capacity design" type of procedure it is essential that the relative strengths of beams and columns are known in order that the columns may be protected from excessive yielding. The possible high flexural overstrength of specimens subjected to high levels of axial load is useful as it provides an extra factor of safety against excessive column yielding.

6.6 MEMBERS IN FRAMES

The effect of inelastic action in the members will determine the behaviour of the frame as a whole. Inelastic action in the members will also be affected by secondary elements in frames, composite action and the non-structural elements. Some aspects of the behaviour of members in frames are discussed below.

6.6.1 Hinging of Beams in Frames

(a) Non-Composite Beams

Yielding may occur in a gravity loaded non-composite beam at the column face as well as within the length of the beam during earthquake attack as shown in Figure 6.17. The hinge locations for loading of the beam in the reverse direction are also shown in Figure 6.17. The locations of the plastic hinges on the beam are different in the two directions of loading. Yielding will

therefore occur in one direction only at each hinge position causing a moment-curvature hysteresis loop such as that shown in Figure 6.18 with accumulation of curvature with every cycle. This effect has also been discussed on work carried out on subassemblages by Bertero, Krawinkler and Popov [6.41]. Fenwick and Davidson [6.42] have also shown that some shakedown of moments may occur in gravity dominated frames where yielding may occur along the member length.

A greater angle of hinge rotation near the column face is required when yielding occurs within the length of the beam, rather than at the beam ends in order to produce the same subassemblage ductility as shown in Figure 6.19. The ductility demand in a non-composite beam may therefore be greater than that implied by the lateral load reduction factor even under monotonic loading.

(b) Composite Beams

All hinging may be forced to the ends of the composite beams by making use of the composite strength along the midspan region of the member. This will reduce the cumulative curvature at any one location. Clifton [6.43] has suggested that this may be achieved by making use of shear studs along the length of the member except for a distance of two and a half times the beam depth ($2.5D_b$) from the column face.

Care must be taken when the slab is in contact with the column that the column is designed for the flexural overstrength of the composite beam. The beam may increase in length because the top of the beam may be in tension for both directions of cyclic loading as shown in Figure 6.20. The slab is in compression during loading in one direction, but may be cracked and resist very little force in the other direction. The column may be designed for a lower moment, and the lengthening of the beams may be stopped if a suitable gap is left between the slab and the column.

If the composite strength of a member is not sufficient to force yielding away from the column face, cracking of the slab along the member length may occur during loading in only one direction also causing an increase in beam length. This has also been observed in a reinforced concrete beam-column subassemblage by Fenwick [6.44], and was found to be significant.

6.6.2 Hinging of Columns in Frames

Hinging in columns in frames has several consequences. Some of these have already been mentioned and others found as a result of the testing are mentioned in 7.13.9.2.

When flexural yielding occurs in a column it will be accompanied by axial shortening. As the column shortens, the beam shears will increase as shown in Figure 6.21. The axial load will be reduced in the shortened column and will be redistributed as increased axial load to the other columns in the storey. Depending on the design approach, the increased axial load may be greater than the design level. Increased axial loading in other columns is not desirable as yielding will occur at a lower flexural strength, the absolute displacement to which it may be subjected before failure will decrease, and the length of flange yield and the possibility of different types of buckling will be greater.

For tall frames, if hinging occurs in a column at every storey level causing a small amount of axial shortening at each hinge, there may be a large difference between the level of this column and other columns in the upper stories of the frame.

As the columns shorten, "non-structural" components may start to contribute to the overall structural behaviour. Popov et al. [6.36] have suggested that the fundamental period of the structure will decrease because of the lowering of the seismic mass thereby possibly attracting larger seismic forces, however, this effect is expected to be negligible. Popov et al. have also found in the testing of a subassemblage that curvature may accumulate during one direction of loading below the joint and in the other direction above the joint causing a progressive increase in curvature with each cycle and deformation of the column into a "C" shape. This deformation causes large P-delta moments to affect the column behaviour.

The strength and ductility capacity of columns are less than for beams and large cumulative effects may occur in columns subjected to cyclic loading. Large distortions caused by local buckling may have an influence on the lateral column stability. A soft-storey mechanism may occur if the columns yield possibly leading to very large column rotation demands and loss of strength. It is suggested, for these reasons, that column yielding should be discouraged during earthquakes.

Although column yielding is generally ductile [6.28] and may be permitted in earthquake-resistant frames, it may be seen from the above discussion that it is less desirable than beam hinging. The weak-beam strong-column approach has been used in the past in order to encourage beam yielding and discourage column yielding and buckling. Various ways of achieving this behaviour in a moment-resisting frame may be made by providing the columns with sufficient strength so that the yielding is predominantly in the beams.

It is recommended that column yielding should be discouraged and that large amounts of column hinging should not occur in frames during a design level earthquake. Some simple, practical methods for achieving this have been described in the previous chapters on moment-resisting and eccentrically-braced frames.

6.7 RELATIONSHIP BETWEEN ANALYSES AND TESTING

In order to compare the results of analytical frame analyses and test results, the loading regime used during testing must be somewhat representative of the number of cycles of loading and the deformations to which the members in a frame are subjected. Two loading regimes are commonly used for testing in New Zealand. These are discussed below.

6.7.1 Loading Regime

The New Zealand draft loadings code commentary [6.20] states that:

> "ductility levels may be established by demonstrating that the structure can sustain 4 cycles to the ultimate limit state displacement without the primary resisting elements losing more than 30% of their maximum lateral resistance to lateral load and the structure as a whole more than 20% of its maximum seismic strength."

This loading regime has been recommended in New Zealand as a benchmark for assessing member performance and is shown in Figure 6.22. Although this loading regime is based on some earthquake analyses it does not represent any real earthquake. It has been the subject of much informal debate as to whether it is too conservative, or not conservative enough in representing the member ductility demands.

In the analyses which have been undertaken in the previous chapters, it was found that the hinges did not yield the same amount in both directions as is commonly assumed in most loading regimes because of the initial gravity loading on the structure. It is felt that from the analyses undertaken in this project that the regime is somewhat conservative as initial gravity moments on the members may cause yielding in one direction only and that during an earthquake there are usually less than four full cycles to the required limit state displacement.

6.7.1.1 Concrete Testing Regime

Although the regime suggested above is recommended in New Zealand, the inelastic cycles of the regime shown in Figure 6.23 have often been used particularly for testing reinforced concrete members at the University of Canterbury [6.45]. This regime consists of the elastic cycles and two complete cycles to displacement ductilities of μ = 2, 4, 6, 8, etc.

The reasons it has been used are that the constant amplitude testing only provides a pass-fail test as to whether of not the member is able to satisfy the requirements to a certain displacement ductility. In order to see if a member would be able to sustain different levels of displacement ductility, several members would have to be tested. Although further cycles of the same magnitude may be applied after the required four cycles, many may be required to cause a decrease in strength, particularly for those members in which the maximum displacement, rather than the energy absorbed is much more critical in the determination of the ductility capacity. The variable magnitude loading regime shown in Figure 6.23 will find the approximate ductility capacity of a member. A guess does not have to be made as to what level of displacement ductility should be used, and it is thought that greater insight into the member behaviour may be gained from the increasing ductility applied. The inelastic cycles of the loading regime shown in Figure 6.23 have been proposed for use in the new draft loadings code [6.46].

It is thought that this loading regime is more representative of the expected behaviour of a member in an earthquake in which there may be several small cycles and only a few cycles of loading to large displacements.

6.7.1.2 Comparison of Loading Regimes

A conservative method of equating the loading regimes has been suggested by Paulay [6.45]. From the previous dynamic analyses, it seems reasonable that if a member is able to sustain two complete cycles to the ultimate limit state displacement without losing more than 30% of its strength when it is subjected to the loading regime of Figure 6.23, it should be considered to behave satisfactorily.

6.7.2 Measurement of Damage

In most loading regimes, the displacement to which a member in a frame is subjected is often described in terms of its displacement ductility. Other parameters such as the member rotation capacity, number of cycles of deformation, and the total energy absorbed have also been used to measure structural performance. Information obtained may be presented using hysteretic diagrams, spine curves, or simply a number indicating a maximum value of one of the above parameters.

The two main forms of measurement described above are energy based methods, such as cumulative ductility, and the maximum deformation approaches such as the rotation, or curvature or displacement ductility.

The energy based form of damage measurement is particularly suitable for elements in frames such as columns, where the energy absorbed is possibly more important than the maximum displacement, while the measurement of damage based on deformation considerations is more relevant for members such as well detailed shear links and beams where the change in the shape of the hysteresis loop and the cumulative member effects are small.

In the past the amount of energy absorbed has sometimes been treated as the most important parameter to predict the strength loss of cyclically loaded members. This is because members were often detailed only for monotonic loading conditions so that when cyclic load was applied, the hysteresis loop was not stable, but degraded reasonably rapidly. However, prediction of the maximum energy absorption capacity is more difficult than estimation of the maximum deformation capacity, and requires an understanding of the energy demands of the members in the frames.

With the detailing guidelines presently in use in New Zealand, very little degradation of the hysteresis loop is expected in the cyclic testing of members, and the maximum deformation is usually major parameter affecting

the strength. This deformation may be measured in terms of ductility, rotation or strain. It is felt by the present writer that while the expected member displacement ductility demand may be estimated for a particular earthquake from the equal displacement assumption, the inelastic member rotation is a better measure of the material behaviour and damage prediction as it is related more directly to the maximum expected strain in the member.

It is desirable that frames be designed so that the components absorbing most of the energy are those in which damage may be measured in terms of the maximum displacement. This will mean that the expected behaviour of a member may be predicted from the displacement to which it is likely to be subjected rather than from both the number of load reversals and the magnitude of each cycle.

6.7.2.1 Rotation

(a) Total Rotation

The rotation capacity generally includes the effects of the elastic as well as the inelastic member rotation. This measurement is an upper bound on the inelastic rotation and does not necessarily indicate the amount of damage sustained because, in some cases, all of the rotation may be elastic.

The total rotation of a column is generally defined as the displacement at the point of contraflexure relative to that at the point of maximum moment divided by the distance between these two points. The column rotation will always be less than the interstorey drift ratio because the flexibility of the beams and panel zone as well as the columns contribute to the interstorey drift. It has been suggested that the maximum level of interstorey drift ratio should not be expected to exceed 3% [6.47] in a very severe earthquake. An upper limit on storey drift is required to control deformations so that P-delta effects do not become too large in a severe earthquake and so that non-structural components are not severely damaged in small earthquakes. The maximum realistic column rotation for testing of specimens should not be required to exceed this value of 3%. Yamada [6.29] has used rotation of a column to relate the number of cycles of loading to the amplitude of loading for a particular axial load level.

(b) Inelastic Rotation

The inelastic rotation, θ_R, is the plastic rotation, θ_P, subtracted from the ultimate rotation, θ_u. The plastic and ultimate rotations are defined as the

plastic displacement, δ_p, and the ultimate displacement, δ_u, respectively divided by the length, L, to where the plastic displacement is measured. Galambos and Lay [6.18] have used inelastic rotation to describe the maximum member deformation.

Cumulative rotation, $\Sigma\theta$, and the inelastic cumulative rotation, $\Sigma\theta_H$, are also used to measure damage when the number of cycles of loading has an effect on the behaviour. Plastic rotation capacity [6.35], often refers to the inelastic displacement ductility, R, which is equal to $\mu_{max} - 1$.

6.7.2.2 Energy Dissipation

The energy absorbed by a member must be less than the capacity of the member to dissipate energy, otherwise failure will occur. Measurement of this quantity is easily computed as the area enclosed by the hysteresis loops. Member hysteresis loops are usually unclosed after an inelastic time-history analysis because of redistribution of load between the members. Popov and Pinkney [6.23] and Mitani et al. [6.17] have shown that the energy absorbed is approximately proportional to the cumulative displacement.

6.7.2.3 Ductility

In measuring ductility of any type, the point of first yield must be well defined. Many materials do not have a well-defined yield point and some arbitrary, yet reasonable definition must be used. For steel sections, the plastic curvature, $\phi_p = (S/Z)\phi_y$, and plastic displacement, $\delta_p = (S/Z)\delta_y$, usually correspond to a curvature ductility and displacement ductility of one respectively. Park [6.48] has suggested several definitions for other structures. The arbitrary nature of the determination of the first yield is a major weakness of using all forms of ductility to estimate damage.

If the axial load on a member is changing, the ductility in a hinge is difficult to define as it is a function of the level of axial load. It is quite common in dynamic analyses for a column to hinge under a certain level of axial load, and the axial load level change before the hinge disappears. To obtain the maximum actual ductility demand, the ductility must be calculated the axial load at each timestep.

In the dynamic time-history analysis program, RUAUMOKO [6.49], plastic hinge rotational ductility, for steel sections, is calculated by adding one to the maximum inelastic hinge rotation divided by the rotation which would cause member plasticity if no axial load were present. Therefore the results

obtained from RUAUMOKO for the curvature ductility demand are a lower bound on the actual curvature ductility demand which includes the effect of axial load.

Some commonly used measures of ductility are discussed below.

(a) Member Curvature Ductility (ϕ/ϕ_p)

Curvature ductility is calculated as the curvature divided by the plastic curvature for steel members. In a test situation the distance over which curvature is measured will affect the curvature obtained. If this length is long, a lower curvature reading results than if a small length is used.

(b) Frame Displacement Ductility

Frame displacement ductility is effectively a load reduction factor for frames designed to the draft NZ loadings code [6.20]. The frame displacement ductility factor of μ_{des} implies that a frame will be designed with a minimum strength of C_μ/C_e multiplied by the elastic design level lateral seismic forces and will be expected to have a maximum displacement of μ_{des} multiplied by the elastic displacement from the design level forces under the design level earthquake.

To measure or define a reasonable first yield in a real frame is arbitrary and of little practical use in long period frames, such as those analysed in this report where the maximum displacement expected is independent of the "yield" displacement according to the equal displacement assumption. Park and Paulay [6.50] have defined first yield in idealised frames in which the columns are assumed to be infinitely stiff as the point at which all of the inelastically responding members yield. In their idealization all members expected to deform inelastically in order to form a mechanism are assumed to yield at the same time.

(c) Subassemblage Displacement Ductility (μ_s)

The expected displacement ductility of a subassemblage or storey in a frame in an earthquake is usually estimated by the equal displacement concept. It has often been seen from the analyses in the preceding chapters that the equal displacement assumption generally provides a slightly conservative estimate of the interstorey drift for design level earthquakes.

(d) Member Displacement Ductility (μ_m)

For steel members the member displacement ductility, μ_m is usually defined as the displacement at the point of contraflexure divided by the displacement at that point causing the plastic section moment to be reached. Member displacement ductility is commonly used to measure member damage. The definition of member first yield usually includes the shear displacement.

(e) Cumulative Displacement Ductility ($\Sigma\mu$)

This is an estimate of the energy absorbed at a particular location and allows some comparison between different loading regimes. Cumulative ductility, or the number of cycles of loading, have been suggested by Paulay [6.45] as a good way of estimating the damage accumulated over many cycles of loading. Inelastic cumulative ductility is another measure of cumulative damage which was used in this report.

6.7.3 Relationships Between Different Forms of Damage Measurement

(a) Relationship between Extreme Fibre Strain and Rotation

The rotation, θ, is assumed to be equal to a constant inelastic curvature, ϕ, which is assumed to be spread over a length of plastic hinge, L_p, multiplied by that length as shown in Equation 6.2a below. The neutral axis of a beam will be in the middle of the section and the extreme fibre strain will be equal to the curvature multiplied by the distance to the extreme fibre of the section as shown in Equation 6.2b.

$$\theta = \phi L_p \qquad \text{Equation 6.2a}$$

$$\varepsilon_f = \phi D/2 \qquad \text{Equation 6.2b}$$

If the plastic hinge length, L_p, is approximately equal to the depth of the beam, D, and θ is measured in radians, then the average extreme fibre strain is

$$\varepsilon_f \approx \theta/2 \qquad \text{Equation 6.2c}$$

The axial strain, ε_{ax}, accumulated from the previous cycles of loading will also contribute to the extreme fibre strain in cyclically loaded columns. The neutral axis will be in one of the flanges for elastoplastic sections with axial load levels greater than A_w/A, and the strain for monotonic loading will approximately be $\varepsilon \approx \phi D$, so

$$\varepsilon_f \approx \phi D + \varepsilon_{ax} \qquad \text{Equation 6.3a}$$

$$\varepsilon_f \approx \phi L_p + \varepsilon_{ax} \qquad \text{Equation 6.3b}$$

Therefore

$$\varepsilon_f \approx \theta + \varepsilon_{ax} \qquad \text{Equation 6.3c}$$

The accumulated axial strain, $\varepsilon_{ax} = 0$, if loading is monotonic, so the column flange strain, ε_f, is equal to the plastic hinge rotation, θ. The maximum monotonic inelastic rotation of columns is approximately one half that of beams with the same extreme fibre strain. This is found when Equation 6.3 is compared with Equation 6.2 giving Equation 6.4. The curvatures, which are related to the rotations, required to obtain the same extreme fibre strain are shown for a section in Figure 6.24.

$$\theta_c \approx \theta_b/2 \qquad \text{Equation 6.4}$$

This result agrees with that of Galambos and Lay [6.18] discussed in section 6.5.2(a), however, it is expected that if buckling were to become severe, a column would not behave as well as a beam with the same flange strain. This is because the web of a column will probably be completely in compression. Web buckling would therefore be more likely to occur in conjunction with flange buckling increasing the rate of strength loss. Axial load will also increase the possibility of member lateral buckling. It is thought for these reasons that the monotonic rotation capacity of columns with high axial loads may well be less than half of the rotation capacity of beams. Further discussion of the effect of the position of the neutral axis in the cyclic loading of members was given in section 6.5.3.

(b) Relationship between Member Displacement and Curvature Ductility

Using the definition for plastic hinge length of section 7.13.6 and Equation 6.5 the relationship between displacement and curvature may be found.

$$\delta - \delta_p = (\phi - \phi_p) L_p L_c$$

$$\Rightarrow (\mu-1)\delta_p/\phi_p = (\phi/\phi_p - 1) L_p L_c \qquad \text{Equation 6.5}$$

If $\delta_p = K\delta_b$ where δ_b is the component of plastic displacement resulting from bending alone and equals $M_p L_c^2/3EI$, $K = (\delta_b + \delta_v)/\delta_b$, where δ_v is the

component of plastic displacement resulting from shear alone, L_c is the distance to the point of contraflexure and $\phi_p = M_p/EI$, then $\delta_p/\phi_p = KL_c^2/3$, and

$$\frac{\phi}{\phi_p} = (\mu - 1)\frac{KL_c}{3L_p} + 1 \qquad \text{Equation 6.6}$$

If K=1.2 say and $L_c/L_p = 5$ then

$$\phi/\phi_p \approx 2\mu - 1 \qquad \text{Equation 6.7}$$

It is thought that the assumptions made to obtain Equation 6.7 are reasonable for most beams and columns.

The plastic hinge length, L_p, in the equations above is used to enable comparison of curvature and displacements between experimental models and theoretical results. In order to obtain realistic ductility demands from inelastic frame analysis programs such as RUAUMOKO [6.49], the plastic hinge length must be specified correctly.

The plastic hinge length is calculated as the length of uniform plastic curvature which will produce the same deflections at the end of the member as does the actual curvature distribution. The magnitude of the uniform inelastic curvature is selected somewhat arbitrarily and is often taken as the curvature from the potentiometers adjacent to the section of maximum moment. In some cases it is taken from the two sets of potentiometers near the region of plastic moment. Due to the random nature of the selection of the length over which the uniform inelastic curvature is measured, differences in the calculated plastic hinge length from the same test may be obtained.

While the plastic hinge length is assumed to be constant, it varies with the amount of plasticity. The inelastic curvature, which is approximated as being uniform within the plastic hinge length in reality also varies considerably as shown in Figure 6.25. For reinforced concrete members, many tests have shown that the plastic hinge length at maximum ductility is a reasonably constant fraction of the section depth, D. Further testing is required to see if the same is true for steel members.

(c) Relationship between Displacement Ductility and Rotational Ductility

Displacement ductility is defined as $\mu = \delta/\delta_p$, while rotational ductility is defined as θ/θ_p. The total rotation, θ, and the plastic rotation, θ_p, are

defined as δ/L_c and δ_p/L_c respectively where L_c is the distance to the point of contraflexure. Because of this the rotational and displacement ductilities are equal.

(d) Relationship between Member and Subassemblage Displacement Ductility

The member displacement ductility, μ_m, will always be greater than or equal to the subassemblage displacement ductility, μ_s, with the amount depending on the flexibility of the non-yielding members in the subassemblage and the structural system used. It is assumed that the beam is the only yielding element in Figure 6.26 of part of a moment-resisting frame subassemblage. The relationship between the member displacement ductility, μ_m, and the subassemblage displacement ductility, μ_s, is described below.

Under design level earthquake loading ($\mu < \mu_e$) the interstorey drift, δ_μ, is given by

$$\delta_\mu = (\theta_b + \theta_c)h \qquad \text{Equation 6.8}$$

As only the beam is expected to yield, the expected interstorey displacement, δ, using the equal displacement concept is

$$\delta = \mu_s \delta_\mu = (\mu_m \theta_b + \theta_c)h \qquad \text{Equation 6.9}$$

therefore

$$\mu_m = (\mu_s \delta_\mu / h - \theta_c)/\theta_b \qquad \text{Equation 6.10}$$

and by substitution of Equation 6.5 into Equation 6.7

$$\Rightarrow \mu_m = (\mu_s (\theta_b + \theta_c) - \theta_c)/\theta_b$$

$$= \mu_s + (\mu_s - 1)\theta_c/\theta_b \qquad \text{Equation 6.11}$$

In the case when the stiffness of the columns is infinite, then $\theta_c = 0$ and the member displacement ductility, μ_m, becomes equal to the subassemblage displacement ductility, μ_s.

Members should be required to sustain the displacements which may be demanded of them in a frame. It may be seen from Equation 6.11 that the displacement ductility which may be demanded of members may be considerably larger than the subassemblage displacement ductilities.

6.7.4 Definition of Failure

Lay and Galambos [6.51] have suggested that the rotation capacity of a beam be calculated as occurring at the time that the strength drops to less than 95% of the maximum strength. Yamada [6.28] has classified failure as occurring when fracture is first observed. Mitani, Matsui and Makino [6.35] have used the rotation at peak moment and after the flexural strength has dropped to 95% of the peak moment.

In the past, many different definitions of failure of specimens have been used. In order to compare results between different countries and different authors a uniform loading regime and definition of failure is required or a correlation between the measures is necessary. Present definitions of failure generally relate to the lateral strength of a frame and not to any secondary effects such as the amount of axial shortening a member may sustain.

In this report the author has used the criterion commonly used in New Zealand that a specimen is assumed to have failed when the moment capacity has became less than 70% of the calculated plastic moment strength [6.20].

6.8 CHAPTER SUMMARY

In this chapter various aspects of the behaviour of steel members were described and as well as some relationships between different measures of member damage.

Discussion was made regarding the material stress-strain behaviour, both under monotonic and cyclic loading. A brief literature summary was presented of the ductility capacity of monotonically loaded beams which have influenced the New Zealand codes and the parameters affecting it.

The failure of steel members was described as occurring as a result of either fracture of buckling or a combination of these. The background to the recommended New Zealand limitations for the section slenderness ratio which is used in order to discourage local buckling was discussed. The way in which buckling contributes to strength loss was shown to be as a result of P-delta effects causing extra bending moments to act. Previous work has shown that low-cycle fatigue fracture is not likely to occur in well detailed steel members.

A summary of previous cyclic testing of steel I-shaped beam-columns has shown that, in fact, very little research has been undertaken. Axial shortening was reported in only one of these papers on column testing and the reasons for the axial shortening of columns are described in this chapter. Reasons for the less rounded hysteresis loop shape of columns, in comparison with beams, which has been observed in previous testing have been put forward. Previous work which found that the maximum overstrength of a member in bending is significantly less than the overstrength of a tensile test piece was also referenced. The tentative New Zealand recommendations for axial load ratio for different levels of ductility demand were described. There is a considerable need for more testing of steel beam-columns because there is relatively little known about their cyclic behaviour.

It was shown that cumulative yielding may occur during load reversals on some members. In particular, yielding in non-composite beams may occur at a particular position along the beam in one direction of loading only. The consequence of axial shortening of columns in a frame was shown to be undesirable.

Loading regimes which are commonly used for testing specimens, and which are meant to be representative of the actual demand on a member during a design level earthquake were discussed. Different forms of damage measurement, such as ductility, rotation and energy which may be obtained from experimental work were described. The benefits of using a particular form of damage measurement and some relationships between these forms were also discussed. Some commonly used definitions of failure were also described.

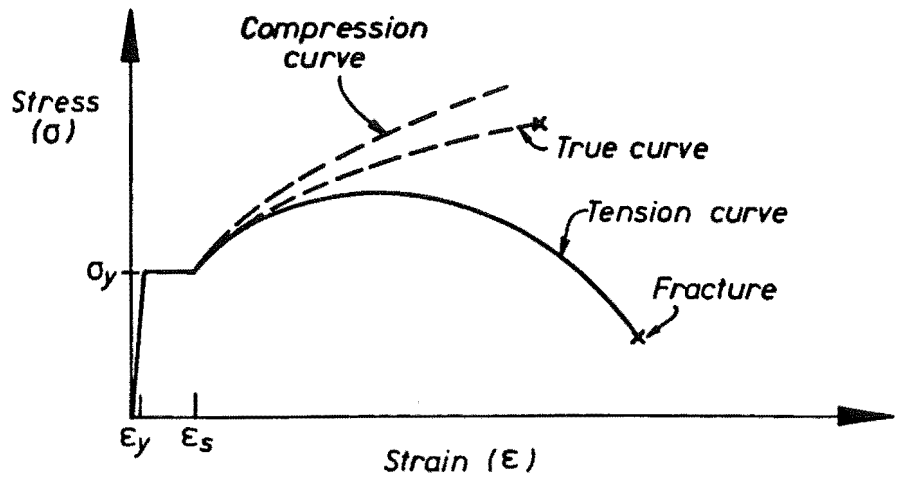

Figure 6.1. Steel Stress-Strain Diagram

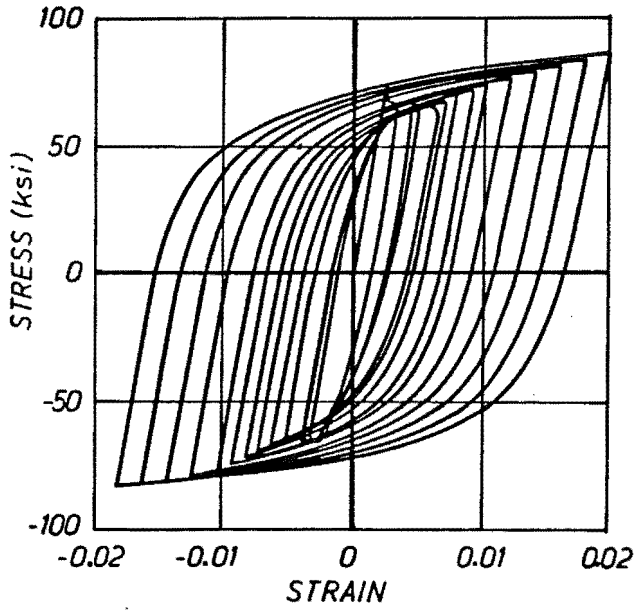

Figure 6.2. Hysteretic Behaviour of Steel (Petersen and Popov)

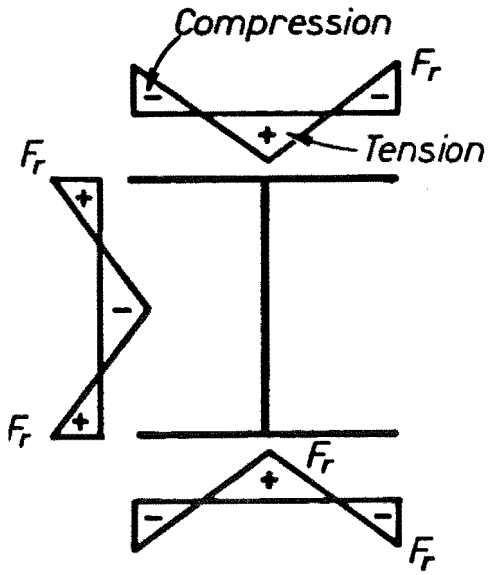

Figure 6.3. Commonly Assumed Residual Stress Distribution

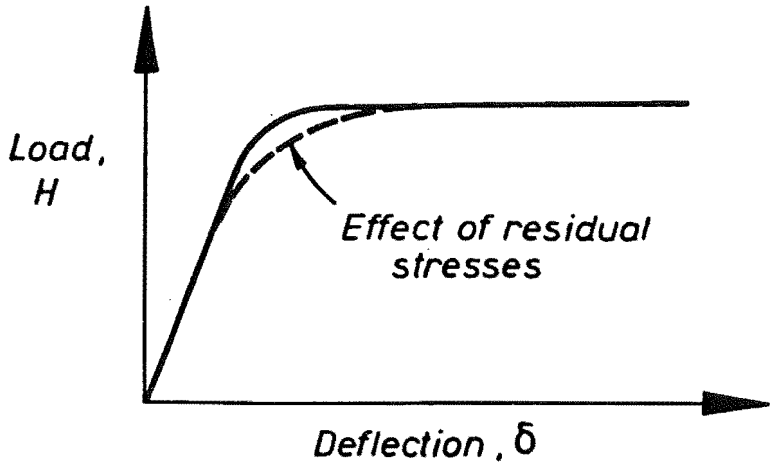

Figure 6.4. Effect of Residual Stresses (Lay)

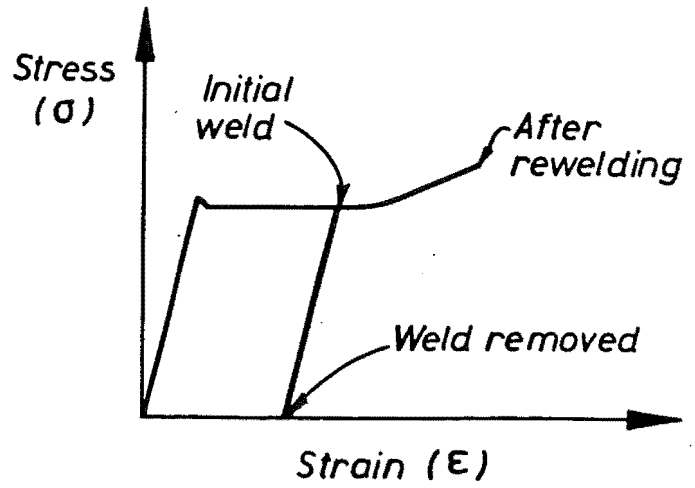

Figure 6.5. Accumulation of Welding Strains

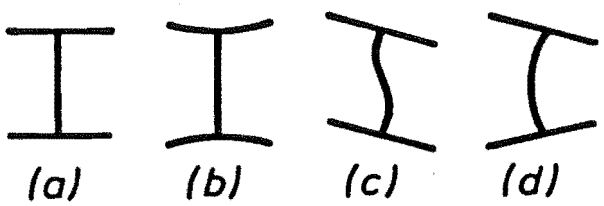

Figure 6.6. Modes of Section Buckling

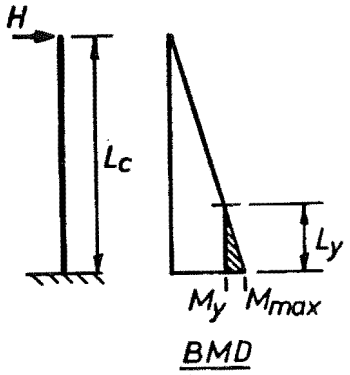

Figure 6.7. Length of Flange Yield

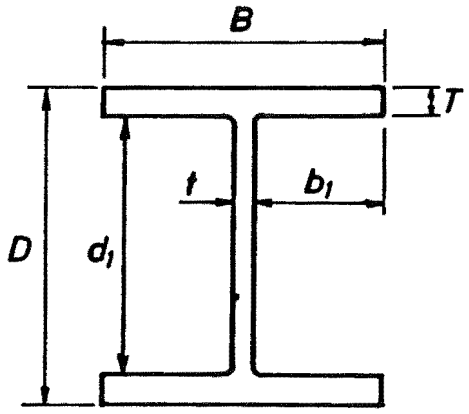

Figure 6.8. Section Dimensions

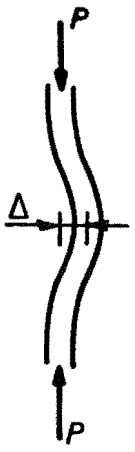

Figure 6.9. Effect of Buckling on Strength of a Flange

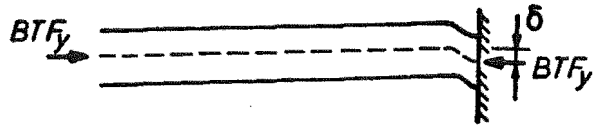

Figure 6.10. Effect of Buckling on Strength of a Beam

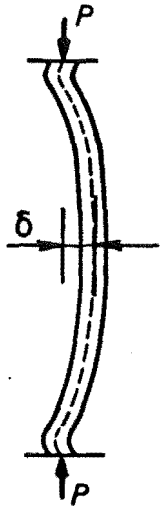

Figure 6.11. Effect of Buckling on Strength of a Column

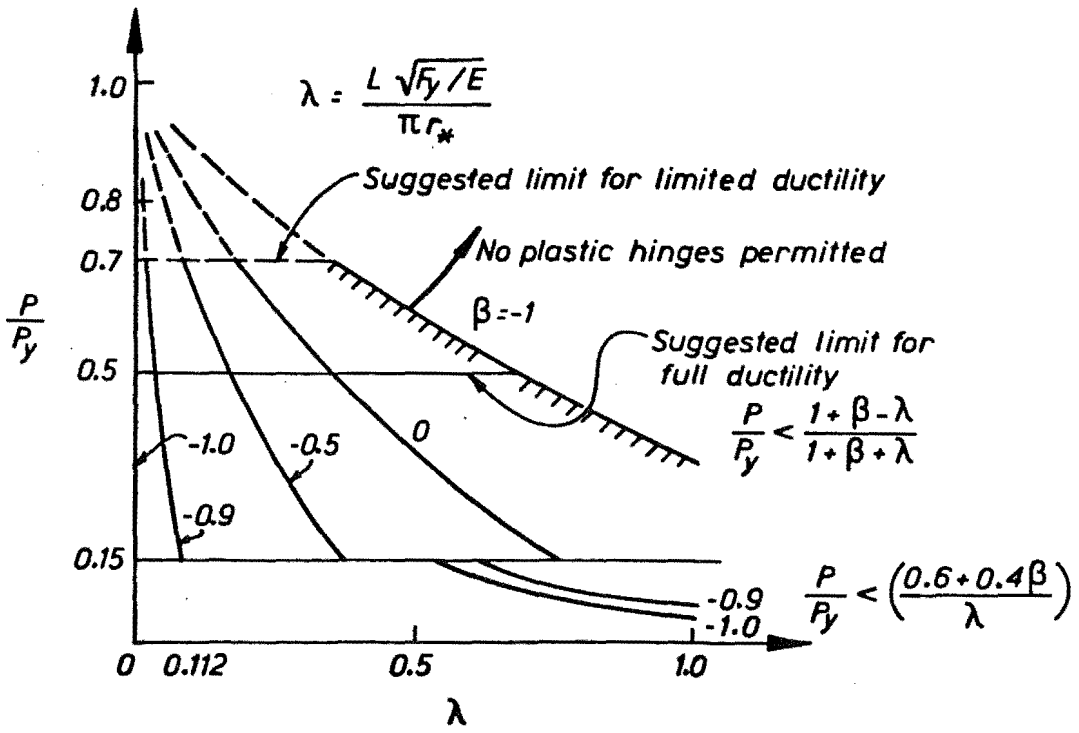

Figure 6.12. Column Axial Load Limits

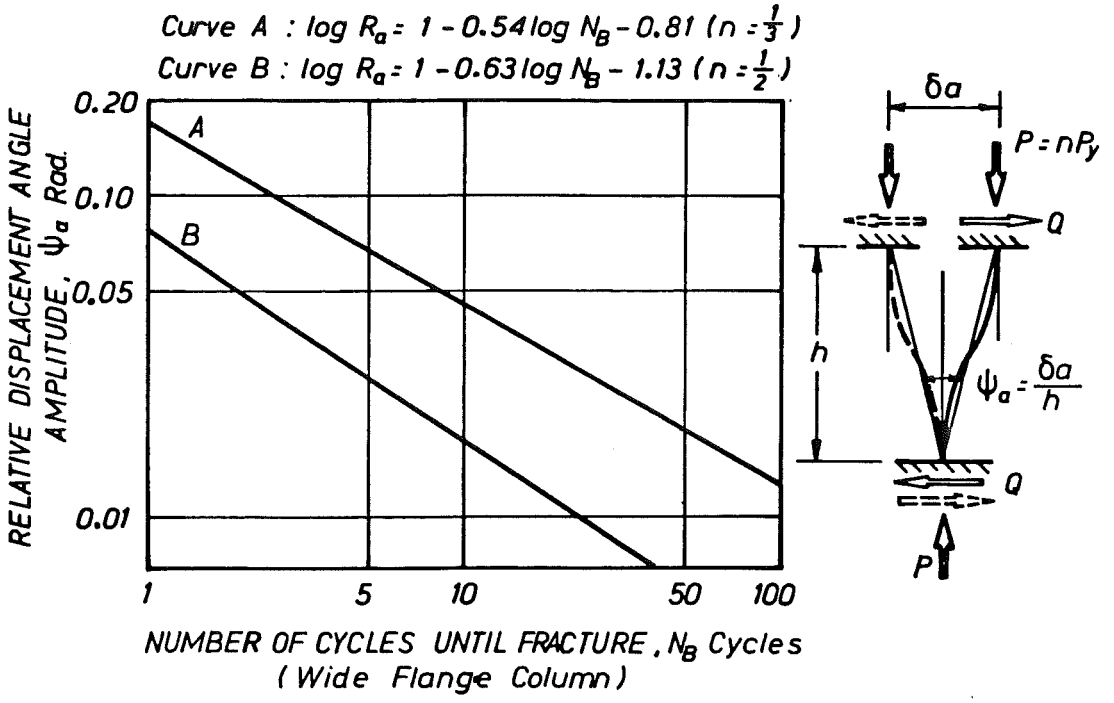

Figure 6.13. Yamada's Fatigue Fracture Limits

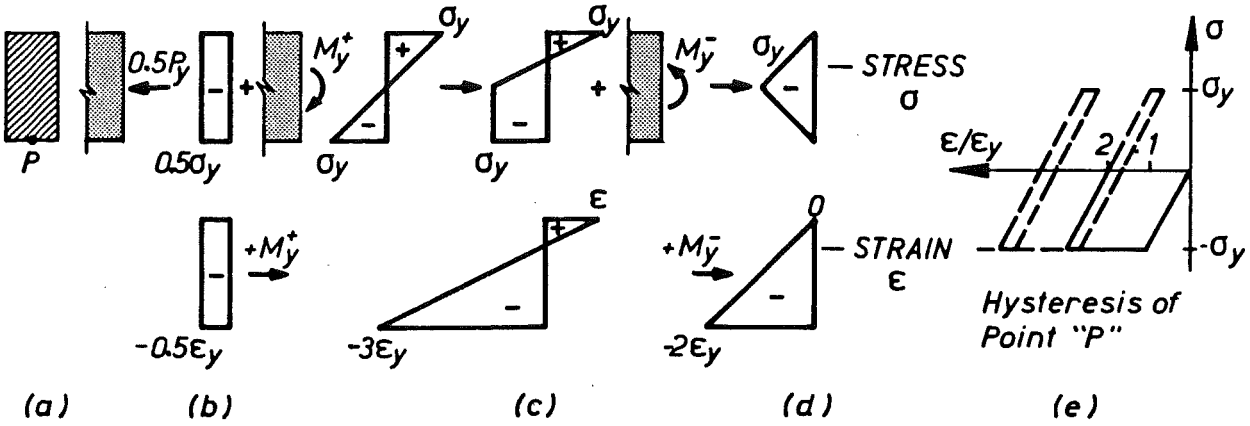

Figure 6.14. Stresses and Strains in a Cyclically-Loaded Section

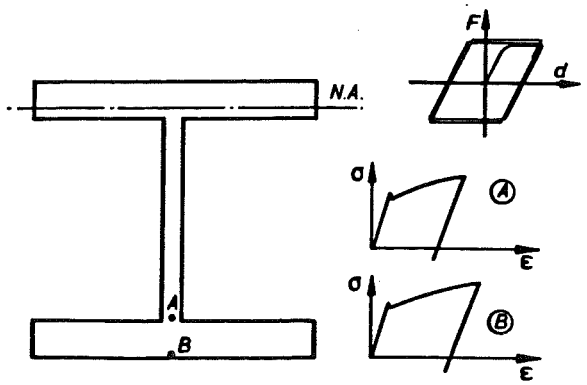

Figure 6.15. Column Hysteresis

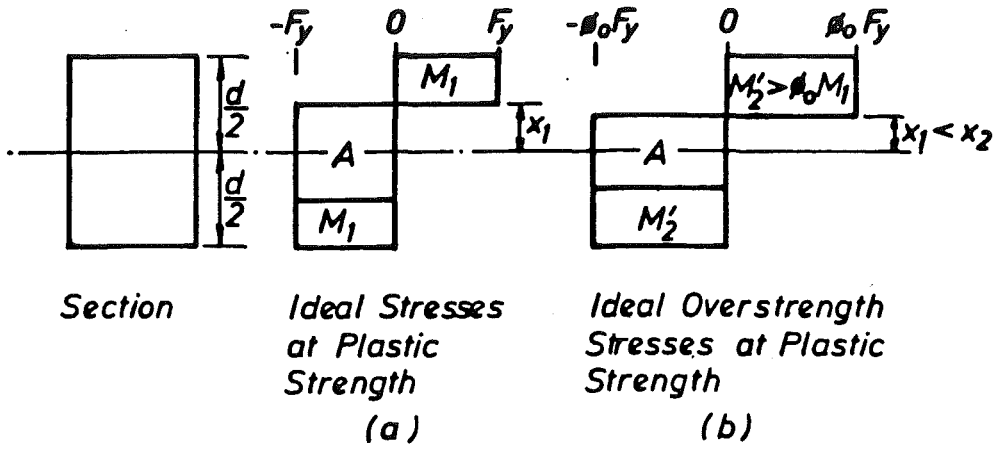

Figure 6.16. Column Maximum Strength

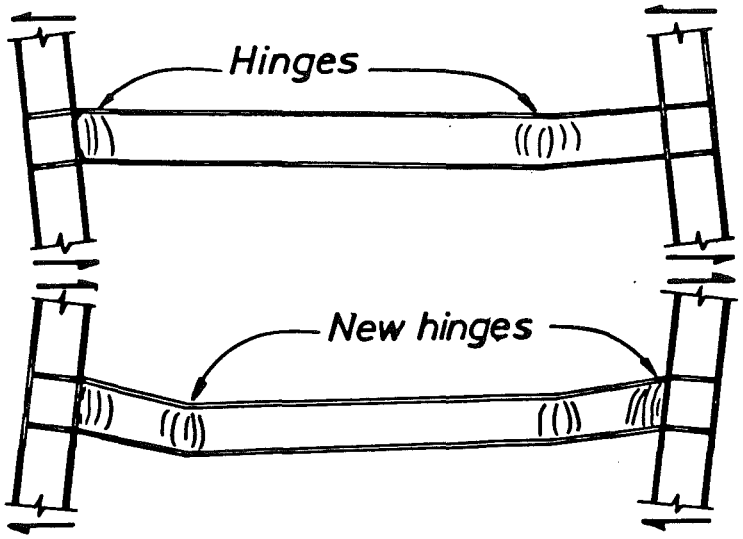

Figure 6.17. Yielding in a Gravity-Loaded Non-Composite Beam

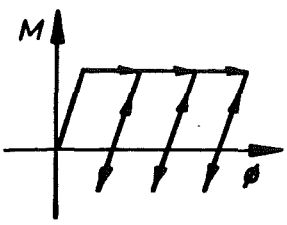

Figure 6.18. Accumulation of Curvature in Hinges of Non-Composite Beams

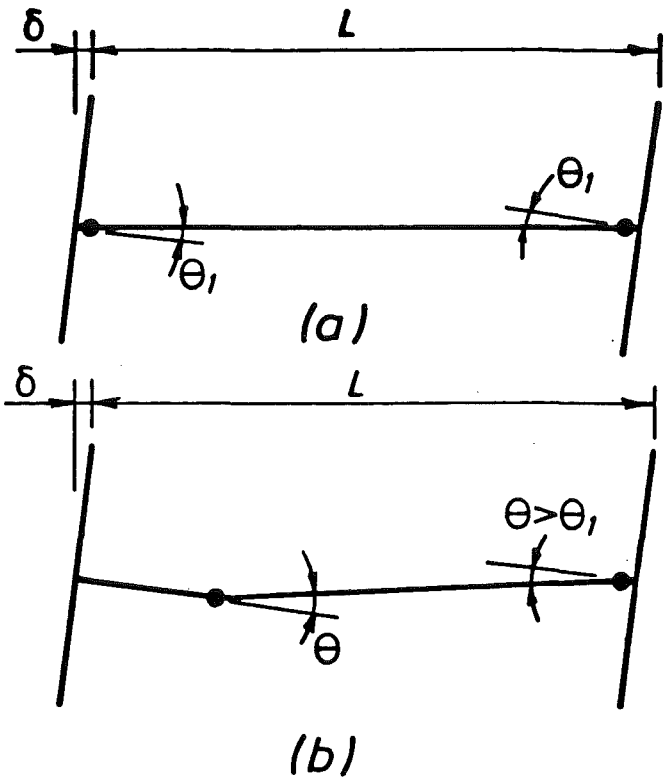

Figure 6.19. Rotation Demand in Gravity-Dominated Non-Composite Members

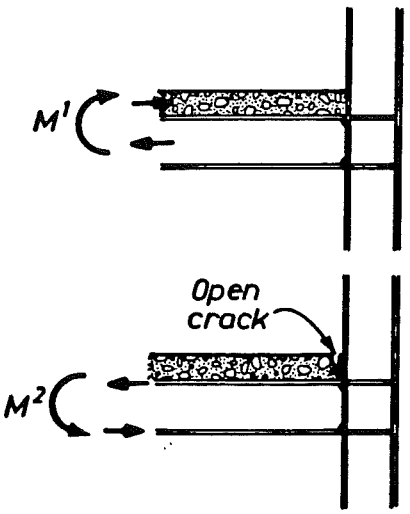

Figure 6.20. Increase in Length of Composite Beams

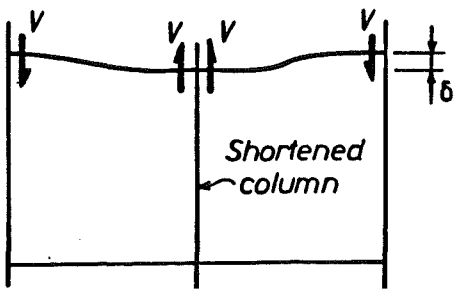

Figure 6.21. Effect of Shortening of a Column in a Frame

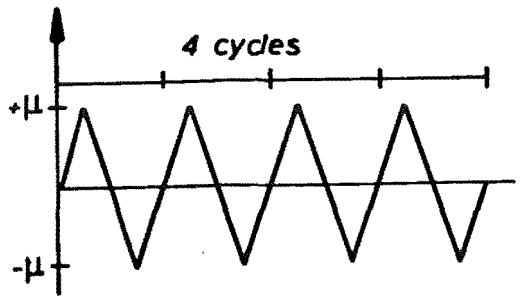

Figure 6.22. Standard Loading Regime

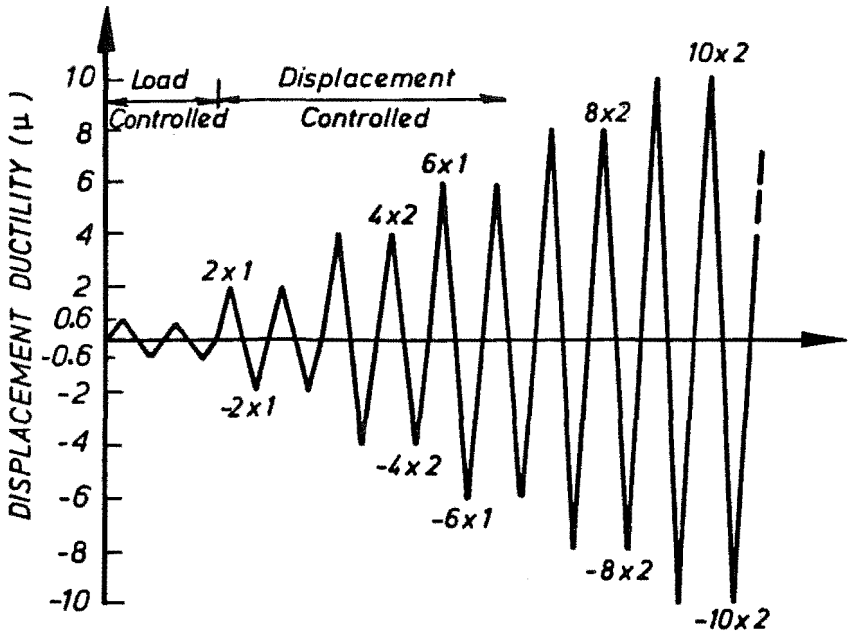

Figure 6.23. Loading Regime for Testing of Specimens

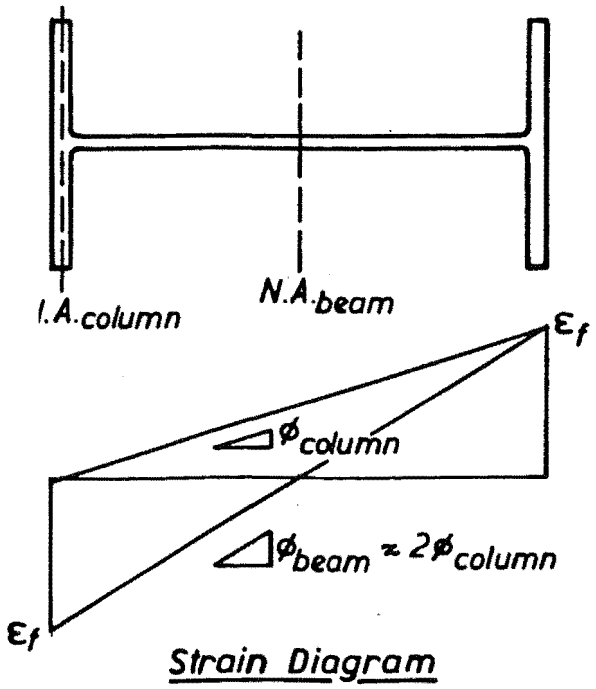

Figure 6.24. Beam and Column Section Strains

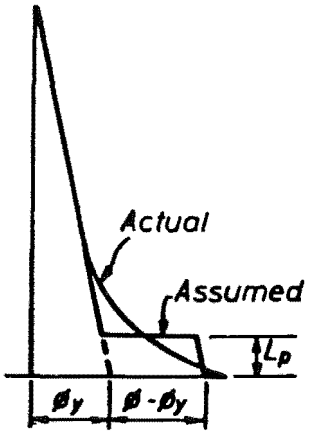

Figure 6.25. Assumed Cantilever Curvature Distribution

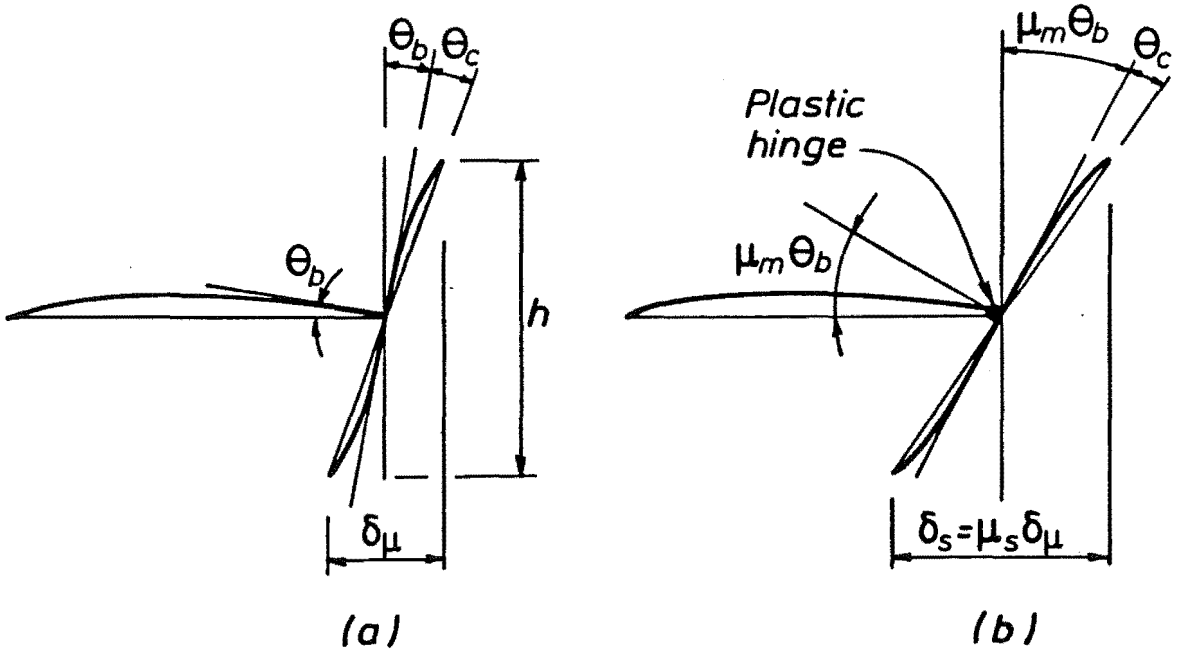

Figure 6.26. Relationship between Member and Subassemblage Displacement Ductilities

6.9 REFERENCES

6.1 Lay M. G. "Structural Steel Fundamentals - an engineering and metallurgical primer", Australian Road Research Board, 1982.

6.2 Mander J. B., Priestley M. N. J. and Park R., "Seismic Design of Bridge Piers", Research Report 84-2, Department of Civil Engineering, University of Canterbury, February 1984.

6.3 Kato B., "Mechanical Properties of Steel Under Load Cycles Idealizing Seismic Actions", Comite Euro-International du Beton, Bulletin D'Information No. 131, Vol. 1, Theme 1a, 1979.

6.4 Petersen H. and Popov E. P., "Constitutive Relations for Generalized Loadings", *Journal of the Structural Division*, ASCE, Vol. 103, EM 4, August, 1977.

6.5 Beamish M., "Seismic Behaviour of Steel Portal Frame Knee Joints", University of Auckland, Dept. of Civil Engineering, Report No. 348, 1984.

6.6 Popov E. P., "Experiments with Steel Members and their Connections under Repeated Loads", International Association of Bridge and Structural Engineering, Lisbon, Portugal, Part 3, pp 125-135, 1973.

6.7 Kikukawa M. and Jono M., "Cumulative Damage and Behaviour of Plastic Strain in High and Low Cycle Fatigue", Int. Conf. Mechanical Behaviour of Materials", Kyoto, Vol. 2, p458-468, August 1971.

6.8 Patton R. N., "Analysis and Design Methods", Section B, Deliberations of the New Zealand Study Group for the Design of Steel Structures, Bulletin of the New Zealand National Society for Earthquake Engineering, Vol. 18, No. 4, December 1985.

6.9 Walpole W. R. and Butcher G. W., "Beam Design", Section C, Deliberations of the New Zealand Study Group for the Design of Steel Bulletin of the New Zealand National Society for Earthquake Engineering, Vol. 18, No. 4, December 1985.

6.10 Kato B. and Akiyama M., "Theoretical Prediction of Load-Deflection Relationship of Steel Members and Frames" International Association of Bridge and Structural Engineering, Lisbon, Portugal, Part 1, pp23-28, 1973.

6.11 Kato B., Akiyama M. and Yamanouchi Y., "Predictable Properties of Material Under Incremental Loading", International Association of Bridge and Structural Engineering, Lisbon, Portugal, Part 3, pp 119-124, 1973.

6.12 Erasmus L. A., "The Mechanical Properties of Structural Steel Sections and the Relevance of these Properties to the Capacity Design of Structures", The Institution of Professional Engineers, New Zealand, Trans., Vol. II, No 3/CE, November 1984.

6.13 Tall L. "Compression Members", Chapter 9, Structural Steel Design, Ed. Lambert Tall, The Ronald Press, New York, 1964.

6.14 Popov E. P., Stephen R. M. and Philbrick R., "Capacity of Columns with Splice Imperfections", Report No. UBC/EERC-76-21.

6.15 Dawe J. L. and Kulak G. L., "Local Buckling of W-Shape Columns and I-Beams", *Journal of the Structural Division*, ASCE, ST June 84, p1292-1304.

6.16 SAA, "Draft Australian Standard for Comment - Steel Structures", DR 87164, August 1987.

6.17 Mitani I., Makino M. and Matsui C., "Influence of Local-Buckling on Cyclic Behaviour of Steel Beam-Columns", 6WCEE, 1977, p3175-3180.

6.18 Galambos T. V. and Lay M. G., "Studies on the Ductility of Steel Structures", *Journal of the Structural Division*, ASCE, Vol 91, ST4 (1965).

6.19 Lay M. G., "Flange Local Buckling in Wide-Flange Shapes", *Journal of the Structural Division*, ASCE, ST6, Dec 1965, p95-116.

6.20 SANZ, "General structural design and design loadings for buildings", DZ4203 Draft for comment, New Zealand Standard, 1986.

6.21 Beamish M., Ph.D. Thesis in preparation, University of Auckland, Department of Civil Engineering.

6.22 Butterworth J. W. and Spring K. C. F., "Column Design" Section D, Deliberations of the New Zealand Study Group for the Design of Steel Structures, Bulletin of the New Zealand National Society for Earthquake Engineering, Vol. 18, No. 4, December 1985.

6.23 Popov E. P. and Pinkney R. B., "Cyclic Load Reversals in Steel Building Joints", *Journal of the Structural Division*, ASCE, ST3:Mar 1969:327:6441.

6.24 Guruparan N. I., "Lateral Buckling rules for seismically-loaded I-beams", ME Report, Department of Civil Engineering, University of Canterbury, 1989.

6.25 Lukey A. F. and Adams P. F., "Rotation Capacity of Beams Under Moment Gradient", *Journal of the Structural Division*, ASCE, ST6:June 69:1173:6599.

6.26 Kemp A. R., "Interaction of Plastic Local and Lateral Buckling", *Journal of the Structural Division*, ASCE, ST Oct 1985, p2181-2196.

6.27 Kemp A. R., "Slenderness Limits Normal to the Plane-of-Buckling for Beam-Columns in Plastic Design", J. Construct. Steel Research, 4, (1984), p135-150.

6.28 Yamada M., "Low Cycle Fatigue Fracture Limits of Various Kinds of Structural Members Subjected to Alternately Repeated Plastic Bending under Axial Compression as an Evaluation Basis of Design Criteria for Aseismic Capacity", Proc. Fourth World Conference on Earthquake Engineering, Santiago, Chile (1969)

6.29 Yamada M., "Effect of Cyclic Load on Buildings", State of Art Report No. 1, Technical Committee 18, International Conference on Planning and Design of Tall Buildings, Lehigh University, Bethlehem, Pa. (1972).

6.30 Johnstone N. D. and Walpole W. R., "Bolted End Plate Beam to Column Connections Under Earthquake Type Loading", Research Report 81-7, Department of Civil Engineering, University of Canterbury, Sept 1981.

6.31 Whittaker D. and Walpole W. R., "Bolted End Plate Connections For Seismically Designed Frames", Research Report 82-11, Department of Civil Engineering, University of Canterbury, June 1982.

6.32 Haaijer G. and Thürlimann B., "On Inelastic Buckling in Steel", *Journal of the Engineering Mechanics Division*, ASCE, Vol. 84, No. EM 2, April 1958.

6.33 Lay M. G., "Source Book for the Australian Steel Structures Code AS1250", Australian Institute of Steel Construction, Sydney, 1975.

6.34 SANZ, "Code for Design of Steel Structures (with commentary)", NZS3404, New Zealand Standard, 1989.

6.35 Mitani I., Makino M. and Matsuì C., "Empirical Formula for Plastic Rotation capacity of Steel Beam-Columns with H-Shaped Cross Section", Proc. Pacific Structural Steel Conference, Vol. 2, p283-382, Auckland, 1986.

6.36 Popov E. P., Bertero V. V. and Chandramoulli S., "Hysteretic Behaviour of Steel Columns", UCB/EERC 75-11, September 1975.

6.37 Yokoo Y., Nakamura T. and Komiyama T., "Nonstationary Stress-Strain Relations of Wide-Flange Steels and Moment-Curvature Relations under Presence of Axial Force", International Association of Bridge and Structural Engineering, Lisbon, Portugal, Part 3, pp 143-149, 1973.

6.38 Igarashi S., Matsui C. and Yoshimura K., "Experimental Study of Bridge Beam-Columns Under Incremental Loading", International Association of Bridge and Structural Engineering, Lisbon, Portugal, Part 3, pp 143-149, 1973.

6.39 De Buen O., "Steel Structures", Chapter 4 of "Design of Earthquake Resistant Structures", edited by E. Rosenblueth, Pentech Press, 1980.

6.40 Stewart W. G., "The Seismic Design of Plywood Sheathed Shear Walls", Ph.D. Thesis, Department of Civil Engineering, University of Canterbury, 1987.

6.41 Bertero V. V., Krawinkler H. and Popov E. P., "Further studies on Seismic Behaviour of Steel Beam-Column Subassemblages" UCB/EERC 73-27, December 1973.

6.42 Fenwick R. C. and Davidson B. J. "Moment-Redistribution in Seismic Resistant Concrete Frames", Pacific Conference on Earthquake Engineering, Wairakei, New Zealand, August 1987, Vol. 1, p95-106.

6.43 Clifton G. C., "Seismic Design Procedures for Ductile Steel Moment-Resisting and Eccentrically Braced Frames", Notes from Seminar on Constructability and Seismic Design of Multistorey Steel Buildings by the New Zealand Heavy Engineering Research Association, Session 4,, 1988.

6.44 Fenwick R. C., Seminar Report - Use of precast concrete in moment-resisting frames and floors designed for earthquake resistance, New Zealand Concrete Society Newsletter No. 1, p12, 1988.

6.45 Paulay T. and Park R. "Joints in Reinforced Concrete Frames Designed for Earthquake Resistance", Research Report 84-09, Department of Civil Engineering, University of Canterbury, June 1984.

6.46 SANZ, "General structural design and design loadings for buildings", DZ4203 Draft for comment, New Zealand Standard, 1989.

6.47 Krawinkler H., Popov E. P. and Bertero V. V., "Inelastic Behaviour of Steel Beam-to-Column Subassemblages", UCB/EERC 71-7, Oct 1971.

6.48 Park R. et al., "Structures of Limited Ductility", Bulletin of the New Zealand National Society of Earthquake Engineering, Vol. 19, No. 4, December 1986.

6.49 Carr A. J., "RUAUMOKO", Computer Program Library, Department of Civil Engineering, University of Canterbury. May 1986.

6.50 Park R. and Paulay T., "Reinforced Concrete Structures", John Wiley & Sons Inc., 1975.

6.51 Lay M. G. and Galambos T. V., "Inelastic Beams Under Moment Gradient", *Journal of the Structural Division*, ASCE, ST1, Feb 1967.

Chapter 7

EXPERIMENTAL PROGRAM

7.1 INTRODUCTION

The eight steel beam-columns studied in this report were intended to represent columns in multistorey moment-resisting steel frame.

All specimens were 250 UC 73 I-shaped universal column sections and were subjected to axial compression and cyclic bending about their strong axis. Axial load ratios (P/P_y) of 0.0, 0.3, 0,4, 0.5, 0.6, 0.7, and 0.8 were adopted for seven of the sections and a further specimen was subjected to both cyclic axial loading and cyclic strong axis bending.

7.2 AIM OF TESTING

The objectives of the study were:

1) to understand the effect of the axial load level on an I-shaped steel member used in a moment-resisting steel frame,

2) to verify that the limits of axial load suggested by Butterworth and Spring [7.1] for members subjected to full and limited ductility demands are realistic, and

3) to isolate the parameters controlling the hysteretic behaviour and the mode of failure of the specimens.

7.3 DESIGN OF SPECIMENS

The 250 UC 73 section was appropriate in that the specified value of the flange slenderness ratio was 8.64 which was only slightly greater than the recommended maximum value by Walpole and Butcher of 8.60 ($136/\sqrt{F_{ys}}$) [7.2] for a member of limited ductility. If these recommendations, which are discussed in section 6.4.4(a), are strictly adhered to then this section shape is only able to be used in buildings designed for the elastic (μ=1) level of earthquake loading, that is, it is not permitted to be designed to yield. Construction drawings for the specimens are shown in Figure 7.1.

The scale of the model was approximately 0.75. The scaled specimen height of 1.100 metres represents one half of the clear height of a column with total clear height equal to approximately 3.00 metres. This is thought to be reasonably representative of a column in a typical moment-resisting steel frame as shown in Figure 7.2.

In the design philosophies described in the previous chapters some column hinging is expected to occur at the base of the frame and may occur over the height of the structure during severe excitations. Columns in all of the frames analysed were expected to be able to sustain at least limited ductility deformation.

Axial load ratios, P/P_y, as high as 0.80 would not be expected in the columns of an ordinary steel ductile moment-resisting frame (DMRF) but tests were performed to this level to verify the work of Popov, Bertero and Chandramoulli [7.3] and the recommendations of Butterworth and Spring [7.1] in which maximum axial load ratios of 0.70 and 0.50 are suggested for members expected to perform to the limited and full ductility requirements respectively.

The out-of-plane slenderness ratio of the members was 17. This was small and would limit the likelihood of lateral buckling. The distance between lateral restraints was 885 mm which is less than the maximum recommended value of 1.96 m corresponding to 480 $r_y/\sqrt{F_y}$ for fully ductile members [7.1].

The axial loads of all columns were less than the recommended upper limits of section 8.4.3.2 of the draft Australian steel code, DR87164 [7.4], so that inelastic rotation capacity was available at the ends of the member [7.5]. It may be seen from Figure 6.12 that the slenderness, λ, of 0.112 was satisfactory for all the axial load levels of the columns tested when the ratio of end moments, β, was taken as zero.

The specimens were designed to deform inelastically in bending rather than in shear. The plastic shear and flexural strengths under zero axial load were approximated as:

$$V_p = 0.55F_{yw}Dt \qquad \text{Equation 7.1}$$

$$M_p \approx F_{yf}BTD \qquad \text{Equation 7.2}$$

therefore if $F_{yw} \approx F_{yf}$:

$$\frac{V_p}{M_p} \approx \frac{0.55t}{BT} \qquad \text{Equation 7.3}$$

In order for yielding to occur in bending rather than shear Equation 7.5, which follows from Equation 7.4, must be satisfied.

$$\frac{M}{M_p} > \frac{V}{V_p} \qquad \text{Equation 7.4}$$

or

$$\frac{V_p}{M_p} > \frac{V}{M} \qquad \text{Equation 7.5}$$

The actual value of moment and shear were M = 1.10m * H, and V = H, where H is the applied lateral load. Therefore V/M = 1.10/m. The specified section properties give:

$$V_p/M_p = 0.55*8.64/(254*14.2)$$
$$= 1.32/m$$

This provides a factor of safety against shear yielding of 1.32/1.10 = 1.20.

If axial load is applied to the specimen this will affect the flexural and shear strengths of the section. Again, for yielding to occur in flexure:

$$\frac{V_{pc}}{M_{pc}} > \frac{V}{M} \qquad \text{Equation 7.6}$$

If no interaction between the shear strength and the flexural strength is assumed, as has been done for links in EBFs [7.6], the flexural strength will decrease more rapidly than the shear strength in the presence of axial loads greater than $0.164P_y$. This is shown in the interaction formulae in Equations 5.1 and 5.2. There is very little reduction in both the flexural and shear strengths for axial loads less than $0.164P_y$. If Equation 7.5 is used to protect axially-loaded columns against shear failure, the factor of safety against shear yielding will be greater than or equal to that found from this equation. If the effect of axial load is considered when the column is designed to yield in bending rather than shear, Equation 7.6 may be used in conjunction with Equations 7.7 which is based upon Equations 5.1 and 5.2.

$$\frac{V_{pc}}{M_{pc}} = \frac{0.55t}{BT}\,\frac{\sqrt{(1-(P/P_y)^2)}}{1.18(1-P/P_y)}, \qquad P/P_y > 0.164, \qquad \text{Equation 7.7a}$$

$$\frac{V_{pc}}{M_{pc}} = \frac{0.55t}{BT}, \qquad P/P_y < 0.164, \qquad \text{Equation 7.7b}$$

7.4 TEST FRAME

The test frame shown in Figure 7.3 was designed and constructed for the project. Axial (vertical) load was applied to the specimen through the Dartec 10 MN Universal testing machine situated at the University of Canterbury (henceforth referred to simply as the "Dartec"). Horizontal load was applied through a separate 1 MN double-acting hydraulic ram which has an actual capacity of 1120 kN in compression and 840 kN in tension, with 400mm maximum travel. A specimen in the test frame is shown in Figure 7.4.

The position of the point of contraflexure was assumed to remain constant at the top loading pin. The two pins shown in Figure 7.5 were held on the same vertical line. An actuator under the floor moved the load frame and bottom pin vertically up and down, to maintain the required axial load. When the horizontal load was applied, the ram extended, so that the load frame at the base of the specimen rotated about the bottom pin causing a bending moment in the specimen. The deflection measuring potentiometers measured the relative deflection of the specimen to the loading frame as shown in Figure 7.5.

7.5 LIMITATIONS OF THE STUDY

The following are some limitations of the test program:

i) The point of contraflexure will move vertically in the columns of real frames during an earthquake. This is not modelled in the test configuration used.

ii) The loads were applied in a pseudo-static manner. However, experiments by Hanson [7.7] show that the difference between static and dynamic hysteretic loops is small for periods greater than 0.3 seconds.

iii) Current construction practice in New Zealand for moment-resisting steel frames is generally to use columns which are continuous through the joint with the beams bolted or welded to the column flange. Columns are usually spliced between floors. The test configuration required that the column be butt-welded at one end possibly resulting in a different residual stress distribution to that commonly expected. This effect was not investigated.

7.6 NOTATION

The column specimens were labeled C0, C3, C4, C5, C6, C7, C8, and CA. The second character distinguishes the level of the axial load ratio which was applied. In the general case, Cn indicates that the axial load level was n/10. For example specimen C5 was subjected to an axial load ratio (P/P_y) of 0.50. The specimen CA was subjected to an alternating axial load which is described in section 7.11.3(a).

7.7 SECTION PROPERTIES

The specimens tested came from three different batches of steel. An offcut from each batch was measured with vernier calipers and a micrometer to obtain the actual offcut cross-section dimensions.

Three samples for tensile testing were taken from three of the flanges of each specimen offcut, and one test sample was taken from the web of each offcut to determine the steel strength and deformation properties of the sections. The samples were taken from positions consistent with the materials code AS1227-1980 [7.8] as shown in Figure 7.6, at least 50mm from any gas cutting. The smallest diameter was cut twice with a round tipped tool before a finishing turn was performed to 7.3mm diameter. Grinding was carried out to 7.155mm before carrying out the finishing grinding in two 0.0125 cuts to get the final size of 7.13mm, as shown in Figure 7.7.

Table 7.1
Geometric, Strength and Stiffness Properties of Section Offcuts

	Batch Number				
	1	2	3	Average	Specified
D (mm)	251.86	251.87	251.84	251.86	254.00
T (mm)	13.83	13.69	13.68	13.73	14.20
B (mm)	251.84	251.86	251.62	251.77	254.00
t (mm)	8.78	8.69	8.57	8.68	8.64
r (mm)	12.7	12.7	12.7	12.7	12.70
F_y flange	305.6	294.4	283.9	294.6	250.0
F_y web	305.6	306.6	308.1	306.8	260.0
F_u flange	486.0	477.8	487.7	483.8	
F_u web (MPa)	500.2	493.9	499.2	497.8	
ϕ_o flange	1.59	1.62	1.72	1.64	
E_{st} (GPa)	5.73	4.96	4.93	5.21	
$E_{1\%}$ (GPa)	.65	.56	.54	.59	
ε_{st} (%)	1.77	1.59	1.21	1.52	
ε_u (%)	35.0	37.2	34.4	35.5	
b_1/T	8.79	8.88	8.88	8.85	8.64
d_1/t	25.54	25.83	26.19	25.85	26.11
B/T	18.21	18.40	18.39	18.34	17.88
D/t	28.69	28.98	29.39	29.02	29.40
A (mm^2)	9073	8985	8947	9002	9301
As (mm^2)	2211	2189	2158	2186	2195
I($10^6 mm^4$)	108.7	107.8	107.5	108.0	113.8
S($10^3 mm^3$)	954.5	945.9	942.9	947.8	990.
Z($10^3 mm^3$)	863.0	855.7	853.4	857.4	895.8
V_p (kN)	675.8	671.1	665.0	670.6	570.6
M_y (kNm)	263.7	251.9	242.3	252.6	223.9
M_p (kNm)	291.7	278.4	267.7	279.2	247.5
P_y (kN)	2773.	2645.	2540.	2652.	2325.

Testing was carried out in accordance with AS1391-1974 [7.9]. A strain rate of 0.02 cm/minute was used up to a strain of 4%, and 0.05 cm/minute was used thereafter. The yield strain, ε_y, was calculated over a 25 mm gauge length, whereas the ultimate strain was computed over the maximum extension length of 30 mm.

To calculate the plastic loads and deflections, Youngs modulus, E, was taken as 200 GPa and a shear modulus, G, of 80 GPa was used. The mean section dimensions, strengths, section properties and maximum values of strain and tangent stiffness, together with calculated values of yield and plastic moments are shown in Table 7.1.

The flanges were slightly thinner than the specified values giving flange slenderness ratios slightly larger than the specified values in Table 7.1. Yield strengths were also greater than the specified values for Grade 250 steel [7.10].

7.7.1 Plastic Displacement and Curvature

In these tests, displacement ductility was defined as the ratio of the lateral displacement (δ) divided by the plastic displacement (δ_s) of the specimen under the axial load, measured at a point 835 mm (L_s) up from the base of the specimen as shown in Figure 7.8 as the expected deformations of the top bracket were unknown.

The plastic displacement, assuming a rigid base, was calculated as

$$\delta_s = \frac{H_p L_s^2}{EI}(L_s/3+L_1/2) + \frac{H_p L_s}{GA_s} \qquad \text{Equation 7.8}$$

where $L_1 = L - L_s$, and

A_s is the shear area which was approximated as Dt.

H_p is the lateral load causing the reduced plastic moment (M_{pc}).

The expected plastic displacement at the top of a uniform member was also calculated as:

$$\delta_t = \frac{H_p L^3}{3EI} + \frac{H_p L}{GA_s} \qquad \text{Equation 7.9}$$

The plastic curvature was calculated using

$$\phi_p = M_{pc}/(EI) \qquad \text{Equation 7.10}$$

Values of plastic moment capacity and plastic curvature reduced by axial load as well as values of plastic displacement for each specimen based on the experimental yield stresses are given in Table 7.2.

Table 7.2
Specimen Capacities, Plastic Curvatures and Displacements

Unit	Batch	Axial Load Ratio (P/P_y)	Axial Load P (kN)	Reduced Plastic Moment M_{pc} (kNm)	Plastic Lateral Load H_p (kN)	Plastic Disp. at Top δ_t (mm)	Plastic Disp. at B δ_s (mm)	Plastic Curv. ϕ_p (rad/m $x10^{-3}$)
C0	3	0.0	-20	268	243	6.57	4.42	12.5
C3	1	0.3	-832	241	219	5.83	3.92	11.1
C4	2	0.4	-1058	197	179	4.82	3.24	9.14
C5	2	0.5	-1323	164	149	4.01	2.70	7.61
C6	1	0.6	-1663	138	125	3.33	2.24	6.35
C7	2	0.7	-1852	99	90	2.41	1.62	4.59
C8	3	0.8	-2032	63	57	1.55	1.04	2.93
CA*	3	Alt						

* Values for unit CA are described in section 7.11.3(a)

7.8 INSTRUMENTATION

(a) Strain Measurements

To measure the strains, 7 mm SHOWA N11-FA-7-120-11 electrical resistance strain gauges with a gauge factor of 2.11 were attached to the flange and web of the specimen in the positions shown in Figure 7.9. They were of the post-yielding type, measuring strains up to 2%. The material surface was prepared first by smoothing the steel with emery paper and then cleaning thoroughly with a 2:1 mixture of Methyl Ethyl Ketone and Xylol before the gauges were mounted. The strain gauges were attached with LOCTITE Cyanoacrylate adhesive 496 and joined to SHOWA FG-7T terminals. The gauges were then waterproofed with one layer of SHINKOH SN/4 strain gauge coating cement.

The gauges were used to find the strains at certain points, and to verify the potentiometer readings. As a limited number of gauges were available, only specimens C0 and C3 were strain gauged.

(b) Displacement Measurements

During the tests, twelve 30 mm linear potentiometers were used to measure displacements. Ten of these were situated over the region of the specimen which was expected to yield. The arrangement of these is shown in Figure 7.10. Measurements from these enabled axial deformation, and rotations over

a portion of the column to be calculated and curvature ductility to be computed at different positions along the hinge length. The potentiometers were attached at the middle of the flange by welding 16mm diameter offstands onto the centre of the specimen flange. The four base potentiometers measured displacement from a plate welded to the flange just above the base of the specimen so that baseplate deformation did not contribute to these potentiometer readings. Six millimetre brackets with the potentiometers were attached to the offstands with 10mm hexagonal headed cap screws.

The other two potentiometers were used to measure the rotation of the specimen base caused by baseplate movement, load frame flexibility and bolt deformation. They were placed approximately 20 mm from the flange tips out from the centres of the flanges along one side of the specimen. All of the 30mm potentiometers measured displacement from thin stainless steel sheet which was glued to the potentiometer brackets or baseplate.

One 100 mm potentiometer was used to measure the horizontal displacement on the specimen, 835 mm from its base. Another 200 mm potentiometer was used to measure the horizontal displacement at the loading point on specimens C4 to CA. These potentiometers were positioned approximately 500 mm from the specimen so that any vertical movement in the specimen would not have a significant effect on the displacement recorded. A Fritz-Staeger demountable mechanical contact-type strain gauge, was used to measure the strains in each flange near the top of specimens C5 to CA. The positions of the measurements made with these demountable mechanical devices are described in section 7.12.4.

(c) Data Recording Equipment

A Metrabyte 128 channel recorder was used to capture information from all the potentiometers and strain gauges on the specimen, as well as the horizontal load, vertical load and Dartec stroke. This enabled full sets of instrument readings to be made virtually instantaneously, and greatly speeded up the testing procedure. The data was then stored and reduced by means of an IBM PC compatible computer. Plotting was carried out using the departmental VAX 11/750 computer and a Hewlett-Packard plotter.

7.9 LOADING

The loading regime shown in Figure 6.22 was used for all columns. Because increasing compressive axial load reduced the plastic displacement, δ_s, the

columns with a higher axial loads were subjected to lower absolute displacements to reach a specified displacement ductility than were the columns with less axial load.

In the following discussion, when behaviour is described as occurring at a certain position on the loading regime the following notation is used. The peak of the nth cycle to a displacement ductility of ±m is often referred to as cycle ±mxn. For example, the second cycle of loading to a displacement ductility, μ, of -6, may be referred to as cycle -6x2. This notation, shown in Figure 6.22, is also used on the photographs.

7.10 PRE-TESTING PROCEDURE

Strips of 3 mm white automobile body tape were stuck to specimens C0 and C3 in the pattern shown in Figure 7.11 so that the buckling deformations would be seen more easily in the photographs. During the tests they peeled off, so white marker pen was used to draw lines on the other specimens. The rust and millscale were not removed so that Lüder lines could be observed.

Each specimen was placed on the loading frame and lined up in the position required, bolts were inserted and snug-tightened. A compressed air impact wrench was used to tighten the nuts on the bolts. Where possible, the nuts on the bolts were rotated through half a turn to attain the bolt proof load. However, the impact wrench managed to turn some of the bolts just over one quarter of a turn. Each set of M30 and M24 bolts was used for two specimens.

The wires from the specimens to the pulleys on the displacement measuring frame were set to horizontal and potentiometers were set at mid travel.

7.11 TESTING PROCEDURE

The sequence of testing of the specimens was carried out in the order of increasing axial load and the specimen with variable axial load was tested last.

7.11.1 Testing Steps

1) A set of zero readings were taken when the specimen was hanging in slight tension in the Dartec. At zero axial load, the displacements and loads were logged, and several further logs were taken before the required axial load level was reached.

2) The specimen was loaded through two full cycles under load control to a load, H, of magnitude $0.60H_p$, where H_p is the lateral load causing the reduced plastic moment, M_{pc}.

3) The stiffness of the whole system ($K = H/\delta$) was calculated as the horizontal load was taken off the specimen. This unloading stiffness was much more linear than the loading stiffness.

4) The total displacement at plastic moment capacity was extrapolated as $\delta_t = H_p/K$.

5) The expected specimen displacement, δ_s, found from Equation 7.1 was subtracted from the total displacement measured, δ_t, to obtain the displacement due to elastic action on the other components δ_c.

6) The stiffness of the other components $K_c = H_p/\delta_c$, was computed.

7) All subsequent cycles were then carried out under displacement control. The specimen was loaded so that it deflected to the desired displacement (δ_μ) which was $\mu\delta_s + H_\mu/K_c$, where H_μ is the expected ram force required (less the friction force). This force was simply taken as H_p in these tests.

8) The test was considered to be finished after the strength (H) of the specimen had dropped to less than 70% of the plastic strength (H_p) calculated using experimental yield values [7.11].

7.11.2 Discussion of Test Procedure

The load value of $0.60H_p$ was selected to keep the member elastic in the initial cycles. Yielding in the extreme fibres of steel sections may begin at an applied moment of $0.65M_p$ due to possible residual stresses caused by rolling (say $0.3F_y$), combined with a shape factor (say 1.18), causing a decrease in member stiffness. A further decrease in stiffness may be due to residual stresses from welding of the base of the specimen to the baseplate. When axial load levels are high, some inelastic action may take place even before any lateral displacement is undergone but the same procedure was used.

After the cycles of load to $0.60H_p$ as shown in Figure 6.22, the horizontal displacement measured was compared with Equation 7.8. The difference between the displacements obtained was from the elastic action of the baseplate, bolts, and test frame underneath the specimen. The elastic stiffness of

these parts was then found. The only part of the whole system expected to deform inelastically was the specimen, the other components were assumed to deform elastically in proportion to the ram force.

The area inside the load displacement hysteresis loop when loading was carried out to $0.60H_p$ is due to the inelastic action from the residual stresses at the weld as well as the friction from the ram. A second cycle was carried out in which the area of the loop was solely dependent on the friction of the ram. The friction force (H_f) may be calculated from the size of the hysteresis loops in the second cycle of loading in the manner of Popov et al. [7.3] as shown in Figure 7.12.

At every increment readings were taken on the datalogger for all potentiometers, strain gauges and loads. Photographs of the specimen were also taken whenever the member geometry altered significantly. Any relevant information such as the length of buckling, and the lateral displacement of the buckle were noted.

7.11.3 Specimen CA

For the column which was to be tested with varying axial load it was intended to make the variation of axial load representative of the behaviour which would be expected in an exterior column of a moment-resisting frame. Initially it was thought that variation of axial load with horizontal load would be most appropriate, but it was realized that this would be realistic only if all the columns in the same level of the frame yielded at the same time, which is neither likely nor desirable. As the variation of axial load is dependent on both displacement and lateral load it was decided, for simplicity, to vary the axial load only in proportion to the displacement of the column. This was felt to better resemble the behaviour of an exterior column in a moment-resisting steel frame where the exterior column may be the only one at that level which yields.

Using this model, a column may be subjected to high axial load while no lateral load is applied. This type of behaviour is shown in the subassemblage of Figure 7.13 in which the members are assumed to behave elasto-plastically and dynamic effects are not considered. At (a) column 3 starts to yield due to the horizontal shear S_3 and the gravity and seismic axial load. As the storey shear, F, increases the other columns remain elastic, but column 3 deforms inelastically with no increase in column shear. The storey shear is maximum in Figure 7.13(b). As the lateral storey shear, F, decreases (c), column 3 will reach a state of zero shear earlier

than the other columns but with significant axial load. When the horizontal load and axial load reduce to zero (d) the total shears of all columns in the storey must sum to zero. The shear in column 3 will have changed sign and there will be a residual displacement. To remove the storey displacement, a storey shear must be applied in the opposite direction (e) to previously. This may mean that column 3 may deform plastically in the other direction before zero displacement is reached. The seismic portion of the axial load will now be acting in tension in column 3.

(a) Specimen CA Strengths and Displacements

The average axial load ratio (P/P_y) was -0.30 corresponding to an axial load of -762 kN. This represented the gravity load on the column. Displacements and ductilities were based on an axial load ratio (P/P_y) of -0.4 at μ=3. The plastic displacement (δ_s), plastic curvature (ϕ_p) and plastic load (H_p) for the axial load ratio (P/P_y) of -0.40 were 3.13mm, 8.30 rad/m and 172kN respectively. As axial load increased with displacement, the ideal section moment capacity decreased, and conversely, the moment capacity decreased with displacement in the other direction until the axial load, P, became less than $0.15P_y$.

The first two cycles were carried out under the average axial load of -762kN to a load of 0.6*201kN = 121kN, where 201kN is the plastic load with P/P_y = -0.30.

After the initial two cycles, the axial load level P/P_y was varied with displacement according to the relationship

$$P/P_y = -0.30-0.03333\mu$$

In order to record the data before significant creep occurred during loading, the axial load was adjusted first, and then the horizontal load. During unloading the lateral load was reduced before the axial load level was altered.

7.12 EXPERIMENTAL RESULTS

7.12.1 Specimen C0

A nominal zero compressive axial load of 20 kN (P/P_y = 0.8%) was applied to hold the specimen in the Dartec. After the first two cycles, an elastic displacement of 1.70 mm was calculated representing all of the elastic effects on displacement apart from the member itself.

Lüder (yield) lines were first observed at cycle 2x2 in the tension flange spaced approximately 10 mm apart at an angle of 45°to the horizontal. The lines did not start at the base of the specimen but were centred 150mm from the base and extended for a length of 110mm along the length of the specimen. Yield lines were also evident on the web at an angle of 25° from the vertical. Web and flange yield lines are shown in Figures 7.14.1 and 7.14.2. As loading continued, further lines were formed. At cycle 4x2 the yield lines in the flange and web had extended to 400mm and 500mm up the specimen respectively. By cycle -6x1 the web yield lines had extended almost to the full height of the specimen. The flaking off of millscale at cycle 8x2 is shown in Figure 7.14.3.

Flange buckling was first observed at cycle 6x1. After the first cycle to a displacement ductility, μ, of -10 the potentiometers were removed because the buckles had become severe enough to twist the potentiometers off the recording plates. The growth of the buckles are shown in Appendix 4. Figures of the buckle formation are shown in Figures 7.14.4 to 7.14.6.

The tips of the flanges on one side of the specimen moved in the same direction deforming the web into double curvature as shown in Figure 6.6c. The inelastic deformations of the specimen seemed to be reversible and the buckles straightened out under tensile loading before the second cycle to a displacement ductility of 10. After this the buckling became severe as the buckles did not completely straighten out during the load reversals and some axial shortening occurred.

The horizontal load-horizontal displacement hysteretic loops were very fat and rounded as shown in Figure 7.14.7.

Strain hardening was evident in the first few cycles increasing the strength of the specimen. This may be seen by comparing cycles 2x1 and 2x2. The maximum strengths were 350 kN and -358 kN which occurred at cycles 8x2 and -

8x2 respectively. This was more than the maximum strength estimated by Lay [7.12] of $H_p(\phi_o+1)/2$ = 331 kN. At the end of the test the maximum strengths were 301 kN and -302 kN.

After cycle 10x2 the specimen strength degraded at a rate of about 2% per cycle because of buckling. The elastic stiffness decreased gradually as the section shape changed and the buckles grew larger. The elastic flexibility of the specimen had increased by 60% at the end of testing.

It may be seen from the horizontal force-axial deformation plot in Figure 7.14.8, obtained from the potentiometers, that the length of this column actually increased in length by about 1 mm during the initial cycles of loading even though it was subjected to a small compressive force. The length of the specimen then remained approximately constant for many cycles. When flange buckling became severe the stiffness of the compressive flange became less than that of the tension flange and progressive shortening occurred. The column had decreased in length approximately 5 mm by the end of the test.

A plot of the curvature at the base of the specimen against the applied load is shown in Figure 7.14.9, and the curvature along the length of the member at peak values of displacement are shown in Figure 7.14.10. The flange hysteresis of this specimen is shown in Figure 7.14.11.

The strain gauges recorded strains of up to 2.1% and behaved satisfactorily until cycle -8x2. Curvatures were computed from average strain gauge measurements, and were plotted in Figure 7.14.12. There is a considerable difference between this figure and Figure 7.14.10 based on potentiometer readings.

As the displacement ductility increases, the curvature ductility along a member must also increase, however, from the strain gauge readings it seems that in the second cycle to a displacement ductility of 6 there was less curvature demand than in the previous loading cycle to a displacement ductility of four. This occurred because the strain gauges measured displacement ductility over a much smaller distance than did the potentiometers. Material damage may be concentrated over a small region over which a strain gauge may or may not be recording. Such a concentration of inelastic action occurs commonly in the necking of a standard test piece. It is thought that longer gauges should be used to record average strains larger than the yield strain. No further use was made of the strain gauges.

After cycle 10x2, the specimen was considered to have behaved very well. Six cycles of loading were then applied without stopping to see if the strength would drop suddenly, and to examine the mechanism causing it. The specimen was still behaving satisfactorily when the testing was terminated after eight cycles of loading to a displacement ductility of 10. There were no signs from the specimen that any large drop in load carrying capacity was about to occur. Loading to larger displacement ductilities was not carried out as the displacement measuring potentiometer was at the limit of its travel.

The cycles to displacement ductility, μ, of 10 correspond to an interstorey drift of 5.2%. This deformation is far beyond the maximum value of 3% expected from an element of an moment-resisting frame during an earthquake which was suggested by Krawinkler et al. [7.13].

7.12.2 Specimen C3

After the first two cycles, an elastic displacement of 0.686 mm was calculated representing all of the elastic effects on displacement apart from the member itself. The compressive axial load ratio of 0.30 corresponded to 832 kN which was maintained throughout the test.

Lüder lines were first observed at cycle 2x1 at 24° to the horizontal and horizontal lines also occurred in the compression flange. As loading continued, more lines formed in the web and flanges and the mill scale started flaking off. Web and flange yield lines are shown in Figures 7.15.1 and 7.15.2. At cycle -2x2, lines in the web were visible at 24° to the horizontal and 28° from the vertical, and in the flange horizontal lines were visible with other lines at 40° to these.

Buckling was first observed at cycle 4x1. The magnitude of the buckles as loading progressed are shown in Appendix 4. This test was different from the previous test C0, in that the buckles did not fully straighten out as the loading was reversed and the flange tips on one side of the specimen moved towards each other as shown in Figure 6.6d bending the web in single curvature. At cycle 6x1 the buckling deformations were severe and the potentiometers were removed. The development of the buckles is shown in Figure 7.15.3.

The hysteretic loops for this specimen are shown in Figure 7.15.4. The loops for this specimen and all others with axial load were much less rounded than those of unit C0. A bilinear elasto-plastic curve would approximate the

response well. Maximum strengths were 279kN and -284kN at cycles 4x2 and -4x2 respectively. The strength increased until cycle 6x1. As loading progressed the elastic stiffness of the load-displacement diagram decreased until it was 28% of the initial stiffness at the end of the test.

This specimen, and all others subjected to axial load, shortened as the specimens became plastic in bending as shown in Figure 7.15.5. The amount of shortening seemed to be dependent on the amount of cumulative plastic lateral deformation, or the number of cycles of loading.

A plot of curvature against the applied moment near the base of the specimen is shown in Figure 7.15.6, and the curvature along the length of the member at peak values of displacement is shown in Figure 7.15.7. The flange hysteresis of this specimen is shown in Figure 7.15.8.

Maximum localised strains of up to 2.5% were recorded from the strain gauges.

The tensile flange fractured over a horizontal length of about 120 mm during loading to cycle -10x1 and a loud bang was heard. The fracture occurred approximately 110 mm up from the base of the specimen as shown in Figures 7.15.9 and 7.15.10. The fracture line coincided with the weld holding a potentiometer mount to the specimen and the fracture was thought to have been initiated at this weld. Upon continuing the loading, the specimen sustained more than the plastic load for a full cycle before testing was terminated. However during this continuation another bang was heard on the way to cycle 10x2 as the crack extended.

The amount of sideways movement and the size of the web buckle grew as the load was applied. After the test, the tip of the compression flange which had initially been at 90° to the plate at the top of the specimen had a slope of 10mm/300mm (2°). Yield lines were also visible in the compressive flange near the top plate as shown in Figure 7.15.11.

The cycles to displacement ductility, μ, of 10 corresponded to an interstorey drift of 4.8%. After testing, compressive yield lines were visible in one of the flanges at the top of the specimen. It seems as though the buckling caused compressive yielding up one side of the specimen. The whole of the column was affected by the buckling deformations. The restraints provided in the test setup limited the deformation. A column in a real frame would not have these restraints and would therefore not be as

likely to sustain the same levels of displacement. Section 7.13.9(b) gives an explanation for this yielding on the flange away from the plastic hinge zone.

7.12.3 Specimen C4

For this and all subsequent specimens, a potentiometer was placed on the bracket connected to the top of the specimen to measure displacement at the pin. Axial load and stroke from the Dartec were also recorded by the Metrabyte data aquisition system. After the first two cycles, an elastic displacement of 0.604 mm was calculated representing all of the elastic effects on displacement apart from the member itself. The compressive axial load ratio of 0.40 corresponded to 1058 kN.

Lüder lines were first observed at cycle 2x1 at 63° and 9° to the horizontal. They were never very clear in the flanges, but rather a general flaking off of millscale occurred.

Buckling was first observed at cycle 2x2. The magnitude of the buckles as loading progressed are shown in Appendix 4. Buckling during testing and at the end of the test are shown in Figures 7.16.1 and 7.16.2. The flange tips initially tended to move away from the web as they did with column C3. One flange deformed severely in this fashion and did not buckle as a whole until cycle 6x2. Potentiometers were removed at cycle -6x1 because of large buckling.

The lateral load-displacement hysteresis diagram is shown in Figure 7.16.3. Maximum strengths occurred at cycle +8x1 and -6x2 and were 281 kN and -264 kN respectively. The stiffness at the end of the test was 46% of the initial stiffness. The strength decreased predominantly in one direction of loading because only one flange moved significantly out-of-plane.

Member axial shortening is shown in Figure 7.16.4. The curvature at the base of the specimen plotted against the applied load is shown in Figure 7.16.5, and the curvature along the length of the member at peak values of displacement is shown in Figure 7.16.6.

The column deformed in local buckling with the web in double curvature as shown in Figure 6.6c. In the final cycle, the strength decreased markedly and positive horizontal load was taken off the member when the hysteretic diagram was near zero displacement. The axial load produced an overturning

moment on the specimen which resulted in additional deformation in the member. The member displacement was stopped when the horizontal ram force became negative and moment equilibrium was reached.

At the end of the test, one of the flanges had moved sideways at an slope of 3% to the plate at the top of the specimen. No fractures were observed during the test but as the axial load was removed, the web of the specimen fractured.

The relationship between the displacement at the pin for specimen C4, and where the displacement was measured along the specimen were not linear as shown in the hysteretic behaviour at the top of the specimen in Figure 7.16.7. During loading in one direction, larger displacement ductilities at the pin were demanded than were anticipated, while in the other direction the same value of displacement was not reached.

The physical reason that this occurred was that centre of plastic rotation was in different positions for each direction of loading causing the displacements recorded on the member and at the pin to be non-proportional. It may be seen from the photograph in Figure 7.16.2 that the centre of the specimen near the region of buckling deformed considerably causing a P-delta moment which made the member keep moving with no lateral load as shown in Figure 7.16.3.

After the testing of this specimen it was observed that yield lines had occurred in the top bracket above the specimen on one side. The yielding was in compression due to lateral buckling of the specimens. An explanation of this behaviour is given in section 7.13.9(c). The cycle to displacement ductility, μ, of 8 corresponded to an interstorey drift of 3.17%.

7.12.4 Specimen C5

A FRITZ STAEGER demountable mechanical contact type strain gauge was used to measure the strains near the top of specimens C5 to CA because of the observed yielding in the flange of specimen C3 near the top. This type of mechanical strain gauge was able to give repeatable readings with a readability of 1μm. Ball bearings were punched into the tips of each flange in the positions shown in Figure 7.17.1. Before any reading was taken on the specimen, a reading was taken on a steel measuring standard so that corrections could be made for any change in length resulting from a temperature change.

After the first two cycles, an elastic displacement of 0.686 mm was calculated representing all of the elastic effects on displacement apart from the member itself.

Lüder lines were first observed at cycle 2x1 at 24° to the horizontal. Horizontal lines also occurred in the compression flange and are shown in Figure 7.17.2. As loading continued, more lines formed in the web and flanges and the mill scale started flaking off. At cycle -2x2, lines in the web were visible at 24° to the horizontal and 28° from the vertical, and in the flange horizontal lines were visible with other lines at 40° to these.

Buckling was first observed at cycle 2x2 in the web and at cycle -2x2 in the compression flange. The formation of buckles is given in Appendix 4 and the buckling deformation is shown in Figure 7.17.3.

The lateral load-displacement hysteresis diagram is shown in Figure 7.17.4. Maximum strength occurred of 220 kN and -218 kN in cycles 6x2 and -6x2 respectively. The final load-displacement stiffness was 45% of the initial stiffness.

Figure 7.17.5 shows the axial deformation of specimen C4. The curvature plotted against the applied moment at the base of the specimen is shown in Figure 7.17.6, and the curvature along the length of the member at peak values of displacement is shown in Figure 7.17.7.

Loss of strength resulted from local buckling in the manner shown in Figure 6.6d. Loading was terminated when the strength dropped to below 70% of the plastic load. The specimen behaved well and attained an interstorey drift of 3.3%.

7.12.5 Specimen C6

After the first two cycles, an elastic displacement of 0.390 mm was calculated representing all of the elastic effects on plastic displacement apart from the member itself.

Lüder lines were first observed in the web cycle 2x1, and at an angle of 33° to the horizontal. Horizontal lines also occurred at that time in the compression flange and at 35° to the horizontal. As loading continued, more lines formed in the web and flanges and the mill scale started flaking off.

Web and flange buckling was first observed at cycle 4x1. The magnitude of the buckles as loading progressed are shown in Appendix 4. At cycle 6x1 the buckling deformations were large so the potentiometers were removed.

The flanges buckled locally putting the web into single curvature. One side of one of the flanges did not start to buckle until cycle 6x1. The deformed shape of the flanges and web are shown at the end of the test in Figure 7.18.1.

The lateral load-displacement hysteresis diagram is shown in Figure 7.18.2. In this specimen, the maximum horizontal load, H_{max}, exceeded the load, H_u, calculated as $(F_u/F_y).H_p$, in the first cycle to a displacement ductility, μ, of -4 as a result of strain hardening.

Maximum strengths were -211 kN and 210 kN occurring at cycles -4x2 and 6x1 respectively. For specimens with higher axial loads the strain hardening became much higher as a proportion of the reduced plastic moment. The strength started to decrease at cycle -6x1. As loading progressed the elastic slope of the specimen decreased and by the end of the test was 51% of the initial stiffness.

Figure 7.18.3 shows the axial deformation of specimen C6. The curvature at the base of the specimen plotted against the moment at that position is shown in Figure 7.18.4, and the curvature along the length of the member at peak values of displacement is shown in Figure 7.18.5.

The deformation of the flange tips caused the web of the specimen to buckle in single curvature. While loading to μ = 10x2 a fracture was observed in the compression side of the web and at cycle –10x2 a fracture occurred in the other side of the web as shown in Figure 7.18.1.

The specimen was considered to have failed on the cycle to μ=-10x3 when the strength of the column dropped to less than 70% of the plastic load of the member. The bending of the column about the weak axis may be seen in Figure 7.18.6. This behaviour was observed in many of the column units. The cycles to displacement ductility, μ, of 10 correspond to an interstorey drift of 2.73%.

7.12.6 Specimen C7

After the first two cycles, an elastic displacement of 0.266 mm was calculated representing all of the elastic effects on the plastic displacement apart from the member itself. A mistake was made in loading to the first cycle and load was taken to H_p rather than 0.6 H_p.

Lüder lines were first observed in the web on cycle 2x1 at angles of 0° and 11° to the horizontal. Lines also occurred at that time in the compression flange at 0° and 35° to the horizontal. As loading continued, more lines formed in the web and flanges and the mill scale started flaking off. The buckle formed further up the specimen than it did in previous tests. Buckling was first observed at cycle 2x2. The magnitude of the buckles as loading progressed are shown in Appendix 4. The flanges buckled locally putting the web into single curvature. Buckling deformation is shown in Figure 7.19.1. At cycle -6x1 the buckling deformations were sufficiently large that the potentiometers were removed.

The lateral load-displacement hysteresis diagram is shown in Figure 7.19.2. In this specimen, the overstrength horizontal load, $\phi_o M_{pc}$, was exceeded in the first cycle to a displacement ductility of -4 because of strain hardening. The rate of strength degradation was approximately 8% per cycle and occurred in both directions of loading. Maximum strengths were -153 kN and +161 kN occurring at cycle -4x2 and cycle 6x1.

Figure 7.19.3 shows the axial deformation of specimen C7. The moment plotted against the curvature at the base of the specimen is shown in Figure 7.19.4, and the curvature along the length of the member at peak values of displacement is shown in Figure 7.19.5. The flange hysteresis is shown in Figure 7.19.6.

The test ended on cycle -10x2. The cycles to displacement ductility, μ, of 10 correspond to an interstorey drift of 1.97%.

7.12.7 Specimen C8

After the first two loading cycles, an elastic displacement of 0.23 mm was calculated representing all of the elastic effects on plastic displacement apart from the member itself. Lüder lines were first observed in the web at cycle 2x1 at angles of 0° and 44° to the horizontal as shown in Figure 7.20.1. As loading continued, more lines formed in the web and flanges and the mill scale started flaking off. Buckling was first observed at cycle

4x1. The buckle formed lower down the specimen than it did in unit C7. The magnitude of the buckles as loading progressed is shown in Appendix 4. The flanges buckled locally deforming the web in single curvature as shown in Figure 6.6d. Potentiometers were removed at cycle -8x2. The buckling is shown in Figure 7.20.2.

The lateral load-displacement hysteresis diagram is shown in Figure 7.20.3. In this specimen, the overstrength horizontal load, $\phi_o M_{pc}$, was exceeded in the first cycle to a displacement ductility of -2. Maximum strengths were -148 kN and 147 kN occurring at cycles -6x1 and +6x2. This maximum strength was approximately 2.6 times the calculated plastic load capacity. The elastic stiffness of the specimen had decreased to 45% of the initial stiffness by the end of the test.

Figure 7.20.4 shows the axial deformation of the specimen C8. Applied moment is plotted against curvature at the base of the specimen as shown in Figure 7.20.5, and the curvature along the length of the member at peak values of displacement is shown in Figure 7.20.6.

The test ended on cycle -14x1 when the strength of the column dropped because of a fracture which occurred in the web. After the cycles to these high ductilities, the strength of the specimen had decreased so that after testing had been completed, and while measurements were being taken, the specimen was unable to carry the axial load applied to it. The specimen shortened axially with large web fracturing until the vertical stroke limit on the Dartec was tripped. The cycles to displacement ductility, μ, of 14 corresponded to an interstorey drift of 1.52%.

7.12.8 Specimen CA

It was decided to test this last specimen under cyclic axial loading as well as lateral loading. In moment-resisting frames, the axial load in the columns is not expected to remain constant on account of large vertical accelerations of the ground, such as those which have been recorded in past earthquakes, and the overturning forces affecting the external columns on a frame.

Lüder lines near the base of the specimen occurred at an angle to the horizontal of 40° while further up the specimen they were at 22° in one direction and 62° in the other direction. Buckling was first observed at cycle 4x1. The magnitude of the buckles as loading progressed are shown in

Appendix 4. At cycle -6x2 the buckling deformations were large so the potentiometers were removed. The flanges buckled locally putting the web into single curvature.

The load displacement curve seemed to follow the shape of the anticipated plastic strength lines shown in Figure 7.21.1. Maximum strengths were 269 kN and -346 kN occurring at cycles 6x1 and -6x1 respectively. As loading progressed the slope of the lateral load-lateral displacement hysteresis diagram decreased to 67% of the initial loading stiffness.

Figure 7.21.2 shows the axial deformation of the specimen with applied load. The moment and curvature at the base of the specimen are shown in Figure 7.21.3, and the curvature along the length of the member at peak values of displacement are shown in Figure 7.21.4. The flange hysteresis of this specimen is shown in Figure 7.21.5.

Fracture occurred while the specimen was being deformed to cycle -10x2. The fracture caused a loud bang and split the tension flange completely and caused a rip approximately one quarter of the specimen depth into the web as shown in Figures 7.21.6 and 7.21.7. The strength dropped immediately to approximately $0.10M_p$. The cycles to displacement ductility, μ, of 10 corresponded to an interstorey drift of 3.8%.

7.13 SUMMARY OF EXPERIMENTAL RESULTS

7.13.1 Lüder Lines

The angle of the Lüder lines would be expected to form at an angle which depends on the orientation of the principal stresses which is dependent upon the level of axial load, and shear and bending stresses. For all of the specimens, angles of the Lüder lines to the horizontal are given in Table 7.3. No pattern was found in the direction of the Lüder lines as the axial load increased on the specimens. Where flange Lüder line orientations are not given, a general flaking off of the mill scale occurred.

Table 7.3
Angles of Lüder Lines

Orientation of Lüder Lines		
Unit	Web Lines	Flange Lines
C0	65°	45° 0°
C3	62° 30°	0°
C4	63° 9°	
C5	51° 35° 0°	45° 0°
C6	33° 0°	35° 0°
C7	11° 0°	
C8	44° 0°	
CA	62° 40° 22°	

7.13.2 Buckling

Buckling was noticed at cycle 6x1 in the beam and occurred as early as cycle 2x2 in the columns. All flanges tips tended to initially buckle out, away from the specimen web as shown in Figure 6.6b. At the peaks of the cycles, the buckle magnitude (x_1), height from the baseplate to the centre of the buckle (x_2), and the halfwave length (x_3) as shown in Figure 7.22 were measured and recorded. As buckling advanced, the flange tips on each side of the specimen would buckle together as shown in Figure 6.6d, except for units C0 and C4 in which the flanges buckled as shown in Figure 6.6c. Buckling deformations are recorded in Appendix 4.

The flanges did not straighten out fully during the load reversals on the axially loaded specimens and the decrease in strength caused by buckling was gradual and not sudden. The height of formation of the buckles seemed to be somewhat erratic. For example, the buckle on specimen C7 formed at a greater distance from the baseplate than in both C6 and C8. It was found that

buckling formed a reasonable distance from the ends of the member. The largest major buckling deformations were not near the welding cope holes and it seems as though these holes made no difference to the behaviour.

7.13.3 Hysteresis

The actual hysteresis loops were not as smooth as those drawn. At each displacement controlled increment, creep of the column units caused the lateral loading ram to lose some load. Similarly, at each load controlled increment, creep of the column unit caused the deflection to increase. The strain rate had a visible effect on the strength. When the peak displacements for each cycle were approached, the loading rate was decreased causing a drop in strength. Overnight relaxation of the specimens caused small steps in the hysteretic diagrams but the specimens usually took up the original curve upon reloading. The curves drawn represent an envelope of the load-deflection and load-curvature behaviour for each cycle. The horizontal displacement is also shown in terms of displacement ductility, μ, and interstorey drift.

7.13.3.1 Friction

During the initial loading cycles some energy was absorbed within the system. The figures of the load-displacement hysteresis show that the amount of energy absorbed was generally small, and was only slightly greater in the first cycle than in the second cycle. Because of the small size of the second loop, the friction in the system was difficult to measure and all values shown are therefore approximate. Values of friction force, H_f, were extrapolated directly from the load-displacement hysteresis curves, as described in section 7.11.2 and Figure 7.12, and are shown in the Table 7.4. There seems to be no dependence of the friction force on the axial load ratio. No correction has been made in any of the results in this report on account of friction. The values of friction in Table 7.4 contributed up to 5% of the maximum load in some cases.

Table 7.4
Loading Friction

Unit	C0	C3	C4	C5	C6	C7	C8	CA
H_f (kN)	10	12	9	9	5	4	7	8

The potentiometers recording the rotation of the specimen baseplate relative to the load frame showed that the rotation occurred almost linearly with applied lateral load.

7.13.3.2 Shape of Hysteresis Loops

It was found in the lateral load-displacement relationships (H-δ) obtained from the experimental work carried out in this chapter that a rounded lateral load-horizontal displacement hysteresis loop was obtained from the beam (unit C0) while the loops obtained from the axial loaded specimens were more rhombic. Similar results were obtained by Yamada [7.14] and Popov et al. [7.3]. Possible reasons for this type of behaviour were described in section 6.5.4(a). No pinching was observed in any of the loops, because there was no slackness in the system. A large amount of energy was absorbed.

The hysteretic loops for column C4 in Figure 7.16.3 show that the strength degraded during loading in one direction, but for the other specimens strength was observed to degrade in both directions of loading. This is because only one of the flanges moved significantly out-of-plane. It was when this flange was in compression that the strength degraded.

7.13.3.3 Strength

The strengths of the specimens increased over the first few cycles as the strain hardening ratio increased and then decreased when the effects of buckling become large.

(a) Strength at Different Cycles

For the beam, specimen C0, the peak force occurred on the cycle to a displacement ductility of 8 and was 1.15 (358kN/311kN) times that occurring at cycle 4x2. Patton, in the New Zealand study group for steel structures [7.15] has recommended a factor of 1.10 to represent the difference between members subjected to full and limited ductility demand in a capacity design type of procedure. On the basis of this one test this value appears to be reasonable. Recent work by Guruparan [7.16] has shown that the maximum strength of one beam was as high as 1.62 times the assumed plastic load at cycle 4x1.

The maximum column strength was obtained after only a few cycles of loading, while the maximum strength did not occur until after many cycles have been carried out in the beam. For example, for specimen C6 with an axial load ratio (P/P_y) of 0.60, the peak strength was almost reached at cycle 4x2 whereas for the beam, specimen C0, the maximum strength was occurred on

cycle 8x1. The reason for this may be that the rate of strain hardening in the columns is higher than in the beams because of the column cumulative shortening.

(b) Maximum Member Strength

The flexural overstrength factor, ϕ_{ob}, which is the ratio of the maximum lateral load, H_{max}, divided by the lateral force, H_{pc}, to cause the reduced plastic moment capacity, M_{pc}, calculated using the measured yield stress and section dimensions for each specimen, is plotted in Figure 7.23. The flexural overstrength is shown to be a function of the applied axial load.

The maximum flexural overstrength, ϕ_{ob}, obtained from column C3, with an axial load ratio, P/P_y, of 0.30 was less than that found from the beam (unit C0). Column C4, with an axial load ratio, P/P_y, of 0.40, had a larger flexural overstrength factor than the columns with axial load ratios of 0.30 and 0.50. Reasons for these phenomena are at present unknown and further understanding of the behaviour is required. However, a possible reason for the increase of flexural overstrength factor in the columns with higher levels of axial load was described in section 6.5.4(b).

Care should be taken when finding appropriate flexural overstrength factors from these results, as they are based on the maximum strength observed which may have occurred after several cycles of loading. When designing columns against yielding, the plastic strength on the first cycle should probably be used in conjunction with the maximum strength of beams during the expected number of cycles of loading.

7.13.3.4 Stiffness

The second moment of area of the beam decreased in the buckled region when significant buckling occurred leading to a degradation of beam stiffness.

7.13.4 Curvature

Rotation was calculated from the differential movement of the potentiometers on either side of the column using Equation 7.11 as shown in Figure 7.24.

$$\phi_{av} = \frac{\theta}{l_h} = \frac{\delta - \bar{\delta}}{l_h D'} \qquad \text{Equation 7.11}$$

Potentiometers had to be removed from the specimen when buckling became severe as the potentiometer brackets would rotate and give incorrect readings.

Curvatures for the hysteresis diagrams were measured by the potentiometers over the bottom 100 mm of the specimen. The moment at the centre of the potentiometers was calculated as $H_p L_p$, where L_p was 1100-13-50 = 1037mm.

All of the moment-curvature diagrams were fat showing no sign of pinching. In units C3, C4, C6, C6 and C8, it may be seen that the curvature at the base of the specimen tends to accumulate in one direction more than in the other.

Plots of curvature along the length of the specimen are also shown at peak values of displacement ductility. In some specimens (such as unit C8) the curvature at the base increases for loading in one direction while for loading in the other direction, the curvature further up the member is greater.

7.13.5 Plastic Hinge Length

An equivalent length of uniform curvature which, concentrated at the base of the specimen, would provide the same displacement at the top of the specimen as the real curvature distribution is known as the "plastic hinge length". It may be found from Equation 7.12 which is obtained from Figure 7.25a.

$$(\delta_T - \delta_t) = (\phi - \phi_p) L_p L \qquad \text{Equation 7.12}$$

The plastic hinge length used by Plugge and Walpole [7.17] which is commonly used for reinforced concrete members [7.18] may be found from Equation 7.13 as shown in Figure 7.25b.

$$(\delta_T - \delta_t) = (\phi - \phi_p) L_p (L - L_p/2) \qquad \text{Equation 7.13}$$

The hinge length, L_p, defined by Equation 7.12, may be slightly less realistic than that used in Equation 7.13, but it is of most use as it may be used directly in computer programs such as RUAUMOKO [7.19], which treat the hinges as concentrated points occurring at the end of a member.

The value of displacement at the pin, δ_T, was approximated as $\mu\delta_t$ from Table 7.2 according to the linearity relationship described in section 7.13.8(c).

The plastic displacement at the point of contraflexure, δ_t, in Equations 7.12 and 7.13 is dependent on the actual lateral load applied when the plastic hinge length is computed. However, in the past the nominal plastic displacement resulting from the nominal plastic load, H_p, has been used. In this report the same approximation was made.

Values of plastic hinge length are given in Table 7.5 below at cycles 2x1 and 4x1 for all specimens except for CA. Values for specimen CA are not given as plastic displacement is dependent on axial load which changes with lateral displacement. The length to the point of contraflexure, L, used in the equations above was 1100 mm.

Table 7.5
Plastic Hinge Lengths

Unit	δ_T (μ=2) mm	δ_T (μ=4) mm	ϕ 2x1 (rad/m x10^{-3})	ϕ 4x1 (rad/m x10^{-3})	L_p μ=2 Eq. 1 mm	L_p μ=4 Eq. 1 mm	L_p μ=2 Eq. 2 mm	L_p μ=4 Eq. 2 mm
C0	13.14	26.28	52.2	125.4	150	159	162	172
C3	11.66	23.32	50.7	87.2	134	209	143	234
C4	9.64	19.28	37.7	82.5	153	179	166	197
C5	8.02	16.04	30.4	58.6	160	215	174	241
C6	6.66	13.32	24.8	50.0	164	208	179	233
C7	4.82	9.64	15.5	34.6	201	219	224	247
C8	3.10	6.20	10.1	24.4	197	197	218	219

It may be seen from Figure 7.26 on which the values of plastic hinge length of Table 7.5 are plotted, that Equation 7.13 gives values of hinge length up to 20% greater than Equation 7.12. This is to be expected as the further up the member that the centre of rotation is, the larger the plastic curvature will have to be to obtain the same displacement at the top.

At cycle 2x1, shown in Figure 7.26, the plastic hinge length seems to increase with the axial load ratio, whereas at cycle 4x1 the dependency seems to be less. Specimen C0 sustained no large cumulative shortening and the hinge length remained approximately constant with increased ductility. For the columns, the hinge length seemed to increase with increasing ductility, however, for column C8 the hinge length remained approximately constant. Potentiometers were removed from some of the specimens at higher displacement ductilities.

The plastic hinge lengths at cycle 4 for these specimens varied from between 64% and 100% of the section depth. The length of plastic hinge increases with increasing ductility so it was thought that at higher displacement

ductilities, which are of most interest, a plastic hinge length equal to the depth of the section should be used in the analyses of members in frames. Further test results are required to confirm this estimation.

7.13.6 Axial Deformation

Axial deformation was found from the potentiometers for specimens C0 and C3, and from the axial movement of the Dartec for the other specimens. The average axial strain in the plastic hinge zone is calculated from Figure 7.24 as

$$\varepsilon_{av} = \frac{\delta + \bar{\delta}}{2\, l_h} \qquad \text{Equation 7.14}$$

(a) Axial Deformation of Beams

The increase in length of the specimen C0, with a very small nominal compressive axial load, is thought to have resulted from the material stiffness, EA, being greater in compression than in tension. Possible reasons for this are that the strain hardening stiffness in compression is greater than that in tension, particularly at large strains, as is shown in Figure 6.1 due to the effect of Poisson's ratio and the length of yield plateau in compression is shorter than in tension. The length of the yield plateau in compression was observed to be about one half of the length of the yield plateau in tension of some reinforcing steel tested by Mander et al. [7.20]. These two effects will mean that the strain hardening stiffness is more in tension than in compression. Therefore during loading, the neutral axis of the section will move toward the compression flange causing the tension flange to yield more. When load is reversed, the tension and compression flanges are reversed and the tensile flange again deforms more. This is accentuated by the new compression flange having strain-hardened in tension more than the new tension flange. After several cycles of loading, the beam will have yielded more in tension than in compression and will, as a result, have increased in length. It should be emphasized that the amount of axial elongation which was approximately one millimetre is insignificant for practical engineering purposes.

When buckling became severe, the member shortened because the compression flange was less stiff than the tension flange causing the neutral axis of the section to move toward the tension flange. When loading was reversed the neutral axis moved toward the tension flange on the other side of the section. Cumulative compressive strains resulted in the section causing

axial shortening. This phenomena of the increase and subsequent decrease in beam length has also been observed in all of the six beam tests recently carried out by Guruparan [7.16].

(b) Column Cumulative Displacement and Axial Shortening

The axially loaded specimens which did not fail from flange fracture shortened between 65 mm and 95 mm over the 300 mm or so of the member which yielded significantly before testing was terminated. This equates to an average strain of over 30%. In some locations the strain would have been greater than this. The ultimate strain of the steel tensile test pieces shown in Table 7.1 was between 30% and 35%.

The graphs of axial displacement versus horizontal displacement show that axial shortening occurred while the member was deforming plastically in bending. Figure 7.27 shows that the relationship between the cumulative inelastic ductility and the axial displacement is approximately linear for small strains before buckling becomes severe. At higher cumulative ductilities the rate of axial shortening increased because of section buckling. The cumulative inelastic displacement ductility was calculated from the loading regime as shown in Figure 7.28. The only parts of the loading regime which cause an inelastic displacement of the specimen, as shown in this figure, contribute to the cumulative inelastic displacement ductility. The elastic parts of the regime, also shown in the figure, are not included in the calculation of the cumulative inelastic ductility.

The relationship between cumulative inelastic rotation and axial deformation are shown in Figure 7.29. The cumulative inelastic rotation, $\Sigma\theta_R$, was found by multiplying the cumulative inelastic displacement ductility by the member theoretical plastic displacement, δ_s, and dividing by the height from the baseplate to which the displacement was measured. The rate of accumulation of axial deformation for members with axial load ratios greater than 0.60 is approximately constant, whereas the rate of axial deformation for specimens with lower axial loads was less than this and depended on the magnitude of the load.

The reason for the members with high levels of axial load having the same rate of accumulation of axial deformation is thought to be because the neutral axis was in the flange of the specimen thereby allowing very little yielding of the flange in tension. A change in axial load level would lead to a small change in the position of the neutral axis. Approximately the same flange strains would then be required in a section with the neutral

axis in the flange, as shown in Figure 7.30, to obtain the same member inelastic rotation. These assumptions lead to the formula given in Equation 7.15a for high levels of axial load where the amount of axial deformation is independent of the level of axial load. A constant plastic hinge length is assumed over which the inelastic curvature is assumed to be uniform. This assumption is the same as that used in the calculation of member inelastic rotation.

For members with lower applied axial loads, the flanges may yield in tension because the neutral axis may be in the web. If there is no axial load and no buckling then no axial shortening is expected. A linear interpolation between zero axial load and the axial load which causes the neutral axis to be in the flange is used to predict the displacement in Equation 7.15b.

The expected column axial deformation, δ_a, before severe buckling takes place may be predicted using Equation 7.15, where α and β are parameters found by experiment.

$$\delta_a \approx \alpha L_p \Sigma\theta_H \qquad \text{if } P/P_y \geq \beta A_w/A \qquad \text{Equation 7.15a}$$

$$\delta_a \approx \left[\frac{P/P_y}{\beta A_w/A}\right] \alpha L_p \Sigma\theta_H \qquad \text{if } P/P_y \leq \beta A_w/A \qquad \text{Equation 7.15b}$$

This equation is non-dimensional and of general form and may be used for any column or beam. The two portions of the equation are required depending on whether the neutral axis of the section is in the web or in the flange as this affects the amount of flange yielding in tension. It may be seen that for beams, in which the neutral axis is in the web that Equation 7.15b should be used and the axial displacement predicted before buckling becomes significant is zero as required. For the experimental tests carried out in this report the values of 0.446 and 2.54 for α and β respectively match the experimental results well and give the lines shown in Figure 7.29 when the length of plastic hinge, L_p, is approximated as the depth of the section, D. It is expected that these values will give a good approximation to the axial deformation of all I-shaped steel members.

When $P/P_y = \beta A_w/A$, it is assumed that the neutral axis of the section is at the interface between the web and the flange and that the web is fully yielded. The value of β then represents the overstrength factor relating to the maximum axial load that may be carried by the web. The value of β of 2.54 is larger than an overstrength value would be expected to be. This is because although it was assumed that the neutral axis was at the web-flange

interface, the neutral axis may be within the flange while significant yielding of the flange in tension occurs. The flange of the specimen with an axial load ratio of 0.60 sustained significant tension yielding showing that this assumption is not correct and that further refinement of this equation is therefore possible. Further variables may be required to account for the position of the neutral axis in the flange when significant tension yielding occurs in the flange. However, for most members it is thought that Equation 7.15 will give a good estimate of the amount of axial shortening expected although verification on other section shapes is required.

7.13.7 Flange Hysteresis

Hysteretic curves of the flange strain verses lateral load at the base of the specimens were calculated by Equation 7.16.

$$\varepsilon_f = \varepsilon_{av} + \phi_{av} (D - T)/2 \qquad \text{Equation 7.16}$$

It may be seen in Figure 7.14.11 that with the application of cyclic load on specimen C0, the flange deformed approximately equally in tension and compression. The flange of specimen C3, shown in Figure 7.15.8, deformed more in compression than in tension, and the flange of specimen C7, shown in Figure 7.19.6, yielded in compression but very little in tension because of the positions of the neutral axes in the sections caused by the amount of axial loading. This behaviour was explained in section 6.5.3.

(a) Prediction of Flange Strain

The flange strain may be calculated using Equation 7.16 in which the axial strain before buckling, ε_{av}, may be calculated as δ_a/L_p from Equation 7.15. Further work is required to estimate the axial shortening which occurs in beams and columns as a result of buckling, and the maximum flange strain which may be sustained by a particular member before the strength loss becomes unacceptable. The maximum sustainable flange strain is expected to be dependent on the section and member slenderness ratios. It is expected that most compact members would behave in a similar way to those tested and described in this report, with the flange strain from axial deformation being much more significant than that arising purely from curvature. All members were able to sustain axial displacements of 43mm before any type of fracture occurred. This displacement corresponds to an axial strain of 0.17 if the length of yielding is assumed to be equal to the section depth. It is

expected that simple plane stress computer programs may be used in order to model the axial deformation of sections if the material stress-strain characteristics are known.

7.13.8 Rotation and Ductility Capacity

It was found that all of the specimens tested sustained at least two cycles of loading to a displacement ductility of eight. This ductility capacity is much more than the expected ductility demand of columns in frames subjected to limited ductility. Some columns with low axial loads sustained rotations of over 5%, while 3% is generally regarded as the maximum rotation a subassemblage in a building would be required to sustain [7.13].

The number of cycles of loading, the cumulative inelastic displacement capacity, the cumulative ductility and the observed axial shortening, before failure are given in Table 7.6. The predicted axial displacement, from Equation 7.15 at failure is also given. It should be noted that the load dropped off slowly for most of these specimens making it difficult to observe when the failure criterion was reached, so the values below cannot be regarded as very accurate and give only an indication of the member deformation capacity. For example, the cumulative ductility capacity of specimen C6, was recorded as being much greater than that of specimen C7 because it sustained one more cycle.

Table 7.6
Cumulative Displacements, Ductilities and Axial Shortening

Unit	Axial Load Ratio	Cycles	Maximum Disp. (mm)	Cumulative Disp. (mm)	Cumulative Ductility	Axial Disp. Predicted (mm)	Axial Disp. Observed (mm)
C0*	0.0	10x8	44.2	1719	389	0	≈5
C3*	0.3	10x2	39.2	678	173	47	62
C4	0.4	-8x2	25.9	392	121	36	51
C5	0.5	10x1	27.0	370	137	42	60
C6	0.6	10x3	22.4	468	209	62	78
C7	0.7	10x2	16.2	280	173	38	60
C8	0.8	14x1	14.6	313	301	42	48
CA*	Varying	10x2	31.3	-	173	-	43

From Table 7.6 it may be seen that the inelastic cumulative ductility was lowest for the specimen C4 which had axial load ratio of 0.40 and was greater for the more highly loaded members. The cumulative inelastic displacement decreased slightly for axial load ratios greater than 0.30. The amount of axial shortening is approximately constant, ranging from 48mm to 62mm for all of the beam-columns failing by buckling except for specimen C6.

The asterisks (*) indicate that these columns either didn't fail or that flange fracture caused failure. The ductility capacity was approximately constant for the specimens with axial load ratios between 0.3 and 0.7, however the maximum displacement which was sustained decreased with axial load. This displacement was measured 835mm from the base of the specimen.

It is thought that the maximum strain in the section is the most important parameter in determining the deformation capacity of a compact column subjected to the type of loading carried out in these tests. The extreme fibre strains are made up of both the axial deformation from the previous cycles plus the strains from the curvature on the section during the cycle under consideration. The axial shortening is thought to be the main parameter determining when failure will occur in compact sections because the strains from section curvature are small compared to the strains from axial deformation alone.

While the members with high levels of axial load had very little flange tension yielding and those with lower axial loads sustained significant amounts of flange tension yielding, the fact that the members failed at the approximately same amount of axial deformation indicates that the effect of load reversal and energy dissipation within the flange is not large. This finding is consistent with research into the cyclic behaviour of shear links [7.6], in which the maximum absolute deformation was found to be far more important than the number of load reversals.

Failure occurred in the columns when the observed axial displacement was greater than 48mm and the predicted axial displacement was greater than 36mm. The observed axial shortening was less than 1.6 times that predicted by Equation 7.15. The difference between the observed and predicted values of axial shortening result from buckling making the section less stiff.

(a) Comparisons with Other Studies

The formulae by Mitani et al. [7.21] for members subjected to monotonic loading predicts that the 250 UC 73 members tested would sustain curvature ductilities greater than 10. Mitani et al. found that the ductility capacity of a member is approximately independent of the axial load level if the axial load ratio (P/P_y) is between 0.30 and 0.60. This was also found to be the case in the testing carried out in this report. The reason for this is that although members with low levels of axial load are subjected to greater levels of displacement than are the more highly axially loaded columns, the amount of tensile yielding of the flanges of specimens subjected to lower

levels of axial load is greater. The net amount of axial shortening during loading to a certain displacement ductility is approximately the same for columns within this range of axial loads. Members with higher levels of axial load, in which no tension yielding occurs, require higher displacement ductilities to obtain the same rotation because the calculated yield displacement is smaller. The higher ductility capacity of highly axially loaded columns is shown in that specimen C8 sustained a displacement ductility of 14.

Yamada [7.14] found that for a particular level of axial load, the number of cycles of loading was dependent on the amplitude of those cycles and that an empirical log-log relationship could be used to predict the behaviour. The relationships have been derived for a specific section type and the number of cycles of loading and displacement magnitude were the main parameters investigated. In this report the main influence investigated was that of the level of axial load, the inelastic rotation rather than the total rotation was used and different failure criteria were selected. The extreme cases of monotonic loading and high cycle fatigue in the elastic range have not been investigated in this report. Although it is difficult to make a direct comparison with Yamada's work for these reasons it was found that in both studies the deformation capacity was found to decrease with increasing axial load. An increase in the number of cycles of loading to a certain displacement, or of the displacement magnitude of those cycles was found to increase the likelihood of failure.

Popov, Bertero and Chandramoulli [7.3] found that the behaviour of members with axial load ratios greater than 0.50 was not desirable. In this report it was found that the behaviour of members was good even under axial loads of up to $0.8P_y$. The reason for this difference is that Popov et al. were testing the specimens to approximately the same level of absolute displacement, rather than to the same level of ductility. This means that the specimens with high levels of axial load were subjected to greater inelastic rotations than were the more lightly loaded columns. It was also found in this report that the maximum displacement to which a member may be subject before failure decreases with axial load. Another effect which decreased the deformation capacity of the specimens tested by Popov et al. was that curvature accumulated in one direction in the columns above and below the joint. This effect could not be modelled in the testing carried out in this report as only one column section, rather than a full subassemblage was tested.

(b) Recommendations on the Axial Load Limitations of Members

The recommendations for the axial load ratios for members subjected to full and limited ductility demands made by Butterworth and Spring [7.1] seem to be reasonable based on the testing carried out.

For members of limited ductility in frames, the achievable member displacement ductility of 8 was much greater than that which would be expected to be demanded of a member of limited ductility. This was achieved in all columns. However, slender columns subjected to high levels of axial load may yield along their lengths because of residual stresses before lateral loading is started. This effect may decrease the member lateral stability [7.22]. Vertical accelerations may increase the column axial load to greater than the testing level. No account of this is taken in the New Zealand design procedures. A recommended maximum column design axial load level should be less than that found during testing to allow for these vertical accelerations. For these reasons the recommended maximum axial load level of $0.70P_y$ [7.1] seems to be a reasonable upper limit for columns subjected to limited ductility.

For members of full ductility in frames, the member displacement ductility demand may exceed 8 in some cases because a member displacement ductility much larger than a specified subassemblage displacement ductility may be required as shown in Equation 6.11 of section 6.7.3(d). However the members tested with low levels of axial load sustained large rotations. For example the member with an axial load ratio of 0.60 sustained a rotation of 0.027. If this column were in a frame, the elastic displacement of the beams would possibly allow the subassemblage to sustain an interstorey drift ratio of 0.03. Interstorey displacements of no more than 0.03 are often considered to be the maximum expected in any large earthquake [7.13]. It is suggested that the value of axial load ratio of 0.50 be used as the maximum axial load permitted for members expected to be subject to limited ductility demand as recommended by Butterworth and Spring. For columns expected to sustain full ductility demands this value was reduced from 0.60 to allow for

1) the effects of vertical accelerations, and
2) the possibility that cumulative curvatures may occur in one direction in the columns of a real frame as has been observed by Popov et al. [7.3].

It recommended, based on this testing, that the axial load limitations by Butterworth and Spring [7.1] be used for members expected to sustain limited ductility demand. However, it is also suggested that more testing be carried

out because a more critical combination of flange and web slenderness ratios could lead to an earlier loss of strength.

(c) Ductility Measurement

There is no recognized standard stating where displacement ductility is to be measured, however it is common that the displacement ductility was computed from measurements taken at the point of contraflexure of a member. In these tests the displacement ductility was based on displacements measured further down the member because of the change in section properties at the top of the column due to the bolted bracket and the possibility of some non-linear deformation occurring there.

The relationship between the equivalent displacement ductility at the point of contraflexure, δ_T, and that measured further down the section, δ_μ, is dependent on the length of member and the length of the plastic hinge, which in turn is a function of the level of displacement ductility. It is therefore a complex relationship.

However, when δ_μ was plotted against δ_T, the relationship was found to be approximately linear as shown in Figure 7.31 for all specimens except column C4. The displacement ductilities at the point of contraflexure and those used in the testing were therefore considered to be the same. Further comments were given about column C4 in section 7.12.3.5.

Measurement of ductility from the side of the specimen was thought to be satisfactory because of the linear of the relationship between the ductility here and that at the top of the specimen and because rotation was thought to be a more important parameter in the understanding of the overall behaviour of the specimens.

7.13.9 Mechanisms

Approximate yield line patterns are shown in Figure 7.32 for local buckling in which the flange tips on one side of the specimen moved in the same direction, and in which the flange tips on the opposite side of the specimen moved apart.

(a) Buckling of Flange Tips

It was observed from the experimental tests described in this chapter that initially the tips of the flanges all seemed to buckle away from the web as

shown in Figure 6.6b. Later the flanges tended to buckle as one unit with the tip at one end of the flange buckling toward the web and the tip at the other end buckling away from the web. The flange tip which is most heavily loaded tended to buckle toward the web in order to decrease the bending resistance of the specimen by lowering the second moment of area of the section about the axis of bending. This was shown for the specimens tested in this chapter by the demountable strain gauge readings. Once each flange had buckled significantly as a whole, the buckled shape was maintained and loading moved more to the other side of the flange.

It was found from the specimens tested that it is difficult to predict the exact behaviour of a member subject to cyclic loading. There seems to be a degree of variation determined by the way in which the flanges buckle and the height of the buckle. Both web and flange buckling were required before there was any real strength loss.

(b) Flange Forces

It was observed in some specimens, such as Unit C3, that the yield lines were observed in some flanges a considerable distance from the plastic hinge region. For this to have occurred, an uneven distribution of flange forces must have been present. In Figure 7.33 it is shown that a moment about the minor axis of the member (d), or a torsional moment (c) when combined with axial load (a) or bending about the major axis (b) may cause yielding in a flange (e) which would not be expected to occur under the directly applied loads.

In the second specimen, Unit C3, yield lines were found on the flange near the top of the specimen. The demountable mechanical contact type strain gauge mounts were placed on the flanges near the top of the specimens C5 to CA to measure the effect of buckling further up the column. The readings of the demountable mechanical contact type strain gauge showed that when axial load was applied to a specimen almost all of it was carried on the flange tips on one side of the web as shown in Figure 7.34a. This resulted in a moment about the minor axis being applied to the specimen.

This may have been because of the yielding and shortening of the bracket on one side of the load frame top bracket as discussed in section 7.12.4. Buckling of specimens C5 to CA all occurred in the same manner, with the flange tips on the side of the specimen with most of the axial load moving together thereby reducing the bending resistance and causing the web to deform in single curvature as shown in Figure 6.6d.

The specimen deformed in the shape shown in Figure 7.34b as the buckles increased in size. The side of the specimen in which the flange tips moved together did not decrease in length as much as the other side. Axial load was gradually transferred to the longer side as further cycles of loading were applied. The demountable mechanical contact type strain gauges showed this effect.

(c) Modes of Failure

Descriptions of the type of failures are given in the discussion of the behaviour of each specimen. A summary of the modes of failure for the specimens is given in Table 7.7. Local buckling[1] and local buckling[2] in this table indicate that the flanges moved in the way shown in Figure 6.6c and 6.6d respectively.

Table 7.7
Specimen Failure Mechanisms

Unit	Failure Mechanism
C0	No failure
C3	Partial Flange fracture
C4	Local buckling[1]
C5	Local buckling[2]
C6	Local buckling[2] with web fracture
C7	Local buckling[2]
C8	Local buckling[2] with inability to sustain axial load and web fracture
CA	Total flange fracture

(d) Fracture

Flange fracture occurred in Column C3 which was subjected to an axial load ratio (P/P_y) of 0.30, and in Column CA with varying axial load after severe local buckling. The specimen with no axial load did not fracture because there was not enough buckling to concentrate the material strains. Although there was significant buckling of the members with axial load ratios greater than 0.40, it is thought that the flange was not subjected to enough tension for flange fracture to take place. In the flanges which did fracture, there was both significant buckling from the compressive loading, and enough tension from reverse loading to initiate the fracture. In the tests the possibility of fracture was also accentuated by the residual stresses caused by the welding of the potentiometer studs to the flange, and the material discontinuity on the flange surface caused by the weld itself.

Web fracture only occurred in specimens C6 and C8 after severe local buckling had taken place as a result of a large amount of column axial shortening.

(e) Degrees of Freedom of the Test Column

The experimental set up restricted some of the degrees of freedom at the top of the column. They are:

i) the out-of-plane displacement (d_1),

ii) the out-of-plane rotation at the top of the specimen (d_2), and

iii) the torsional degree of freedom at the top of the column (d_3), as shown in Figure 7.35,

iv) the distance to the flange stiffener is less than the recommended maximum distance thereby providing additional restraint. In a column of a real building, the upper half column connected to the top of the specimen would provide some restraints but these may be less restrictive than those applied here in the test frame.

7.13.10 Effect of Alternating Axial Load

In the tests undertaken it was found that a cyclically-varying axial load caused less buckling than if the axial load was maintained at the maximum value throughout the tests, however the possibility of flange fracture was greater than with a high level of axial load. Because of the uncertainty of the value of the column axial load expected during an earthquake it is suggested, if fracture is not expected, that the maximum expected axial load ratio be applied to the column during testing in order to conservatively estimate the most critical buckling behaviour.

7.13.11 P-Delta Effects

The P-delta moments were small in the testing undertaken because the displacement at the top of the columns was high for columns with no axial load, and low for columns with high axial load levels, at the same level of displacement ductility. The magnitude of the P-delta moment was calculated by the method of Pam [7.23] as shown in Figure 7.36.

$$Pd' = \frac{Pad}{b}$$

In the test rig the values of a and b were 320 mm and 1100 mm respectively. The maximum displacements at the top pin produced P-delta moments at the

base of the specimens of less than 18 kNm in all cases. This value was small, and no correction for P-delta was included in the hysteretic diagrams in this report.

7.14 CHAPTER SUMMARY

Within the limitations of this study the following observations may be made.

1) All of the columns tested behaved well and attained at least two cycles to a displacement ductility of eight. The achievable displacement ductility seemed to be independent of the axial load ratio, however, smaller column rotations were achieved with greater axial load ratios.
2) Significant axial deformation may occur before buckling starts. The amount of this axial deformation may be predicted.
3) Significant local buckling may occur before the lateral strength of a specimen decreases.
4) The number of cycles of loading is a very important parameter in the response of a beam-column member.
5) Strength loss and failure may occur because of different forms of buckling or fracture.
6) Because of the different ways in which flanges buckle and the different heights at which the major deformation forms, it is necessary to be careful when testing a few specimens to make sure that the correct conclusions are drawn.
7) The present limits for axial load ratios for members in earthquake resistant frames seem to be reasonable from the testing undertaken.

The test set-up and the testing of eight beam-columns was described in this chapter. The key parameter affecting the deformation capacity of compact columns failing by buckling and loaded cyclically was identified and a method for the prediction of the axial shortening of a column was developed. It is suggested that further work be carried out in order to verify the assumptions made herein, to predict the axial shortening occurring as a result of member buckling in both beams and columns and to study the deformation capacity of different member types. The introduction of the axial shortening into a dynamic time-history analysis model would then be desirable.

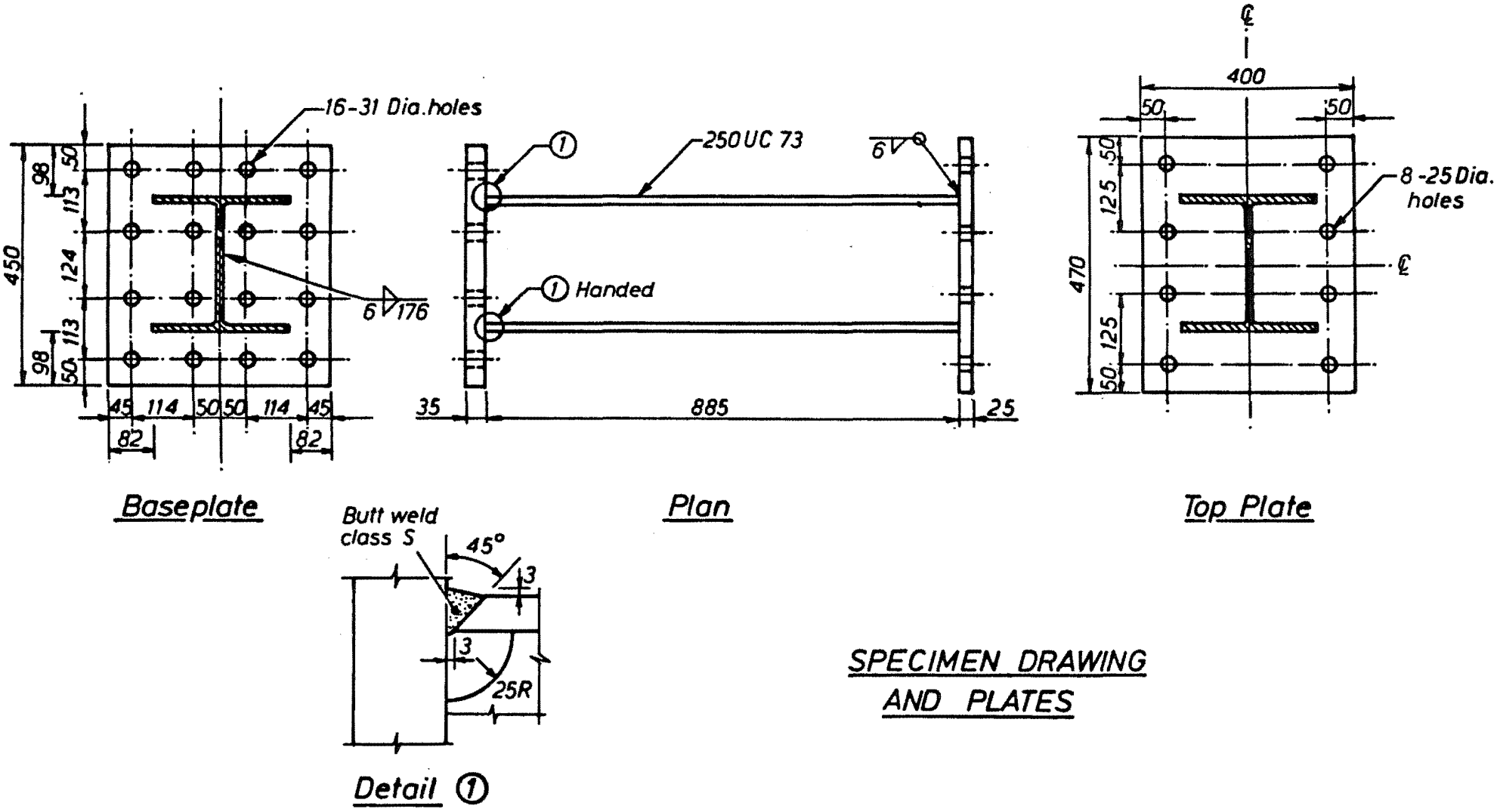

SPECIMEN DRAWING AND PLATES

Figure 7.1. Test Specimen Construction Drawings

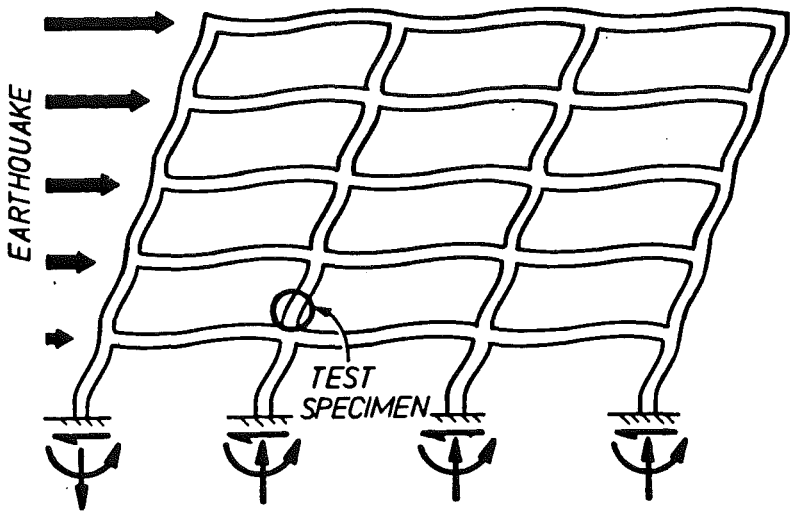

Figure 7.2. Assumed Position of Test Specimen in Multistorey Frame

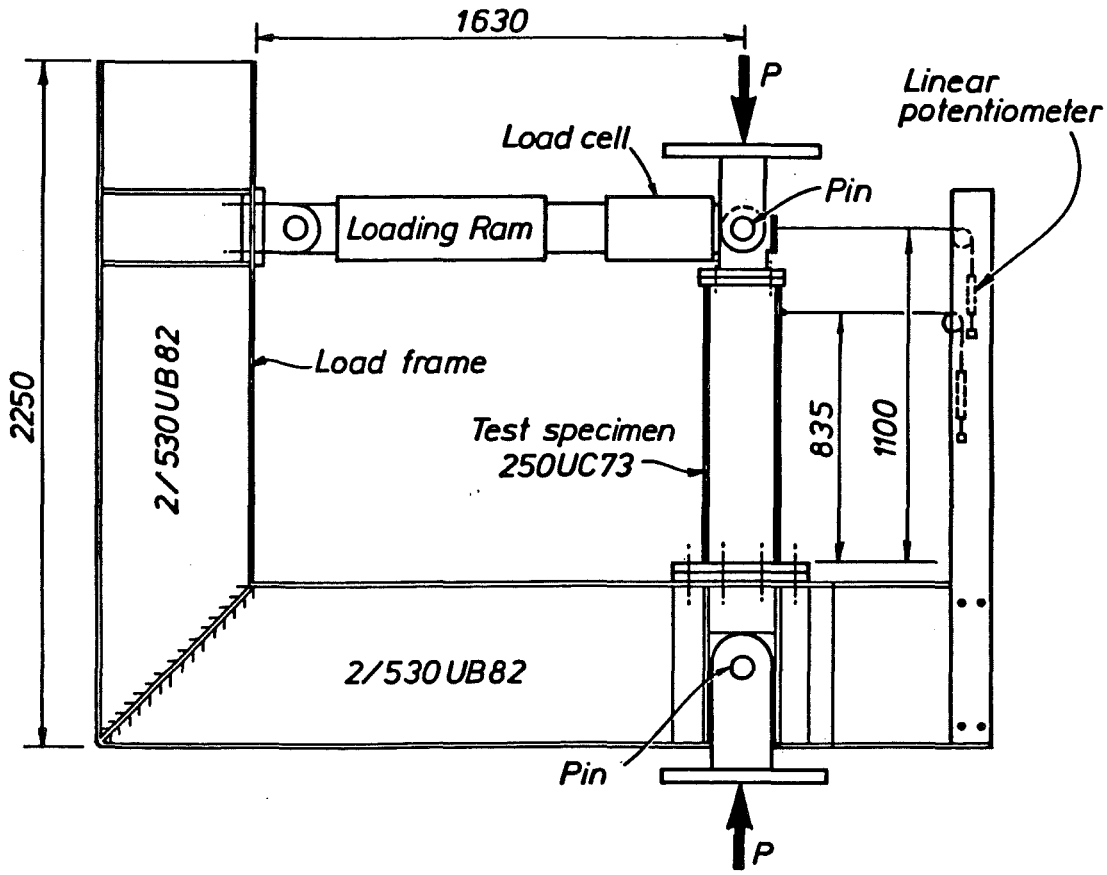

Figure 7.3. Test Specimen in Load Frame

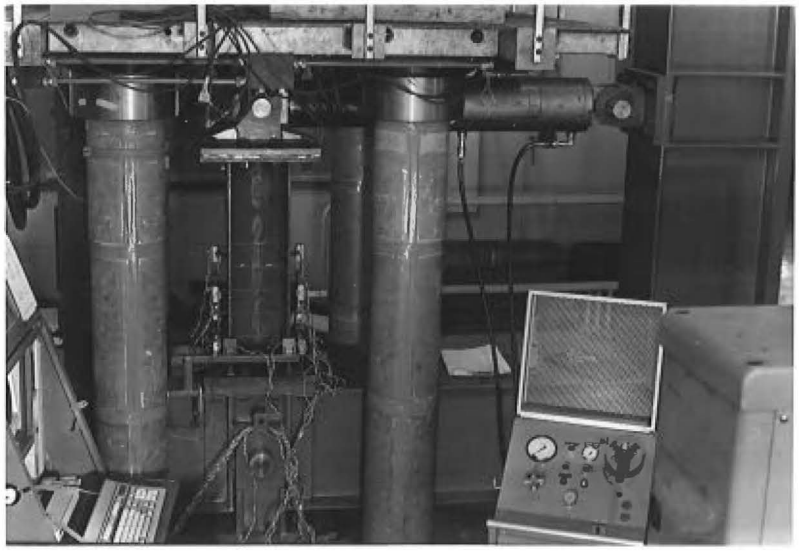

Figure 7.4. Photograph Specimen in Load Frame

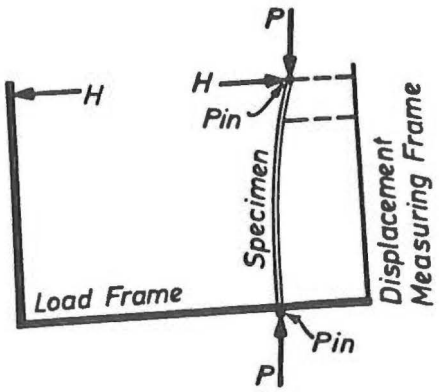

Figure 7.5. Deformation of Specimen in Load Frame

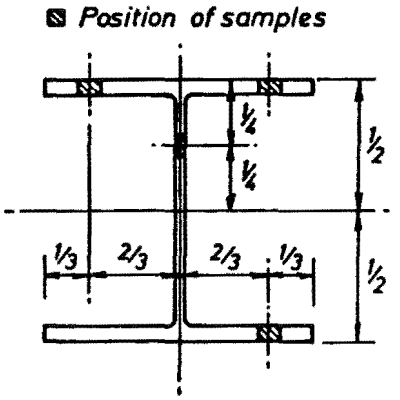

Figure 7.6. Positions from which Samples were taken from the Column Section

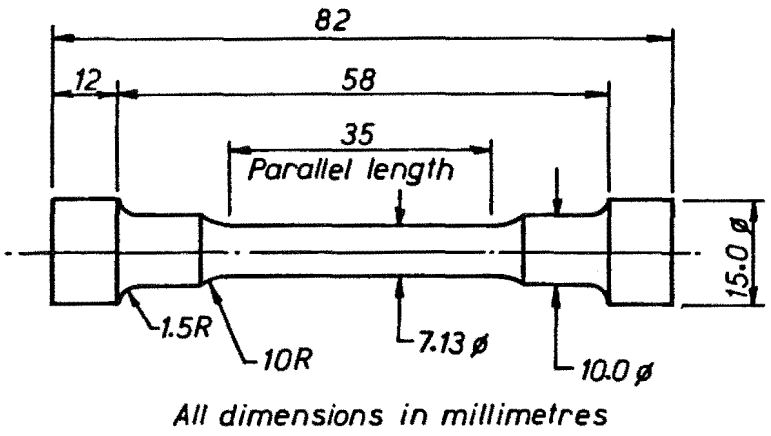

Figure 7.7. Shape of Tensile Test Sample

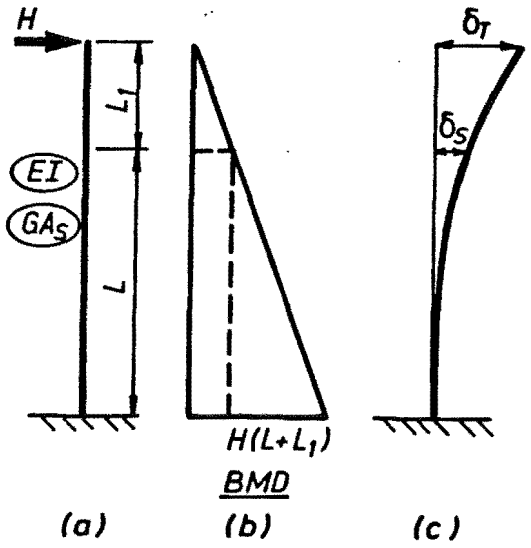

Figure 7.8. Positions of Displacement Measurement

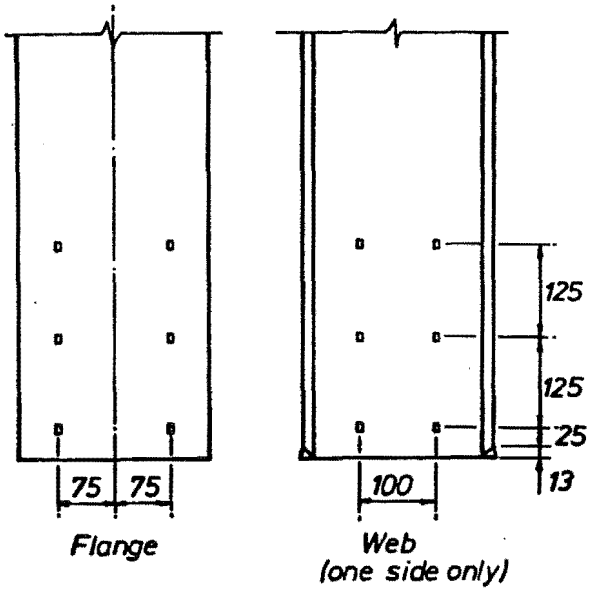

Figure 7.9. Positions of Strain Gauges

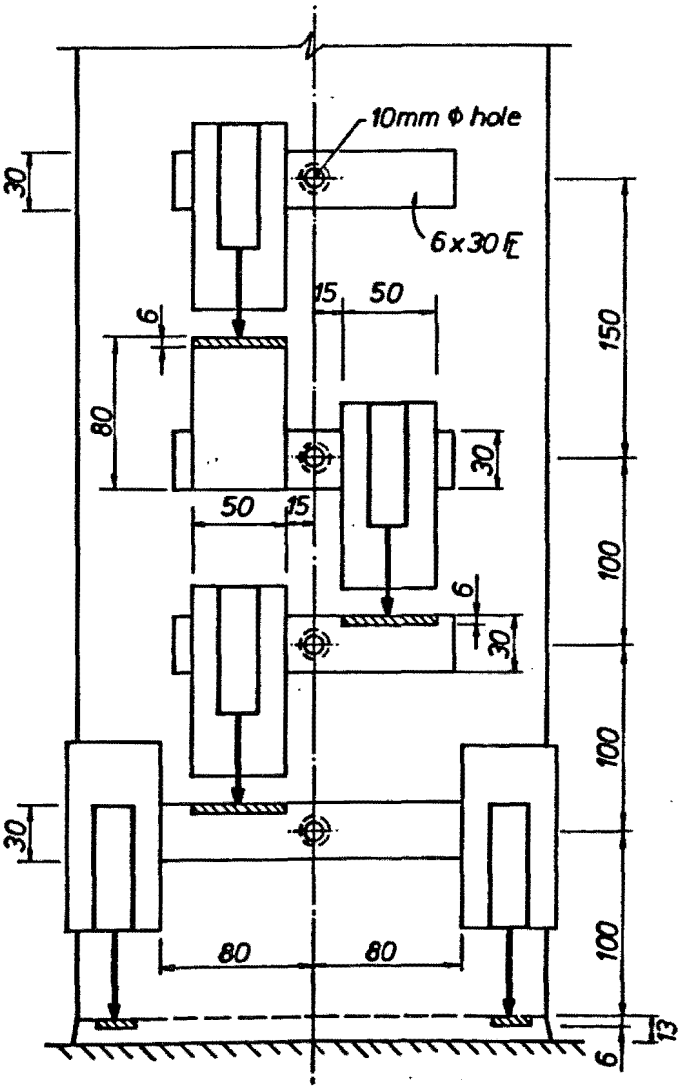

Figure 7.10. Potentiometer Positions

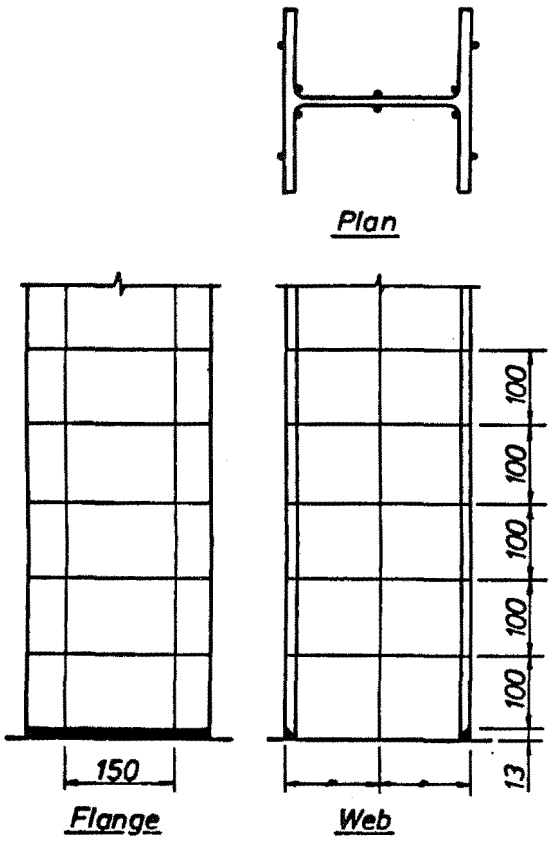

Figure 7.11. Positions of Grid Lines

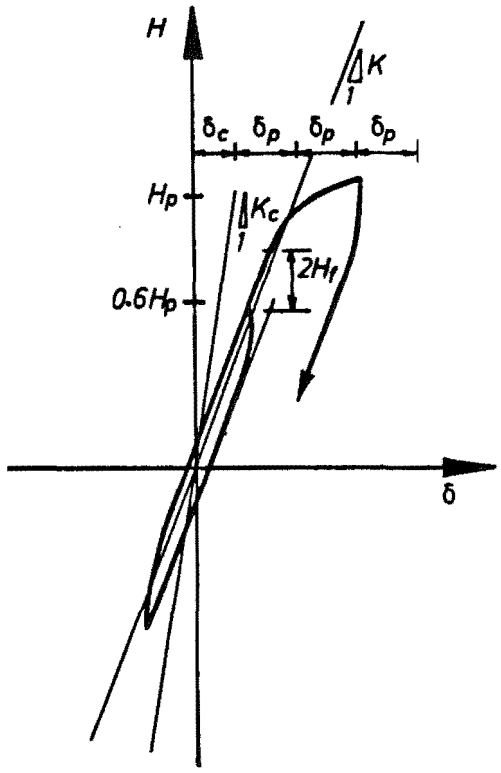

Figure 7.12. Load-Displacement Hysteresis of Initial Cycles

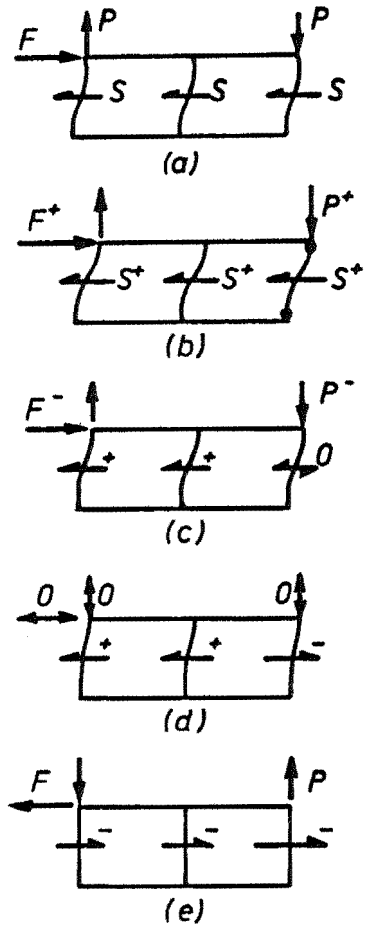

Figure 7.13. Possible Forces on External Column

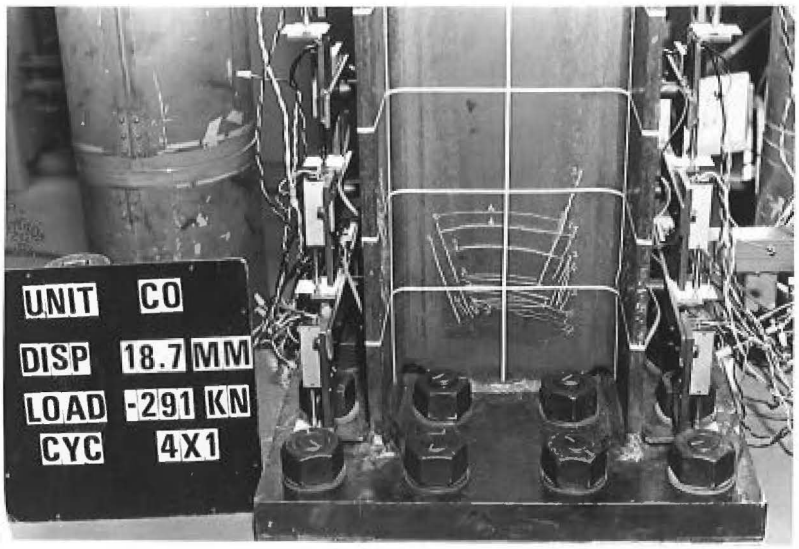

Figure 7.14.1. Column CO Web Yield Lines - Cycle 4x1

Figure 7.14.2. Column CO Flange Yield Lines - Cycle -4x1

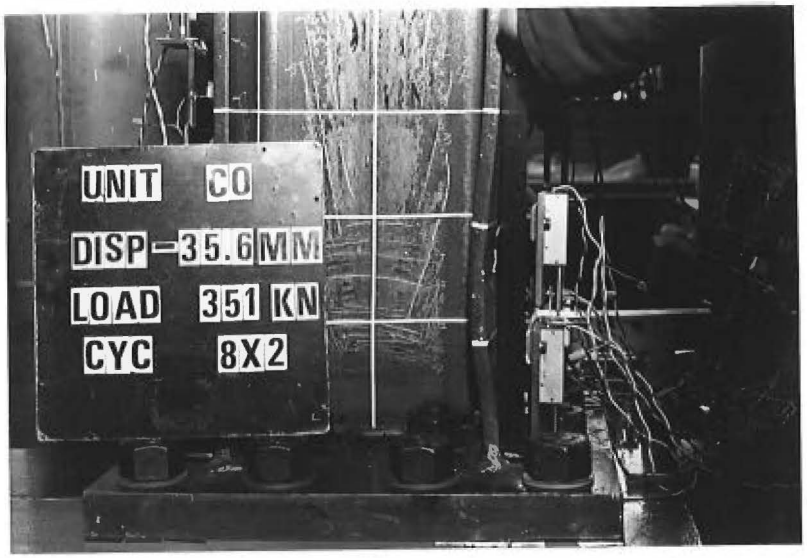

Figure 7.14.3. Flaking off of Millscale - Cycle 8x2

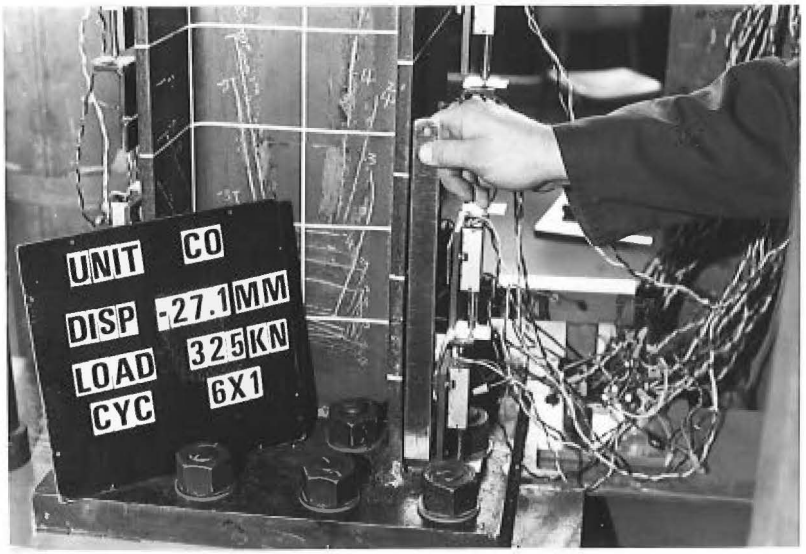

Figure 7.14.4. Column CO Flange Buckling - Cycle 6x1

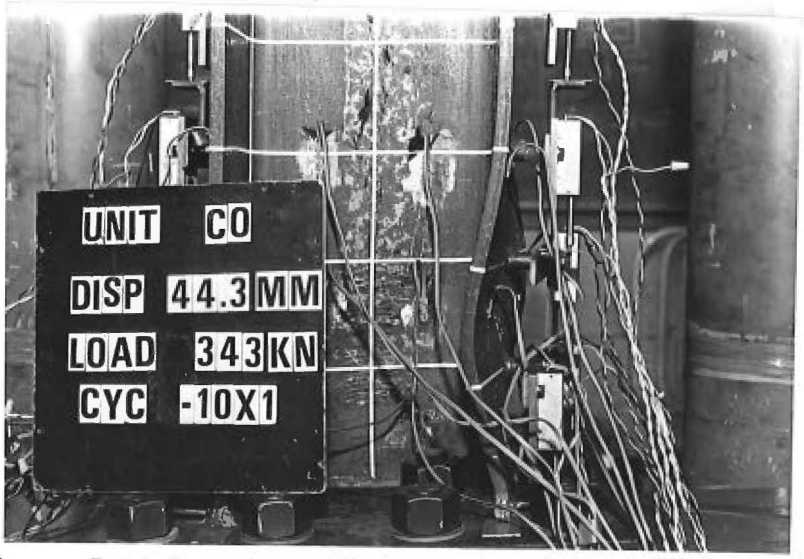

Figure 7.14.5. Column CO Flange Buckling - Cycle -10x1

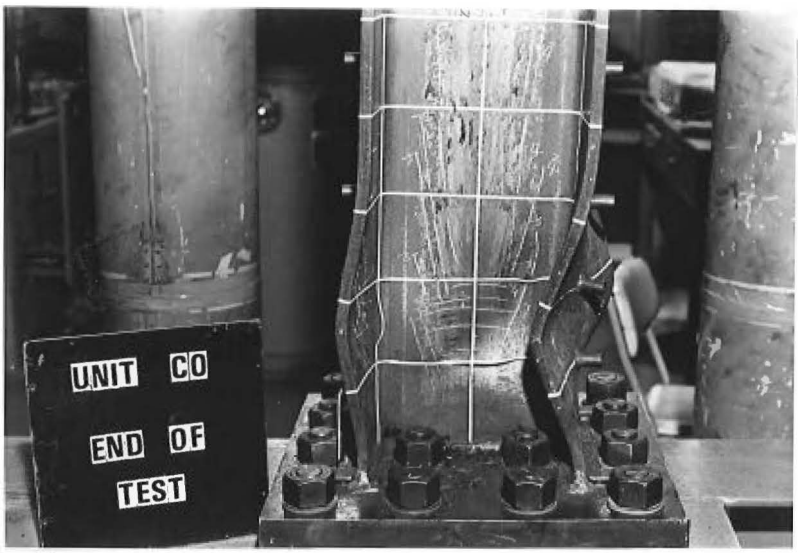

Figure 7.14.6. Column CO Flange Buckling - End of Test

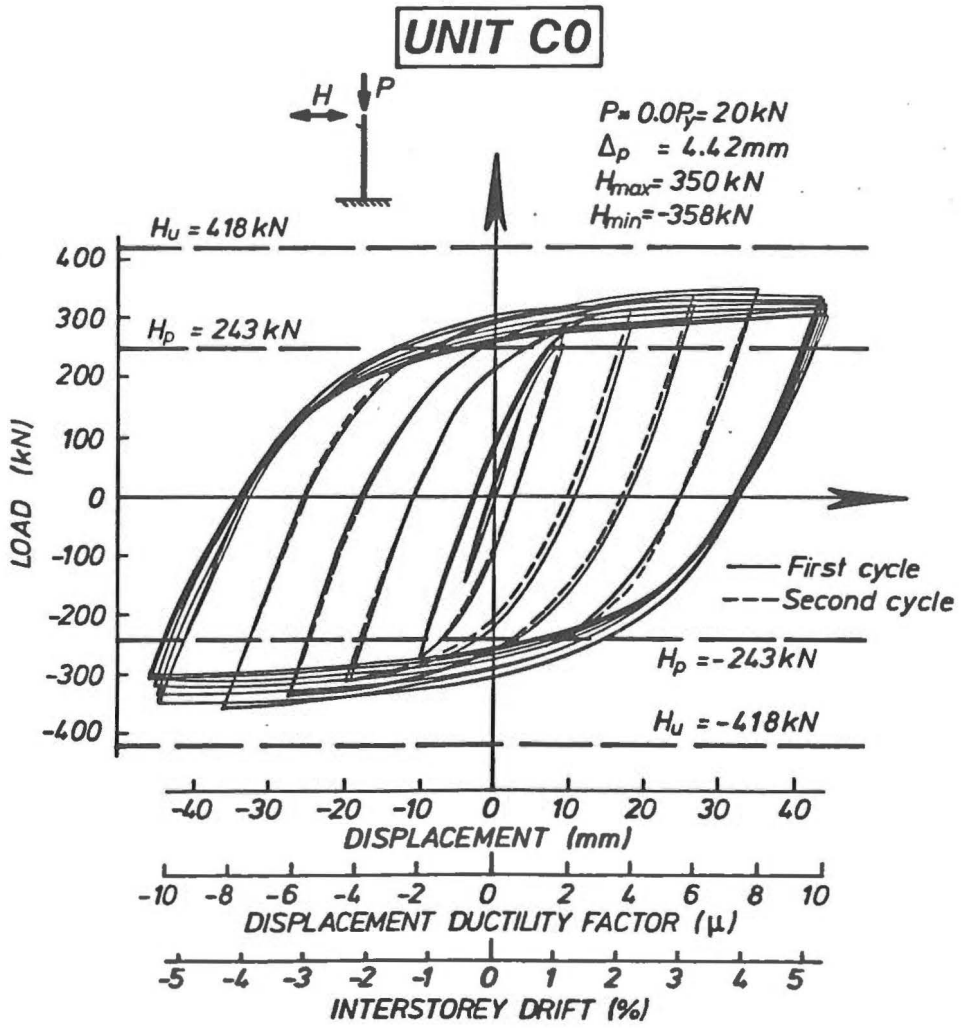

Figure 7.14.7. Column CO Lateral Load - Displacement Hysteresis

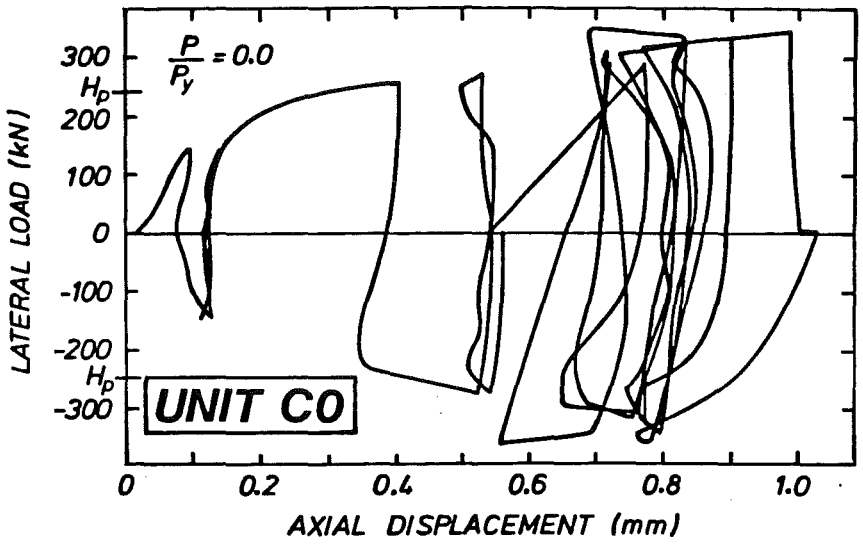

Figure 7.14.8. Column CO Horizontal Load - Axial Displacement

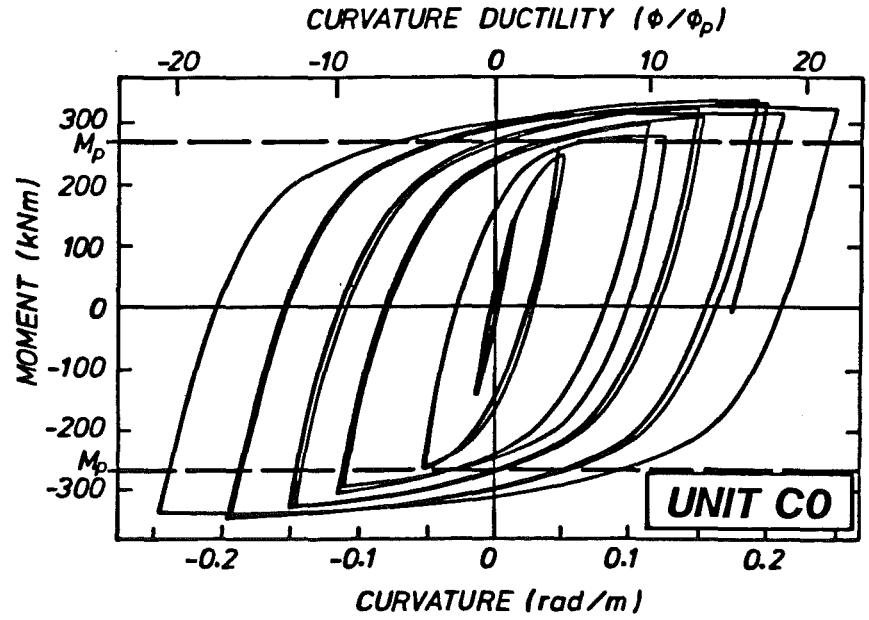

Figure 7.14.9. Column CO Moment - Curvature Hysteresis

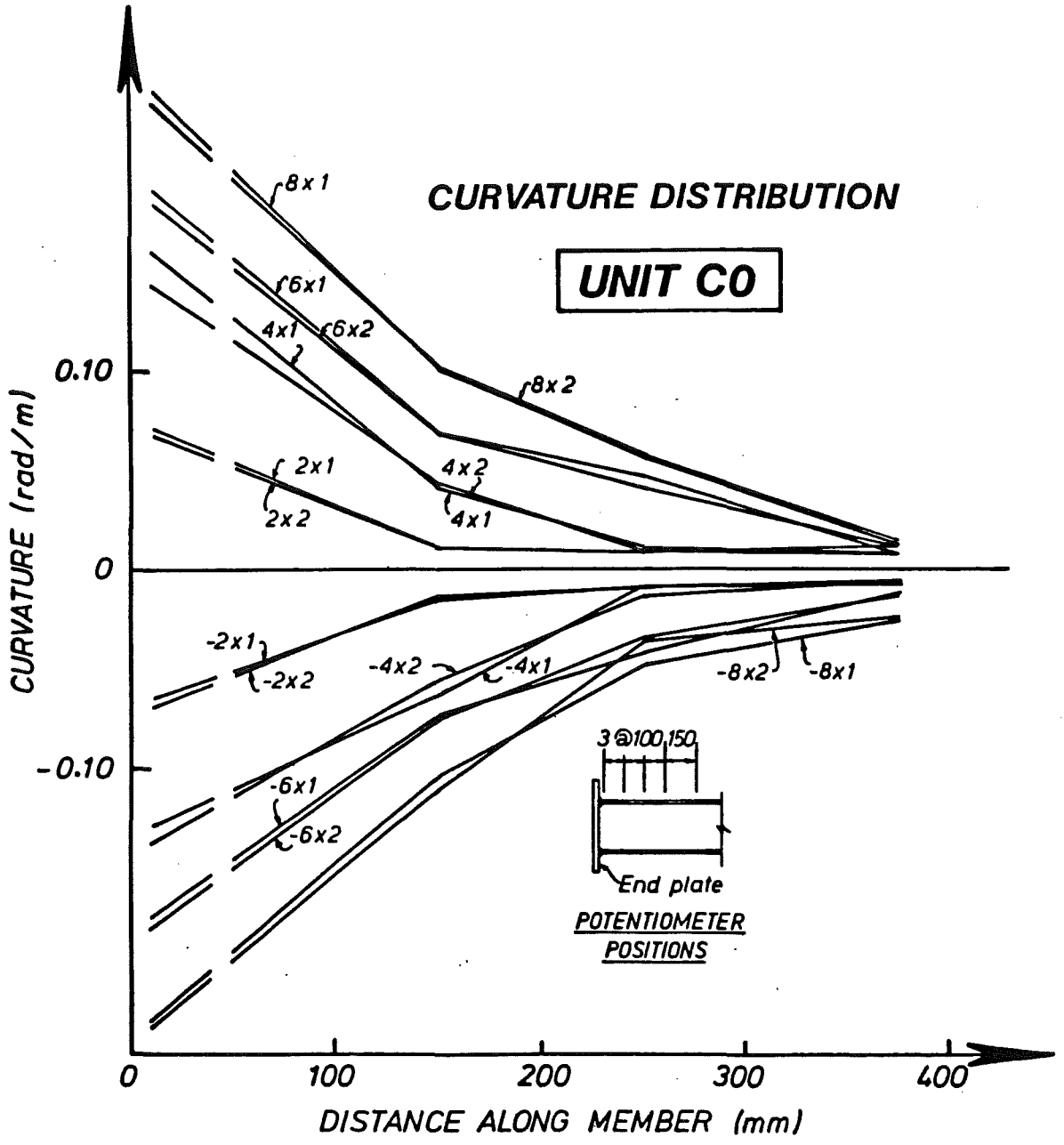

Figure 7.14.10. Column CO Curvature Distribution

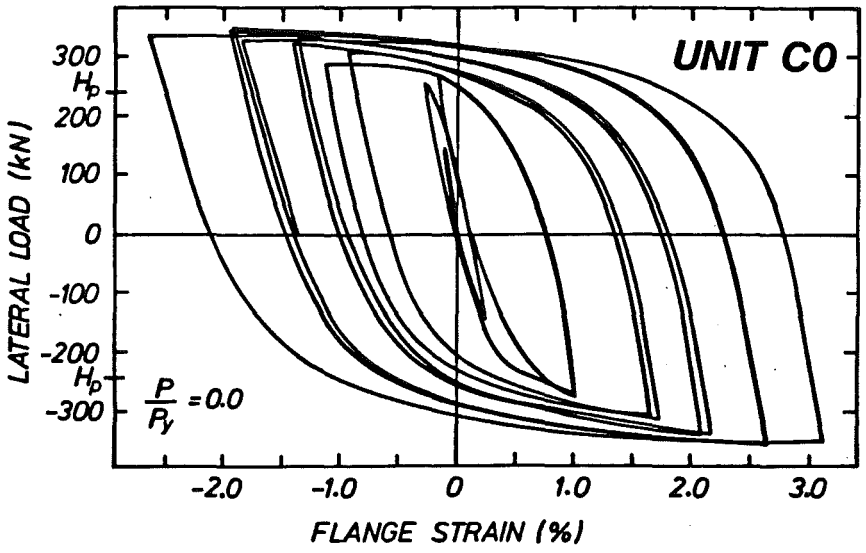

Figure 7.14.11. Column C0 Lateral Load - Flange Strain

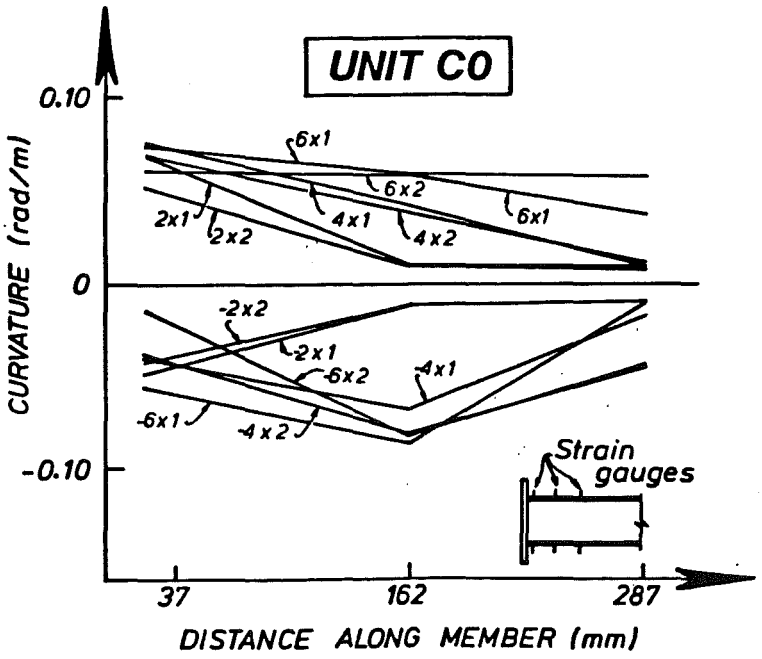

Figure 7.14.12. Column C0 Curvature Distribution from Strain Gauges

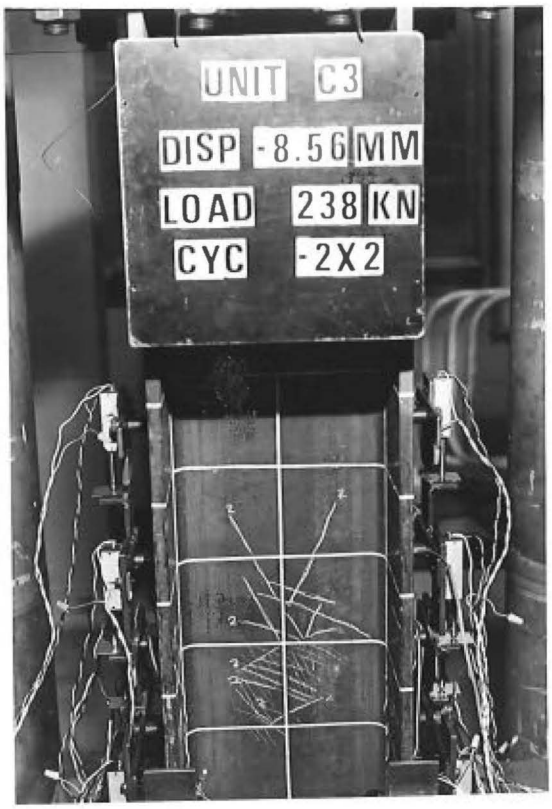

Figure 7.15.1. Column C3 Web Yield Lines - Cycle -2x2

Figure 7.15.2. Column C3 Flange Yield Lines - Cycle 4x1

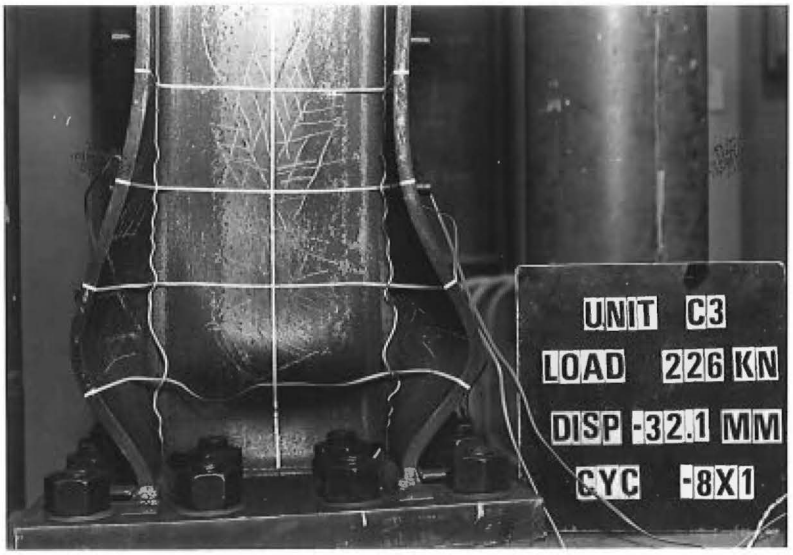

Figure 7.15.3. Column C3 Buckling - Cycle -8x1

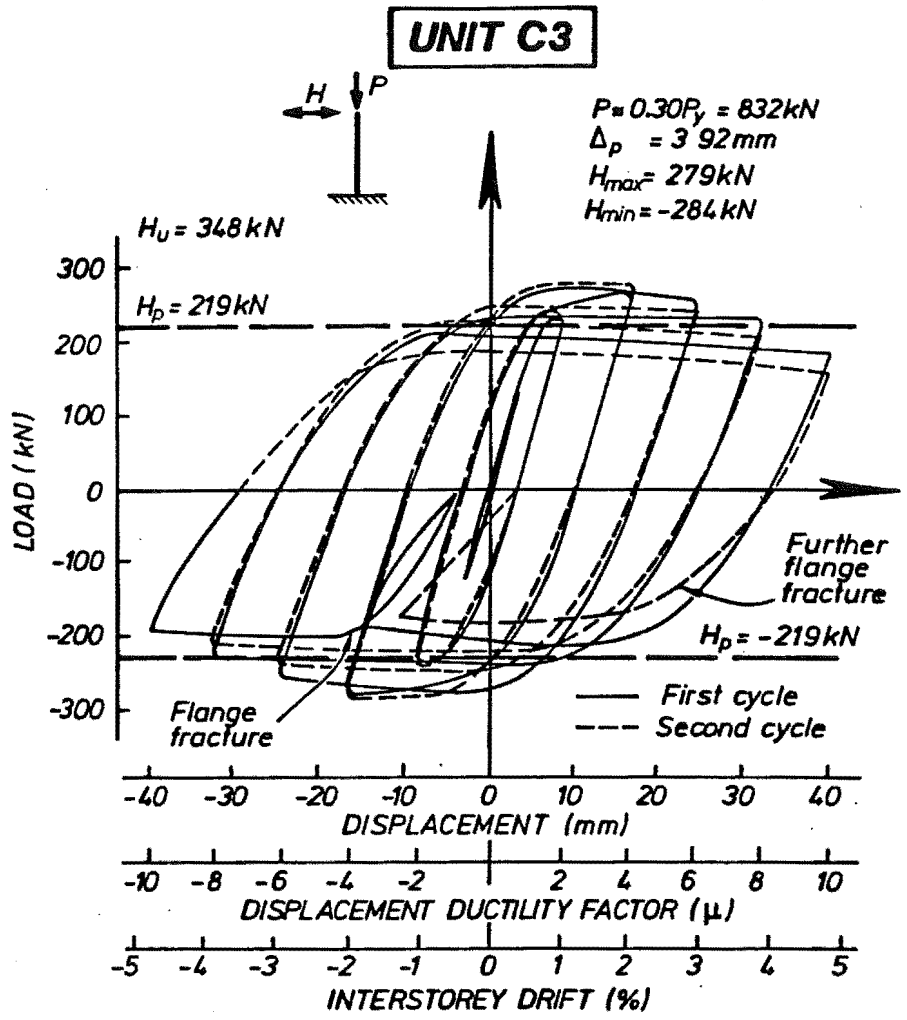

Figure 7.15.4. Column C3 Lateral Load - Displacement Hysteresis

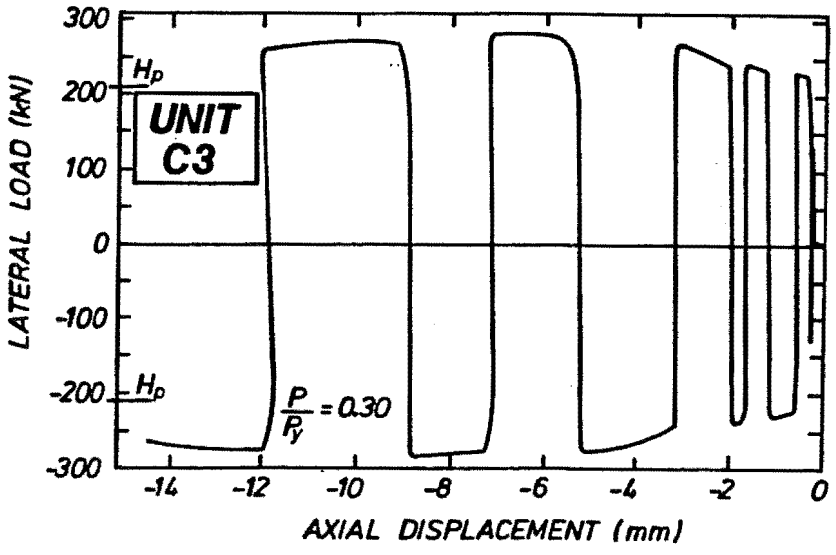

Figure 7.15.5. Column C3 Horizontal Load - Axial Displacement

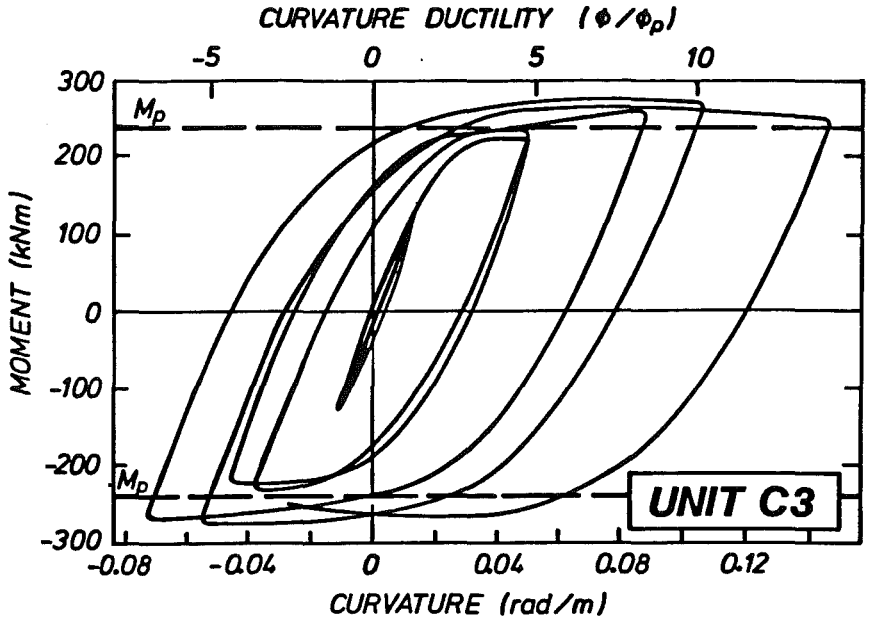

Figure 7.15.6. Column C3 Moment - Curvature Hysteresis

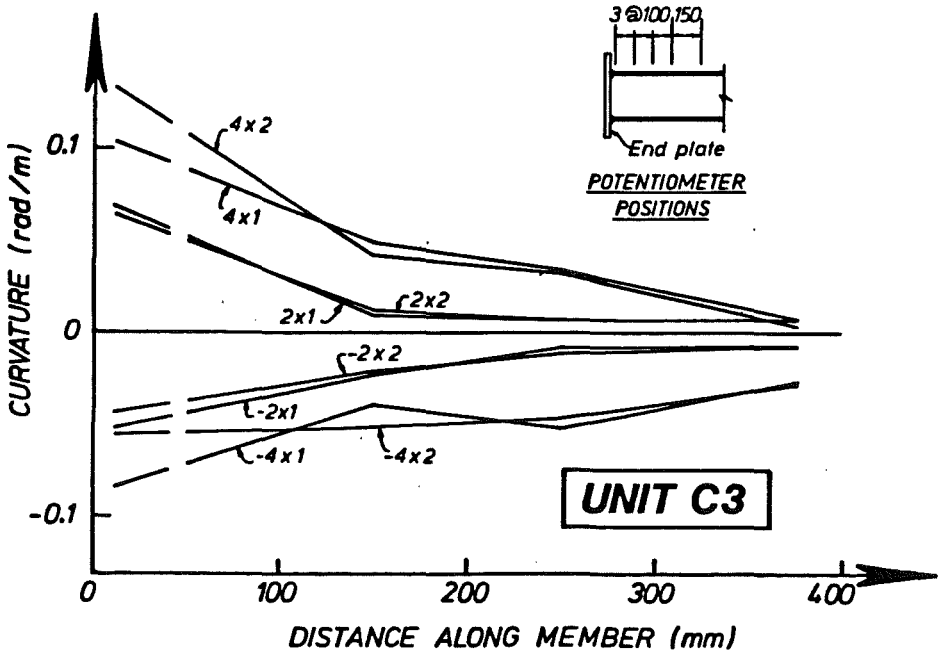

Figure 7.15.7. Column C3 Curvature Distribution

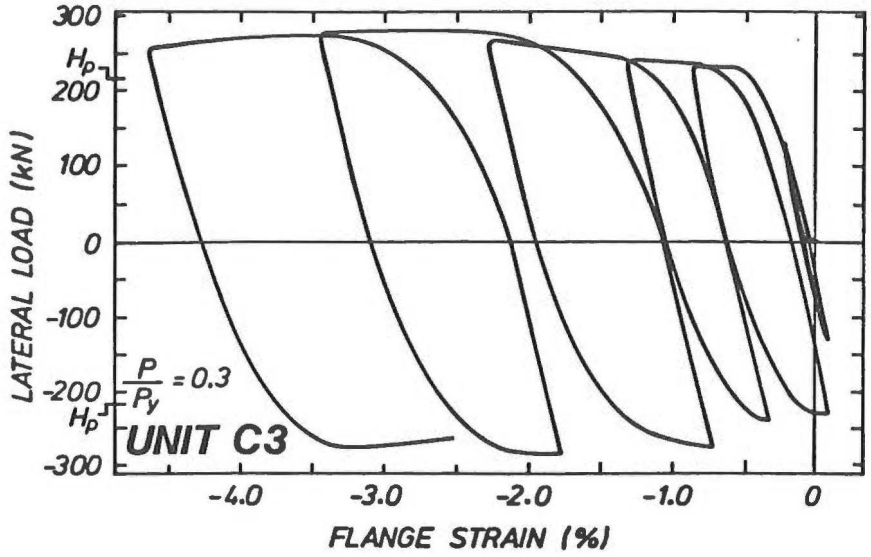

Figure 7.15.8. Column C3 Lateral Load - Flange Strain

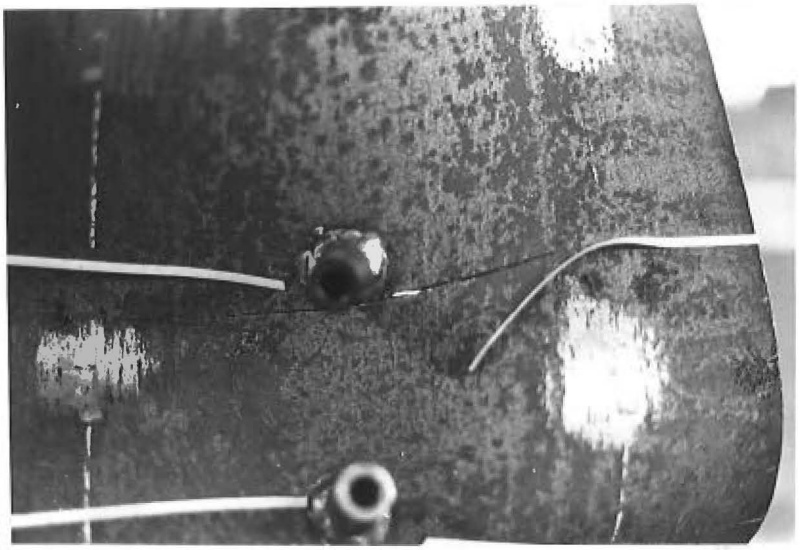

Figure 7.15.9. Column C3 Fracture

Figure 7.15.10. Column C3 Fracture

Figure 7.15.11. Column C3 Yield Lines near Top of Specimen

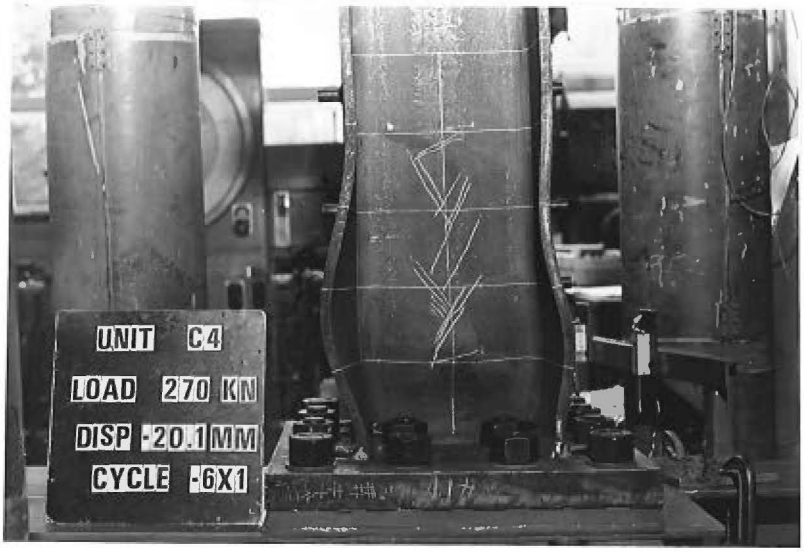

Figure 7.16.1. Column C4 Buckling - Cycle -6x1

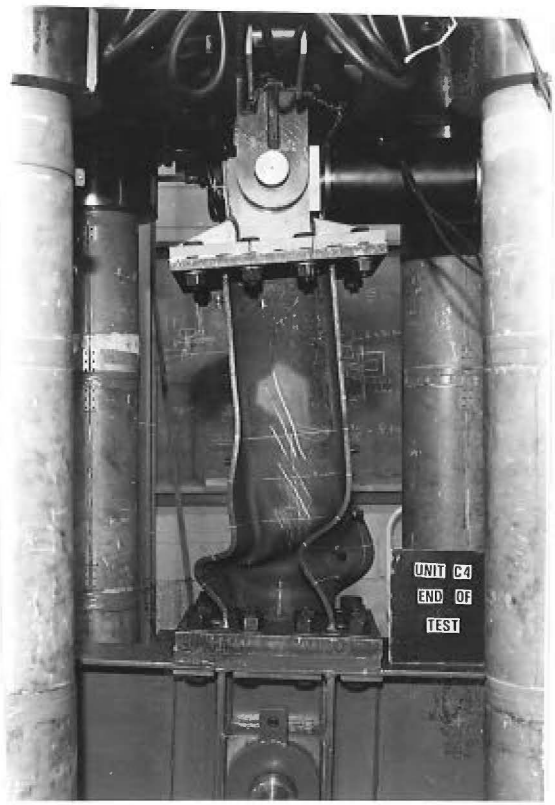

Figure 7.16.2. Column C4 Buckling - End of Test

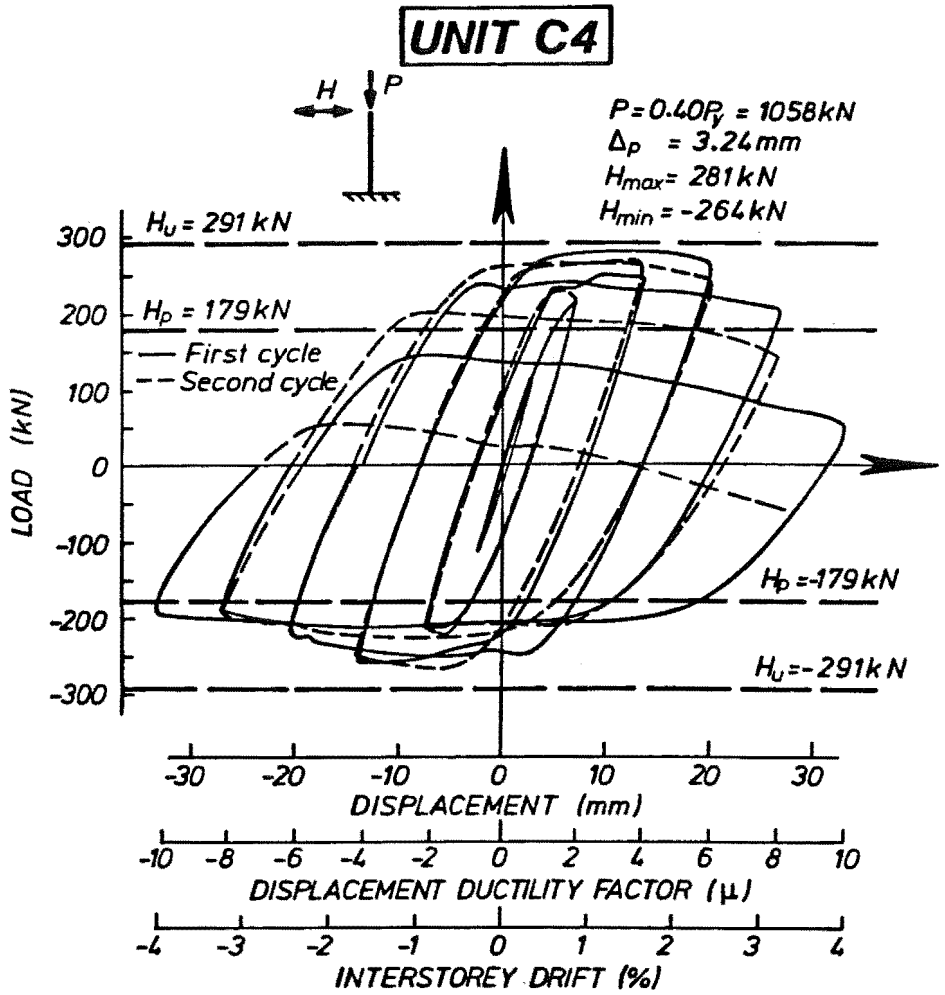

Figure 7.16.3. Column C4 Lateral Load - Displacement Hysteresis

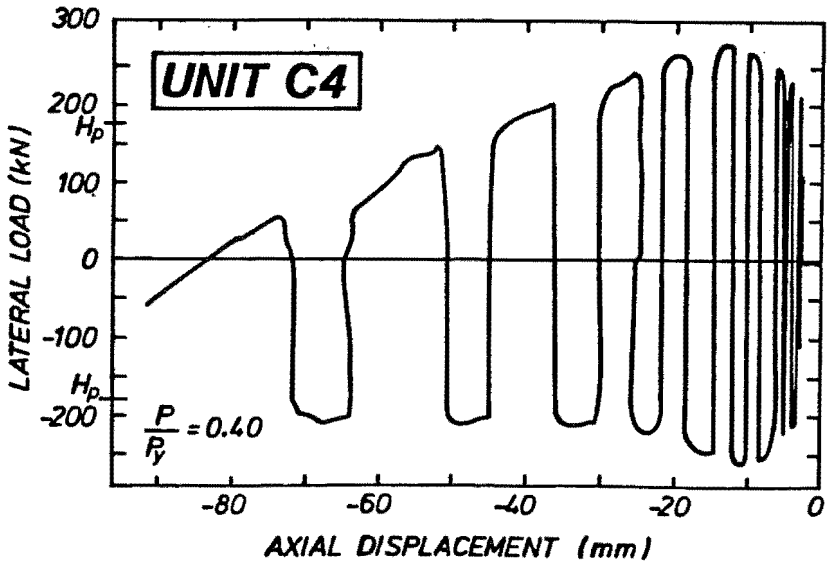

Figure 7.16.4. Column C4 Horizontal Load - Axial Displacement

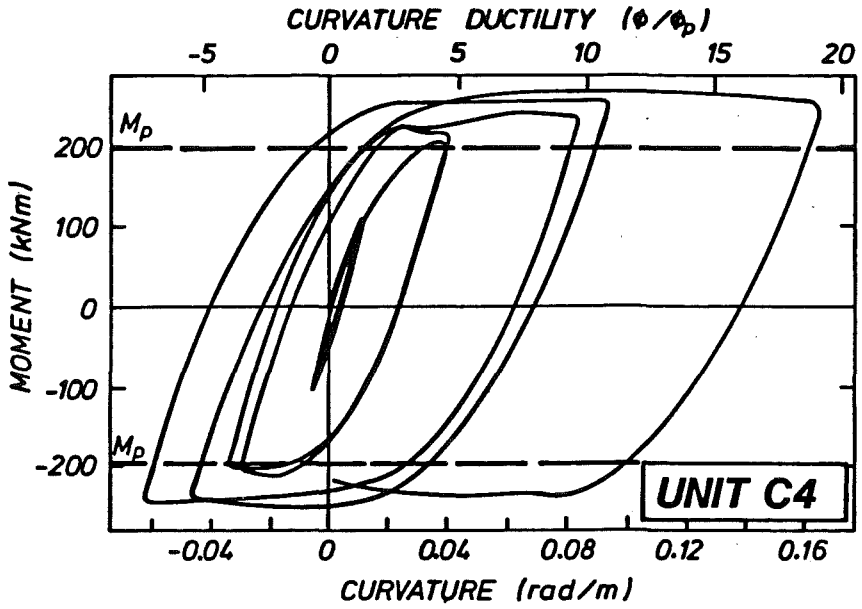

Figure 7.16.5. Column C4 Moment - Curvature Hysteresis

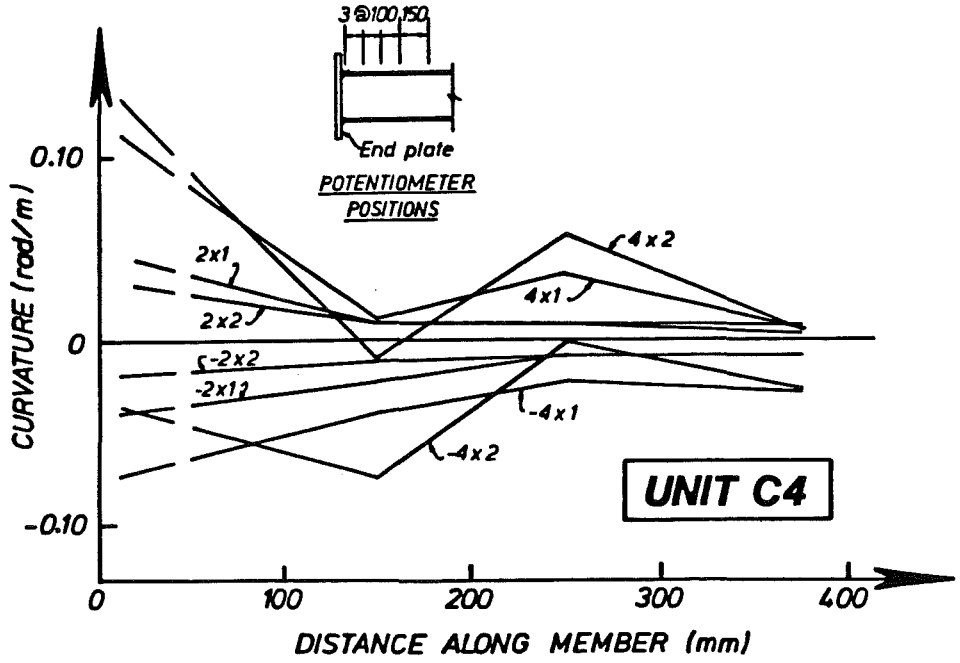

Figure 7.16.6. Column C4 Curvature Distribution

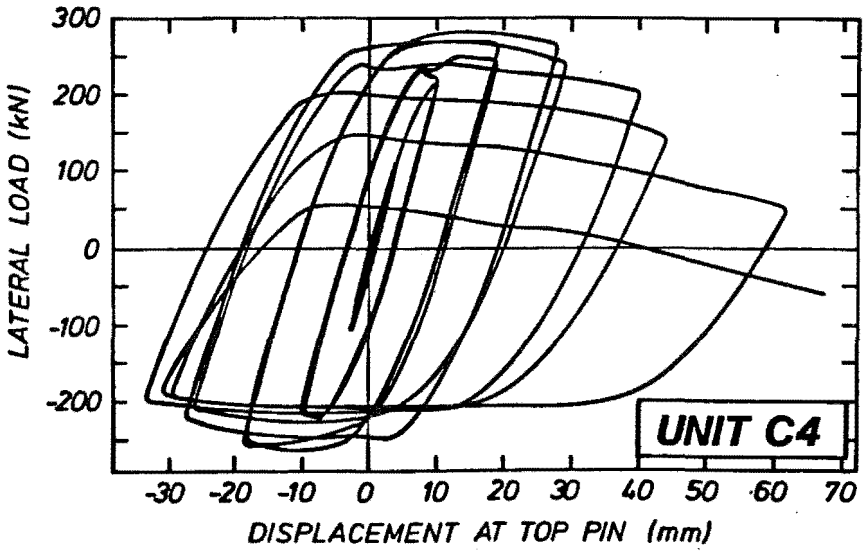

Figure 7.16.7. Column C4 Horizontal Load - Axial Displacement at Pin

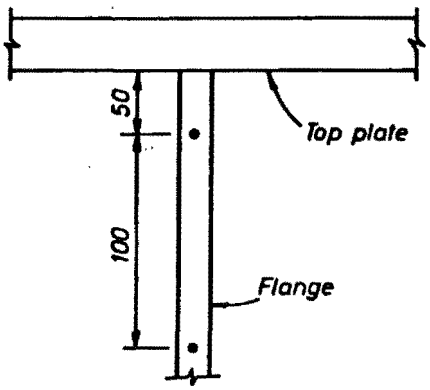

Figure 7.17.1. Positions of Steel Balls for Strain Measurement

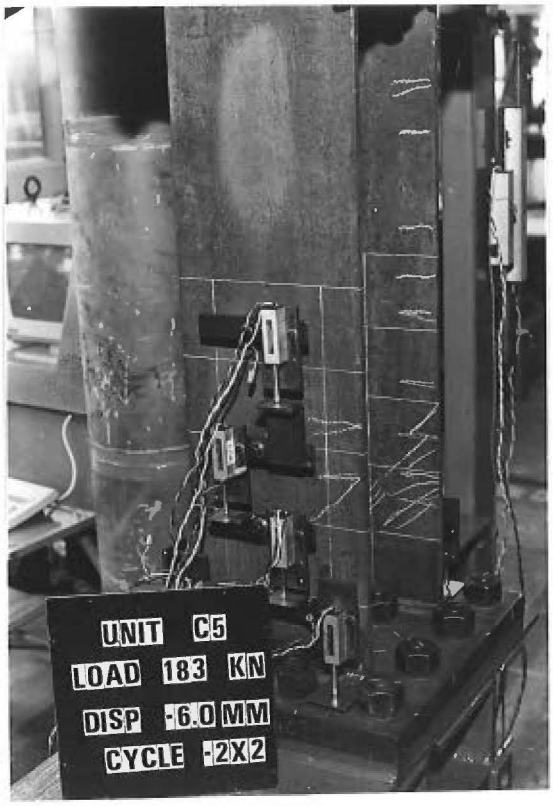

Figure 7.17.2. Column C5 Flange Yield Lines - Cycle -2x2

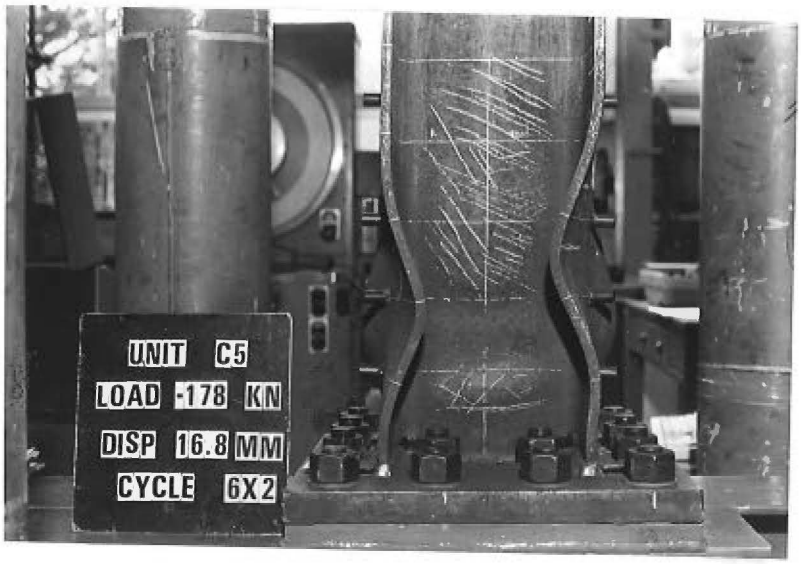

Figure 7.17.3. Column C5 Buckling - Cycle 6x2

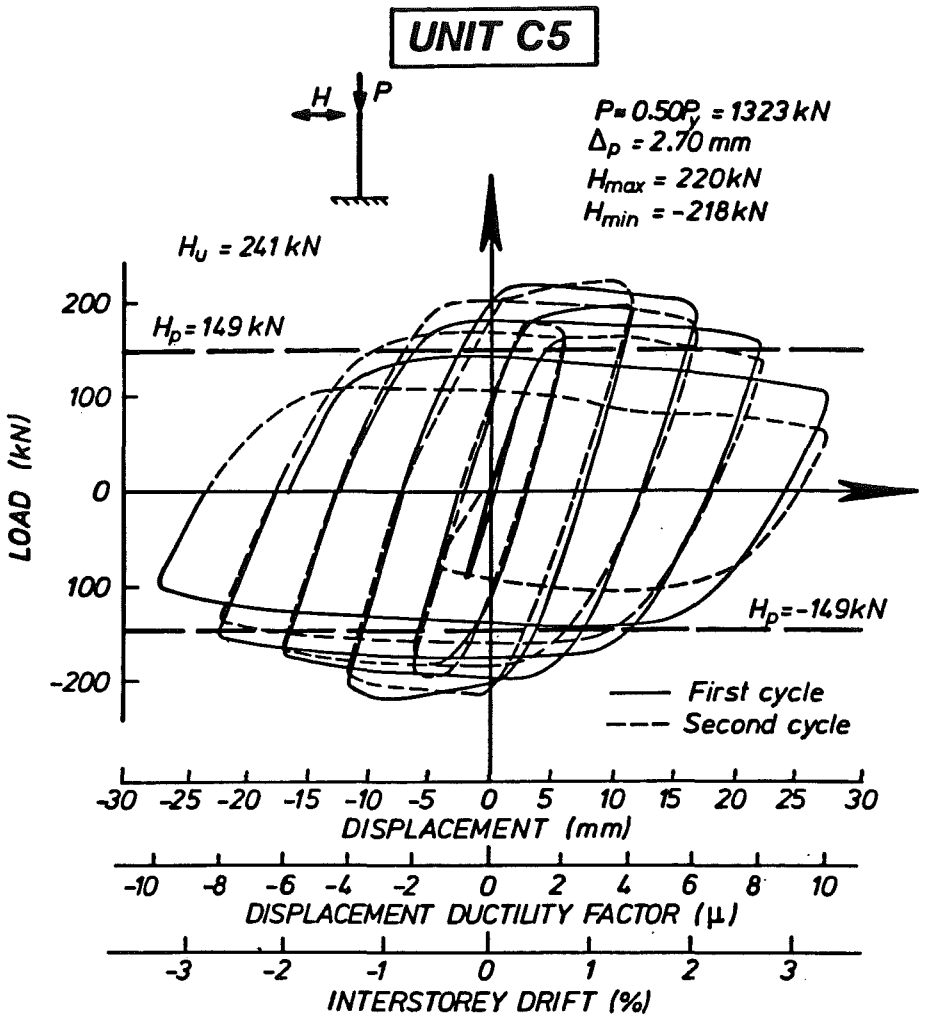

Figure 7.17.4. Column C5 Lateral Load - Displacement Hysteresis

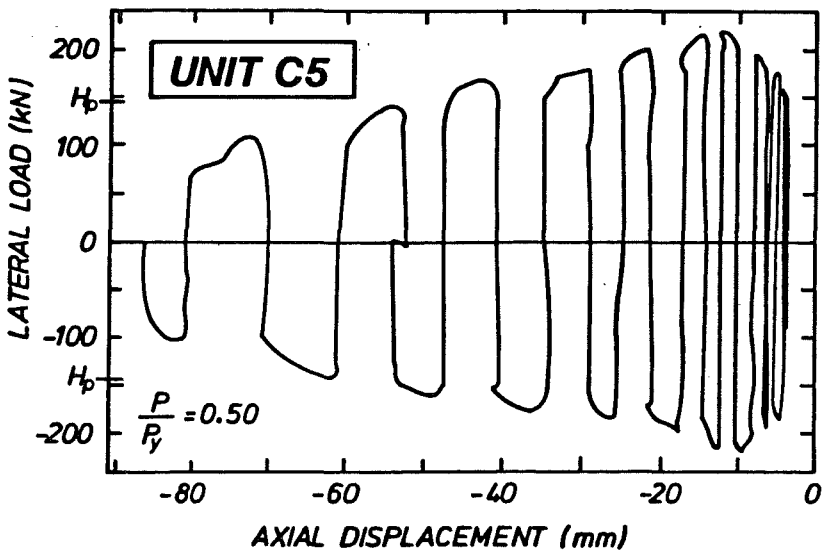

Figure 7.17.5. Column C5 Horizontal Load - Axial Displacement

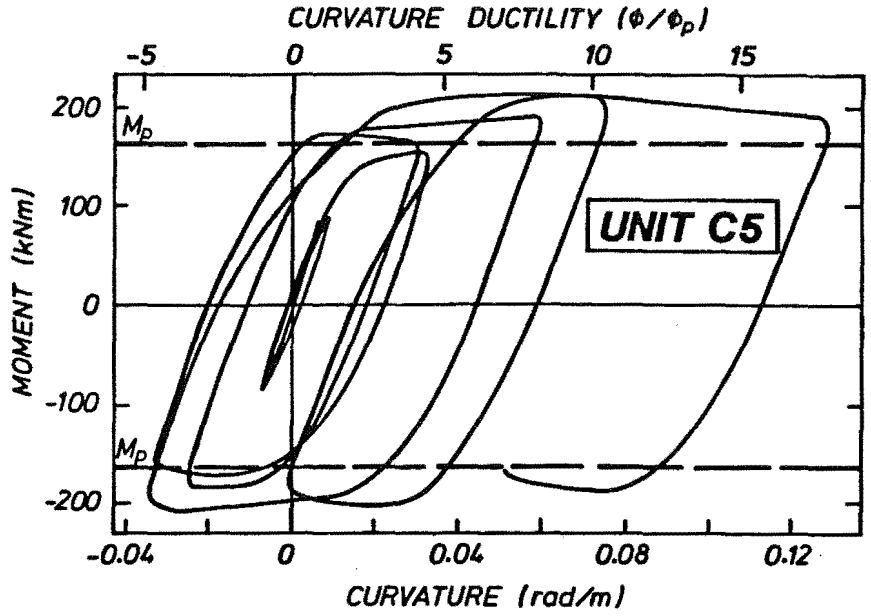

Figure 7.17.6. Column C5 Moment - Curvature Hysteresis

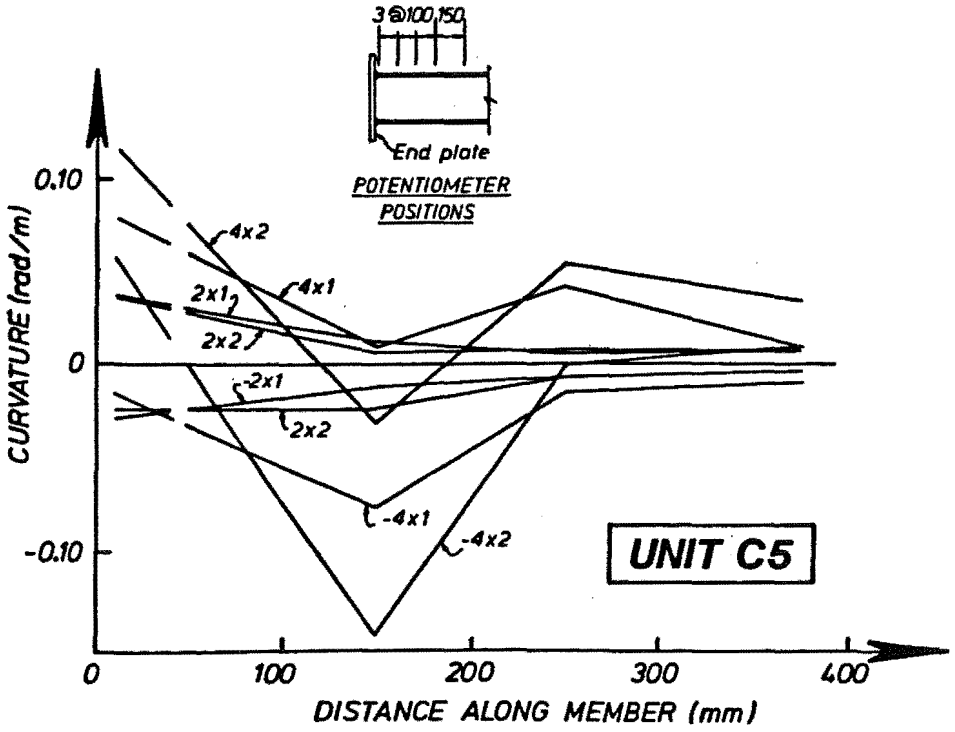

Figure 7.17.7. Column C5 Curvature Distribution

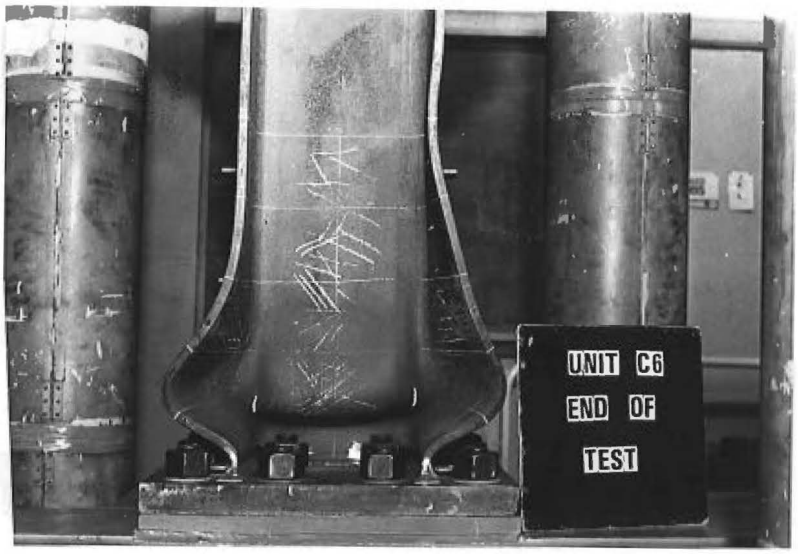

Figure 7.18.1. Column C6 Buckling and Web Fracture - End of Test

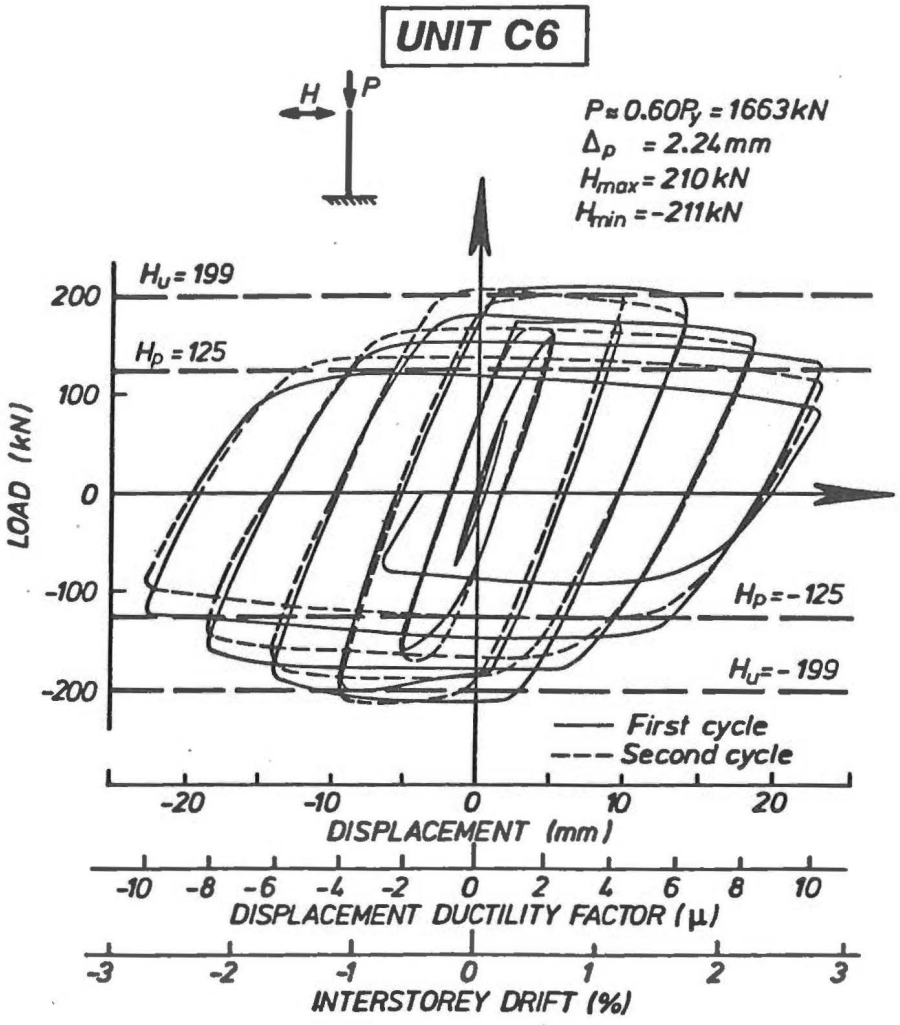

Figure 7.18.2. Column C6 Lateral Load - Displacement Hysteresis

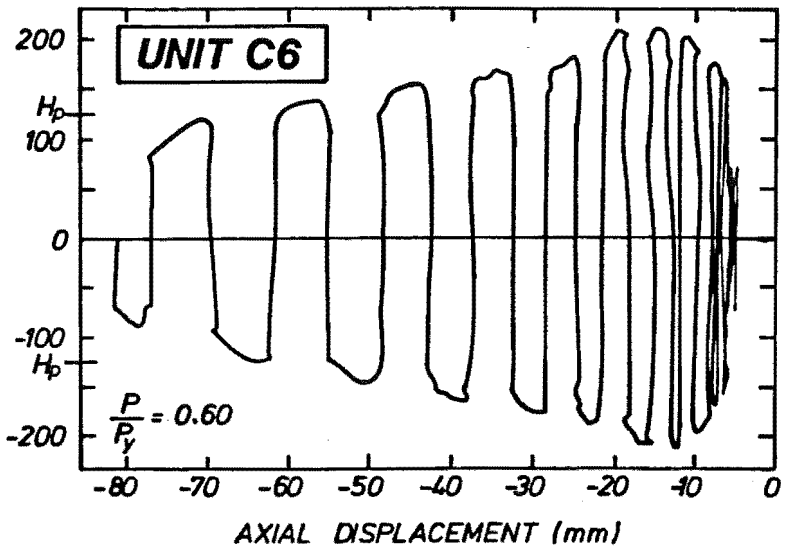

Figure 7.18.3. Column C6 Horizontal Load - Axial Displacement

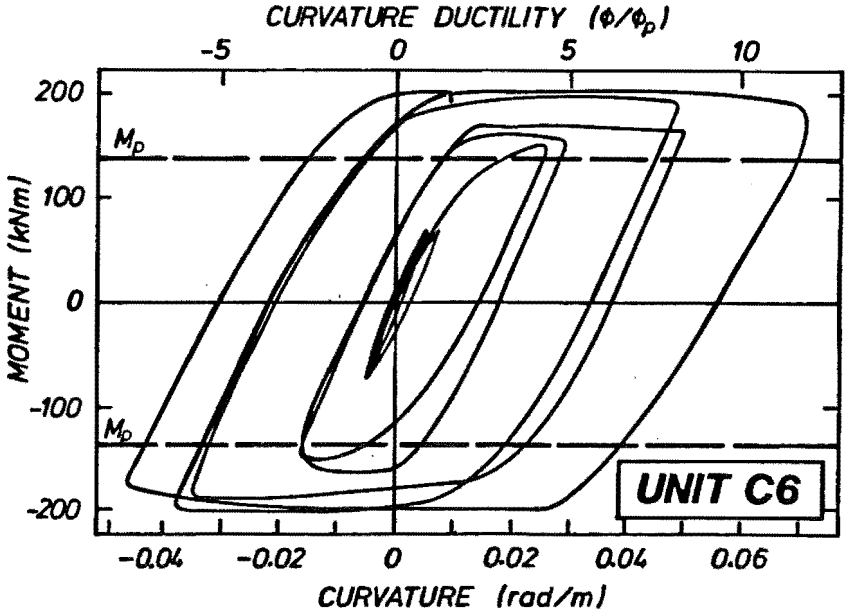

Figure 7.18.4. Column C6 Moment - Curvature Hysteresis

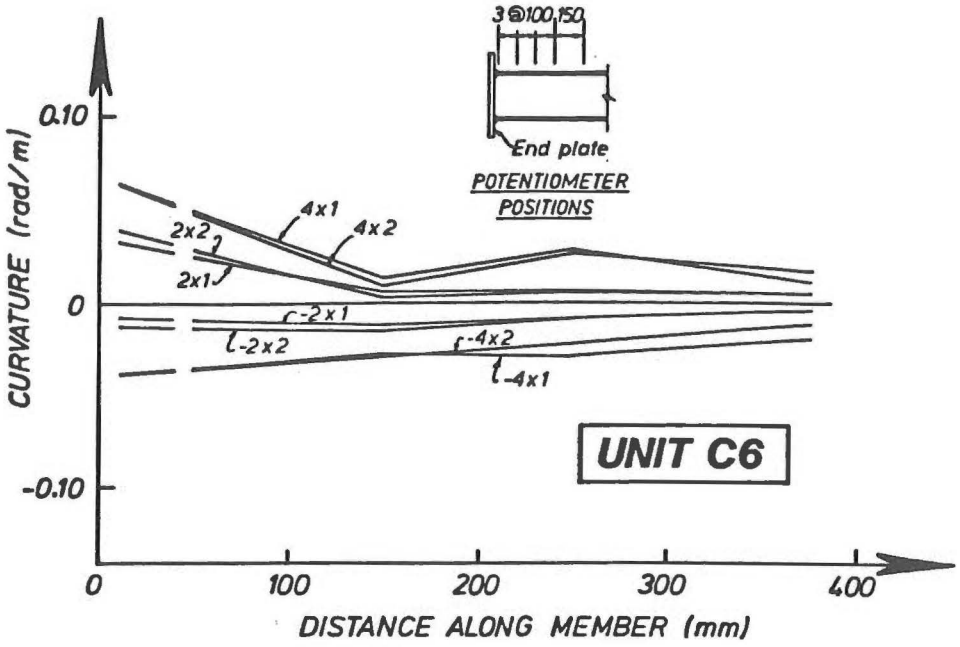

Figure 7.18.5. Column C6 Curvature Distribution

Figure 7.18.6. Column C6 Deformation about Weak Axis - End of Test

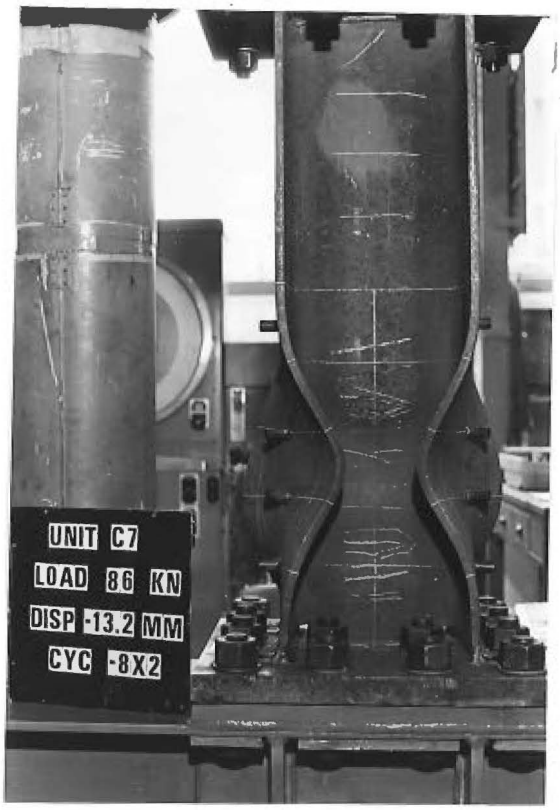

Figure 7.19.1. Column C7 Buckling - Cycle -8x2

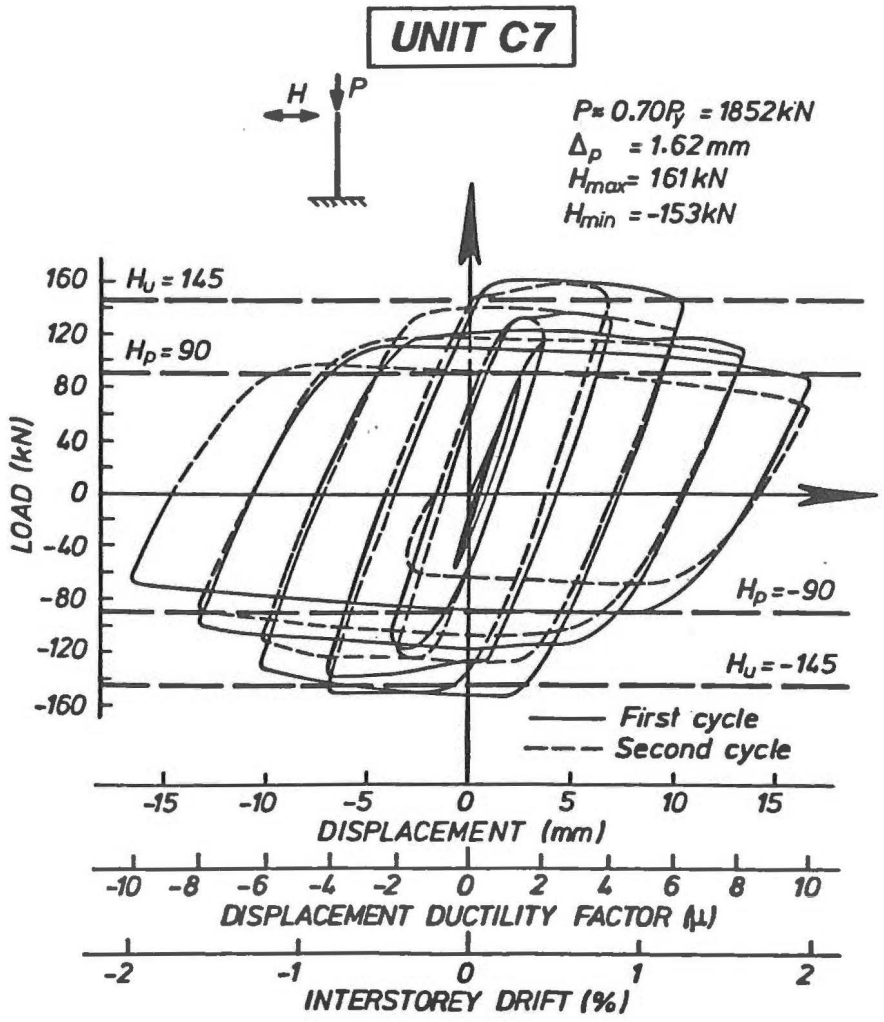

Figure 7.19.2. Column C7 Lateral Load - Displacement Hysteresis

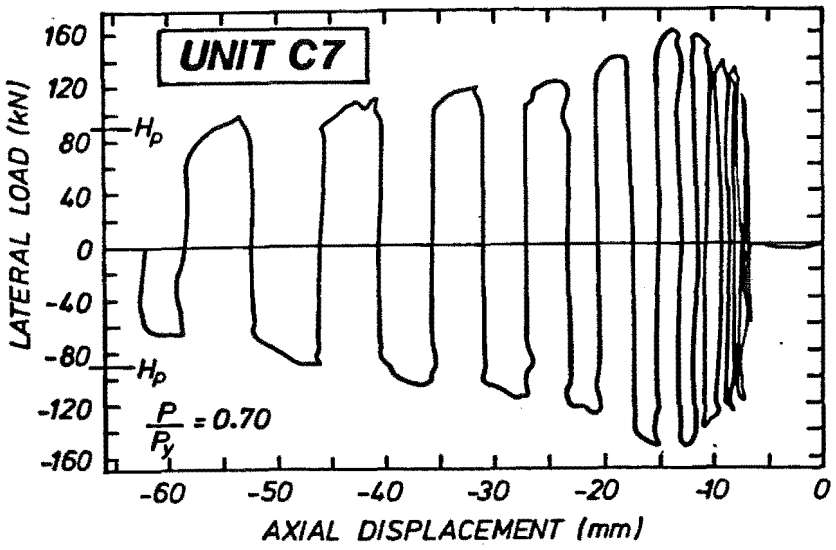

Figure 7.19.3. Column C7 Horizontal Load - Axial Displacement

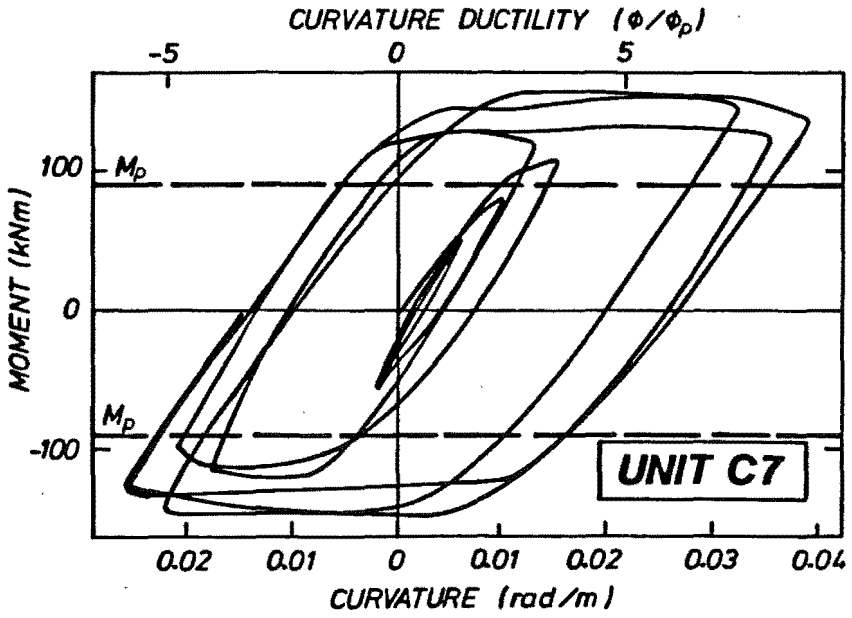

Figure 7.19.4. Column C7 Moment - Curvature Hysteresis

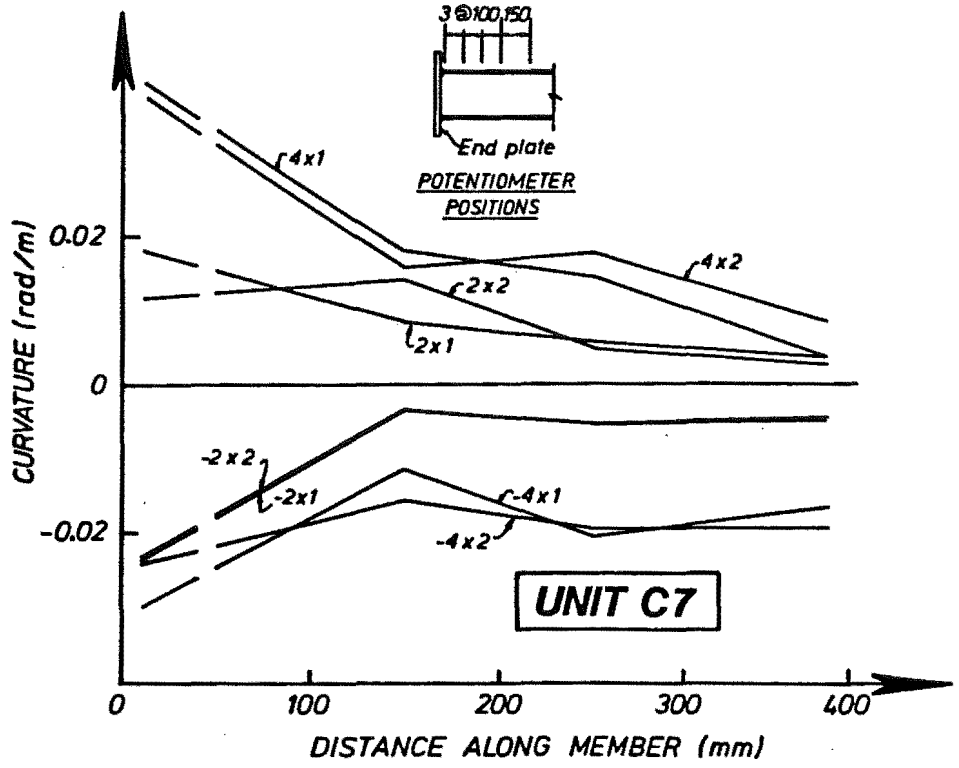

Figure 7.19.5. Column C7 Curvature Distribution

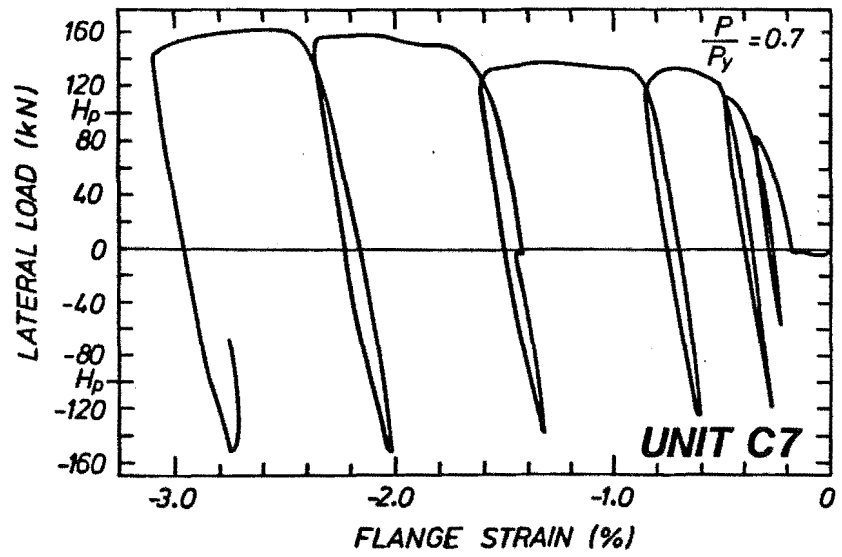

Figure 7.19.6. Column C7 Lateral Load - Flange Strain

Figure 7.20.1. Column C8 Web Yield Lines - Cycle -6x2

Figure 7.20.2. Column C8 Buckling - Cycle -10x2

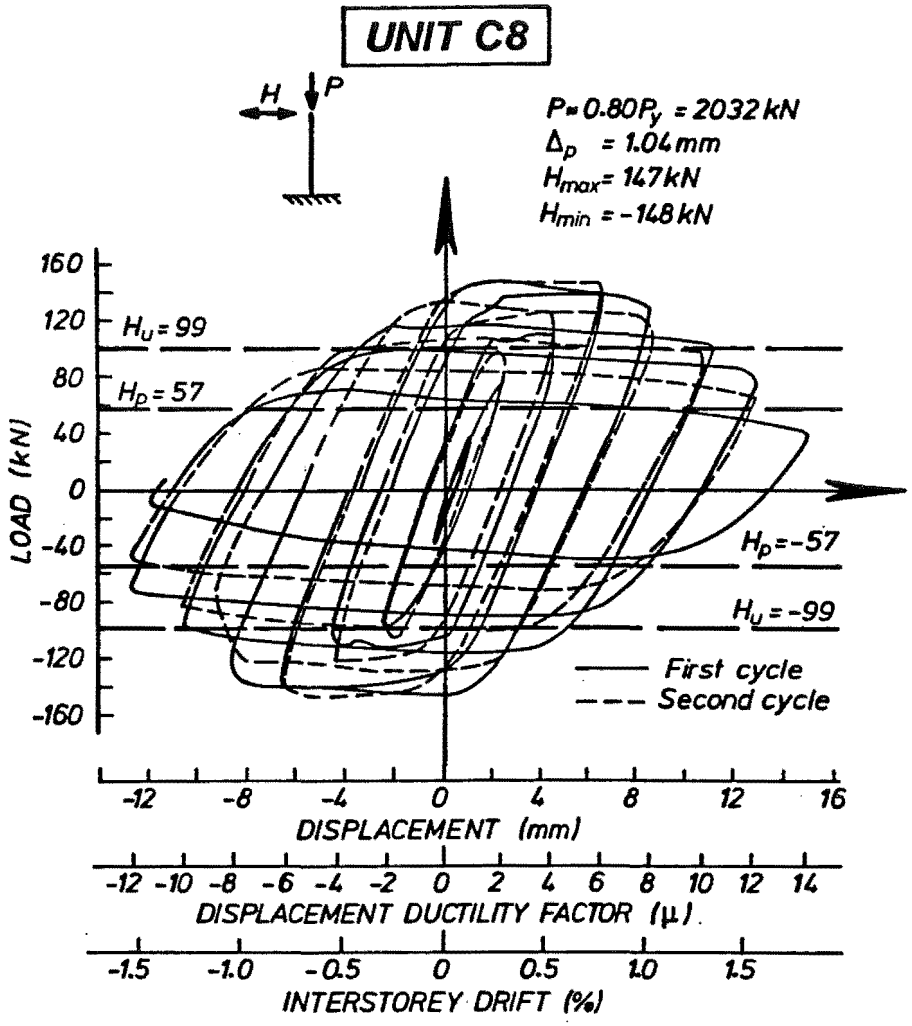

Figure 7.20.3. Column C8 Lateral Load - Displacement Hysteresis

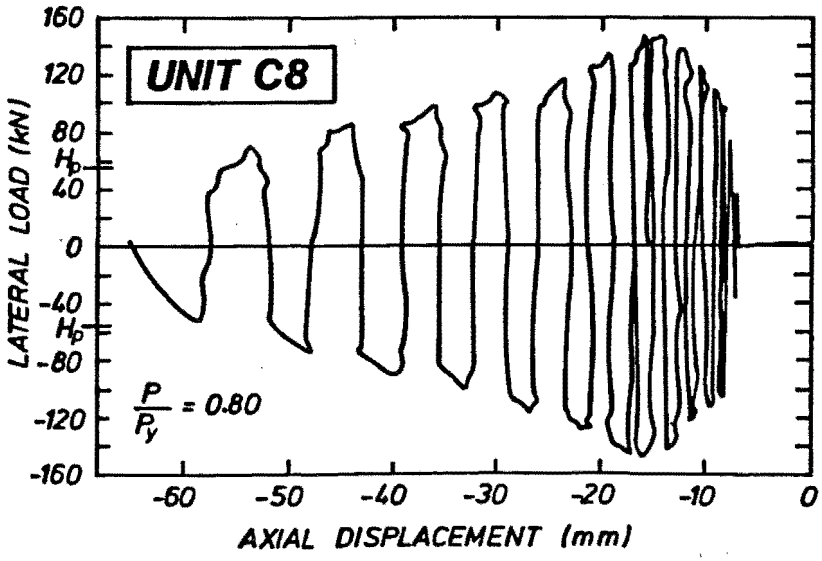

Figure 7.20.4. Column C8 Horizontal Load - Axial Displacement

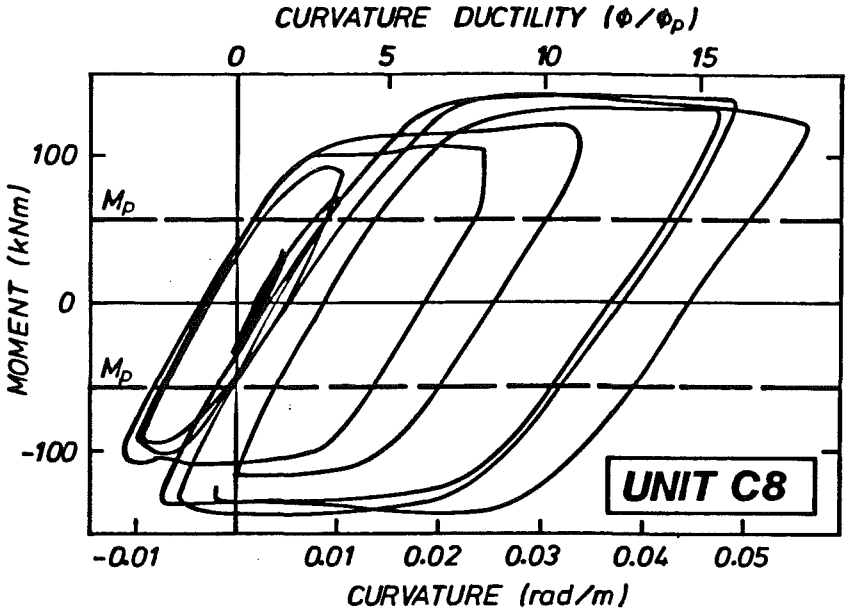

Figure 7.20.5. Column C8 Moment - Curvature Hysteresis

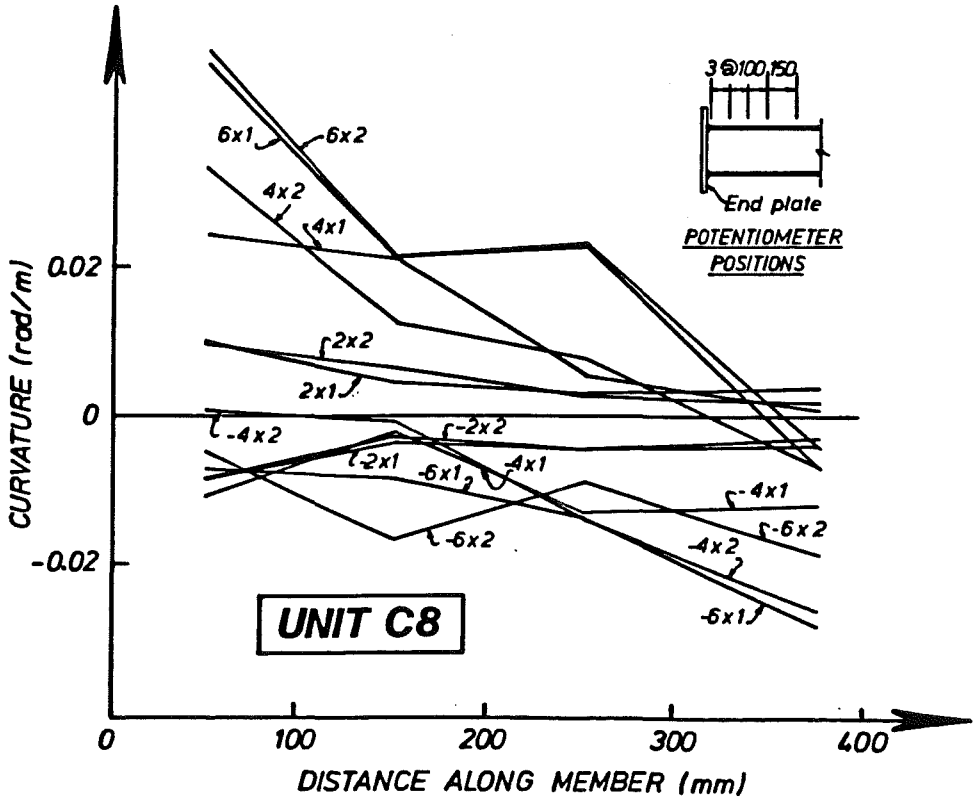

Figure 7.20.6. Column C8 Curvature Distribution

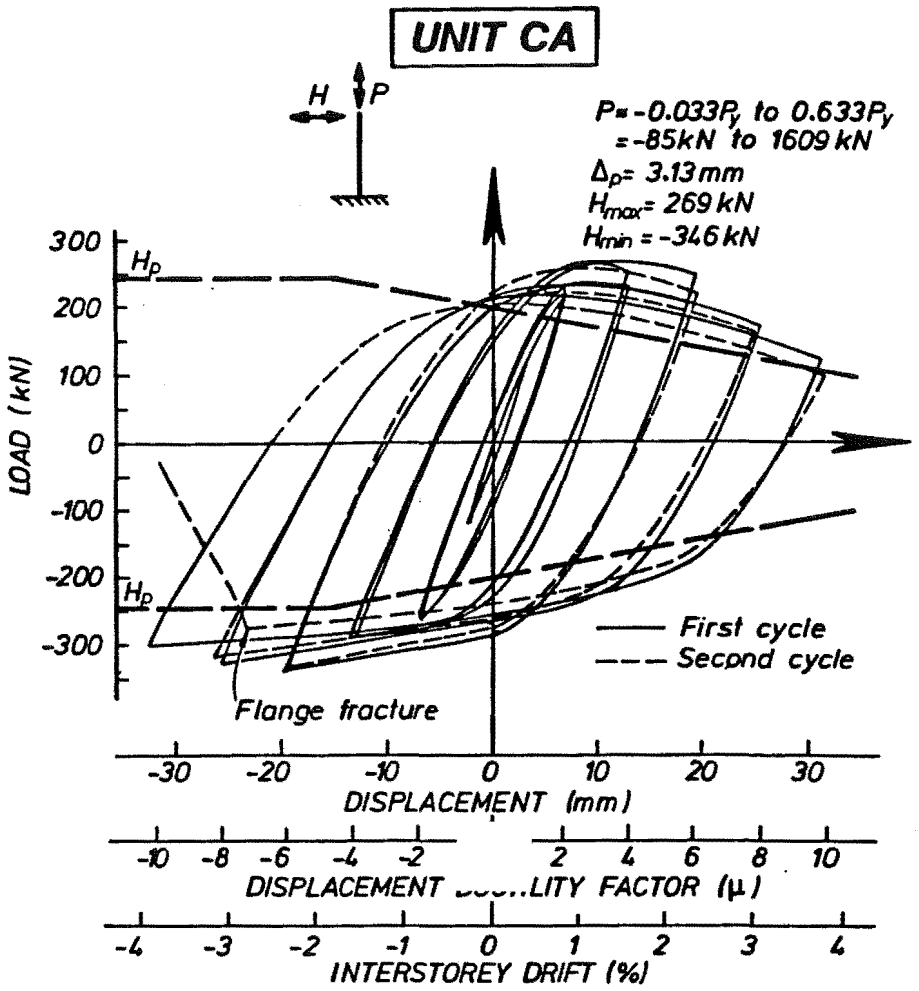

Figure 7.21.1. Column CA Lateral Load - Displacement Hysteresis

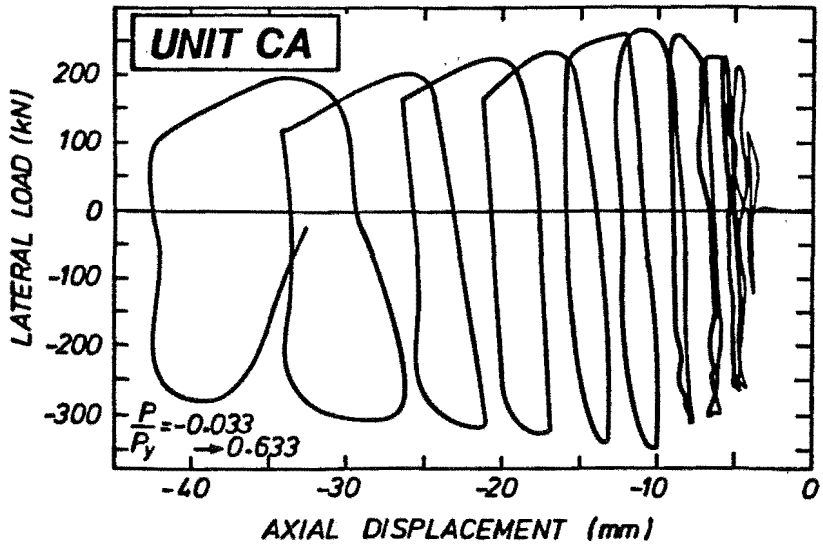

Figure 7.21.2. Column CA Horizontal Load - Axial Displacement

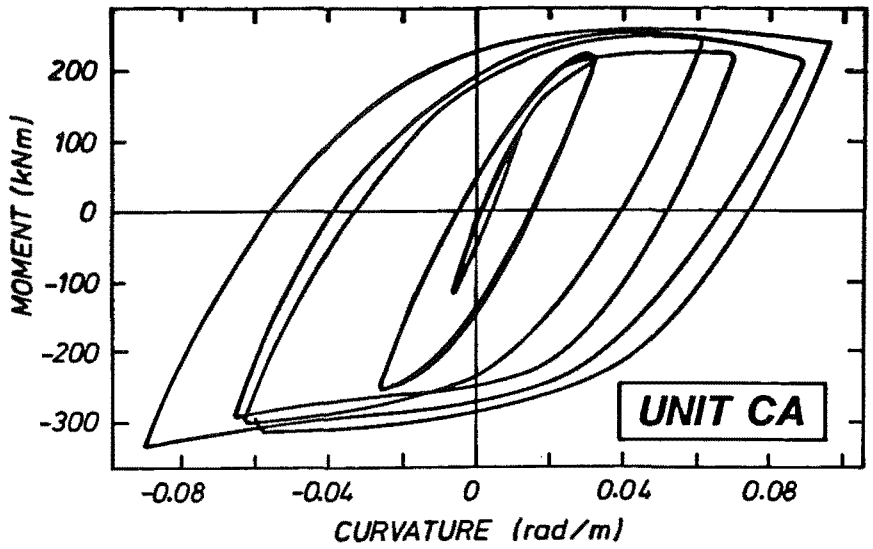

Figure 7.21.3. Column CA Moment - Curvature Hysteresis

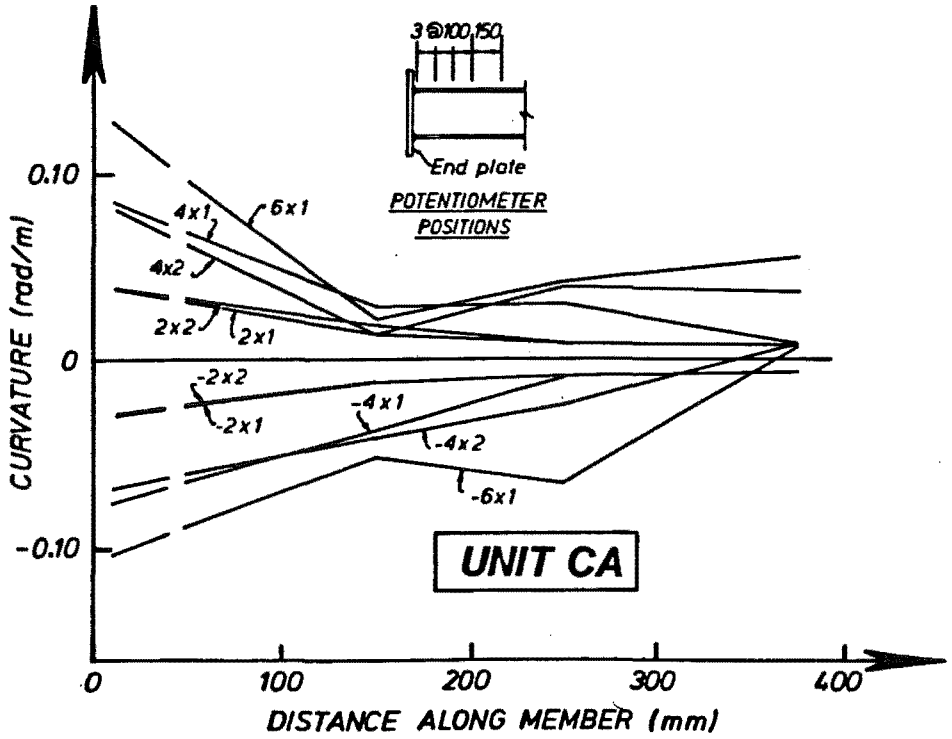

Figure 7.21.4. Column CA Curvature Distribution

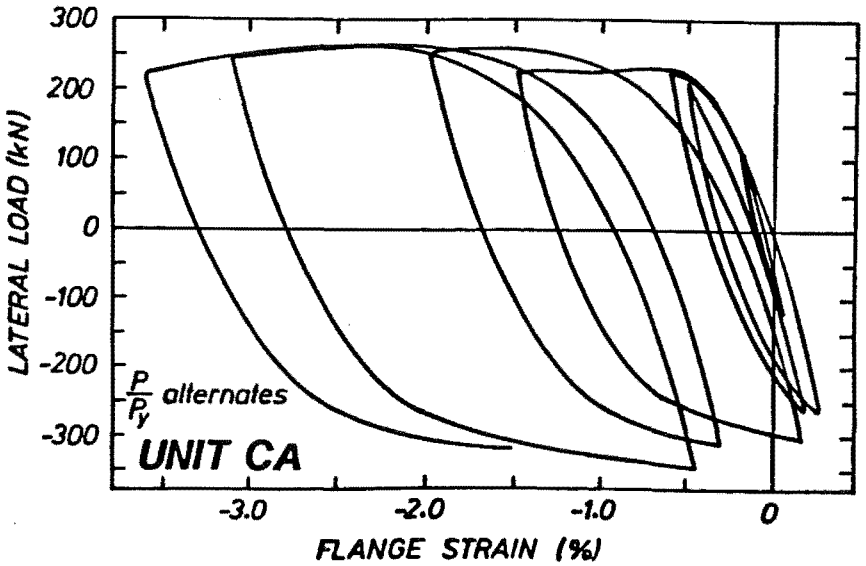

Figure 7.21.5. Column CA Lateral Load - Flange Strain

Figure 7.21.7. Column CA Fracture

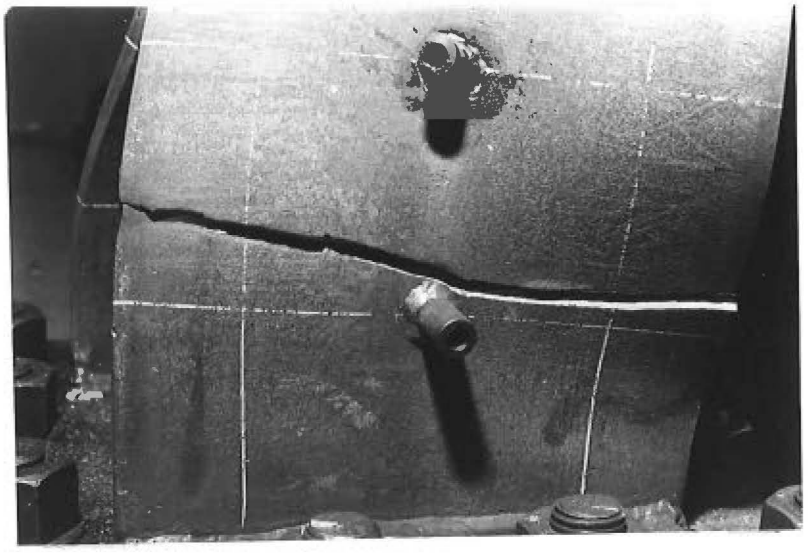

Figure 7.21.8. Column CA Fracture

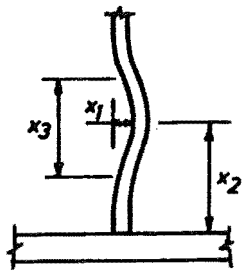

Figure 7.22. Measurement of Buckling

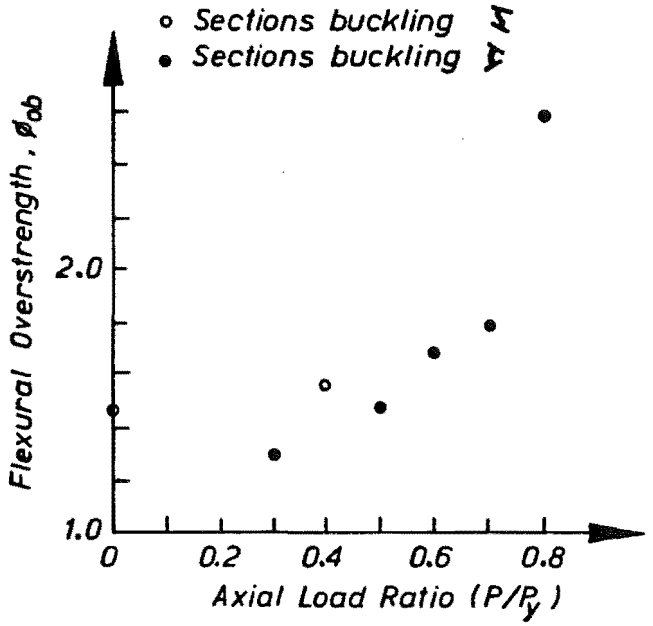

Figure 7.23. Flexural Overstrength of Members

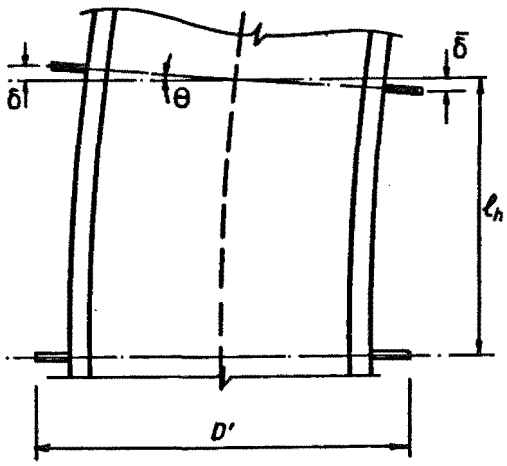

Figure 7.24. Measurement of Curvature

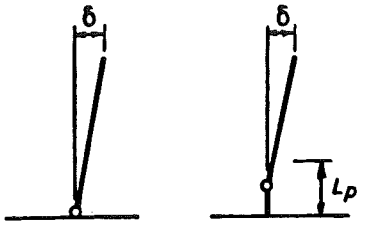

(a) (b)

Figure 7.25. Assumed Plastic Hinge Positions

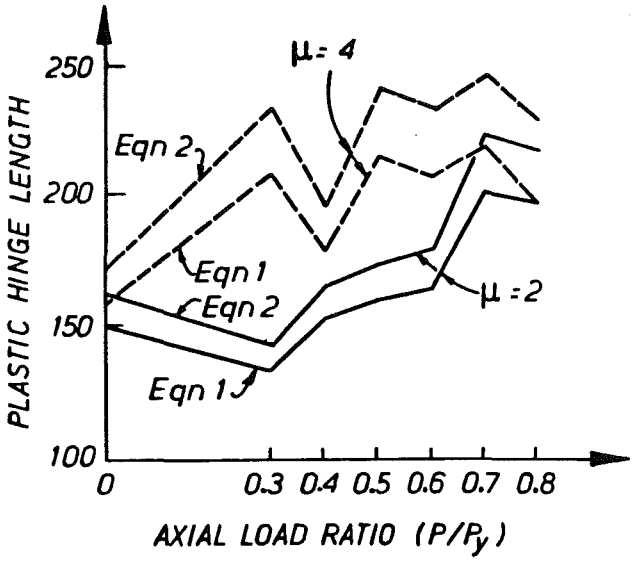

Figure 7.26. Specimen Plastic Hinge Lengths

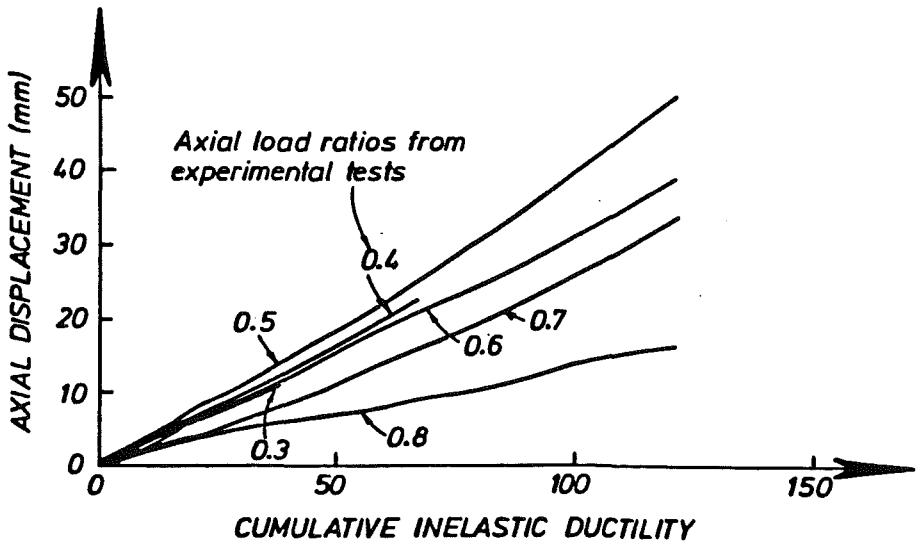

Figure 7.27. Axial Displacement - Cumulative Inelastic Ductility

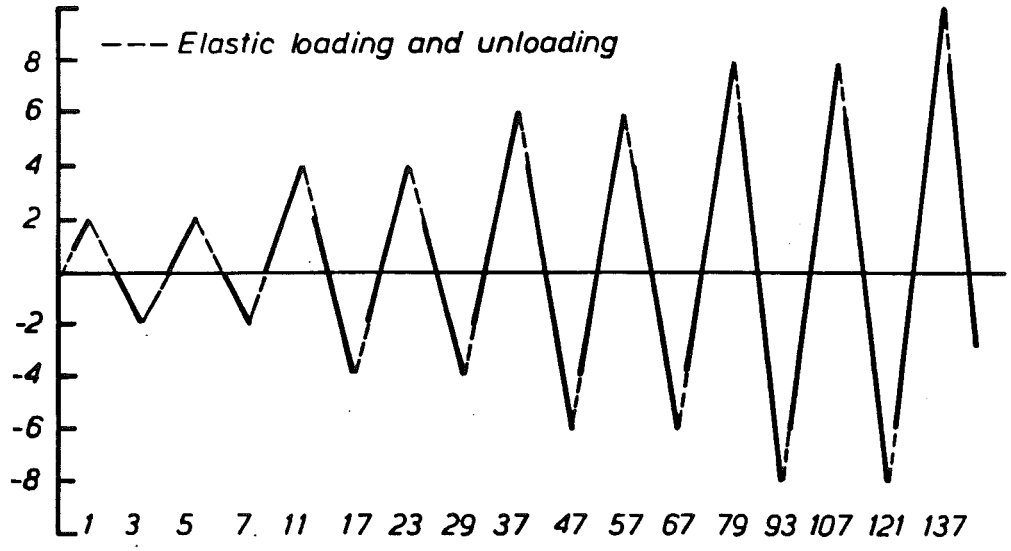

Figure 7.28. Cumulative Inelastic Displacement Ductility

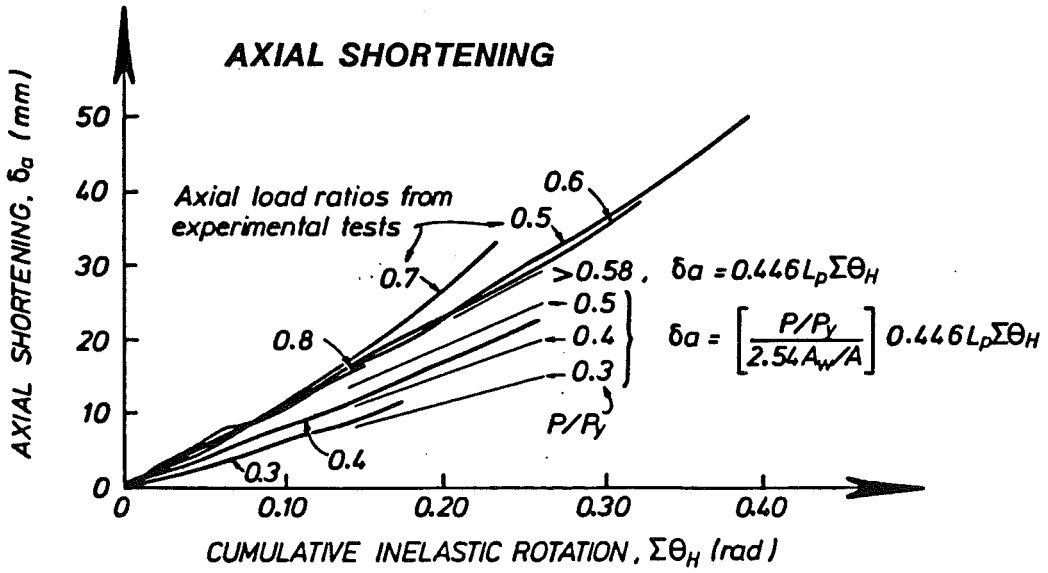

Figure 7.29. Axial Shortening - Cumulative Inelastic Rotation

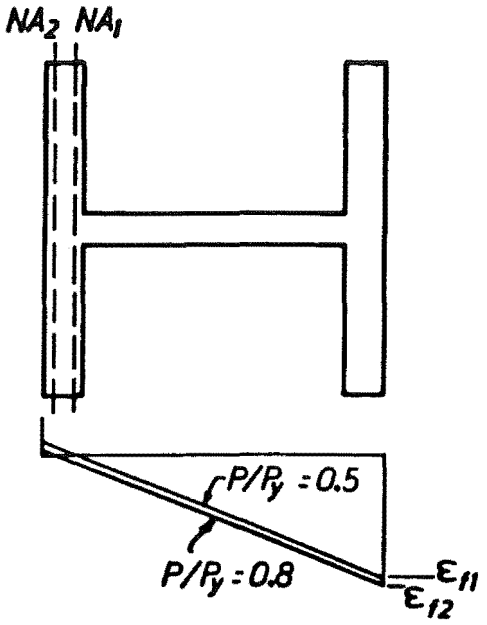

Figure 7.30. Column Section Strains
at a Particular Hinge Rotation

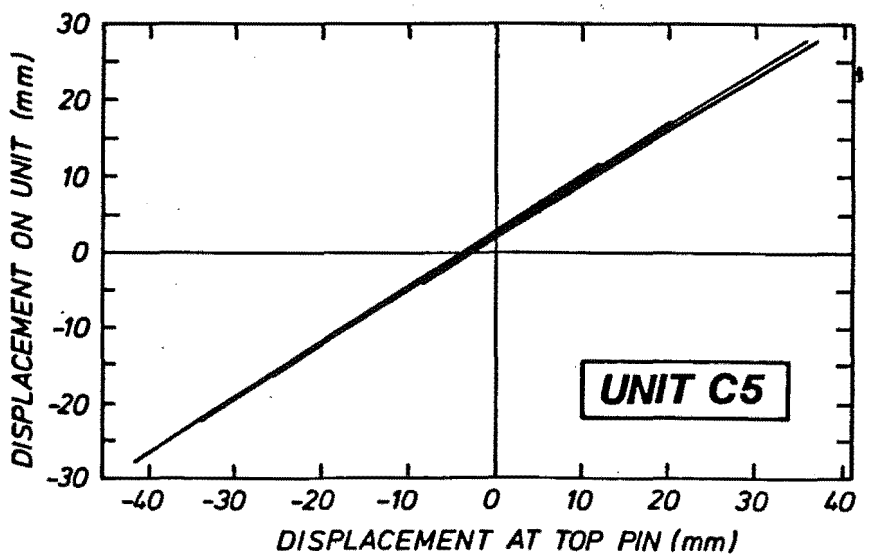

Figure 7.31. Linearity of Displacement Measurement

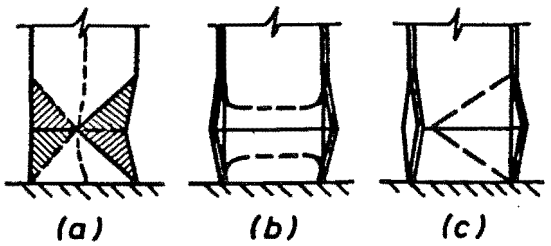

Figure 7.32. Member Yield Line Mechanisms

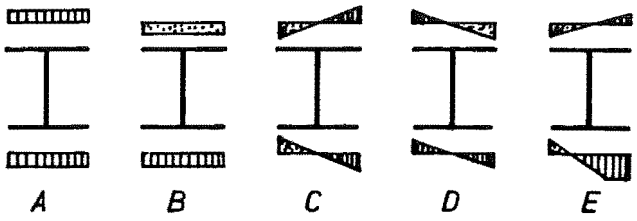

Figure 7.33. Possible Flange Stresses

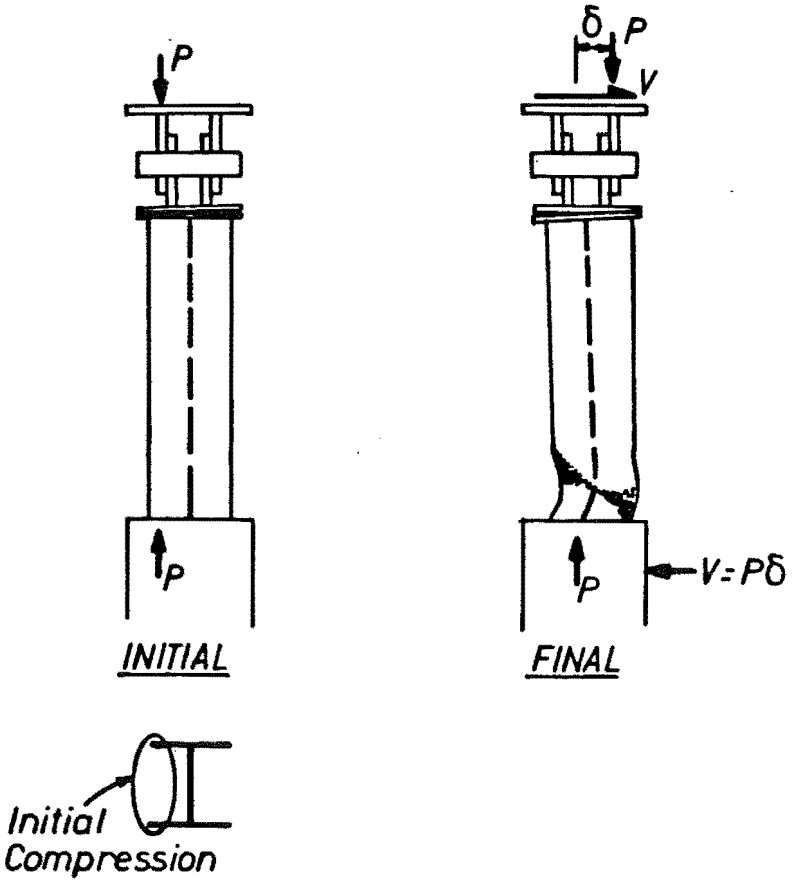

(a) (b)

Figure 7.34. Loading on Specimens

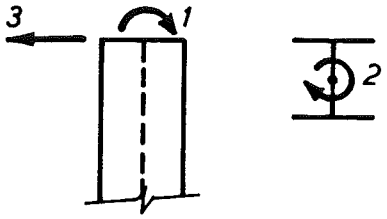

Figure 7.35. Restricted Degrees of Freedom of Test Column

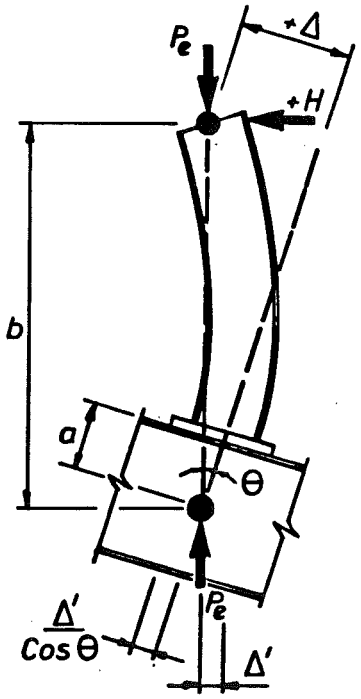

$$P_e \Delta' = P_e \frac{a}{b} \Delta$$

Figure 7.36. P-Delta Forces at the Base of The Specimen

7.15 REFERENCES

7.1 Butterworth J. W. and Spring K. C. F., "Column Design" Section D, Deliberations of the New Zealand Study Group for the Design of Steel Structures, Bulletin of the New Zealand National Society for Earthquake Engineering, Vol. 18, No. 4, December 1985.

7.2 Walpole W. R. and Butcher G. W., "Beam Design", Section C, Deliberations of the New Zealand Study Group for the Design of Steel Bulletin of the New Zealand National Society for Earthquake Engineering, Vol. 18, No. 4, December 1985.

7.3 Popov E. P., Bertero V. V. and Chandramoulli S., "Hysteretic Behaviour of Steel Columns", UCB/EERC 75-11, September 1975.

7.4 SAA, "Draft Australian Standard for Comment - Steel Structures", DR 87164, August 1987.

7.5 Trahair N. S., "Behaviour and Design of Steel Structures", Chapman and Hall, London, 1977.

7.6 Kasai K. and Popov E. P., "General Behaviour of WF Steel Shear Link Beams", *Journal of the Structural Division*, ASCE, Vol. 112, No. 2, February 1986.

7.7 Hanson R. D., "Comparison of Static and Dynamic Hysteresis Curves", *Journal of the Engineering Mechanics Division*, ASCE, Vol. 92, Oct 1966.

7.8 SAA, "Australian Standard - General Requirements for Supply of Hot-Rolled Steel Plates, Sections, Piling and Bars for Structural Purposes", AS 1227, 1980.

7.9 SAA, "Australian Standard - Methods of Tensile Testing of Metals", AS 1391, 1974.

7.10 SAA, "Australian Standard - Structural Steel Ordinary Weldable Grades", AS 1204, 1980.

7.11 SANZ, "General structural design and design loadings for buildings", NZS 4203, New Zealand Standard, 1982.

7.12 Lay M. G., "Flange Local Buckling in Wide-Flange Shapes", *Journal of the Structural Division*, ASCE, ST6, Dec 1965, p95-116.

7.13 Krawinkler H., Popov E. P. and Bertero V. V., "Inelastic Behaviour of Steel Beam-to-Column Subassemblages", UCB/EERC 71-7, Oct 1971.

7.14 Yamada M., "Low Cycle Fatigue Fracture Limits of Various Kinds of Structural Members Subjected to Alternately Repeated Plastic Bending under Axial Compression as an Evaluation Basis of Design Criteria for Aseismic Capacity", Proc. Fourth World Conference on Earthquake Engineering, Santiago, Chile (1969)

7.15 Patton R. N., "Analysis and Design Methods", Section B, Deliberations of the New Zealand Study Group for the Design of Steel Structures, Bulletin of the New Zealand National Society for Earthquake Engineering, Vol. 18, No. 4, December 1985.

7.16 Guruparan N. I., "Lateral Buckling rules for seismically-loaded I-beams", ME Report, Department of Civil Engineering, University of Canterbury, 1989.

7.17 Plugge H. B. and Walpole W. R., "The Tenacity of Bolted Beam End-Plate to Column Connections Under Simulated Seismic Loading" Research Report 83-2, Department of Civil Engineering, University of Canterbury, September 1983.

7.18 Priestley M. N. J. and Park R. "Strength and Ductility of Bridge Substructures", Road Research Unit Bulletin 71, National Roads Board, Wellington, New Zealand, 1984.

7.19 Carr A. J., "RUAUMOKO", Computer Program Library, Department of Civil Engineering, University of Canterbury. May 1986.

7.20 Mander J. B., Priestley M. N. J. and Park R., "Seismic Design of Bridge Piers", Research Report 84-2, Department of Civil Engineering, University of Canterbury, February 1984.

7.21 Mitani I., Makino M. and Matsui C., "Empirical Formula for Plastic Rotation capacity of Steel Beam-Columns with H-Shaped Cross Section", Proc. Pacific Structural Steel Conference, Vol. 2, p283-382, Auckland, 1986.

7.22 Wood B. R., Beaulieu D., and Adams P. F., "Further Aspects of Design by the P-delta Method", *Journal of the Structural Division*, ASCE, Vol. 102, ST3, March 1976.

7.23 Pam H. J., "Seismic Performance of Prestressed Concrete Piles and Pile-cap connections", Ph.D. Thesis, Department of Civil Engineering, University of Canterbury, 1987.

Chapter 8

CONCLUSIONS

8.1 SUMMARY

In this report on the seismic response of steel structures, two aspects of earthquake resistance were studied. They are:

i) the response of steel frames to earthquakes and their resulting member deformation demands, and

ii) the available inelastic deformation capacity of some actual steel members.

In addition to this, relationships between the expected deformation demands of members and the actual deformation demands were discussed. Earthquake resistance of structures may be provided with the knowledge of both the expected member deformation demands and of the member deformation capacities.

As most of the conclusions have generally been described at the end of each chapter, only some of the most important findings are reported here.

The inelastic dynamic response multi-degree-of-freedom steel structures to earthquake inertia loading was found to be complex. However, some patterns in the behaviour of these frames were observed. It was found that column axial load levels greater than that implied by the earthquake lateral load reduction factor may occur in moment-resisting frames and this higher level of axial load should be designed for. Shakedown of gravity moments was observed in the beams during cyclic yielding. Columns may dissipate energy during the first mode response during the later cycles. The equal displacement assumption was found to predict the frame displacements and interstorey drifts of all types of frames reasonably accurately when no soft-storey mechanisms formed during the design level earthquakes. However, it was found that the shape of the displacement envelopes for some frames may be significantly different than that predicted by the equal displacement assumption as most of the deformation tends to occur at the base of the frame. The maximum storey shears observed during actual earthquake records were often greater than that expected using the code loading distribution even when a full frame mechanism occurred because the centroid of the loading distribution moved. It was found that it was very difficult to force a soft-storey mechanism to occur in a regular steel moment-resisting frame.

Several different methods for the design of steel ductile moment-resisting frames were discussed and a design philosophy and methodology were presented based on the results of inelastic time-history analyses. In the proposed design method, the ductility capacity of different components is recognised. Yielding is encouraged to occur predominantly in the beams as well-detailed beams have a large rotation capacity. However, during large ground excitations yielding may occur in the panel zones or in the columns in order to reduce the ductility demand in the beams. Although panel zones and columns may possess reasonable ductility capacity there may be problems in these components if they are subjected to very large amounts of inelastic cyclic deformation. All of the frames analysed behaved well.

A simple tentative design method for P-delta effects in inelastically-responding frames was proposed. In this procedure an extra set of lateral forces were applied to the structure to account for the storey masses being translated through the expected displacements. The results given by this method seem reasonable although further study of this effect is required.

The eccentrically braced frames studied were of two types, the V-braced frame, and the D-braced frame. It was shown that although the columns of V-braced frames are generally not designed for moment, if no moment-capacity is provided, a soft-storey mechanism and large link deformations may result. To predict the actual moments in columns was found to be difficult. It was recommended that the maximum axial load level used in the design of columns be limited. Columns would therefore possess a minimum flexural strength by virtue of the moment-axial load interaction diagram, and if the moment demand did exceed the column flexural strength, sufficient ductility capacity would be available in the columns if a soft-storey mechanism did not occur. In D-braced frames the column moments next to the link must be known if the column is to be designed to remain elastic. It was found that the moment magnification factors commonly applied to reinforced concrete moment-resisting frames in New Zealand estimated the column moments of the D-braced frame well. It was also found that the reinforced concrete procedure may be simplified with little loss of accuracy when large dynamic magnification factors are used in D-braced frames.

The effects of cyclic loading on steel test samples, steel sections, and steel members in frames was discussed in chapter 6. It was shown that one of the reasons that the ductility capacity of columns was less than that of beams was that the neutral axis of a column may be in the flange so larger extreme fibre strains are required to obtain the same displacement ductility. The mechanism by which axial shortening may occur in columns was

described. Axial shortening was shown to affect the distribution of axial load among the columns of a frame. Cumulative effects, such as the column axial shortening, accumulation of curvature in gravity loaded non-composite beams and the "shakedown" of beam gravity loads were shown to occur during cyclic loading. A literature summary of beam testing which has affected the New Zealand codes was given. Very little work on the deformation capacity of cyclically-loaded steel columns was found to have been carried out and the need for further research in this area was described. Some different methods of damage measurement to describe member behaviour, such as energy, rotation and ductility to describe member behaviour and the relationships between these methods were discussed.

The testing of several steel I-shaped beam-columns under various levels of axial load and cyclic lateral load was described in chapter 7. The columns tested had flange slenderness ratios greater than that presently recommended in New Zealand for members expected to sustain limited ductility demand. All of the columns tested were found to behave well sustaining at least two cycles of loading to a member displacement ductility of eight. However, during the testing large amounts of column axial shortening occurred. Strength was found to be lost by means of either buckling or fracture. It was found that all of the members which lost strength by buckling failed after sustaining approximately the same amount of axial shortening. The amount of axial shortening was considered to be the main parameter governing the deformation capacity of these members. A rational formula was developed with empirical factors which estimated the amount of axial shortening of the members before buckling became severe. The members which lost strength as a result of fracture had sustained large inelastic deformations and large amounts of buckling before fracture occurred. Previously suggested values for the maximum axial load ratios for members expected to be subjected to both limited and full ductility demand were confirmed. As a result of the testing a greater understanding of the cyclic behaviour of beam-column members was developed than that which had been reported previously.

There was usually no column ductility demand in the columns above the ground floor level in moment-resisting frames designed according to the recommendations in chapter 3 and analysed under design level excitations. The columns at the base of the frames in which large ductility demands were demanded during the analyses were usually subjected to less than one full cycle of loading. The inelastic rotations associated with these ductility demands were of approximately the same size as the inelastic rotations obtained from the testing of columns with a similar level of axial load after several displacement cycles had been carried out. The testing carried

out did not study the ductility capacity of columns subjected large displacements with few load reversals. Frames in which column hinging was permitted over the height of the structure demanded several cycles of displacement to low displacement ductilities, usually of a magnitude of about 2, during design level earthquakes. These demands could easily be met with columns of the type tested and described in this report. It is thought that the displacement ductilities demanded of all members by the design level earthquakes could easily have been satisfied by well-detailed members.

Many facets of the behaviour of steel frames and of steel members have been studied in this report. Although the seismic response of frames is complex, it may be seen that properly-designed steel frames behave well. Steel is an ideal material for structures in earthquake-prone areas as it requires very little or no detailing to ensure good deformation capacity. The variety of structural forms of steel framed structures now available provide many opportunities for full advantage to be taken of the properties of steel.

It should be emphasized that many of the observations and design recommendations made are based on the authors judgement and on the interpretation of limited data. It is recognized that some of these recommendations may change as further research is carried out.

8.2 FURTHER RESEARCH

It is thought that further research may be carried out profitably into the following areas:

1) The study of seismic response, particularly in relation to the formation and behaviour of soft-storey mechanisms.

2) The study of the influence of P-delta effects on response and the likelihood of instability within structures. It is thought that studying this limit state may provide a new perspective on P-delta behaviour and highlight the sensitivity of the various parameters involved. Further work should be carried out to predict the behaviour of single degree of freedom oscillators with negative bilinear stiffnesses thereby providing insight into the P-delta response.

3) The effects of vertical accelerations, soft-soil behaviour and different types of earthquake record on the response of structures.

4) Analyses of irregular structures or those with different structural configurations should be carried out in order to further verify the proposed design procedures for these structures. Further study is required into the behaviour of hybrid structures which may consist of both braced frames and moment-resisting frames resisting the seismic forces together.

5) Further study is required to investigate the effects of different damping models on inelastically responding structures and an effort should be made to obtain a better knowledge of the true damping mechanism in building frames so that more appropriate analytical models may be used leading to more reliability in the results of analyses.

6) Further analytical and experimental testing of steel sections is required to find the maximum section slenderness limits which will permit satisfactory performance of steel members under seismic load conditions. A simple model should be developed to estimate the amount of strength loss occurring as a result of buckling in the columns.

7) The bi-axial inelastic cyclic flexural behaviour of I-shaped beam-columns should be studied further. This behaviour may occur during uni-axial loading of steel beam-columns, as out-of-plane buckling may induce secondary forces, but will be further exaggerated by bi-axial loading.

Appendix 1

METHOD FOR RAPID DETERMINATION OF FRAME PERIOD AND BASE SHEAR

Steps:

1. Assume member sizes for the frame.
2. Calculate the gravity loads and seismic masses of the frame.
3. Calculate:
   $F_x/V = W_x*h_x/\Sigma W_x*h_x$ at each level for frames with fundamental period, T, less than 0.7 seconds, or
   $F_x/V = 0.92\ W_x*h_x/\Sigma W_x*h_x$ at each level for frames with $T \geq 0.7$ seconds with an extra 0.08 applied at the top of the structure.
4. Apply F_x/V to structure in a 2-D structural analysis to obtain the structural deformations.
5. Using deflections from the static analysis output, the fundamental period may be calculated by Rayleighs method.

$$T = 2\pi\sqrt{(\Sigma(W_x d_x^2)/(g\Sigma(F_x d_x)))}$$
$$= 2\pi\sqrt{(\Sigma(W_x \delta_x^2)/(g\Sigma(W_x h_x \delta_x/\Sigma(W_x h_x))))}$$
where $\delta_x = d_x/V$

6. Using the period the elastic seismic force coefficient, C_e, may be found by interpolation from the elastic acceleration spectra.
7. By selecting a lateral load reduction factor, μ, the inelastic seismic force coefficient, C_μ, may be calculated as:
   $C_\mu = C_e/\mu$, for periods, $T \geq T_1$ seconds, or
   $= C_e/((\mu-1).T/T_1 + 1)$, for periods, $T \leq T_1$ seconds, and
   T_1 is the time period greater than which the equal displacement assumption is used for the acceleration spectra.
8. Calculate the base shear, V, as $C_\mu RZW_t$.
9. Find d_x $(=V\delta_x)$ to find displacements and hence interstorey drifts (ISD).
   $ISD = (d_{x2}-d_{x1}).\mu$
10. Compare the interstorey drifts (ISD) with the allowable interstorey drift limit, Z/50. If the drifts exceed this limit go back to step 1.
11. Multiply the input data for the seismic load case by the base shear, V, in the structural analysis to obtain the lateral force, F_x at each level. Other load cases should also be calculated and combined, as required, to determine the design forces on the members.

Steps 3 and 5-10 may be computerised. The period calculated by Rayleigh's method and is generally accurate to within 2% of that obtained by modal analysis for a regular rectangular frame.

Appendix 2

GENERATION OF ARTIFICIAL EARTHQUAKE RECORDS

Artificial earthquake records were generated using Simqke [2.51] to matcl the design acceleration response spectra of structures on hard soil given i1 the draft New Zealand loadings code [2.2].

A suite of two artificial earthquake records were generated. These may b(used for any stiff soil site in New Zealand or for any return period b1 simple scaling of the records by the appropriate zone and return perio(factors.

Typical input information into the program Simqke used to obtain th(artificial records is given below:

Smallest period of desired response spectrum	=	0.1 sec
Largest period of desired response spectrum	=	4.0 sec
Trapezoidal intensity function used - Build up time	=	2.0 sec
- Level time	=	15.0 sec
Duration of generated accelerogram	=	20.0 sec
Discretization time interval for generated accelerogram	=	0.02 sec
Desired maximum ground acceleration	=	0.4g
Number of iteration cycles of matching to target spectrum	=	3
Number of points used to describe target spectrum	=	18
Percentage of critical damping appropriate to target spectrum	=	5%

An arbitrary seed value was also used for the selection of random phas(angles.

Appendix 3

Loading and Analysis Input Data for the Frames

Loading for Ordinary Six Storey Frames - Frame #1 and Frame #3

Number of Bays	3	Distance to next frame	7 m
Span	7 m	No. of sec beams	0
Interstorey hght	3.5 m	Gravity	9.81 N/kg

DEAD LOAD				
Slab	2.7 kPa	=	18.9 kN/m	
Partitions	.45 kPa	=	3.15 kN/m	
Beams		=	1.05 kN/m	
Curtain wall	.5 kPa Vert			= 12.25 kN
Column weight	283 kg/m			= 9.72 kN
Beam in other dir	0 kg/m			= .00 kN
Total Dead UDL		=	23.1 kN/m	
Total Dead Exterior Node				= 21.97 kN
Total Dead Interior Node				= 9.72 kN
LIVE LOAD	2.5 kPa	=	17.5 kN/m	
Total Live Exterior Node				= .00 kN
Total Live Interior Node				= .00 kN

Nodal Load Combinations	
Total Exterior Nodal Load - D+Ls	= 21.97 kN
Total Interior Nodal Load - D+Ls	= 9.72 kN
Total Exterior Nodal Load - 1.2(D+Ls)	= 26.36 kN
Total Interior Nodal Load - 1.2(D+Ls)	= 11.66 kN
Total Exterior Nodal Weight	= 122.42 kN
Total Interior Nodal Weight	= 210.62 kN
Exterior Rotational Weight	= 93.75 kNm
Interior Rotational Weight	= 187.51 kNm

Uniformly Distributed Load, Loading Combinations	
D+Ls	28.70 kN/m
1.2(D+Ls)	34.44 kN/m
1.2D+1.6L	55.72 kN/m

Fixed End Forces		
Moment	D+Ls	117.2 kNm
Shear	D+Ls	100.5 kN
Moment	1.2(D+Ls)	140.6 kNm
Shear	1.2(D+Ls)	120.5 kN

Weight/level 666.1 kN

Loading for Six Storey Frame with Strong Outer Columns - Frame #2

Number of Bays	2		Distance to next frame		7 m
Span	7 m		No. of secondary beams =		0
Interstorey hght	3.5 m		Gravity	9.81 N/kg	

DEAD LOAD

Slab	4 kPa	=	28 kN/m	
Partitions	.7 kPa	=	4.9 kN/m	
Beams		=	1.35 kN/m	
Curtain wall	1.587 kPa Vert			= 38.88 kN
Column weight	283 kg/m			= 9.72 kN
Beam in other dir	0 kg/m			= .00 kN
Total Dead UDL		=	34.25 kN/m	
Total Dead Exterior Node				= 48.60 kN
Total Dead Interior Node				= 9.72 kN

LIVE LOAD	2.5 kPa	=	17.5 kN/m	
Total Live Exterior Node				= .00 kN
Total Live Interior Node				= .00 kN

Nodal Load Combinations

Total Exterior Nodal Load - D+Ls	= 48.60 kN
Total Interior Nodal Load - D+Ls	= 9.72 kN
Total Exterior Nodal Load - 1.2(D+Ls)	= 58.32 kN
Total Interior Nodal Load - 1.2(D+Ls)	= 11.66 kN
Total Exterior Nodal Weight	= 188.07 kN
Total Interior Nodal Weight	= 288.67 kN
Exterior Rotational Weight	= 130.18 kNm
Interior Rotational Weight	= 260.35 kNm

Uniformly Distributed Load, Loading Combinations

D+Ls	39.85 kN/m
1.2(D+Ls)	47.82 kN/m
1.2D+1.6L	69.10 kN/m

Fixed End Forces

Moment	D+Ls	162.7 kNm
Shear	D+Ls	139.5 kN
Moment	1.2(D+Ls)	195.3 kNm
Shear	1.2(D+Ls)	167.4 kN

Weight/level 664.8 kN

FRAME #1 Six storey 3 bay frame

Beam span = 7 m Bilinear column factor = .001
Damping = 5% in Modes 1 and 6
Interstorey height = 3.50 m

MEMBER PROPERTIES

Level	Axial Area (mm**2)			Shear Area (mm**2)			Moment of Inertia (x10**6 mm**4)		
	Int Col	Ext Col	Beam	Int Col	Ext Col	Beam	Int Col	Ext Col	Composite Beam
1	17500	17500	7600	4420	4420	3170	328	328	258
2	17500	17500	7600	4420	4420	3170	328	328	258
3	17500	17500	7600	4420	4420	3170	328	328	258
4	15000	15000	6840	3050	3050	3060	305	305	223
5	15000	15000	6840	3050	3050	3060	305	305	223
6	15000	15000	6840	3050	3050	3060	305	305	223

MEMBER STRENGTHS

Level	Flexural Strength (kNm)		Axial Strength (kN)				Beam Gravity Loads		Plastic Hinge Length	
							Moment (kNm)	Shear (kN)	(mm)	(mm)
	Int Col	Ext Col	Beam	Int Col	Ext Col	Beam			Column	Beam
1	575	575	298	4375	4375	3300	117	100	.320	.406
2	575	575	298	4375	4375	3300	117	100	.320	.406
3	575	575	298	4375	4375	3300	117	100	.320	.406
4	488	488	262	3750	3750	3154	117	100	.315	.403
5	488	488	262	3750	3750	3154	117	100	.315	.403
6	488	488	262	3750	3750	3154	117	100	.315	.403

NODAL LOADS AND WEIGHTS

Level	Gravity Nodal Vertical Loads		Nodal Weights Internal Nodes		Nodal Weights External Nodes	
	External Nodes (kN)	Internal Nodes (kN)	Horiz. and Vert (kN)	Rotat'l (kNm)	Horiz. and Vert (kN)	Rotat'l (kNm)
1	22	9.7	211	187	122	94
2	22	9.7	211	187	122	94
3	22	9.7	211	187	122	94
4	22	9.7	211	187	122	94
5	22	9.7	211	187	122	94
6	22	9.7	211	187	122	94

FRAME #2 Six storey 2 bay frame with elastic outer columns

Beam span = 7 m Column bilinear factor = 0.0005
Damping = 5% in Modes 1 and 6
Interstorey height = 3.50 m

MEMBER PROPERTIES

Level	Axial Area (mm**2)			Shear Area (mm**2)			Moment of Inertia (10^6 mm**4)		
	Int Col	Ext Col	Beam	Int Col	Ext Col	Beam	Int Col	Ext Col	Int Beam
1	16000	23000	11100	0	0	0	280	550	450
2	14500	23000	11100	0	0	0	225	550	450
3	13200	23000	11100	0	0	0	190	550	450
4	11300	19000	10600	0	0	0	140	400	400
5	8700	19000	10600	0	0	0	850	400	400
6	5500	19000	10600	0	0	0	350	400	400

MEMBER STRENGTHS

Level	Flexural Strength (kNm)			Axial Strength (kN)			Beam Gravity Loads: Moment (kNm)	Shear (kN)	Plastic Hinge Length (mm)		
	Int Col	Ext Col	Beam	Int Col	Ext Col	Beam			Int Col	Ext Col	Beam
1	631	1071	631	4760	6842	3300	196	167	.300	.300	.650
2	536	1071	631	4328	6842	3300	196	167	.300	.300	.650
3	464	1071	631	3940	6842	3300	196	167	.300	.300	.650
4	369	833	583	3370	5653	3154	196	167	.300	.300	.650
5	250	833	583	2600	5653	3154	196	167	.300	.300	.650
6	125	833	583	1642	5653	3154	196	167	.300	.300	.650

NODAL LOADS AND WEIGHTS

Level	Gravity Nodal Vertical Loads		Nodal Weights Internal Nodes		Nodal Weights External Nodes	
	External Nodes (kN)	Internal Nodes (kN)	Horiz. and Vert (kN)	Rotat'l (kNm)	Horiz. and Vert (kN)	Rotat'l (kNm)
1	49	10	290	262	189	131
2	49	10	290	262	189	131
3	49	10	290	262	189	131
4	49	10	290	262	189	131
5	49	10	290	262	189	131
6	49	10	290	262	189	131

FRAME #3 Six storey 3 bay frame with P-delta design

Beam span = 7 m Bilinear column factor = .001
Damping = 5% in Modes 1 and 6
Interstorey height = 3.50 m

MEMBER PROPERTIES

Level	Axial Area (mm**2)			Shear Area (mm**2)			Moment of Inertia (x10^6 mm**4)		
	Int Col	Ext Col	Beam	Int Col	Ext Col	Beam	Int Col	Ext Col	Composite Beam
1	17500	12300	5700	4420	3050	2420	328	222	121
2	17500	12300	5700	4420	3050	2420	328	222	121
3	17500	12300	5700	4420	3050	2420	328	222	121
4	15000	11400	5700	3050	2730	2420	305	143	121
5	15000	11400	5700	3050	2730	2420	305	143	121
6	15000	11400	5700	3050	2730	2420	305	143	121

MEMBER STRENGTHS

Level	Flexural Strength (kNm)			Axial Strength (kN)			Beam Gravity Loads: Moment (kNm)	Shear (kN)	Plastic Hinge Length (mm)		
	Int Col	Ext Col	Beam	Int Col	Ext Col	Beam			Int Col	Ext Col	Beam
1	575	397	194	4375	3075	1425	117	100	.320	.307	.352
2	575	397	194	4375	3075	1425	117	100	.320	.307	.352
3	575	397	194	4375	3075	1425	117	100	.320	.307	.352
4	488	308	194	3750	2850	1425	117	100	.315	.260	.352
5	488	308	194	3750	2850	1425	117	100	.315	.260	.352
6	488	308	194	3750	2850	1425	117	100	.315	.260	.352

NODAL LOADS AND WEIGHTS

Level	Gravity Vertical Nodal Loads		Nodal Weights Internal Nodes		Nodal Weights External Nodes	
	External Nodes (kN)	Internal Nodes (kN)	Horiz. and Vert (kN)	Rotat'l (kNm)	Horiz and Vert (kN)	Rotat'l (kNm)
1	22	9.7	211	187	122	94
2	22	9.7	211	187	122	94
3	22	9.7	211	187	122	94
4	22	9.7	211	187	122	94
5	22	9.7	211	187	122	94
6	22	9.7	211	187	122	94

V-Braced Frame Loads and Analysis Input

Assumed Seismic Load ($D + L_s$) = 5 kPa
Load/Level/Frame = 5 kPa * 32 m * 24 m/2 = 1920 kN

Mass and loads were only considered on the external nodes
Weight/Node = 1920/2 = 960 kN horizontally
= 5 kPa * 32 m^2 = 160 kN vertically
Rotational weight/internal node = 195 kNm
Vertical load = 160 kN vertically

MEMBER PROPERTIES

	Area	Shear Area	Second Moment of Area	Plastic Moment	Axial Strength
	A (m^2)	A_s (m^2)	I (m^4)	M_p (kNm)	P_y (kNm)
Columns					
310 UC 240	0.03060	0.00811	$642.0*10^{-6}$	1062.	7650.
Braces					
200 UC 60	0.00758	0.00194	$60.9*10^{-6}$	163.	1895.
Beams (Top 5 stories)					
360 UB 51	0.00646	0.00285	$142.0*10^{-6}$	224.	1615.
Links (Top 5 stories)					
360 UB 51	0.00646	0.00285	$142.0*10^{-6}$	178.	1615.
Beams (Bottom 5 stories)					
310 UC 46	0.00589	0.00207	$99.5*10^{-6}$	181.	1472.
Links (Bottom 5 stories)					
310 UC 46	0.00589	0.00207	$99.5*10^{-6}$	142.	1472.

Damping was constant at 5% in every one of the 120 modes
Bilinear factor for all members = 0.01

D-Braced Frame Loads and Analysis Input

Dead Load -	Slab	2.70 kPa * 18 m * 30 m	=	1458	kN
	Partitions	0.45 kPa * 18 m * 30 m	=	243	kN
	Columns	18 * 300 kg/m * 3.5m * 9.81 N/kg	=	185	kN
	Beams	(7 * 18 m + 4 * 30 m) * 1.35 kN/m	=	332	kN
	Curtain Walls	0.5 kPa * 3.5 m * 96 m	=	168	kN
		D	=	2386	kN
Serviceability Live Load -		0.80 kPa * 18 m * 30 m	L_s =	432	kN
$D + L_s$ /level			=	2818	kN
Load/level/frame ($D + L_s$)		2816 kN/4	=	705	kN

NODAL LOADS

Dead (Ext)	2386 kN * 5 m * 4.5 m / 2 / 18 m / 30 m	=	49.7	kN
(Int)	2386 kN * 5 m * 6.75 m / 18 m / 30 m	=	149.1	kN
Live (Ext)	0.80 kPa * 5 m * 4.5 m / 2	=	9.0	kN
(Int)	0.80 kPa * 5 m * 6.75 m	=	27.0	kN
Total Exterior Nodal Load ($D + L_s$)		=	58.7	kN
Total Interior Nodal Load ($D + L_s$)		=	176.1	kN

MEMBER PROPERTIES

	Area	Shear Area	Second Moment of Area	Plastic Moment	Axial Strength
	A (m^2)	A_s (m^2)	I (m^4)	M_p (kNm)	P_y (kNm)
Columns					
200 UC 60	0.00758	0.00475	$60.9*10^{-6}$	220.	2558.
Braces					
200 UC 60	0.00758	0.00475	$60.9*10^{-6}$	220.	2558.
Beams					
250 UB 37	0.00475	0.00164	$55.6*10^{-6}$	121.	1188.
Links					
250 UB 37	0.00475	0.00164	$55.6*10^{-6}$	112.5	1188.

LOADS & WEIGHTS

	LOAD	NODAL WEIGHTS	
		Horizontal	Rotational
	(kN)	(kN)	(kN)
Column Near Link	58.7	235.	10.
Column Not Near Link	176.1	470.	10.

Damping was constant at 5% in every one of the 45 modes
Beam bilinear factor = 0.0005
Column and brace bilinear factor = 0.0100

Appendix 4

TABLES OF BUCKLING

Values of buckle displacement, buckle half wave length and distance from the baseplate to the centre of the buckle during the testing are given in the tables below for the different specimens.

Flange buckle displacement is designated as positive toward the west, and web buckling positive toward the south. All numbers are given in units of millimetres. For cycles of loading to positive values of ductility the compression flange was the west flange.

Estimation of the magnitude of the buckles was thought to be accurate to ±1mm and approximately ±10mm in the estimation of the half wavelength and the height of the buckles. Some of the flanges buckled in such a way that there were several points of contraflexure along the flange making estimation of the half-wave length and distance to the centre of the buckle difficult. This is one reason for some of the variation in the buckling patterns obtained in the specimens.

Specimen CO

Cycle	Flange Buckle Magnitude Flange West		East		Compression Flange Height to centre		Half wave length		Web	
	North	South	North	South	North	South	North	South	Magn-itude	Height
6x1	-3		0	0	160					
-6x1	0	0	-2		110					
6x2	-3	1			165					
-6x2	0	0	-2	3	80	100				
8x1	-8	3	0	0	166	80	160			
-8x1	0	0	-3	8	70	160		180		
8x2	-13	10	0	0	170	170	180	180		
-8x2	0	0	-7	13						
10x1	-23	22	0	0	165	170	160	170	4	160
-10x1	0	0	-19	23	170	170	210	200		
10x2[a]	-39	39	0	0	170	185				
10x8[b]	-48	22	-47	22	180	170	155	160	35	160
10x8[c]	-48	22	-47	22	180	170	155	180	35	160

a) Buckles straighten out completely up to this stage
b) East flange
c) West flange

Specimen C3

Cycle	Flange Buckle Magnitude Flange West		East		Compression Flange Height to centre		Half wave length		Web Magnitude	Web Height
	North	South	North	South	North	South	North	South		
4x1	1	3								
-4x1	1	3	-2	-5					6	125
4x2	-8	12	-2	-5	190	140	200	200	10	120
-4x2	-8	12	10	-18	185	140	150	190	15	135
6x1	-30	30	10	-18	187	140	200	250	22	130
-6x1	-30	30	36	-36		130	165	170	22	130
6x2	-52	50	36	-36			170	170	32	
-6x2			50	-50		130	135	135	35	125
8x1	-65	65							39	
-8x1			70	-65					51	135
8x2	-82	75				160				
-8x2			79	-75			135	135	55	
10x1	-98	87			160	100	145	140	56	115
-10x1	-104	98	97	95	132	95	110	110	60	

Specimen C4

Cycle	Flange Buckle Magnitude Flange West		East		Compression Flange Height to centre		Half wave length		Web Magnitude	Web Height
	North	South	North	South	North	South	North	South		
2x2	1	1								
-2x2			1	1						
4x1	4	4			130	140				
-4x1			-6	4	150	180			5.5	130
4x2	8	10			130	135	145	160	8	120
-4x2			-14	15	155	195	180	180	13	
6x1	20	22			135	140	135	125	16.5	120
-6x1			-37	40	170	190	185	125		
6x2*	-38	36			280	135				
6x2*	28	36			130	135			26	125
-6x2			-50	50	160	180	175	150	31	130
8x1	-61	56			270	130	170	120	37	
-8x1			-67	70	158	172	155	130	42	125
8x2	-84	63			255	125	160	110	46	
-8x2							175	135	51	
10x1		76					145	97	60	
-10x1			-98	96	145	163	180	130	57	
EOT	-126	86	-103	93	215	125	160	80	68	125

* Double Buckle

Specimen C5

Cycle	Flange Buckle Magnitude Flange West		East		Compression Flange Height to centre		Half wave length		Web Magnitude	Web Height
	North	South	North	South	North	South	North	South		
2x2				-1		140				
4x1	3	1			140	150			5	
-4x1			10	-10	195	155			8	165
4x2	-7	7			270	155		125	12	
-4x2			23	-23	185	150	175	210	16	175
6x1	-28	26			258	150	180	165	20	
-6x1			46	-43	187	158	145	190	30	180
6x2	-47	44			250	158		170	33	
-6x2			61	-55	185	145	135	180	36	
8x1	-65	65			240	160	175		43	
-8x1			77	-71	175	147	130	165	49	184
8x2	-80	78			230	140	145	125	54	
-8x2			90	-83	175				58	
10x1	-97	90			220	126	160		72	
-10x1			105	-92	160	113	105	125	78	
10x2	-104	105			205	113	130	105	83	
EOT	-112	106	114	-97	150	105	125	120	85	150

Specimen C6

Cycle	Flange Buckle Magnitude Flange West		East		Compression Flange Height to centre		Half wave length		Web Magnitude	Web Height
	North	South	North	South	North	South	North	South		
2x2				-2						
4x1		3				135			4	135
-4x1			-1	-7	130	143		140	5	
4x2		12				125		140	7	130
-4x2			7	-17	230	150		130	10	
6x1	-12	27				130			14	
-6x1			30	-35	215	150	165	140	19	
6x2	-28	41			150	130	170	135	23	
-6x2			44	-50	215	145			25	
8x1	-48	53			155	130	160	130	31	
-8x1		51	65	-62	200		170	160	34	130
8x2	-60	64			150	130			37	
-8x2			75	-70	190	140	160	130	40	
10x1	-75	75			144	117	140	120	46	
-10x1			91	-82	185	125	155	130	50	
10x2	-86	84			135	110	110	115	55	
-10x2			102	-91	170	110	155	130	60	105
EOT	-100	92	102	-96	125	98	120	145	64	95

Specimen C7

Cycle	Flange Buckle Magnitude Flange West		East		Compression Flange Height to centre		Half wave length		Web Magnitude	Web Height
	North	South	North	South	North	South	North	South		
2x2	1	1	-1	-1						
4x1	3	1			140					
-4x1			-3	-3						
4x2	-4	4			265	155			3	125
-4x2			8	-7	250	160			6	200
6x1	-17	14			255	190	195	195	12	210
-6x1			28	-22	260	180	150	230	18	210
6x2	-35	33			250	205	165	190	23	
-6x2			43	-36	255	200	160	250	30	
8x1	-52	50			255	205	170	240	35	
-8x1			60	-55	255	205	160	310	41	
8x2	-65	60			250	200	175	220	47	
-8x2			78	-65	245	185	180	270	52	
10x1	-79	79							57	
-10x1			80	-74					64	
10x2	-99	87			235	175	135	238		
EOT	-92	90	97	-80	235	168	130	270	68	210

Specimen C8

Cycle	Flange Buckle Magnitude Flange West		East		Compression Flange Height to centre		Half wave length		Web Magnitude	Web Height
	North	South	North	South	North	South	North	South		
4x1	1	1								
-4x1				-2						
4x2	2	2								
-4x2				-5					3	
6x1	3	6			150	140			5	
-6x1			2	-10	200	140			6	160
6x2	-9	13			245	155	175	195	8	150
-6x2			7	-19	155	135	120	135	11	150
8x1	-18	24			235	155	180	185	13	155
-8x1			18	-30	170	135	155	115	18	
8x2	-30	36			230	165	165	155	20	155
-8x2			34	-39	180	130	150	130	25	
10x1	-44	47			220	160	150	195	26	155
-10x1			48	-52	178	133	150	125	30	
10x2	-60	60			215	165	145	140	34	
-10x2			57	-60	172	135	145	135	37	155

The specimen collapsed before end-of-test readings could be taken.

Specimen CA

Cycle	Flange Buckle Magnitude Flange West			East	Compression Flange Height to centre		Half wave length		Web	
	North	South	North	South	North	South	North	South	Magn-itude	Height
4x1	2									
-4x1			-2	-1						
4x2	4	1								
-4x2			3	-2					3	
6x1	-10	6				205			6	
-6x1			12	-9	235	150	145	210	7	
6x2	-29	22			270	223	145	270	16	210
-6x2			24	-19	245	130	130	165	16	
8x1	-47	45			275	225	150	220	25	210
-8x1			40	-32	245	140	145	170	25	
8x2	-64	55			270	205	135	210	36	210
-8x2			50	-46	235	140	140	165	36	
10x1	-75	70			263	195	145	240	45	
-10x1			64	-59	235	140	160	220	42	
10x2	-86	82			258	190	132	190	52	
EOT			77	-67	235	135	155	210	50	245